VOLUME 64 [W. B. No. 1181] NUMBER 4

MONTHLY WEATHER REVIEW

APRIL 1936

CONTENTS

	Page
On the Relation Between Rainfall and Stream-flow. (5 figs.) Richmond T. Zoch	105
Cooling in the Lower Atmosphere and the Structure of Polar Continental Air. (9 figs.) H. Wexler	122
Duststorms in the United States, April 1936. (1 fig.) Robert J. Martin	137
Bibliography	137
Solar Observations	139
Aerological Observations	143
Rivers and Floods	145
Weather on the Atlantic and Pacific Oceans	149
Climatological Tables	152
Charts I-X.	

UNITED STATES DEPARTMENT OF AGRICULTURE

WEATHER BUREAU

WASHINGTON, D. C.

For sale by the Superintendent of Documents, Washington, D. C. - See page 4 of cover for price

DEPOSITED BY THE
UNITED STATES OF AMERICA
AUG 7 '36

MONTHLY WEATHER REVIEW

Editor, EDGAR W. WOOLARD

VOL. 64, No. 4
W. B. No. 1181

APRIL 1936

CLOSED JUNE 3, 1936
ISSUED JULY 22, 1936

ON THE RELATION BETWEEN RAINFALL AND STREAM FLOW—II

By RICHMOND T. ZOCH

[Washington, D. C., March 1936]

PART I

This article, the second of a series on the subject,[1] presupposes an acquaintance with the first article. Here, instead of considering the drainage area to be rectangular, the theory is extended to irregularly-shaped drainage areas such as are actually met with on the earth's surface.

Throughout this article, as in the first paper, the rate of rainfall, the dryness of the soil, and the velocity of the water are considered to be constant. Moreover, evaporation is neglected as before. However, in the last section of this paper it is pointed out that the methods here employed for irregularly-shaped drainage areas are entirely general and can be readily used when the aforementioned restrictions are removed.

In the first paper no mention was made of the tributaries that streams which exceed the size of brooks invariably have; neither was anything said about the distance which water has to flow overland in order to reach stream channels. Furthermore, while the first paper discussed the discharge from a rectangular drainage area, no precise explanation was given as to what was meant by a rectangular drainage area. Does a rectangular drainage area imply one whose divide outlines a rectangle regardless of how the river and its tributaries meander within the rectangle? These questions were purposely ignored for several reasons: The first paper was essentially introductory; the conditions there treated were very much idealized; it was believed that the discussion of the questions just mentioned belonged in this second article. It is necessary that these neglected features be made clear before irregularly shaped drainage areas can be adequately treated, and therefore they will now be discussed. In discussing them it will be simplest to explain certain steps essential to the application of this theory, which explanations at first sight might appear more properly to belong in the second group of articles.

Despite the features neglected in the first paper, it will have been observed that the distance which water has to travel in order to reach the gage plays an important part in determining the discharge from rainfall. Clearly, in the case of a specific drainage area there may be a large subarea from which water has to travel an approximate distance of a certain number of miles, while for an approximate distance of a different number of miles the corresponding subarea may be much less. In other words, for any given interval of distance which water has to travel, the subareas may be quite different; for example, the subarea from which water has to travel from 10 to 20 miles to reach the gage may be much less than the subarea from which water has to travel from 40 to 50 miles. In order to develop a general theory it is necessary to take this fact into account. Such is the main purpose of this second paper, and it is here shown that, regardless of how irregular any natural drainage area may be, systematic methods can be used for predicting its discharge from rainfall.

In order to apply the theory which will be developed in part II it is necessary to have accurate maps of the river basin whose discharge it is desired to predict. Maps like the topographic maps made and issued by the United States Geological Survey will answer the purpose very nicely.

If the proper maps are available, then the first step in applying the theory is to outline the drainage area on the maps. This is accomplished by drawing a line which begins at the gaging station, follows the divide, and finally ends at the gaging station, thus inclosing the drainage area. After this it is necessary to determine the greatest distance which water has to travel in order to reach the gaging station. This distance should then be divided into a convenient number of equal parts. Say the greatest distance which water has to travel is 300 miles. If this distance of 300 miles be divided into 12 equal parts, each part will be of length 25 miles. Steps should now be taken to outline the several subareas from which water, in order to reach the gaging station, has to travel more than 0 miles and less than 25 miles, more than 25 miles and less than 50 miles, more than 50 miles and less than 75 miles, and so on. To carry this out it is necessary to measure, with a suitable measuring device such as a chartometer, up the main stream and up each tributary, marking off points corresponding to 25 miles, 50 miles, 75 miles, and so on, always being careful to follow the thread of the stream while measuring. After these points have been located, all of them which are 25 miles from the gage should be connected by a smooth line (curve) beginning at the divide[2] on one side of the main stream and ending at the divide on the opposite side. All points which are 50 miles from the gage should be similarly connected, and so on. Clearly each tributary may have tributaries of its own and these tributaries may also have tributaries and so on to mere brooks or ditches. Hence, the process of finding the boundaries of the several aforementioned subareas is a slow and tedious task, but it is perfectly straightforward and can be carried out easily (though slowly) if the proper maps are available.

From the above explanation it will be seen that the lines (curves) which outline the subareas are lines such that from all points on any one of them water has to travel equal distances in order to reach the gage. For this reason they will, in the future, be called *equal water travel* lines.

Where equal water travel lines cross stream channels they do so at right angles. Thus, in a certain sense, the

[1] The first paper appears in MONTHLY WEATHER REVIEW, 62: 315-322, September 1934.

[2] The term "divide" will be used in this series of articles for the line representing the ridge of high ground inclosing the drainage area that contributes to the discharge at the gaging station. The four terms "drainage area", "drainage basin", "river basin", and "watershed" will be used synonymously for the area inclosed by the divide. The term "water parting" will be used for any line representing a ridge of the high ground *within* the river basin which separates the areas drained by two tributaries.

net of stream channels and the equal water travel lines form a mutually orthogonal system. In this respect equal water travel lines are like contour lines, for the latter also cross stream channels at right angles. However, equal water travel lines should not be confused with contour lines, as the two have no other property in common.

After the equal water travel lines have been drawn on the maps as explained above, the subareas comprised between successive equal water travel lines should be measured. These subareas can be quickly and easily obtained by means of a planimeter.

If these subareas be plotted on a diagram, on which the midpoint distances of the subareas above the gaging station are abscissas (in the above example these midpoint distances are 12½, 37½, 62½ miles, and so on, respectively) and the corresponding subareas divided by the distance between consecutive equal water travel lines are ordinates, a histogram of the drainage area is obtained. This histogram shows the true shape of the drainage area.

The channel which is followed by the water that flows the greatest distance in reaching the gage will be considered as the main stream. On the above-mentioned diagram the main stream, *rectified*, forms the axis of abscissas.

Clearly in the above example it was not necessary to divide the 300 miles into 12 equal parts. The 300 miles could have been divided into a greater number of equal parts, thus making the distance between consecutive equal water travel lines smaller. Obviously, a very accurate histogram can be constructed by making the distance between consecutive equal water travel lines very small. After the histogram has been completed, a mathematical curve can be fitted to it, the equation of which will give the width of the drainage area at any distance above the gaging station.

In this paper no histogram has been constructed for a specific river basin; the above explanation has been given to show that the theory developed in this second paper is very general and can be applied to any river basin for which maps are available. In the second group of papers the complete process of making one or more histograms for one or more actual river basins will be given.

The distance which water has to travel from where it falls as rain over a drainage area, to a gaging station on the stream, can be divided into two parts, viz: (1) that part where the water travels in the stream channel (or the stream channel with its adjacent flood plain), and (2) that part where the water travels over the land before reaching a permanent stream channel such as a gully or brook. The question of overland travel of water was tacitly ignored in the first paper; this was done in order to keep the mathematical developments there (the first paper being essentially introductory in character) as simple as possible. The first section of part II discusses the question of overland travel. It is there shown that the error involved in neglecting overland travel entirely, as was done in the first paper, is small. A helpful corollary can be drawn from this conclusion: In drawing lines of equal water travel on maps it is not necessary to use extreme care in drawing an equal water travel line *overland* from one tributary to the adjacent tributary. As the location of the points on the tributaries where equal water travel lines cross them is a slow process, the fact that the lines can be drawn from tributary to tributary by personal judgment rather than by exact measurement adds to the ease with which the theory can be applied. Of course, when the points where equal water travel lines cross the several tributaries are being located, great care should be exercised.

The question of the number of parts into which the greatest distance that water has to travel in order to reach the gage (the 300 miles in the illustration above) should be divided, i. e., how many equal water travel lines should be drawn when dealing with a given watershed, in order to obtain reasonably accurate results, will be taken up in the second group of articles on this subject.

If the greatest distance which water has to travel in order to reach the gage be divided into a very large number of parts, the histogram obtained by the above described procedure will approach a smooth curve; or, putting it differently, if the distance between consecutive equal water travel lines be made infinitely small, then the histogram approaches a smooth curve as a limit. This curve will be termed the *drainage area curve*. Its abscissas are distances above the gaging station, and its ordinates are the widths of the drainage area. These widths must be obtained by the processes above outlined. Thus, in general, the width of the drainage area at an arbitrary distance above the gage will not be the length of an equal water travel line corresponding to this distance; neither will it be the width of the watershed as a crow flies.

Obviously, it is impracticable in constructing a histogram of a drainage area to make the distance between consecutive equal water travel lines very small. Hence the actual mathematical curve which is fitted to the histogram of the drainage area will not coincide with the theoretical drainage area curve. However, it should approximately follow the theoretical drainage area curve. This point will be further discussed in the second group of articles; in the present paper we assume that this problem will cause no difficulty, and the two terms *drainage area curve* and *histogram of the drainage area* are used more or less synonymously in the first group of articles.

Summing up the above explanations, we can say that the shape of the divide has no bearing whatever on what is meant by the shape of the drainage area. The true shape of the drainage area is obtained by an involved process. In particular we say a drainage area is rectangular when the areas comprised between consecutive equal water travel lines are all equal to each other. Since the main stream is the axis of abscissas, we can also say a drainage area is rectangular when its drainage area curve is a straight line parallel to the axis of abscissas. In general, by the shape of a drainage area is meant the shape of the area enclosed by the drainage area curve and the axis of abscissas.

Two new terms are introduced in this paper; they will now be defined. The first derivative of the discharge with respect to time is here defined as the *rate of discharge*. The *rate of discharge* at any given time is the change in discharge per unit time at that time, and is measured in mile inches per hour per hour. The second derivative of the discharge with respect to time is here defined as the *discharge tendency*. The *discharge tendency* at any given time is the change in the rate of discharge per unit time at that time, and is measured in mile inches per hour per hour per hour.

As pointed out in the first paper, both the volume of discharge and the discharge are functions of the time. Likewise, the rate of discharge and the discharge tendency are functions of the time. If any one of the four quantities, volume of discharge, discharge, rate of discharge, or discharge tendency, be plotted as ordinates on a graph

with time as abscissas we obtain a curve. The nomenclature used for these curves is in accordance with the variable that forms the ordinate. To illustrate, figure 4 is a volume-of-discharge *curve;* figure 5 is a discharge *curve*, and so on.

Having considered the questions of overland travel, tributaries, and the precise meaning to be attached to the term "shape of the drainage area", and having defined the new terms introduced in this paper, it now remains, in order to carry out the plan of describing in the first part of each paper what is done mathematically in the second part, to explain the remaining sections of part II:

In section 2 of part II a drainage area whose histogram has the shape of a triangle is discussed. It is there pointed out that even so simple a drainage area leads to equations which cannot be explicitly solved in literal form. It is also pointed out that in this special case, for short rains, that is to say, rains whose duration is less than the time required for water to flow from the most distant part of the drainage area to the gage (compare the comments made in connection with equation (9) in the first paper), a different equation must be solved to obtain the maximum discharge from that which is necessary when the rains are long.

The third section takes up the special case of a drainage area whose histogram has the shape of an ellipse. The discussion there shows that in selecting a curve by which the histogram is to be represented, great care must be taken lest expressions which cannot be integrated be encountered. It is also shown that even though we may not always be able to solve explicitly for the time of the crest, we can, nevertheless, always express the maximum discharge explicitly in literal form. This is a very important point, and will be of the utmost assistance in applying the theory.

Clearly there will be few drainage areas whose histograms can be reasonably well represented by simple geometrical curves such as a rectangle, triangle, or ellipse. For this reason the fourth section takes up the general case where the drainage area curve is expressed by any function whatever.

In this fourth section equations analogous to the equations of the first paper are derived. In addition to enabling us to predict the maximum discharge and its time of occurrence, these equations reproduce the complete hydrograph which results from a single rain. It is there pointed out that for some drainage areas a single rain can cause only one crest, while in other drainage areas it may cause more than one crest, and the precise conditions which the drainage area curve must satisfy in order that a single rain may cause a single crest are given. However, it is further pointed out that if the rain lasts long enough for water to flow from the farthest part of the watershed to the gage, then a single rain can cause only one crest, regardless of the shape of the drainage area.

It is also shown in section 4 that the maximum discharge from a watershed which results from a given rain is equal to the discharge from that portion of the watershed which lies between two equal water travel lines in a steady state. The expression "steady state" here means that the rain has lasted so long that there is just as much water flowing off the soil as there is rain falling upon it; one of the equal water travel lines is that which lies at the greatest distance which water has to travel to reach the gage, the other lies at that distance above the gage which water would travel in the interval beginning with the end of the rain and ending with the time of the crest. However, for infinitely short rains, it is shown that the maximum discharge has a still simpler interpretation, and is equal to the product of the depth of the rain times the velocity of the water times the width of the drainage area at the equal water travel line corresponding to the time of the crest.

Finally, section 4 shows that both the discharge and rate of discharge curves are everywhere continuous, except that for infinitely short rains the rate of discharge curve may have a discontinuity at the time of the crest; and that the discharge tendency curve is continuous except at certain points.

The fifth section discusses a drainage area curve which overcomes all the difficulties raised in the second and third sections. The purpose of the sixth and last section was mentioned in the second paragraph above.

PART II

FOREWORD

The figures in this series of articles are numbered consecutively for the series as a whole, and not separately for each article.

Two methods are used in numbering the equations. When an equation of any preceding paper is generalized in a subsequent paper, then the number of the equation as it first appears in the series will be preceded by a letter. Thus in this paper all of the equations in section 2 of the first article are generalized, hence these generalized equations are preceded by the letter B. The letter C will be similarly used in the third article, and so on. Should it be necessary to give the same equation two separate generalizations in the same subsequent article then the letter will be primed.

Those equations which are not generalizations of equations previously given will be numbered consecutively for the entire series. It is hoped that this dual system of numbering the equations will cause no confusion.

The mathematics used in this article is but slightly more advanced than that in the first one; and every effort has been made, consistent with keeping the cost of publication reasonable, to have all developments clear.

SECTION 1: OVERLAND TRAVEL

In order to facilitate the mathematical treatment of overland travel, it is here assumed that the water travels overland in a direction perpendicular to the stream channel. Naturally this is not always the case, but it will be clear to the reader that this assumption is permissible since the complete neglect of overland travel involves only a small error.

Consider a rectangle whose width is W and whose length is L. Take the X-axis as the line parallel to and midway between the lines forming the sides (length) of the rectangle. Take the origin at one end of the rectangle and assume that the gaging station is at the origin and that the stream channel coincides with the X-axis. Let w be the distance from the stream channel to the infinitesimal *area* $dwdx$; the definitions of all other symbols were given in the first paper.

Now at the time t each infinitesimal area, $dwdx$, contributes to the discharge at the gaging station, y, not its discharge at the time t but its discharge at the time t diminished by the time required for the water to flow from $dwdx$ to the gaging station. Clearly the time required for the water to flow from $dwdx$ to the gaging station is the time required for the water to flow from $dwdx$ to the stream channel plus the time required for the water to flow from where the discharge from $dwdx$ reaches the stream channel to the gaging station. Since the velocity of the water is v, these times are w/v and x/v, respec-

tively; and therefore the time required for the water to flow from $dwdx$ to the origin is $(w+x)/v$. The discharge, y, is the sum of all the discharges from the infinitesimal areas $dwdx$; it is therefore (under properly chosen conditions) equal to the double integral (see fig. 2):

$$\int\int r\left\{1-e^{-\frac{1}{c}\left(t-\frac{x+w}{v}\right)}\right\}dwdx.$$

If the time t be taken sufficiently large so that the water from the area $dwdx$ farthest from the gaging station has had time to reach the gage (in other words if $tv \geqq L+\frac{1}{2}W$), then the limits on the above integrals are $\frac{1}{2}W$ and $-\frac{1}{2}W$, and L and 0; and on performing the indicated integration and substituting these limits we obtain the equation:

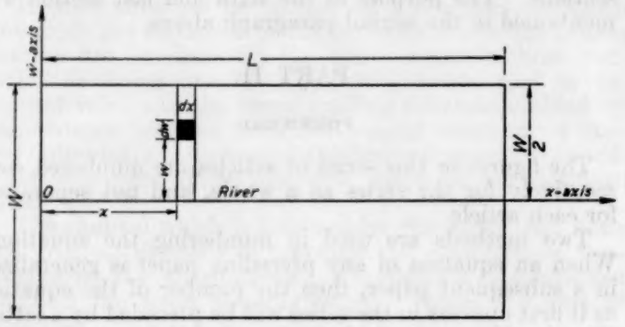

FIGURE 2.

$$y=r\left[WL-2c^2v^2e^{-\frac{t}{c}}\left(e^{\frac{W}{2cv}}-1\right)\left(e^{\frac{L}{cv}}-1\right)\right]. \quad (10)$$

Equation (10) holds on the range $\frac{L+\frac{1}{2}W}{v} \leqq t \leqq \infty$, with the additional restriction that $t \leqq t_0$. That is to say, as long as the rain lasts, equation (10) applies. As $t \to \infty$, y approaches the limit WLr. It should be noted that equation (4) has this same limit as $t \to \infty$. In other words, for equations (4) and (10), if the rain lasts sufficiently long a steady state will eventually be reached when there is just as much water flowing away from the area as there is rain falling upon it; this is just as would be expected, and moreover the discharge in this steady state is not dependent on whether overland travel is considered or neglected. From the nature of the problem, and without going into any involved mathematics, it is clear that the discharge at the time of a steady state is independent of the size and shape of the drainage area.

When the time $t < \frac{L}{v}$, the discharge, y, will not be given by the above integral, but will be the sum of the discharges from a rectangle whose width is W and length is $tv-\frac{1}{2}W$ and from a triangle whose base is W and altitude is $\frac{1}{2}W$. (See fig. 3.) The discharge from the rectangle is

$$\int_0^{tv-\frac{1}{2}W}\int_{-\frac{1}{2}W}^{\frac{1}{2}W}\left\{1-e^{-\frac{1}{c}\left(t-\frac{x+w}{v}\right)}\right\}dwdx,$$

and the discharge from the triangle is

$$\int_{tv-\frac{1}{2}W}^{tv}\int_{-(tv-x)}^{(tv-x)}\left\{1-e^{-\frac{1}{c}\left(t-\frac{x+w}{v}\right)}\right\}dwdx.$$

On performing the above integration, substituting the indicated limits, simplifying and adding, we get the equation:

$$y=r\left[Wtv-Wcv-\tfrac{1}{4}W^2+2c^2v^2e^{-\frac{t}{c}}\left(e^{\frac{W}{2cv}}-1\right)\right]. \quad (11)$$

Equation (11) holds only on the range $\frac{W}{2v} \leqq t \leqq \frac{L}{v}$ with the restriction that $t \leqq t_0$. When overland travel was neglected, the curve, y, representing the discharge from the time the rain begins to the time after the rain stops when the discharge has receded to its value when the rain began, was a continuous curve whose first derivative with respect to time, dy/dt, was continuous and whose second derivative with respect to time, $\frac{d^2y}{dt^2}$, was also continuous except at three points, viz., $t=Lv$, $t=t_0$, and $t=t_0+L/v$. The effect of these three points of discontinuity in $\frac{d^2y}{dt^2}$ was to divide the curve for y into four sections represented by equations (3), (4), (6), and (5), respectively. Figure 4 illustrates the integral of the discharge curve. Figures (5), (6), and (7) illustrate a theoretical discharge curve, its first derivative, and its second derivative for a rectangular drainage area where overland travel is neglected. Figure (7) clearly shows the three points of discontinuity. As the derivative of a function is discontinuous at every point where the function is discontinuous, it follows that the third derivative of y with respect to t will also be discontinuous at these three points. Now when the question of overland travel is considered, as above, then not only both y and dy/dt

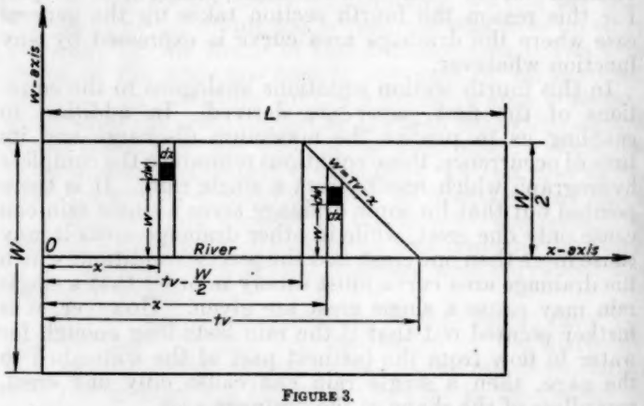

FIGURE 3.

but also $\frac{d^2y}{dt^2}$ are everywhere continuous. However, $\frac{d^3y}{dt^3}$ is continuous except at, not three points, but seven points, and the y-curve is thus divided into eight sections. The following table gives the range of t for each of the eight sections and the number of double integrals required to obtain y:

Range of t:	Number of double integrals
$0 \leqq t \leqq \frac{W}{2v}$	1
$\frac{W}{2v} \leqq t \leqq \frac{L}{v}$	2
$\frac{L}{v} \leqq t \leqq \frac{L+\frac{1}{2}W}{v}$	2
$\frac{L+\frac{1}{2}W}{v} \leqq t \leqq t_0$	1
$t_0 \leqq t \leqq t_0+\frac{W}{2v}$	3
$t_0+\frac{W}{2v} \leqq t \leqq t_0+\frac{L}{v}$	4
$t_0+\frac{L}{v} \leqq t \leqq t_0+\frac{L+\frac{1}{2}W}{v}$	3
$t_0+\frac{L+\frac{1}{2}W}{v} \leqq t \leqq \infty$	1

The foregoing table is based on the assumption that $t_0 \geqq (L+\frac{1}{2}W)/v$. Clearly t_0, the duration of the rain, may be less than $(L+\frac{1}{2}W)/v$. In such a case the above table would have to be modified, and it may happen that as many as five double integrals would be required to obtain y.

Equations for y as a function of t on each of the above ranges will not be given here; should they be desired, their derivation is perfectly straightforward, though tedious, as the above two equations show. As the main purpose of these papers is to devise a scheme for predicting flood crests, only one more equation for these ranges will be obtained, viz., that for the range $t_0+W/2v \leqq t \leqq t_0+L/v$, as this range contains the time of the crest.

It follows by reasoning similar to that given in the first article, together with that already given here, that the discharge on this last-mentioned range is given by the sum of (1) the discharge of a rectangle of width W and length $x_0-\frac{1}{2}W$ where the rate of run-off is decreasing; (2) the discharge of a triangle of base W and altitude $\frac{1}{2}W$ where the rate of run-off is decreasing; (3) the discharge of *two* triangles, each of base $\frac{1}{2}W$ and altitude $\frac{1}{2}W$, adjacent to the triangle of (2) and where the rate of run-off is increasing; and (4) the discharge of a rectangle of width W and length $L-x_0$, where the rate of run-off is increasing. The discharge is, therefore, the following sum of four double integrals:

$$y=\int_0^{x_0-\frac{1}{2}W}\int_{-\frac{1}{2}W}^{\frac{1}{2}W} r\left(1-e^{-\frac{t_0}{c}}\right)e^{-\frac{1}{c}\left(t-t_0-\frac{x+w}{v}\right)}dwdx+$$
$$\int_{x_0-\frac{1}{2}W}^{x_0}\int_{-(x_0-x)}^{x_0-x} r\left(1-e^{-\frac{t_0}{c}}\right)e^{-\frac{1}{c}\left(t-t_0-\frac{x+w}{v}\right)}dwdx+$$
$$2\int_{x_0-\frac{1}{2}W}^{x_0}\int_{x_0-x}^{\frac{1}{2}W} r\left\{1-e^{-\frac{1}{c}\left(t-\frac{x+w}{v}\right)}\right\}dwdx+$$
$$\int_{x_0}^{L}\int_{-\frac{1}{2}W}^{\frac{1}{2}W} r\left\{1-e^{-\frac{1}{c}\left(t-\frac{x+w}{v}\right)}\right\}dwdx.$$

On performing the above integrations, substituting the indicated limits, simplifying, remembering here that $x_0=r(t-t_0)$, and adding, we get the equation:

$$y=2r\left[c^2v^2\left(e^{\frac{t_0}{c}}-1\right)\left\{e^{-\frac{t_0}{c}}-e^{-\frac{1}{c}\left(t_0+\frac{W}{2v}\right)}-e^{-\frac{1}{c}\left(t-\frac{W}{2v}\right)}+e^{-\frac{t}{c}}\right\}+\right.$$
$$cv\left(1-e^{-\frac{t_0}{c}}\right)\left\{\tfrac{1}{2}W-cv+cve^{-\frac{W}{2cv}}\right\}+$$
$$\tfrac{1}{8}W^2+cve^{-\frac{t_0}{c}}\left\{\tfrac{1}{2}W+cv-cve^{\frac{W}{2cv}}\right\}+$$
$$\left.\tfrac{1}{2}WL-\tfrac{1}{2}Wv(t-t_0)-c^2v^2\left(e^{-\frac{1}{c}\left(t-\frac{L}{v}\right)}-e^{-\frac{t_0}{c}}\right)\left(e^{\frac{W}{2cv}}-1\right)\right]. \quad (12)$$

We can find the time of the maximum discharge by differentiating equation (12) with respect to t, and setting this derivative equal to zero. On doing this and simplifying, the following equation is obtained which gives the time of the crest:

$$t_c=c\log\left(e^{\frac{L}{cv}}+e^{\frac{t_0}{c}}-1\right)+c\log\frac{2cv}{W}\left(e^{\frac{W}{2cv}}-1\right). \quad (13)$$

Equation (13) agrees exactly with equation (7) except for the addition of the term $c\log\frac{2cv}{W}\left(e^{\frac{W}{2cv}}-1\right)$. It will now be shown that in all practical cases equation (7) gives t_c with sufficient accuracy:

Consider L to be 50 miles (for a value of L this small, it is doubtful if it would be practicable to make flood crest forecasts). L is purposely taken this small because as L increases the effect of the term $c\log\frac{2cv}{W}\left(e^{\frac{W}{2cv}}-1\right)$ on t_c becomes less and less. Take W as 2 miles; this means that the greatest distance that water would have to travel overland is 1 mile. It is believed that this value is greater than is usually found in nature. It may be well to point out here that the fact that a stream has tributaries, thus increasing the width of the *drainage basin*, will not increase W; $W/2$ is the greatest distance that water would have to travel *overland* to reach *some* tributary (i. e. a permanent stream channel). Except on extremely flat land, $W/2$ would not ordinarily exceed 1 mile; a glance at any topographic map will bear this out. Moreover, increasing the number of tributaries will have no effect on t_c; it will affect y_c but not t_c.

Consider now the constant c. This is a time constant, and when we say that a certain parcel of ground in a specified condition has a constant c equal to a certain number of hours (say 4 hours) we mean that at the end of 4 hours from the beginning of the rain the rate of run-off from the parcel of ground will be $\left(1-\frac{1}{e}\right)$ times the rate of rainfall which is falling upon the ground. Thus the time constant is the time in which the rate of run-off reaches $\left(1-\frac{1}{e}\right)=\frac{1.71828\ldots.}{2.71828\ldots.}=0.63212$ (approximately) of its final value (steady state). Clearly, the longer the time necessary for the rate of run-off to reach 0.63212 of the rate of rainfall, the greater is the amount of water which the soil retains; but the point to be emphasized is that we measure the capacity (dryness) of the soil in time (hours) and *not* in volume as might be supposed. It is believed that c is always greater than 1 hour. For soils covered with growing vegetation, 24 hours would probably be a good average value of c.

When streams are low, v may be as small as ¼ mile per hour or even less; but when a stream rises sufficiently to cause a flood, v will usually be much greater. Summing up, we can assume that in practice $\frac{2cv}{W}>1$, $c>1$ and $v>1$. Under these conditions it can be shown that $\log\frac{2cv}{W}\left(e^{\frac{W}{2cv}}-1\right)$ is everywhere positive but less than 0.541. It has the value 0.541 when $2cv/W=1$, and approaches zero very rapidly when $2cv/W$ is greater than 1. Of course, it is necessary to multiply the small quantity $\log(2cv/W)\left(e^{\frac{2cv}{W}}-1\right)$ by c, and the product might be appreciable. Accordingly the following table has been prepared showing the relative values of the two terms on

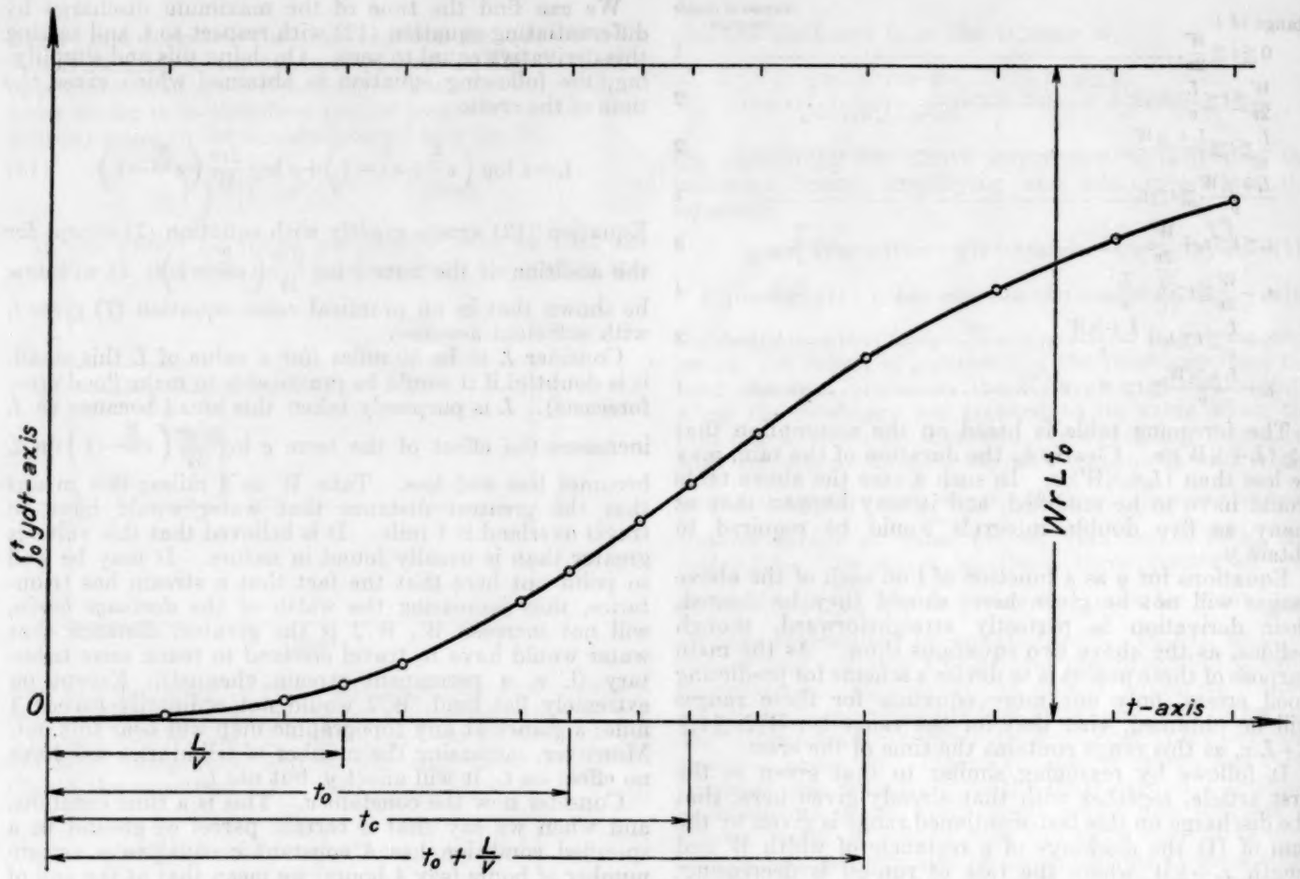

FIGURE 4.

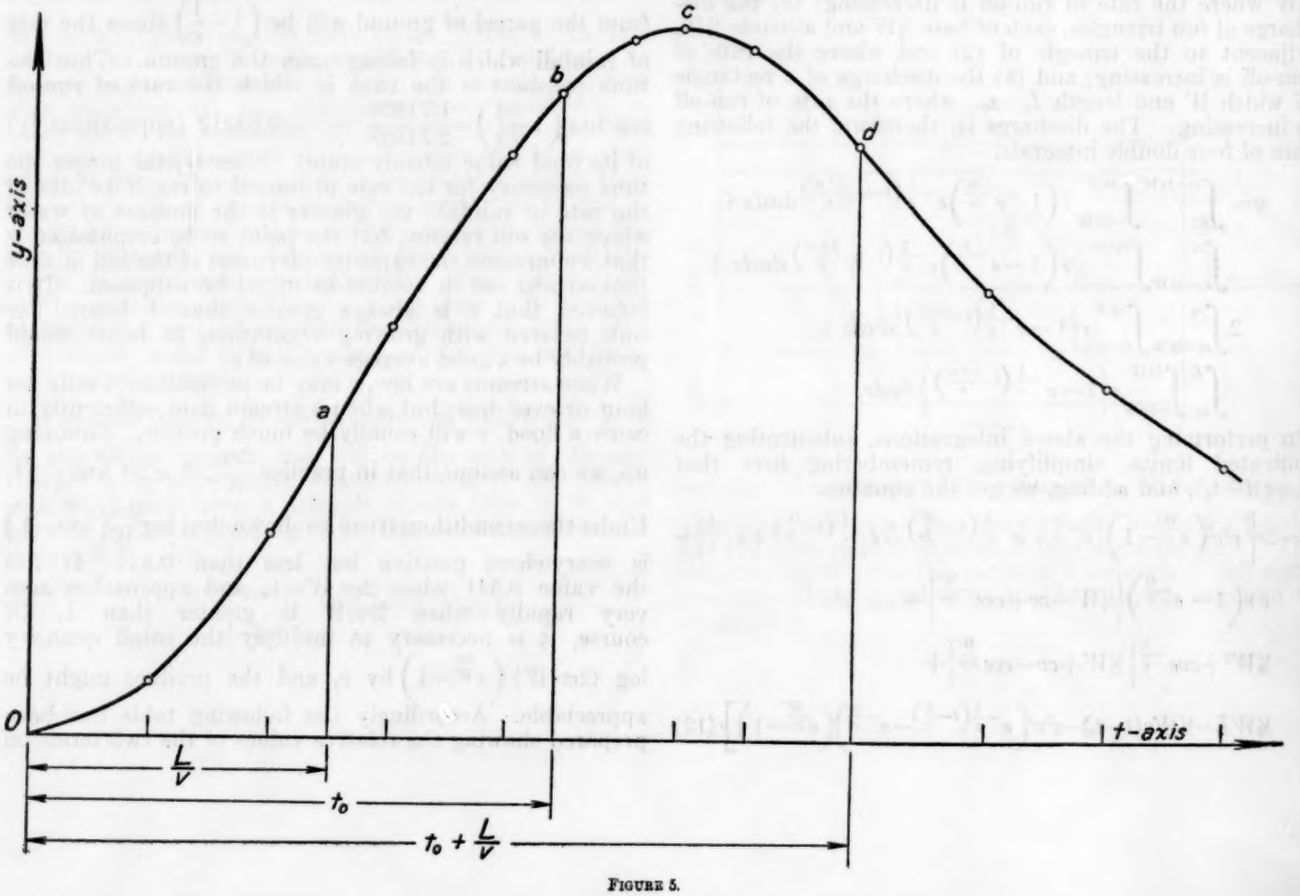

FIGURE 5.

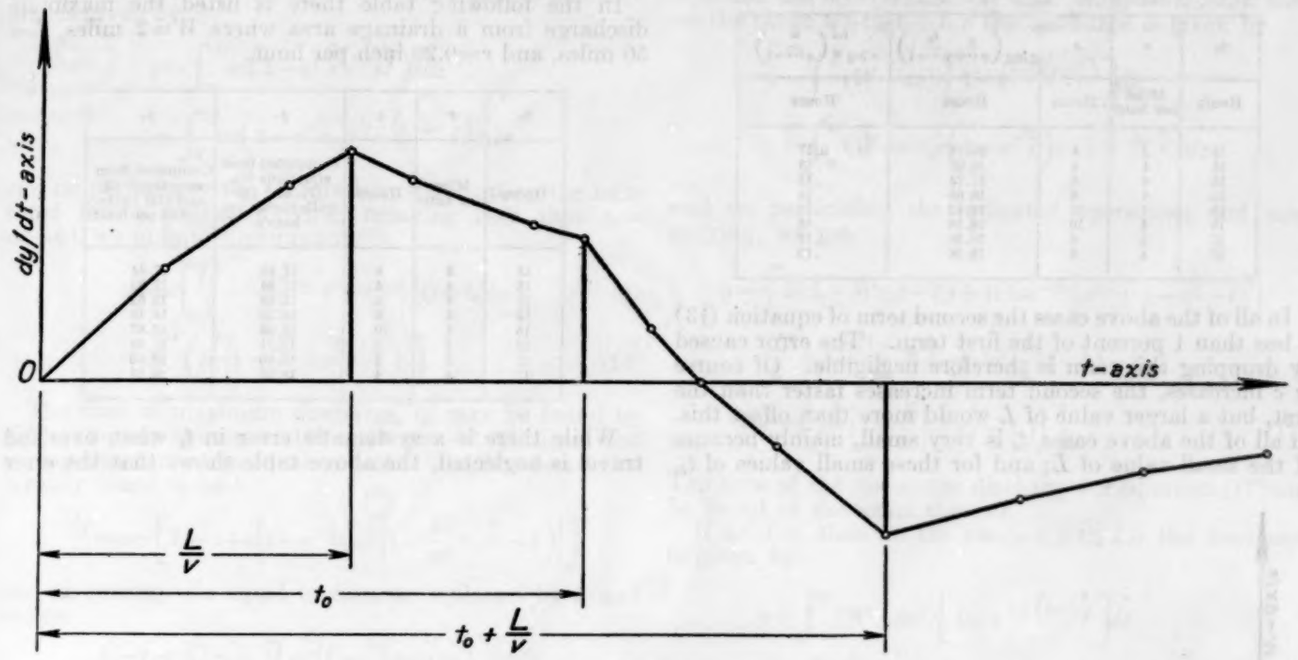

FIGURE 6.

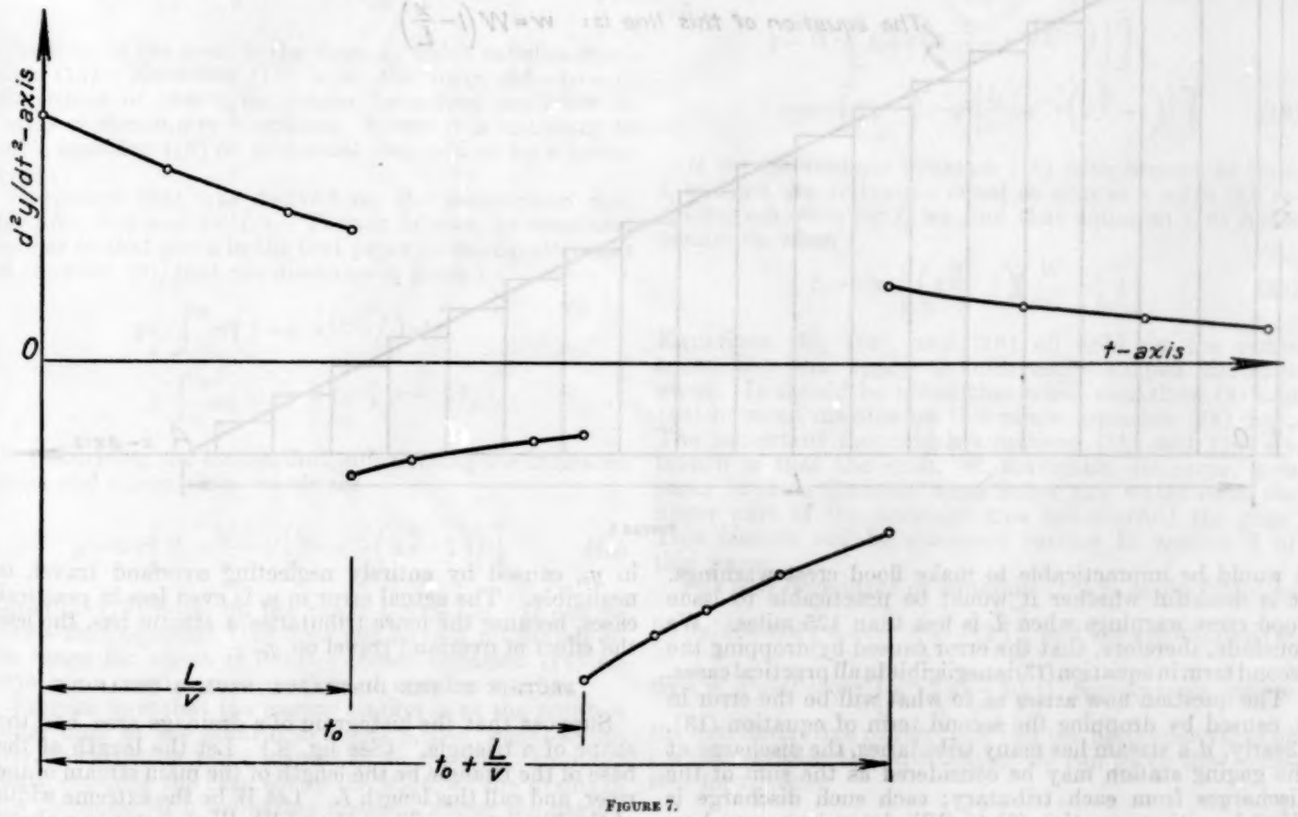

FIGURE 7.

the right-hand side of equation (13) for selected values of t_0, v, and c. In all cases $L=50$ miles and $W=2$ miles.

t_0	v	c	$c\log\left(e^{\frac{L}{cv}}+e^{\frac{t_0}{c}}-1\right)$	$c\log^{\frac{2cv}{W}}\left(e^{\frac{W}{2cv}}-1\right)$
Hours	Miles per hour	Hours	Hours	Hours
18	3	4	20.14	0.17
15	4	4	16.65	.13
15	4	6	17.73	.13
15	4	8	18.65	.14
15	4	10	19.42	.16
13	4	10	18.18	.16
17	3	4	19.58	.17
17	4	4	18.08	.13

In all of the above cases the second term of equation (13) is less than 1 percent of the first term. The error caused by dropping this term is therefore negligible. Of course as c increases, the second term increases faster than the first, but a larger value of L would more than offset this. In all of the above cases, t_c is very small, mainly because of the small value of L; and for these small values of t_c, it would be impracticable to make flood crest warnings. It is doubtful whether it would be practicable to issue flood crest warnings when L is less than 125 miles. We conclude, therefore, that the error caused by dropping the second term in equation (13) is negligible in all practical cases.

The question now arises as to what will be the error in y_c caused by dropping the second term of equation (13). Clearly, if a stream has many tributaries, the discharge at the gaging station may be considered as the sum of the discharges from each tributary; each such discharge is given by either equation (6) or (12), depending upon how much accuracy is desired. Thus the more tributaries a stream has, the less the error involved by using equations (6), (7), and (8) in place of the more accurate equations (12) and (13).

In the following table there is listed the maximum discharge from a drainage area where $W=2$ miles, $L=50$ miles, and $r=0.20$ inch per hour.

t_0	v	c	y_c	y_c
Hours	Miles per hour	Hours	Computed from equations (6), (7), and (8) (mile-inches per hour)	Computed from equations (12) and (13) (mile-inches per hour)
18	3	4	17.43	17.44
15	4	4	17.36	17.35
15	4	6	15.63	15.62
15	4	8	14.16	14.15
15	4	10	12.93	12.87
13	4	10	11.71	11.65
17	3	4	16.90	16.90
17	4	4	18.27	18.21

While there is a systematic error in t_c when overland travel is neglected, the above table shows that the error in y_c, caused by entirely neglecting overland travel, is negligible. The actual error in y_c is even less in practical cases, because the more tributaries a stream has, the less the effect of overland travel on y_c.

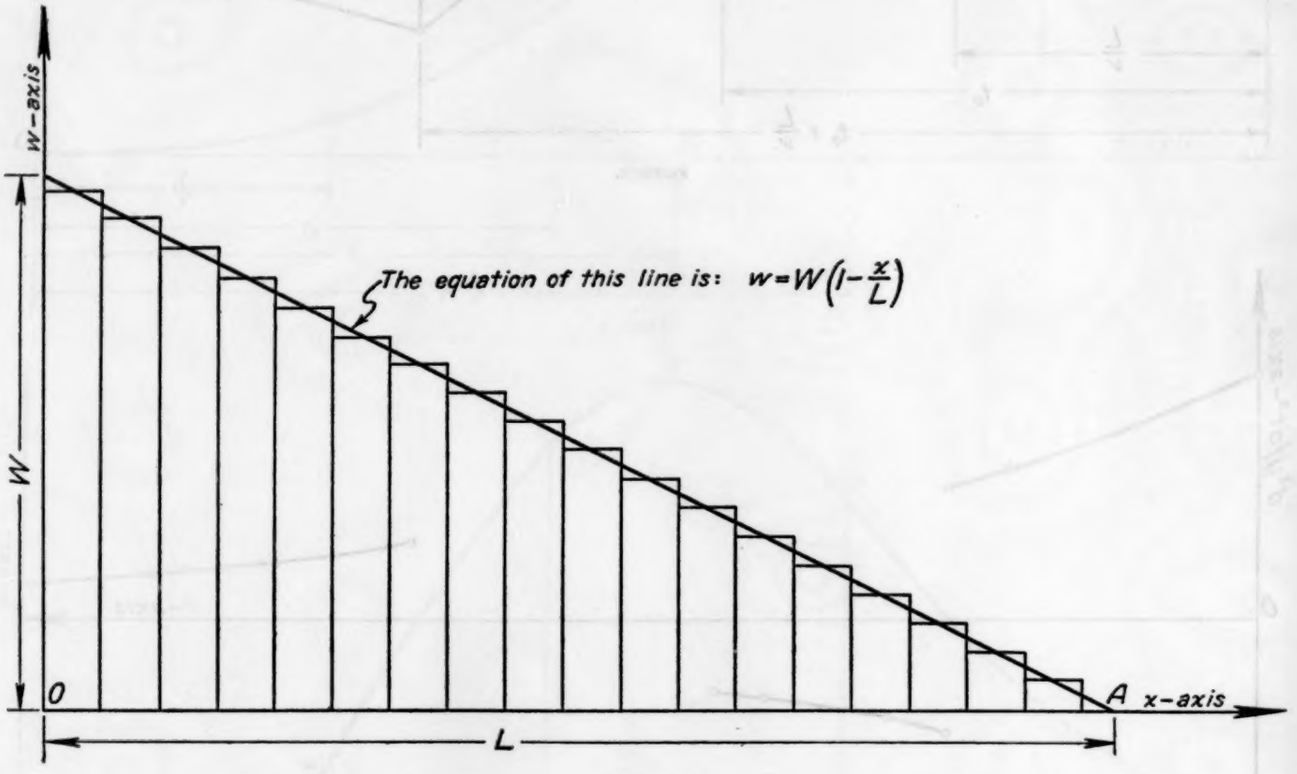

FIGURE 8.

SECTION 2: THE DISCHARGE FROM A TRIANGLE

Suppose that the histogram of a drainage area has the shape of a triangle. (See fig. 8.) Let the length of the base of the triangle be the length of the main stream of the river, and call this length L. Let W be the extreme width of the histogram. Then the width W at distance x above the gaging station will be $(W/L)x$. For the sake of brevity put $W/L=a$. Suppose that $t_0>L/v$. Then it follows, by

reasoning similar to that in the first paper, that the discharge on the range $t_0 \leqq t \leqq t_0 + L/v$ from such a drainage area is given by

$$y = \int_{x_0}^{L} ar\left(1 - e^{-\frac{1}{c}\left(t - \frac{x}{v}\right)}\right)dx + \int_{0}^{x_0} ar\left(1 - e^{-\frac{t_0}{c}}\right)e^{-\frac{1}{c}\left(t - t_0 - \frac{x}{v}\right)}dx$$

and on performing the integration, substituting the indicated limits and simplifying, recalling here that $x_0 = v(t - t_0)$, we obtain the equation:

$$y = ar\left[\frac{L^2}{2} - \frac{(t-t_0)^2}{2}v^2 + c^2v^2\left\{\frac{1}{c}(t-t_0) - 1 + e^{-\frac{t}{c}}\left(e^{\frac{L}{cv}}\left\{1 - \frac{L}{cv}\right\} + e^{\frac{t_0}{c}} - 1\right)\right\}\right]. \quad (14)$$

The time of maximum discharge, t_c, may be found by differentiating equation (14) with respect to time, and setting this derivative equal to zero. The first derivative is easily found to be

$$\frac{dy}{dt} = arv^2\left[t_0 - t + c\left\{1 - e^{-\frac{t}{c}}\left(e^{\frac{L}{cv}}\left\{1 - \frac{L}{cv}\right\} + e^{\frac{t_0}{c}} - 1\right)\right\}\right],$$

and on setting this equal to zero we replace t by t_c and obtain

$$t_0 - t_c + c\left\{1 - e^{-\frac{t_0}{c}}\left(e^{\frac{L}{cv}}\left\{1 - \frac{L}{cv}\right\} + e^{\frac{t_0}{c}} - 1\right)\right\} = 0;$$

if the terms be rearranged, we finally have the equation

$$\left(1 + \frac{t_0}{c}\right)e^{\frac{t_0}{c}} - \frac{t_c}{c}e^{\frac{t_0}{c}} = e^{\frac{L}{cv}}\left\{1 - \frac{L}{cv}\right\} + e^{\frac{t_c}{c}} - 1. \quad (15)$$

The time of the crest is the time, t_c, which satisfies equation (15). Equation (15) is of the form $Ae^t - \xi e^t = B$. Equations of this type cannot be solved explicitly in terms of elementary functions. Hence it is necessary to solve equation (15) by numerical methods, or by a nomogram.

Equation (14) was derived on the assumption that $t_0 > L/v$. Suppose $t_0 < L/v$. Then it follows, by reasoning similar to that given in the first paper in the development of equation (9), that the discharge is given by

$$y = \int_{x_0}^{tv} ar\left(1 - e^{-\frac{1}{c}\left(t - \frac{x}{v}\right)}\right)dx + \int_{0}^{x_0} ar\left(1 - e^{-\frac{t_0}{c}}\right)e^{-\frac{1}{c}\left(t - t_0 - \frac{x}{v}\right)}x\,dx.$$

On performing the integration, substituting the indicated limits and simplifying, we obtain

$$y = arv^2\left[tt_0 - \frac{t_0^2}{2} - c^2\left\{\frac{t_0}{c} - e^{-\frac{t}{c}}\left(e^{\frac{t_0}{c}} - 1\right)\right\}\right]. \quad (16)$$

Equation (16) holds on the range $t_0 \leqq t \leqq L/v$. It can be shown that equation (16) does not have a maximum on the range for which it holds. Hence equation (14) always has a maximum regardless of whether $t_0 \leqq L/v$.

Suppose now that the gaging station is at the point A rather than at the point 0 in figure 8, i. e., suppose the river flows to the right instead of to the left. In other words, consider the case where the width of the drainage area decreases with increasing distance above the gaging station, rather than increases with increasing distance as formerly. Then w is not given by $(W/L)x$, but by the equation $w = W - (W/L)x = W - ax$. Suppose $t_0 > L/v$; then on the range $t_0 \leqq t \leqq t_0 + L/v$ the discharge is given by

$$y = \int_{x_0}^{L} (W - ax)r\left[1 - e^{-\frac{1}{c}\left(t - \frac{x}{v}\right)}\right]dx + \int_{0}^{x_0} (W - ax)r\left(1 - e^{-\frac{t_0}{c}}\right)e^{-\frac{1}{c}\left(t - t_0 - \frac{x}{v}\right)}dx;$$

and on performing the indicated operations and simplifying, we get

$$y = r\left[WL - Wv(t - t_0) + Wcve^{-t/c}\left\{e^{t/c} + 1 - e^{\frac{L}{cv}} - e^{\frac{t_0}{c}}\right\} - \frac{aL^2}{2} + \frac{av^2(t-t_0)^2}{2} - ac^2v^2\left\{\frac{1}{c}(t - t_0) - 1 + e^{-t/c}\left(e^{\frac{L}{cv}}\left\{1 - \frac{L}{cv}\right\} + e^{\frac{t_0}{c}} - 1\right)\right\}\right]. \quad (17)$$

The time of the maximum discharge for equation (17) can be found in the usual manner.

If $t_0 < L/v$, then on the range $t_0 \leqq t \leqq L/v$ the discharge is given by

$$y = \int_{x_0}^{tv} (W - ax)r\left[1 - e^{-\frac{1}{c}\left(t - \frac{x}{v}\right)}\right]dx + \int_{0}^{x_0} (W - ax)r\left(1 - e^{-\frac{t_0}{c}}\right)e^{-\frac{1}{c}\left(t - t_0 - \frac{x}{v}\right)}dx.$$

On carrying out the indicated operations we get

$$y = Wrv\left[t_0 + c\left\{e^{-\frac{t}{c}} - e^{-\frac{1}{c}(t - t_0)}\right\}\right] - arv^2\left[tt_0 - \frac{t_0^2}{2} - c^2\left\{\frac{t_0}{c} - e^{-\frac{t}{c}}\left(e^{\frac{t_0}{c}} - 1\right)\right\}\right]. \quad (18)$$

If we differentiate equation (18) with respect to time, t, and set the derivative equal to zero and solve the resulting equation for t_c we find that equation (18) has a maximum when

$$t_c = c\log\left[\left(e^{\frac{t_0}{c}} - 1\right)\left(\frac{W}{avt_0} + \frac{c}{t_0}\right)\right]. \quad (19)$$

Equations (9), (16), and (18) all hold on the range $t_0 \leqq t \leqq L/v$, but apply to differently shaped drainage areas. It should be noted that while equations (9) and (16) have no maxima on this range, equation (18) does. The important fact which equations (18) and (19) establish is that the crest, or maximum discharge, *may* occur in some drainage areas *before* any water from the upper part of the drainage area has reached the gage. This feature will be discussed further in section 4 of this paper.

The first derivative of equation (16) is easily found to be $dy/dt = arv^2\left[t_0 - ce^{-t/c}\left(e^{\frac{t_0}{c}} - 1\right)\right]$, and the second derivative is $d^2y/dt^2 = arv^2\left[e^{-t/c}\left(e^{\frac{t_0}{c}} - 1\right)\right]$. Suppose we equate the first derivative to zero, and call the particular value of t which satisfies the equation t_c; we can solve this equation for t_c; thus

$$t_c = c\log\frac{c}{t_0}\left(e^{\frac{t_0}{c}} - 1\right). \quad (20)$$

If we substitute this value of t_c in the second derivative, we get $d^2y/dt^2=arv^2c/t_0$, which is a positive quantity, hence equation (2) gives the value of a *minimum* for equation (16). Now from the physical nature of the problem, we should not expect equation (16) to have a proper minimum on the range for which it applies, viz., $t_0 \leqq t \leqq L/v$. It will now be shown that the value of t_c given by equation (20) is less than t_0. Write equation (2) in the form $\frac{t_0}{c}e^{\frac{t_c}{c}}=\left(e^{\frac{t_0}{c}}-1\right)$, and for brevity put $\frac{t_c}{c}=\eta$ and $\frac{t_c}{c}=\zeta$; then we get $e^{\zeta}=\frac{1}{\eta}(e^{\eta}-1)$. Now expand the exponentials in a series, thus:

$$1+\zeta+\zeta^2/2!+\zeta^3/3!+\zeta^4/4!+\ \ldots\ .=$$

$$\frac{1}{\eta}\left(\eta+\frac{\eta^2}{2!}+\eta^3/3!+\eta^4/4!+\eta^5/5!+\ \ldots\ .\right)$$

$$=1+\eta/2!+\eta^2/3!+\eta^3/4!+\ \ldots\ .$$

If $\zeta \geqq \eta$, then each term of the second series, $\eta^n/(n+1).'$ is *less* than the corresponding term, $\zeta^n/n.'$ of the first, hence in order that the equality may be satisfied, $\zeta<\eta$, i. e., $t_c<t_0$; and equation (16) has no minimum on the range for which it applies.

In the case of the rectangle it is always possible to find the time of the crest, t_c, explicitly. In the case of the triangle, the time of the crest can be expressed explicitly in some instances but not in all; thus the derivatives of equations (16) and (18) can be solved explicitly for t_c, while those of equations (14) and (17) cannot. We shall now consider drainage areas where in no case is it possible to express the time of the crest explicitly.

SECTION 3: THE DISCHARGE FROM AN ELLIPSE

Consider now the case when the histogram may be fitted by a semiellipse; if L be the length of the histogram and W the extreme height of the histogram, then the equation is $(w/W)^2+(2x/L-1)^2=1$. (See figure 9.) It follows readily that the width of the drainage area at distance x from the gaging station, with the origin at the latter, is given by the equation $w=W\sqrt{1-(2x/L-1)^2}$. Instead of obtaining at once the equation on whose range the crest occurs, as was done in section 2, consider the range $L/v \leqq t \leqq t_0$; this was the range for equation (4) in the first paper. On this range the discharge is given by the integral:

$$y=\int_0^L Wr\sqrt{1-(2x/L-1)^2}\left[1-e^{-\frac{1}{c}\left(t-\frac{x}{v}\right)}\right]dx.$$

As this integral cannot be evaluated in terms of elementary functions, each step in performing the above integration will be given in detail. First dividing by Wr, and then multiplying the expressions under the integral sign, we get:

$$y/Wr=\int_0^L \sqrt{1-(2x/L-1)^2}dx$$

$$-\int_0^L \sqrt{1-(2x/L-1)^2}e^{-\frac{1}{c}\left(t-\frac{x}{v}\right)}dx.$$

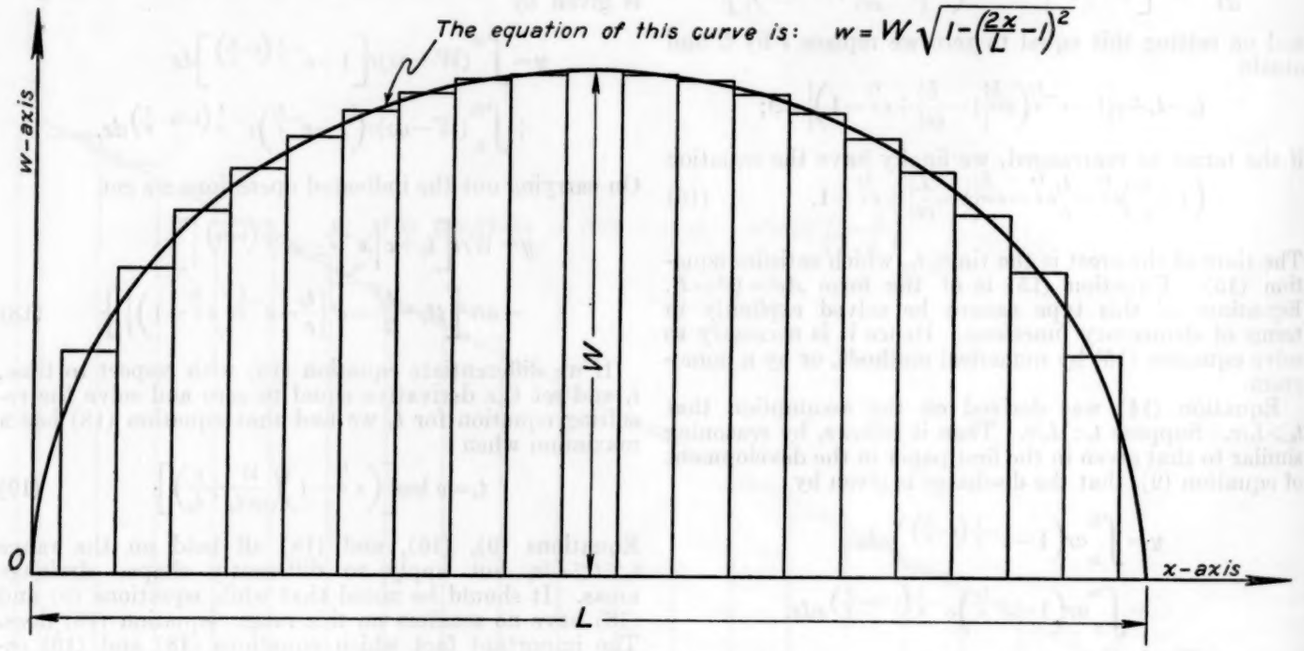

FIGURE 9.

The first integral in this last equation can be evaluated in terms of elementary functions, and is readily found to be

$$\frac{L}{2}\ \frac{1}{2}\Big[(2x/L-1)\sqrt{1-(2x/L-1)^2}$$

$$+\text{arc sin}\ (2x/L-1)\Big]_0^L=\frac{\pi L}{4}.$$

The second integral can be written in the form:

$$e^{-\frac{t}{c}}\int_0^L \sqrt{1-(2x/L-1)^2}e^{\frac{x}{cv}}dx.$$

Now replace x by $\frac{1}{2}L\theta+\frac{1}{2}L$; then when $x=0$, $\theta=-1$,

and when $x=L$, $\theta=1$; also $dx=(L/2)\,d\theta$. Making these substitutions, we have

$$\begin{aligned}
&e^{-\frac{t}{c}}\int_{-1}^{+1}\sqrt{1-\theta^2}\,e^{\frac{L}{2cv}(\theta+1)}\,(L/2)d\theta\\
&=\frac{1}{2}Le^{-\frac{1}{c}\left(t-\frac{L}{2v}\right)}\int_{-1}^{+1}\sqrt{1-\theta^2}\,e^{L\theta/2cv}\,d\theta\\
&=\frac{1}{2}Le^{-\frac{1}{c}\left(t-\frac{L}{2v}\right)}\int_{-1}^{+1}\sqrt{1-\theta^2}\,e^{\frac{L}{2cv}\theta}\,d\theta\\
&=\frac{1}{2}Le^{-\frac{1}{c}(t-L/2v)}\left(\frac{\pi}{L/2cv}\right)I_1(L/2cv)\\
&=\pi cve^{-\frac{1}{c}(t-L/2v)}\,I_1(L/2cv),
\end{aligned}$$

where $I_1(L/2cv)$ is the *modified Bessel Function of the first kind of order one* with argument $L/2cv$. The discharge from the semiellipse on the range $L/v\leqq t\leqq t_0$ is therefore given by

$$y=\frac{1}{4}WLr\pi-Wrcv\pi e^{-\frac{1}{c}(t-L/2v)}\,I_1(L/2cv). \qquad (21)$$

Next consider the range $0\leqq t\leqq L/v$, where also $t\leqq t_0$; here the discharge is given by the integral:

$$y=\int_0^{tv}Wr\sqrt{1-(2x/L-1)^2}\left[1-e^{-\frac{1}{c}\left(t-\frac{x}{v}\right)}\right]dx.$$

In trying to evaluate this integral we divide the equation by Wr and multiply the expressions under the integral sign and get

$$\begin{aligned}
y/Wr=&\int_0^{tv}\sqrt{1-(2x/L-1)^2}\,dx\\
&-\int_0^{tv}\sqrt{1-(2x/L-1)^2}\,e^{-\frac{1}{c}\left(t-\frac{x}{v}\right)}\,dx.
\end{aligned}$$

By evaluating the first integral, and making the substitution $x=(L/2)\,(\theta+1)$ in the second, we have

$$\begin{aligned}
\frac{Y}{Wr}=&\frac{L}{2}\cdot\frac{1}{2}\Big[(2x/L-1)\sqrt{1-(2x/L-1)^2}+\arcsin(2x/L-1)\Big]_0^{tv}\\
&-e^{-\frac{t}{c}}\int_{-1}^{2tv/L-1}\sqrt{1-\theta^2}\,e^{\frac{L(\theta+1)}{2cv}}\,(L/2)d\theta.
\end{aligned}$$

On further simplification, we find that on the range under consideration the discharge is given by

$$\begin{aligned}
y=&WLr\pi/8+\tfrac{1}{4}WLr\{(2t/L-1)\sqrt{1-(2tv/L-1)^2}\\
&+\arcsin\,(2tv/L-1\}\\
&-\frac{1}{2}WLre^{-\frac{1}{c}\left(t-t_0-L/2v\right)}\int_{-1}^{2tv/L-1}\sqrt{1-\theta^2}\,e^{\frac{L\theta}{2cv}}\,d\theta. \qquad (22)
\end{aligned}$$

The integral occurring in equation (22) cannot be evaluated explicitly in terms of any mathematical functions now known. It is necessary to use numerical methods to evaluate it.

Consider now the range $t_0+L/v\leqq t\leqq\infty$. It follows, by reasoning similar to that used in deriving equation (5) in the first paper, that on this range the discharge from a semiellipse is given by

$$y=\int_0^L Wr\sqrt{1-(2x/L-1)^2}\,e^{-\frac{1}{c}\left(t-t_0-\frac{x}{v}\right)}\,dx,$$

and clearly this equation can be written in the form

$$y/Wr=e^{-\frac{1}{c}\left(t-t_0\right)}\int_0^L\sqrt{1-(2x/L-1)^2}\,e^{\frac{x}{cv}}\,dx.$$

On making the same substitutions used in deriving equation (21), we obtain

$$\begin{aligned}
y/Wr=&e^{-\frac{1}{c}\left(t-t_0\right)}\int_{-1}^{+1}\sqrt{1-\theta^2}\,e^{L(\theta+1)/2cv}\,(L/2)d\theta\\
=&\frac{1}{2}Le^{-\frac{1}{c}\left(t-t_0-L/2v\right)}\int_{-1}^{+1}\sqrt{1-\theta^2}\,e^{L\theta/2cv}\,d\theta\\
=&\pi cve^{\frac{1}{c}\left(t-t_0-L/cv\right)}\,I_1(L/2cv),
\end{aligned}$$

where $I_1\,(L/2cv)$ has the same meaning as in equation (21). On multiplying by Wr we finally obtain

$$y=Wrcv\pi e^{-\frac{1}{c}\left(t-t_0-L/2v\right)}\,I_1(L/2cv). \qquad (23)$$

To complete the treatment of the semiellipse where $t_0>L/v$, it remains to consider the range $t_0\leqq t\leqq t_0+L/v$. It is on this range that the crest occurs. It follows by reasoning similar to that used in deriving equation (6) that on this range the discharge from a semiellipse is given by

$$\begin{aligned}
y=&\int_{x_0}^L Wr\sqrt{1-(2x/L-1)^2}\left[1-e^{-\frac{1}{c}\left(t-\frac{x}{v}\right)}\right]dx\\
&+\int_0^{x_0}Wr\sqrt{1-(2x/L-1)^2}\left(1-e^{-\frac{t_0}{c}}\right)e^{-\frac{1}{c}\left(t-t_0-\frac{x}{v}\right)}\,dx.
\end{aligned}$$

On dividing by Wr and multiplying the expressions under the integral signs, we get

$$\begin{aligned}
y/Wr=&\int_{x_0}^L\sqrt{1-(2x/L-1)^2}\,dx-e^{-\frac{tc}{c}}\int_{x_0}^L\sqrt{1-(2x/L-1)^2}\,e^{\frac{x}{cv}}dx\\
&+e^{-\frac{1}{c}\left(t-t_0\right)}\int_0^{x_0}\sqrt{1-(2x/L-1)^2}\,e^{\frac{x}{cv}}dx\\
&-e^{-\frac{t}{c}}\int_0^{x_0}\sqrt{1-(2x/L-1)^2}\,e^{\frac{x}{cv}}dx.
\end{aligned}$$

The first integral in this last equation can be evaluated in terms of elementary functions; the second and fourth can be combined, using the limits 0 and L. On doing this and making the same substitution used in deriving equation (21), we finally obtain

$$\begin{aligned}
y/Wr=&\frac{1}{4}\Big[\pi-(2x_0/L-1)\sqrt{1-(2x_0/L-1)^2}\\
&-\arcsin\,(2x_0/L-1)\Big]\\
&-\pi cve^{-\frac{1}{c}\left(t-L/2v\right)}\,I_1(L/2cv)\\
&+\frac{1}{2}Le^{-\frac{1}{c}\left(t-t_0-L/2v\right)}\int_{-1}^{2x_0/L-1}\sqrt{1-\theta^2}\,e^{L\theta/2cv}\,d\theta.
\end{aligned}$$

On multiplying by Wr and recalling that $x_0=v(t-t_0)$, we now get

$$\begin{aligned}
y=&Wr\Big[\frac{1}{4}L[\pi-(2v\{t-t_0\}/L-1)\sqrt{1-(2v\{t-t_0\}/L-1)^2}\\
&-\arcsin\,(2v\{t-t_0\}/L-1)]-\pi cve^{-\frac{1}{c}\left(t-\frac{L}{2v}\right)}\,I_1(L/2cv)\\
&+\frac{1}{2}Le^{-\frac{1}{c}\left(t-t_0-L/2v\right)}\int_{-1}^{2v(t-t_0)/L-1}\sqrt{1-\theta^2}\,e^{L\theta/2cv}\,d\theta\Big]. \qquad (24)
\end{aligned}$$

Equation (22) expresses y as a function of t, but the function is not an elementary one; in fact it is not possible

to evaluate the integral in this equation in terms of any known mathematical functions. In no one of the four ranges which have been considered is it possible—except for the particular values $t=0$, $t=\infty$, and also as will be pointed out presently $t=t_c$—to express y as a function of t by means of the elementary functions. In the cases of equations (21) and (23), y involves the modified Bessel function of the first kind of order one, while equations (22) and (24) are still more complex and involve a different and unnamed function. This is readily seen when we observe that in the development of these four equations the integrand encountered is the same; and, while in deriving equations (21) and (23) the upper limit is fixed, for the other two equations the upper limit is variable. Now it is an interesting fact that, while in general y is not an elementary function of t on the range $t_0 \leqq t \leqq t_0+L/v$, for the particular value of t when the maximum discharge occurs y can be expressed in terms of elementary functions.

The maximum discharge, y_c, can be obtained from equation (24) as follows: Multiply both sides of equation (24) by $e^{t/c}$. Then differentiate both sides of the resulting equation with respect to t; recall here that the formula for differentiating under the integral sign is

$$\frac{d}{d\alpha}\int_a^b f(x,\alpha)dx=\int_a^b \frac{\partial f}{\partial \alpha}dx+f(b,\alpha)\frac{db}{d\alpha}-f(a,\alpha)\frac{da}{d\alpha}.$$

Then put $dy/dt=0$ and finally multiply by $ce^{-t/c}$. Then on collecting terms on the right, we have:

$$y_c=\tfrac{1}{4}WLr[\pi-(2v\{t_c-t_0\}/L-1)\sqrt{1-(2v\{t_c-t_0\}/L-1)^2} \\ -\text{arc sin }(2v\{t_c-t_0\}/L-1)]. \qquad (25)$$

No equations will be derived for the case when $t_0<\frac{L}{v}$. It is not likely that they would be of practical value; but if they should be desired, the reader should have no difficulty in obtaining them by using steps quite similar to those given above.

It will now be clear that the triangular and elliptically shaped drainage areas involve considerably more difficulties than the rectangular. For these reasons, and also because comparatively few watersheds would have a histogram whose shape is that of a simple geometric figure, no further equations will be given for geometric configurations. The difficulties mentioned in connection with the triangle and the ellipse should be kept in mind as one reads the remainder of this paper.

SECTION 4: THE DISCHARGE FROM ANY DRAINAGE AREA

In this section all of the formulas of both this article and the first article are summarized. This summary should be of much convenience to those who wish to apply the theory developed in this series of articles.

Instead of considering a drainage area whose histogram is of a special shape, as an ellipse or a triangle, or one to whose histogram a particular mathematical equation has been fitted, consider the more general case of a drainage area whose histogram may be represented by the function $w=W(x)$. When for $W(x)$ we substitute special functions we get special cases; thus, if $W(x)=W$, a constant, we have the case of a rectangle, if $W(x)=W-(W/L)x$, we have one of the triangular cases, and if $W(x)=W\sqrt{1-(2x/L-1)^2}$ we have the case of a semiellipse, all of which have already been discussed.

Let the greatest distance that water has to travel in order to reach the gage be L. Then the following mathematical restrictions will be placed on $W(x)$:

1. $W(x)$ shall be single-valued, except at points of discontinuity where it shall be two-valued;
2. $W(x)$ shall be everywhere finite (in other words, $W(x)$ is bounded);
3. $W(x)$ shall be everywhere positive, except possibly at $x=L$ where it may have the value zero;
4. $W(x)$ shall not have more than a finite number of discontinuities on a finite range.

Each of the above restrictions is justified by the physical nature of the problem. Thus a drainage area curve which is not single-valued, or is infinite, or is negative, would have no practical meaning. It may be thought that the last restriction is more general than is necessary practically, and that to say $W(x)$ shall be everywhere continuous would be sufficiently general. However, a mountain range, or a divide between two tributaries, within a drainage area, may cause a discontinuity in the drainage area curve. Thus, if a river has cut a gorge through a range of mountains, and if the tributaries downstream from the gorge and range are of such nature that the range itself corresponds to an equal water travel line, then there will be a discontinuity in the drainage area curve.

It follows, by reasoning similar to that used in deriving equation (3) in the first paper, that on the range $0 \leqq t \leqq L/v$ where $t \leqq t_0$ the discharge from a drainage area whose histogram is represented by $w=W(x)$ is given by

$$y=r\int_0^{tv} W(x)\left[1-e^{-\frac{1}{c}\left(t-\frac{x}{v}\right)}\right]dx \\ =r\left\{\int_0^{tv} W(x)dx-e^{-\frac{t}{c}}\int_0^{tv} W(x)e^{\frac{x}{cv}}dx\right\}. \qquad (B\text{-}3)$$

We may say that the generalized form of equation (3) is equation (B-3). When $t=0$ then $y=0$, and when $t=L/v$ equation (B-3) takes the form:

$$y=r\left\{\int_0^L W(x)dx-e^{-\frac{L}{cv}}\int_0^L W(x)e^{\frac{x}{cv}}dx\right\}, \qquad (B\text{-}3a)$$

which is the generalized form of equation (3a).

On the range $L/v \leqq t \leqq t_0$ the discharge is given by

$$y=r\int_0^L W(x)\left[1-e^{-\frac{1}{c}\left(t-\frac{x}{v}\right)}\right]dx \\ =r\left\{\int_0^L W(x)dx-e^{-\frac{t}{c}}\int_0^L W(x)e^{\frac{x}{cv}}dx\right\}, \qquad (B\text{-}4)$$

which is the generalized form of equation (4). Since $\int_0^L W(x)dx$ is the area of the drainage basin, and since as $t\to\infty$, $e^{-t/c}\to 0$, equation (B-4) shows that if the rain continues sufficiently long the discharge approaches the product $Ar\equiv r\int_0^L W(x)dx$, the area of the watershed times the rate of rainfall, as a limit. Equation (1) shows that if the rain continues sufficiently long, then the *volume of rate of run-off* also approaches Ar as a limit. However, the *volume of rate of run-off* approaches the limit Ar more quickly than does the *discharge*, because in equation (1) the coefficient of $e^{-t/c}$ is $\int_0^L W(x)dx=A$, while in equation (B-4) the coefficient of $e^{-t/c}$ is $\int_0^L W(x)e^{\frac{x}{cv}}dx$, and

$$\int_0^L W(x)e^{\frac{x}{cv}}dx > \int_0^L W(x)dx.$$

On the range $t_0+L/v \leqq t \leqq \infty$, the discharge is given by the generalized form of equation (5), viz,

$$y=r\int_0^L W(x)e^{-\frac{1}{c}\left(t'-x/v\right)}\left(1-e^{-t_0/c}\right)dx$$

$$=re^{-\frac{t}{c}}\left(e^{\frac{t_0}{c}}-1\right)\int_0^L W(x)e^{\frac{x}{cv}}dx. \qquad (B\text{-}5)$$

As $t\to\infty$, the discharge as given by equation (B-5) approaches the limit zero. Likewise equation (2) shows that as $t\to\infty$, then the volume of rate of run-off approaches zero as a limit. As in the case of equations (1) and (B-4), equation (2) approaches the limit 0 more quickly than equation (B-5), and for the same reason.

When $t=L/v$, equation (B–4) takes the form of equation (B–3a); and when $t=t_0$, equation (B–4) becomes

$$y=r\left\{\int_0^L W(x)dx-e^{-\frac{t_0}{c}}\int_0^L W(x)e^{\frac{x}{cv}}dx\right\}. \qquad (B\text{–}4a)$$

When $t=t_0+L/v$, equation (B–5) takes the form:

$$y=re^{-\frac{L}{cv}}\left(1-e^{-t_0/c}\right)\int_0^L W(x)e^{\frac{x}{cv}}dx. \qquad (B\text{–}5a)$$

Equations (B–4a) and (B–5a) are the generalized forms of equations (4a) and (5a).

On the range $t_0 \leqq t \leqq t_0+L/v$ where $t_0>L/v$, the discharge is given by [recall here that $v(t-t_0)=x_0$]

$$y=r\int_{x_0}^L W(x)\left[1-e^{-\frac{1}{c}\left(t-\frac{x}{v}\right)}\right]dx$$
$$+r\int_0^{x_0} W(x)e^{-\frac{1}{c}\left(t'-\frac{x}{v}\right)}\left(1-e^{-\frac{t_0}{c}}\right)dx.$$

On multiplying the expressions under the integral sign and dividing by r, we get

$$y/r=\int_{x_0}^L W(x)dx-e^{-t/c}\int_{x_0}^L W(x)e^{\frac{x}{cv}}dx-e^{-t/c}\int_0^{x_0} W(x)e^{\frac{x}{cv}}dx$$
$$+e^{-\frac{1}{c}(t-t_0)}\int_0^{x_0} W(x)e^{\frac{x}{cv}}dx.$$

In this last equation the second and third integrals can be combined, using the limits 0 and L, whence we finally obtain

$$y=r\left\{\int_{x_0}^L W(x)dx-e^{-\frac{t}{c}}\int_0^L W(x)e^{\frac{x}{cv}}dx\right.$$
$$\left.+e^{-\frac{1}{c}(t-t_0)}\int_0^{x_0} W(x)e^{\frac{x}{cv}}dx\right\}. \qquad (B\text{–}6)$$

When $t=t_0$ then equation (B–6) reduces to equation (B–4a); and when $t=t_0+L/v$, equation (B–6) becomes equation (B–5a).

By applying the rule for differentiating under the integral sign, we find the derivative of equation (B–6) to be

$$dy/dt=r\left\{-vW(tv-t_0v)+\frac{1}{c}e^{-\frac{t}{c}}\int_0^L W(x)e^{\frac{x}{cv}}dx\right.$$
$$\left.-\frac{1}{c}e^{-\frac{1}{c}(t-t_0)}\int_0^{tv-t_0v} W(x)e^{\frac{x}{cv}}dx+ve^{-\frac{1}{c}(t-t_0)}W(tv-t_0v)e^{\frac{1}{c}(t-t_0)}\right\}.$$

Clearly the first and last terms on the right cancel, whence the above simplifies to

$$\frac{dy}{dt}=\frac{r}{c}e^{-\frac{t}{c}}\left\{\int_0^L W(x)e^{\frac{x}{cv}}dx-e^{\frac{t_0}{c}}\int_0^{tv-t_0v} W(x)e^{\frac{x}{cv}}dx\right\}.$$

Then on equating dy/dt to zero, we get

$$e^{\frac{t_0}{c}}\int_0^{t_ev-t_0v} W(x)e^{\frac{x}{cv}}dx=\int_0^L W(x)e^{\frac{x}{cv}}dx. \qquad (B\text{–}7)$$

Equation (B–7) is not a generalized form of equation (7); but the time of the crest, t_e, is given by the solution of equation (B–7).

The maximum discharge can be obtained by multiplying both sides of equation (B–6) by $e^{t/c}$, differentiating the resulting equation with respect to t, putting $dy/dt=0$, and finally solving for y_e by multiplying by $\frac{1}{c}e^{-t/c}$. On carrying out these steps we get

$$y_e=r\int_{v(t_e-t_0)}^L W(x)dx, \qquad (B\text{–}8)$$

which is the generalized form of equation (8). It should be noted that in the first paper equation (8) could have been derived from equation (6) by the procedure here suggested, instead of the more straightforward method used there; and moreover that equation (8) can be written in the form:

$$y_e=Wr\int_{v(t_e-t_0)}^L dx.$$

Equation (B–8) is an exceptionally neat way in which to express the maximum discharge, and further comments will be made on it later.

Equations (B–6), (B–7), and (B–8) were derived on the assumption that $t_0>L/v$. If $t_0<L/v$, then the discharge on the range $t_0 \leqq t \leqq L/v$ is given by

$$y=r\left\{\int_{x_0}^{tv} W(x)dx-e^{-\frac{t}{c}}\int_0^{tv} W(x)e^{\frac{x}{cv}}dx\right.$$
$$\left.+e^{-\frac{1}{c}\left(t-t_0\right)}\int_0^{x_0} W(x)e^{\frac{x}{cv}}dx\right\}. \qquad (B\text{–}9)$$

When $t=t_0$, equation (B–9) takes the form

$$y=r\left\{\int_0^{tv} W(x)dx-e^{-\frac{t_0}{c}}\int_0^{tv} W(x)e^{\frac{x}{cv}}dx\right\}; \qquad (B\text{–}9a)$$

and when $t=L/v$, equation (B–9) takes the form

$$y=r\left\{\int_{L-t_0v}^L W(x)dx-e^{-\frac{L}{cv}}\int_0^L W(x)e^{\frac{x}{cv}}dx\right.$$
$$\left.+e^{-\frac{1}{c}\left(L/v-t_0\right)}\int_0^{L-t_0v} W(x)e^{\frac{x}{cv}}dx.\right. \qquad (B\text{–}9n)$$

It should be noted that when $t=t_0$, equation (B–3) reduces to (B–9a); and when $t=L/v$, equation (B–6) reduces to (B–9b). Equations (B–9), (B–9a), and (B–9b) are the generalized forms of equations (9), (9a), and (9b), respectively.

It can be shown that the first derivative of equation (B–9) with respect to t can be written in the form

$$dy/dt=\frac{r}{c}e^{-t/c}\left\{\int_0^{tv} W(x)e^{\frac{x}{cv}}dx-e^{\frac{t_0}{c}}\int_0^{v(t-t_e)} W(x)e^{\frac{x}{cv}}dx\right\};$$

and the second derivative of equation (B–9) with respect to time can be written

$$\frac{d^2y}{dt^2}=-\frac{1}{c}\frac{dy}{dt}+\frac{rv}{c}\left\{W(tv)-W(tv-t_0v)\right\}.$$

If we set the first derivative just obtained equal to zero, we get the equation

$$e^{\frac{t_e}{c}}\int_0^{v(t_e-t_0)} W(x)e^{\frac{x}{cv}}dx=\int_0^{t_ev} W(x)e^{\frac{x}{cv}}dx. \qquad \text{(B–7a)}$$

By multiplying both sides of equation (B–9) by $e^{t/c}$ differentiating the resulting equation with respect to t, putting $dy/dt=0$, and lastly solving for y_c by multiplying by $\frac{1}{c}e^{-t-c}$, we get

$$y_c=r\int_{v(t_c-t_0)}^{t_cv} W(x)dx. \qquad \text{(B–8a)}$$

It follows from the conditions for a maximum that are given by the elementary calculus, and from the form of the second derivative of equation (B–9) above, that equation (B–8a) gives the maximum discharge when the solution of equation (B–7a) for t_c gives at least one value such that $t_0<t_c<L/v$, and when $W(t_cv)<W(t_cv-t_0v)$ for the value of t_c in question. If the width of the histogram of the drainage area increases with increasing distance from the gaging station, i. e., if $W(x)$ increases as x increases, even if in this case $W(x)$ is discontinuous, then $W(t_cv)>W(t_cv-t_0v)$ for all admissible values of t_c, and therefore equation (B–8a) cannot furnish the maximum discharge. If the width does not everywhere increase with increasing distance from the gage, the equation (B–8a) may furnish the maximum discharge.

A method of showing that the equations (B–3), (B–4), (B–6) and (B–5) are correct is to integrate them with respect to t between the limits for which they apply, and ascertain that the sum of the four integrals thus obtained is equal to the volume of rainfall which falls during the rain-causing freshet. This process was carried out in the first paper for the special case there discussed. In the same way it can be shown that the volume of discharge for the general case is $rt_0\int_0^L W(x)dx$, which is also the volume of rainfall.

Concerning equations (B–6) and (B–7) we can draw the following conclusions: If we evaluate $(dy/dt)_{t=t_0}$ for equation (B–6), we get $(r/c)e^{-t_0/c}\int_0^L W(x)e^{\frac{x}{cv}}dx$. Clearly this quantity is positive. If we evaluate $(dy/dt)_{t=0}+L/v$ for equation (B–6), we get $-(r/c)e^{-\frac{L}{cv}}(1-e^{-t_0/c})\int_0^L W(x)e^{x/cv}dx$. Clearly this quantity is negative. Now dy/dt is continuous for all values of t, even though $W(x)$ be discontinuous. Therefore, it follows that equation (B–7) has at least one real root t_c on the range $t_0\leqq t_c\leqq t_0+L/v$. Moreover equation (B–7) has only one real root on this range. For even if $W(x)$ be discontinuous, the left-hand member of equation (B–7) exists and is an increasing function of t_c. Since the left-hand member is an increasing function of t_c, it will equal the right-hand member at but one point. This root of equation (B–7) corresponds to a maximum and not a minimum. For the second derivative of equation (B–6) is

$$\frac{d^2y}{dt^2}=(r/c)\Big\{-\frac{1}{c}e^{-\frac{t}{c}}\int_0^L W(x)e^{\frac{x}{cv}}dx+$$

$$\frac{1}{c}e^{-\frac{1}{c}(t-t_0)}\int_0^{(vt-t_0)} W(x)e^{\frac{x}{cv}}dx-vW(tv-t_0v)\Big\}.$$

Since the first two terms vanish when $dy/dt=0$, and since $W(x)$ is not less than zero, it must follow that $d^2y/dt^2<0$ when $dy/dt=0$, and we have the necessary conditions for a maximum fulfilled. Thus the unique solution of equation (B–7) is the time of the crest. We have now proved that equation (B–6) has one and only one maximum point. By similar reasoning it can be shown that on the range $t_0\leqq t\leqq t_0+L/v$ where $t_0>L/v$, the discharge curve has no point of inflection at which the change in discharge with respect to time is zero.

We now turn to a similar discussion of equation (B–9) and its derivative. The first derivative of this equation evaluated at $t=t_0$ is $\frac{r}{c}e^{-\frac{t_0}{c}}\int_0^{t_0v} W(x)e^{\frac{x}{cv}}dx$. Clearly this quantity is positive. Moreover dy/dt is everywhere continuous. Now the first derivative evaluated at the point $t=L/v$ is

$$\frac{r}{c}e^{-\frac{L}{cv}}\Big\{\int_0^L W(x)e^{\frac{x}{cv}}dx-e^{\frac{t_0}{c}}\int_0^{L-t_0v} W(x)e^{\frac{x}{cv}}dx\Big\}.$$

Clearly this quantity is positive or negative according as the first term in the bracket is greater or less than the second term. If $(dy/dt)_{t=L/v}$ is negative, then dy/dt, being continuous, will have an odd number of real roots. If $(dy/dt)_{t=L/v}$ is positive, then dy/dt will have either no real root or an even number of real roots.

Consider now the range $L/v\leqq t\leqq t_0+L/v$ where $t_0<L/v$. On this range the discharge is given by an equation of the *same literal form* as equation (B–6); but as equation (B–6) was derived on the assumption that $t_0>L/v$, we shall, for the sake of definiteness, call the equation of discharge on this range where $t_0<L/v$ equation (B–6a). Recall here that when $t=L/v$, equation (B–6) and hence also equation (B–6a) reduce to equation (B–9b). Now if $(dy/dt)_{t=L/v}$ is negative then equation (2–6a) will not have a maximum. For its derivative is everywhere continuous, and as $e^{t_0/c}\int_0^{v(t-t_0)} W(x)e^{x/cv}dx$ is an increasing function of t, and all other quantities in the derivative of equation (B–6a) are positive, it follows that once this derivative becomes negative it remains negative. Furthermore, if $(dy/dt)_{t=L/v}$ is positive, then by the same reasoning as that used for equation (B–6) it follows that equation (B–6a) will have one and only one maximum point.

We now want two tests: (1) one to show whether $(dy/dt)_{t=L/v}\gtrless 0$; and (2) the other, to be used when $(dy/dt)_{t=L/v}>0$, to show whether the first derivative of equation (B–9) will have no root or an even number of roots.

Test (1) is easily devised, thus: Solve equation (B–7) for t_c. If $t_cv\geqq L$, then $(dy/dt)_{t=L/v}\geqq 0$, and equation (B–6a) furnishes a maximum. The convenient thing about this test is that the test itself furnishes the time of the maximum discharge, provided of course $(dy/dt)_{t=L/v}\geqq 0$ and not <0. If $t_cv<L$, then equation (B–6a) will not have a maximum.

It appears impracticable to devise a convenient test for (2) to use on the general case of $W(x)$. However, a few special cases of $W(x)$ will be discussed:

Case I: Suppose that in addition to the conditions stated at the beginning of this section, $W(x)$ is such that at discontinuities $W(x-0)>W(x+0)$ and that $(d/dx)W(x)$ is never positive. In this case equation (B–9) may have a maximum, but it can never have more than one maximum. For since both equation (B–9) and

its first derivative are continuous, then in order for it to have two maxima it must have one minimum. Now in this case d^2y/dt^2 satisfies the conditions for a maximum point everywhere, but at no point are the conditions for a minimum point satisfied.

Case II: Suppose that in addition to satisfying the conditions first stated, $W(x)$ also satisfies the following conditions: to the *left* of a certain point, say $x=a_1$, $W(x)$ is such that at discontinuities $W(x-0)<W(x+0)$, and $(d/dx)W(x)$ is never negative; while to the *right* of this point $W(x)$ is such that at discontinuities $W(x-0)>W(x+0)$, and $(d/dx)W(x)$ is never positive. Then in this case equation (B–9) may have a maximum, but it can never have more than one maximum. For it cannot have a maximum such that vt_c lies to the left of $x=a_1$; and to the right of a_1, the reasoning in the first case holds.

Case III: Suppose that in addition to the conditions first stated $W(x)$ contains a point, say $x=b$, to the left of which $W(x)$ satisfies the conditions of case II (the point a_1 may of course be the point $x=0$), and to the right of which $W(x)$ also satisfies the conditions of case II (the greatest value of $W(x)$ to the right of b being at the point $x=a_2$), and such that the point $(b-0)$ furnishes a minimum on the range $a_1<x<b$ while the point $(b+0)$ furnishes a minimum on the range $b<x<a_2$. In this case equation (B–9) may have two maxima. For suppose equation (B–7a) yields three roots for t_c; then call these three roots t_{c1}, t_{c2}, and t_{c3}. Now, if $a_1<t_{c1}v<a_2$ and $W(t_{c1}v)<W(t_{c1}v-t_0v)$, we have a maximum. If $b<t_{c2}v<L$ and $W(t_{c2})>W(t_{c3}v-t_0v)$, we haye a minimum. Lastly, if $a_2<t_{c3}v<L$ and $W(t_{c2}v)>W(t_{c2}v-t_0v)$, we again have a maximum. In this case, if $t_0v>a_2$ then equation (B–9) can furnish but one maximum point.

When the drainage area is of such shape that a steady rain may cause two or more crests it will always be necessary to apply both test (1) and test (2). For if $(dy/dt)_{t=L/v}>0$, we have to determine whether equation (B–7a) has no root or an even number of roots; while if test (1) shows the inequality sign reversed, we know equation (B–7a) has an odd number of roots but we have to determine how many roots it has.

The question naturally arises whether a watershed can be of such shape that a crest may occur before the rain stops. In other words, can equation (B–3) furnish a maximum? Now the first derivative of equation (B–3) can be written

$$(r/c)e^{-t/c}\int_0^{tv} W(x)e^{\frac{x}{cv}}dx.$$

Clearly this expression never vanishes, and therefore no drainage area can be of such shape that a crest will occur before the rain stops. It should be emphasized here that we are assuming the rate of rainfall to be constant.

Equation (B–8) has a physical interpretation. It shows that the maximum discharge from the entire drainage area is equal to the discharge from that portion of the drainage area lying between two equal water travel lines, corresponding to $x=L$ and $x=v(t_c-t_0)$, respectively, in a steady state. To explain this, put $t^*=t_c-t_0$. Now as $t_0\to\infty$, clearly t_c does also, because t_c is greater than t_0. However, as $t_0\to\infty$, then $t^*\to 0$; for if equation (B–7) be written in the form

$$\int_0^{t^*v} W(x)e^{\frac{x}{cv}}dx=e^{-t_0/c}\int_0^{L} W(x)e^{\frac{x}{cv}}dx,$$

then as $t_0\to\infty$ the right-hand side $\to 0$, and as this equation is true for all values of $t_0>0$ it therefore follows that the left-hand side $\to 0$ also; but in order for the left-hand side $t_0\to 0$, t^* must $\to 0$, as stated above. Moreover, t^* can have the value 0 for no other value of t_0.

Since $t^*\to 0$ as $t_0\to\infty$, it follows from equation (B–8) that $y_c\to r\int_0^L W(x)dx$ as $t_0\to\infty$. In other words, y_c approaches the same limit that y does in equation (B–4) as $t\to\infty$ in that equation. Thus the maximum discharge obtained from equation (B–8) cannot exceed the discharge at a steady state. Also we can see that as $t_0\to\infty$, the equal water travel line given by $x=t^*v$ approaches the gaging station as a limit.

The question arises as to how rapidly $y_c\to r\int_0^L W(x)dx$. Clearly from the above discussion, y_c approaches this limit as quickly as y in equation (B–4) approaches this same limit. The limit may be considered, practically, to have been reached when the second term inside the brackets of equation (B–4) is negligible compared to the first term. Now,

$$\int_0^L W(x)e^{\frac{x}{cv}}dx<\int_0^L W(x)e^{\frac{L}{cv}}dx,$$

whence y has approached the limit in question when $e^{-\frac{1}{c}(t+L/v)}$ is negligible compared to unity. Hence, if the rain lasts such a time that its duration, diminished by L/v, is 2.30------ times c, then the discharge has approached a value which is *more* than 0.9 of the steady state; if the duration less L/v is 4.60------ times c, the discharge has approached a value which is *more* than 0.99 of the steady state; if the duration less L/v is 6.90------ times c, the discharge has approached a value which is *more* than 0.999 of the steady state; and so on. The constant, 2.30------ is the natural logarithm of 10, i. e., the reciprocal of the modulus of common logarithms.

Having discussed the behavior of the maximum discharge for infinitely long rains, we now take up the maximum discharge for infinitely short rains, i. e., cloudbursts. If $t_0=0$, we write the fundamental equation thus: $cZ=AR-\int_0^t Zdt$; from this we develop the equation $Z=\frac{AR}{c}e^{-\frac{t}{c}}$. (Compare with the development of equation (2) in the first paper.) Then the discharge will be given by

$$y=(R/c)\int_0^{tv} W(x)e^{-\frac{1}{c}(t-x/v)}dx=(R/c)e^{-tc}\int_0^{tv} W(x)e^{\frac{x}{cv}}dx.$$

The first derivative of this equation is $-y/c+(Rv/c)W(tv)$, and the second derivative is $-(1/c)(dy/dt)+(Rv^2/c)W'(ty)$; hence if the equation is to furnish a proper maximum it is necessary that $W'(t_cv)$ be negative. Clearly $W'(x)$ may be positive for all values of x; in such a case the point of maximum discharge is a cusp on the discharge curve. This cusp will be at the point $t=L/v$, and in this case the discharge curve does not have a proper maximum. If $W'(x)$ be negative when dy/dt vanishes, then the time of the crest will be given by the solution of the following equation for t_c:

$$cvW(t_cv)=e^{-\frac{t_c}{c}}\int_0^{t_cv} W(x)e^{\frac{x}{cv}}dx.$$

The maximum discharge for infinitely short rains can be found by substituting R/t_0 for r in equation (B–8a)

and then finding the value of the right-hand side as $t_0 \to 0$ by the rule for evaluating indeterminate forms. Thus

$$\underset{t_0 \to 0}{\text{Limit}}\, y_c = \underset{t_0 \to 0}{\text{Limit}} R\left[v\frac{dt_c}{dt_0}W(t_c v) - v\left(\frac{dt_c}{dt_0}-1\right)W(t_c v - t_0 v)\right] = RvW(t_c v).$$

In words, the maximum discharge due to an infinitely short rain is equal to the product of the depth of the rain times the velocity of the water in the stream times the width of the drainage area corresponding to the point $x=t_c v$. Clearly, the width of the drainage area which enters in this product will vary with the capacity of the soil, but we can readily conclude that the maximum discharge from cloudbursts cannot exceed the product of the rainfall times the velocity of the stream times the maximum width of the drainage area. If the drainage area be of such character that equation (B–8a) cannot furnish the maximum discharge, then for infinitely short rains

$$y_c = (R/c)e^{-\frac{L}{cv}}\int_0^L W(x)e^{\frac{x}{cv}}dx.$$

This section will be concluded with a few remarks about the continuity of the rate of discharge and the discharge tendency curves. If equations (B–3), (B–4), (B–5), (B–6) and (B–9) be differentiated with respect to t, then the rate of discharge curve is obtained. If we substitute the various limits of the ranges of these equations in their first derivatives, it will be noted that the rate of discharge curve is continuous at these points. By differentiating the rate of discharge curve with respect to time, we obtain the discharge tendency curve. It can be shown that the discharge tendency curve, when $t_0 > L/v$, is continuous at the point $t=L/v$ if $W(L)$ is zero; otherwise, it is continuous there. At the point $t=t_0$ it would be continuous were $W(O)=0$, but this has been excluded from the physical conditions of the problem, hence the discharge tendency curve is discontinuous at $t=t_0$. At the point $t=t_0+L/v$ it is continuous only if $W(L)$ is zero. It can also be shown that the above statements hold when $t_0 < L/v$. In addition to the above discontinuities, the discharge tendency curve will have other discontinuities if the drainage area curve be discontinuous. Thus that portion of the discharge tendency curve corresponding to equation (B–3) will have the same number of discontinuities as the drainage area curve. However, discontinuities in the drainage area curve will not cause any discontinuities in the rate of discharge curve; hence the rate of discharge curve is everywhere continuous.

SECTION 5: DRAINAGE AREA CURVES

We now turn to some practical considerations connected with the application of the theory in the last section. Suppose we have topographic maps of a drainage area and have carefully constructed a histogram from them and that it is then desired to fit a curve to this histogram. The question arises: What form of curve should be used? Or in other words, what function should be used for $W(x)$?

From the necessity of having equations (B–7) and (B–8) in tractable forms it is essential that both $W(x)$ and $W(x)e^{\frac{x}{cv}}$ be integrable in terms of functions for which tables now exist, preferably elementary functions. The elliptically shaped histogram discussed in section 3 is an illustration of a case in which $W(x)$ is integrable; but $W(x)e^{x/cv}$ is not integrable in terms of tabulated functions.

A number of functions suggest themselves for $W(x)$. We can use a trigonometric series (Harmonic Analysis), a polynomial, an exponential series, or a Gram-Charlier series. All of these satisfy the condition of tractable integrability, but each of them has the same defect which the case of the triangle brought out. In the case of the triangle (as well as these four series) equation (B–7) is transcendental. Of course one can solve a transcendental equation by numerical methods, and no doubt in some applications this will be the best way.

We can make equation (B–7) a polynomial by fitting a curve of the form

$$W(x) = (a_c + a_1 x + a_2 x^2 + a_3 x^3 + \cdots + a_n x^n)e^{-\frac{x}{cv}}$$

to the histogram of the drainage area. As c is not a function of time during any one flood, but does vary from flood to flood, it is necessary to fit a different curve to the histogram for each flood. At first this procedure appears to be very tedious; but consider the following suggestions:

Suppose we fit the curve

$$W(x) = (a_c + a_1 x + a_2 x^2 + a_3 x^3 + \cdots + a_n x^n)e^{-\frac{x}{c_0 v_0}}$$

to the histogram, where $c_0 v_0$ is the arithmetic mean value of all the cv that are ever to be expected in the river basin in question. This will be done once, and will apply to all future floods. In this way the constants $c_0 v_0$ are assumed, so to speak, and then the a_i are determined from the histogram. Now when a particular flood occurs, we want to fit the curve

$$(a_0' + a_1' x + a_2' x^2 + a_3' x^3 + \cdots + a_n' x^n)e^{-\frac{x}{cv}}$$

to the histogram, where cv is now known from the conditions existing at the beginning of the rain. Since these two curves are to fit the same histogram we require that they be equal; equate, and multiply both sides of the equation thus obtained by $e^{x/cv}$:

$$(a_0 + a_1 x + a_2 x^2 + a_3 x^3 + \cdots + a_n x^n)e^{-(x/c_0 v_0 - x/cv)} = a_0' + a_1' x + a_2' x^2 + a_3' x^3 + \cdots + a_n' x^n$$

Now when $x/c_0 v_0 - x/cv$ is small, the power series which represents the function $e^{-(x/c_0 v_0 - x/cv)}$ is rapidly convergent; we assume this condition is fulfilled. Expand the exponential in the last equation in a power series, multiply together the two series on the left, and equate coefficients of like powers of x. On doing this we get the following system of equations:

$$\left.\begin{aligned}
a_0' &= a_0,\\
a_1' &= a_1 - (1/c_0 v_0 - 1/cv)a_0,\\
a_2' &= a_2 - (1/c_0 v_0 - 1/cv)a_1 + (1/c_0 v_0 - 1/cv)^2\frac{a_0}{2},\\
a_3' &= a_3 - (1/c_0 v_0 - 1/cv)a_2 + (1/c_0 v_0 - 1/cv)^2\frac{a_1}{2} - (1/c_0 v_0 - 1/cv)^3\frac{a_0}{3},\\
a_4' &= a_4 - (1/c_0 v_0 - 1/cv)a_3 + (1/c_0 v_0 - 1/cv)^2\frac{a_2}{2} - (1/c_0 v_0 - 1/cv)^3\frac{a_1}{3} + (1/c_0 v_0 - 1/cv)^4\frac{a_0}{4}, \text{ etc.}
\end{aligned}\right\} \text{I}$$

If $|\ x/c_0v_0-x/cv\ |$ is not sufficiently small to insure rapid convergence when the exponential is expanded in a power series, then, instead of fitting just one curve to the histogram, we can fit two or more curves to it. Thus, if two curves are fitted to the histogram, we divide the expected values of cv into two groups, one consisting of large values, the other small, and take the arithmetic mean value of each group. One mean is used in fitting one curve, and the other for the second curve. Then in a particular flood we use the curve for which $1/c_0v_0$ is the nearer to $1/cv$ in order to compute the a_i'.

After having obtained the a_i' from the a_i by means of equations (I), we next solve equation (B–7) for $v(t_c-t_0)$; this is now very quickly accomplished, because we can integrate the functions easily, and after the integration has been performed we can then readily solve the polynomial obtained. In following this method, equation (B–8) takes the form:

$$y_c=r\int_{t_cv-t_0v}^{L}\sum_{i=0}^{i=n}a_i'x^ie^{-\frac{x}{cv}}dx.$$

This expression is readily integrated in terms of elementary functions by the following substitution: Put $x/cv=\theta$, $dx=cvd\theta$; when $x=L$, $\theta=L/cv$; and when $x=v(t_c-t_0)$, $\theta=(1/c)(t_c-t_0)$; and we have

$$y_c=r\sum_{i=0}^{i=n}a_i'(cv)^{i+1}\int_{(1/c)(t_c-t_0)}^{L/cv}\theta^ie^{-\theta}d\theta.$$

If the histogram of the drainage area should have a discontinuity, it will be necessary to fit two different curves, each of the form

$$(a_0+a_1x+a_2x^2+a_3x^3+\text{.....}+a_nx^n)e^{-x/cv},$$

to the histogram, one to the left of the discontinuity and one to the right of it.

SECTION 6: ADDITIONAL DISCHARGE EQUATIONS

Thus far all of the discharge equations have been derived on the assumptions that while it is raining equation (1), viz:

$$Z=Ar(1-e^{-t/c}),$$

gives the volume of rate of run-off; and after the rain stops equation (2), viz.:

$$Z=Z_0e^{-\frac{1}{c}(t-t_0)},$$

gives the volume of rate of run-off. Clearly, when evaporation is considered, or the rate of rainfall is not constant, these equations are no longer true. Furthermore, these equations have been derived on the fundamental assumption that the rate of run-off at any given time is proportional to the rainfall remaining with the soil at that time. While it is believed that this assumption is a very close approximation to what occurs in Nature, it is evident that different underlying assumptions will lead to different forms of equations (1) and (2), even where evaporation is neglected and the rate of rainfall considered constant. A few remarks will now be made about the discharge equations which result when the run-off equations are made more general.

Suppose while the rain is falling the volume of rate of run-off is given by the function $Z=AZ_1(t)$, and after the rain stops the volume of rate of run-off is given by $Z=AZ_2(t)$. For the present no restrictions will be placed on the functions $Z_1(t)$ and $Z_2(t)$ except that they be single-valued, or at points of discontinuity two-valued. Functions which are not single-valued would have no physical meaning.

In the next three papers special forms, nevertheless forms of greater generality than equations (1) and (2), of the functions $Z_1(t)$ and $Z_2(t)$ will be discussed. A portion of each of the next three papers will be taken to show that in most cases the practical problem of predicting flood crests does not warrant the use of run-off equations which are more general than equations (1) and (2). In this section, however, we consider the discharge from a watershed when the general run-off equations are used.

If while it is raining $Z_1(t)$ gives the rate of run-off, and if v be the velocity of the flowing water, a constant, then the discharge from a watershed whose drainage area curve is $W(x)$ is given by the equation

$$y=\int_0^{tv}W(x)\Sigma_1(t-x/v)dx,$$

which holds on the range $0\leqq t\leqq L/v$ and where $t_0\leqq L/v$. This equation is a generalization of equation (B–3).

Similarly, after the rain stops, if $Z_2(t)$ gives the rate of run-off, and v the velocity of the water, the discharge from the watershed is given by the equation

$$y=\int_0^{L}W(x)\Sigma_2(t-x/v)dx,$$

which holds on the range $t_0+L/v\leqq t\leqq\infty$. This is a generalization of equation (B–5).

Analogous equations can be written for the remaining ranges of t. The point to be emphasized is that the method of Section 4 is perfectly general, and involves the underlying relation between discharge and the rate of run-off. The rate of run-off is measured in inches per hour, and the discharge is measured in mile-inches per hour. The last two equations are merely symbolic forms of the following statement in words: The discharge from a drainage area at time t is the sum of the volumes of rate of run-off from all the infinitesimal strips above the gaging station, not at time t but at time t diminished by the interval required for the water to flow from where the rain falls to the gaging station; furthermore, the volume of rate of run-off from an infinitesimal strip is the product of the rate of run-off, be it any single-valued function of time whatever, times the length of the strip (width of drainage area), $W(x)$, times the width of the strip (the differential dx).

In the sixth paper of this series a variable velocity of the water will be considered. It will there be shown that for *special* variations of velocity all the conclusions of this paper, insofar as they relate to the prediction of flood crests, remain unchanged. The theoretical treatment of irregular-shaped drainage areas is now considered complete.

ACKNOWLEDGMENT

It is a pleasure to thank Mr. M. W. Hayes, Chief of the River and Flood Division of the Weather Bureau, for his cooperation and encouragement.

I am very grateful to Dr. W. J. Humphreys and Dr. Edgar W. Woolard, both of the Weather Bureau, who have read the manuscript and offered helpful suggestions.

72457—36——3

COOLING IN THE LOWER ATMOSPHERE AND THE STRUCTURE OF POLAR CONTINENTAL AIR

By H. WEXLER

[Weather Bureau, Washington, D. C., April 1936]

It has been known for some time that during a clear, calm night the temperature of a snow surface falls much below the temperature of the air within even a few centimeters of the surface. The snow surface radiates energy practically as a black body; and receives, by conduction from the snow and air, and also by radiation from the atmosphere, less energy than it loses through its own radiation; and consequently its temperature decreases. However, if the wind movement increases, considerable heat is transported to the surface from the warmer air above, by turbulence, and the surface temperature rises. When the wind ceases, the surface temperature again falls. The question arises as to how much the surface temperature can fall without also a simultaneous decrease of the temperature of large portions of the air above it. It will be shown, from considerations of radiative balance between the air and the snow surface, that it is impossible for the surface temperature to fall below a certain value without a simultaneous decrease of the maximum free-air temperature. In other words, it will be shown how, apart from conduction and mechanical turbulence, cooling from below extends upward through the lower troposphere.

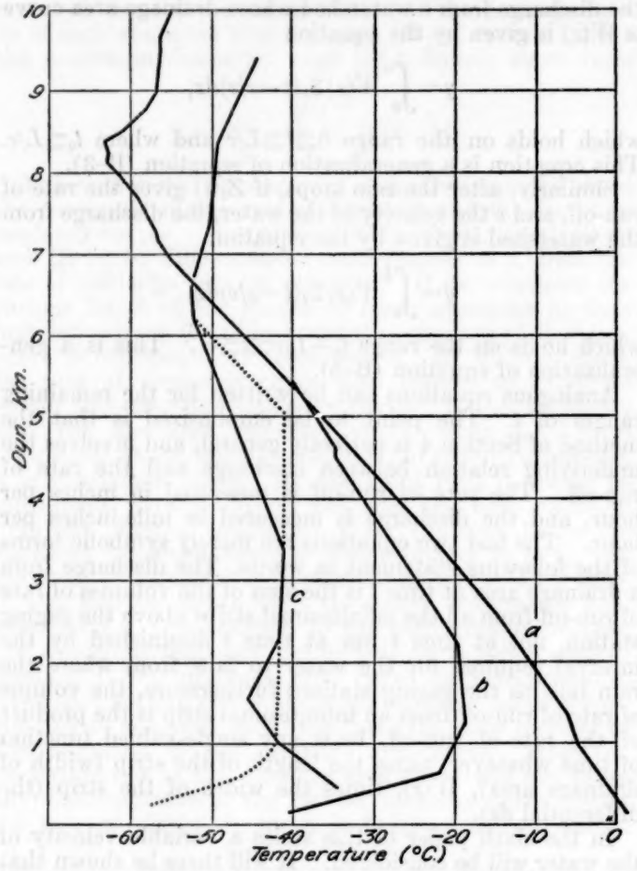

FIGURE 1.—Soundings at (*a*) Ås, Norway, February 2, 1933, 15.11 h; (*b*) Fairbanks, Alaska, December 28, 1932, 9.34 h; (*c*) Ellendale, N. Dak., February 8, 1933, 13.28 h, local time.

THE CHANGE FROM POLAR MARITIME TO POLAR CONTINENTAL AIR MASS CHARACTERISTICS

No better introduction to the problem can be given than by presenting actual soundings showing different types of polar air.

Curve (*a*) in figure 1 shows a portion of a balloon sounding taken through fresh polar maritime air at Ås, Norway (59°40′ N., 10°46′ E.) February 2, 1933. The synoptic situation for this period is discussed by Palmén (1), and it is seen from his maps that the air moved rapidly from the north over the Atlantic Ocean and appeared at Ås with westerly winds. According to Palmén, the air above the surface layer was in almost neutral equilibrium for moist air, and caused numerous showers, hailstorms, and thunderstorms along the Norwegian Coast.

Curve (*b*) is a sounding made at Fairbanks, Alaska (64°51′ N., 147°52′ W.), December 28, 1932, under clear skies and in a calm. An inversion of over 20° occurs between the surface and 1,300 meters, above which is an isothermal layer extending to about 2,200 meters, and a steeper lapse rate above. The wind above the inversion was westerly backing to southwesterly, 15 miles per second, at 3,400 meters, showing that the air above the inversion came from the Pacific Ocean. The temperature of this air differs from that of the Ås air by only a few degrees and is practically the same at 5 kilometers. The lower air was shielded from a maritime influence by the extensive mountain ranges that surround the Yukon Valley, and had probably remained over the snow cover for some time.

Curve (*c*) represents a portion of a balloon sounding made at Ellendale, N. Dak. (45°59′N., 98°34′ W.) on February 8, 1933, at about noon in a northwest wind of about 10 meters per second. It shows a superadiabatic surface layer, a smaller adiabatic layer, then an inversion, and isothermalcy to about 3,300 meters, above which the lapse rate steepens. The synoptic situation for this period is discussed by Willett (2), and it shows that the sounding was taken in a well developed current of polar continental air from the Hudson Bay area. The steep lapse rate in the lower air is a result of mechanical turbulence and heating from below. Before the air started its rapid movement southward it probably possessed a thermal structure in its lower portion similar to that indicated by the dotted line, as will be shown presently.

The problem that confronts us is to explain how sounding (*a*) is transformed into sounding (*c*). That such a transformation takes place over the polar regions during winter can hardly be doubted, for the constant drain of polar continental air from its source region southward must be compensated by an inflow of warmer air. The problem is in no way restricted if we assume as an initial air mass a body of polar maritime air, such as represented by the Ås sounding. In order to transform the Ås sounding into the Ellendale sounding, it is evident that we must seek an explanation that involves radiative transfer; and since the maximum temperature difference occurs at lower levels (38° C. at 1,500 meters) and the two soundings approach each other aloft (5° C. difference at 6,000 meters), it appears that heat is lost to space

mostly by way of the snow surface; we shall therefore examine how this can take place.

According to Falckenberg (3) the amount of radiation emitted by a snow surface (frozen or melting) differs by less than one-half percent from that coming from a black body, and so follows closely the law of Stefan-Boltzmann,

$$I=\sigma T^4,$$

where I is the radiation intensity in gm. cal./cm²/min., $\sigma=82\times10^{-12}$, T=temperature in degrees absolute.

The radiative properties of the atmosphere are much more complex, since the air is composed of several gases, only a few of which are good absorbers of long wave radiation. In the wave-length region for which terrestrial radiation is most intense, carbon dioxide has an important absorption band; but the best absorber is water vapor, and its varying content in the atmosphere combined with the complicated fashion in which its absorption coefficient depends on wave-length, adds to the difficulty of treating the problem analytically. Indeed, judging from the disagreement among various investigators, the exact nature of the water vapor absorption spectrum is still unknown. Some of the chief investigators have been Rubens and Aschkinass (4), Fowle (5), Hettner (6), and, more recently, Weber and Randall (7). Each of these authorities agrees to the existence of a strong, narrow, absorption band at about 7μ, a region of low absorption centered at about 10μ, and increasing absorption beyond 12μ. However, their quantitative results are not in agreement; Hettner's absorption values are the largest, while those of Weber and Randall are the least; in between these two extremes are the determinations of Rubens and Aschkinass and of Fowle.

Hettner's data have usually been used by most meteorologists, especially by Simpson (8), who applied them with considerable success to certain problems concerning the mean heat balance of the atmosphere. Recently, however, Ramanathan and Ramdas (9), in trying to derive theoretically Ångström's formula for atmospheric radiation, found that Hettner's absorption data led to a value of a constant in the formula which was much larger than the observed one, while the data of Weber and Randall gave a value in much better agreement.

In figures 2a and 2b are shown the laboratory results of Hettner and of Weber and Randall. Against wave-length is plotted α, the decimal coefficient of absorption, which, assuming Beer's law to be true for water vapor, is defined in the following manner:

$$10^{-\alpha m}=I_\lambda/I_{0\lambda},$$

where $I_{0\lambda}$ is the intensity of the incident radiation of wave-length, λ, and

I_λ is the intensity after the radiation has passed through m gms. of the absorbing material.

The two curves in figure 2a, and Hettner's curve in figure 2b have been reproduced from the paper of Ramanathan and Ramdas; but the Weber-Randall curve in figure 2b has been prepared by the writer, from the data published by Weber and Randall, together with certain additional information kindly supplied by Professor Randall. Ramanathan and Ramdas evidently assumed the temperature of the absorption tube that contained the saturated water-vapor to be about 30° C., whereas it was actually about 22.5° C. This means that the actual absorption coefficients are higher than those calculated by Ramanthan and Ramdas. This correction has been applied to figure 2b but not to figure 2a, since it is negligible for low values of absorption. Also, due to an error in printing, 10 absorption lines, 21.39μ to 22.55μ, inclusive, were included in the steam absorption data instead of the water vapor data; this accounts for the apparent low absorption shown in this region in the paper of Ramanathan and Ramdas.

The curves in figures 2a and 2b show that Weber and Randall found smaller absorption than did Hettner. The former authorities used a 60° potassium bromide prism twice, resulting in high dispersion and resolution, while Hettner used a 20° potassium chloride prism and larger slit widths. Professor Randall has assured the writer that "it is quite impossible to compare results when such a difference exists." In this study, both sets of absorption data are used, and their respective meteorological consequences examined and compared.

Simpson's use of the absorption data of Hettner (for water vapor) and Rubens and Aschkinass (for carbon dioxide).—We shall assume with Simpson (8) that a layer of air in which each column of unit cross section contains 0.15 millimeters precipitable water and 0.03 gram of CO_2[1] completely absorbs all radiation of wave-lengths between 5.5μ and 7μ, and greater than 14μ; partially absorbs radiation of wave-lengths between 4μ and 5.5μ, 7μ and 8.5μ, 11μ and 14μ; and is practically transparent to wave-lengths between 8.5μ and 11μ. These wave-lengths together cover the range over which terrestrial and atmospheric radiation have appreciable intensity. To avoid repetition, let us call the radiation with wave-lengths in the first group, W-radiation (after Brunt); in the second, S-radiation; and in the last, T-radiation. At a temperature of 273°, the percentages of radiation from a black body included in these three groups are 59%, 26%, 15%, respectively.

The length of a column of air of 1 square centimeter cross section which contains 0.15 millimeter precipitable water is given approximately by

$$L=0.70\frac{T}{e}\text{meters},$$

where T is the mean temperature of the column in °A, and e is the mean vapor pressure in mb; when $T=273°$ and $e=6$ $mb.$, then $L=40$ meters, and when $T=253°$ and $e=1$ $mb.$, then $L=175$ meters.

If we divide the atmosphere into layers each of whose unit columns contains 0.15 millimeter precipitable water, then the amount of CO_2 in each unit column of the layer ordinarily will not be of the order of 0.03 gram. According to Fowle (10), the average sea-level content of CO_2 is 0.6 gram per cubic meter. Assuming this value is the same above the surface (probably it is too high), then a column of air of cross-section 1 square centimeter, and 40 meters long, will contain only 0.0024 gram of CO_2; and a column 200 meters thick, 0.012 gram. Now as found by Rubens and Aschkinass (4), CO_2 absorbs very strongly in a narrow band from 13 to 16μ, with its maximum absorption occurring at 14.7μ and equal to 88 percent for 0.06 gram. Assuming 0.06 gram of CO_2 in the stratosphere, Simpson felt justified in decreasing the lower limit of Hettner's complete absorption region, for radiation passing through the stratosphere, from about 20μ to 14μ. If account is taken of the actual CO_2 content in the layers

[1] Because of the diffuse nature of terrestrial and atmospheric radiation, the mean path of the radiation will include approximately twice the amount of absorbing gas; hence, diffuse radiation passing through a layer, each of whose unit columns contains 0.15 millimeter water and 0.03 gram CO_2 will be absorbed in approximately the same proportion as a parallel beam passing through a layer each of whose unit columns contains 0.30 millimeter of H_2O and 0.06 gram CO_2.

considered above, then the absorption will not be so complete as that assumed by Simpson. However, since in this paper the extreme values of absorption will each be used, it will be assumed that in this case the *W*-radiation is contained in the wave-length regions adopted by Simpson.

Now let us suppose that a body of air in convective equilibrium with an open ocean surface of temperature 1° C., and containing no clouds, comes to rest over an unlimited horizontal snow surface during the polar night. Initially, the temperature of the snow surface will be 0° C. and, after stagnation of the air ensues, will fall very rapidly to a value determined by the amount of radiation that is received from the atmosphere (assuming that conduction from the atmosphere and underlying snow is very small). If we divide the atmosphere into layers, each of whose unit columns contains 0.15 millimeter precipitable water, then practically all of the *W*-radiation reaching the surface will originate in the lowest layer. No *T*-radiation will reach the surface, since it is not emitted in any appreciable quantity by the water-vapor. A certain amount of *S*-radiation will reach the surface, and this will come from various layers, the more intense radiation coming from lower layers and the less intense from the higher layers. It is impossible to determine exactly the amount of *S*-radiation that will reach the surface, but it is clear that the radiation in each band must be bounded by a curve extending from full absorption at the temperature of the lowest layer, to complete transparency, the shape of which will depend on the amount and distribution of water vapor. As Simpson pointed out, almost any reasonable

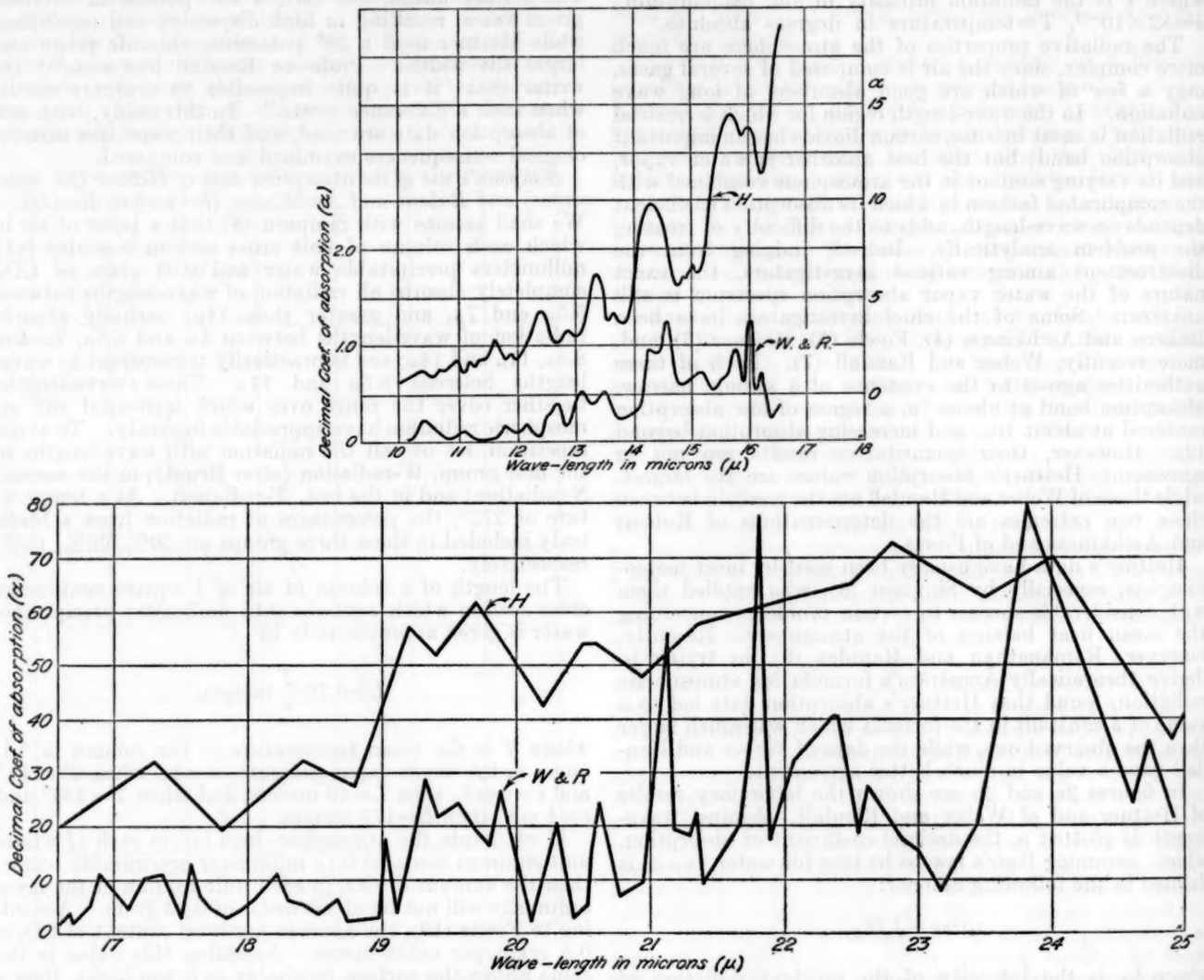

FIGURE 2 (*a* and *b*).—Water vapor absorption spectra as found by Hettner (H), and by Weber and Randall (W & R). (*a*) The left-hand scale refers to Weber and Randall's curve and the right-hand scale to Hettner's curve (after Ramanathan).

curve in these bands, joining full absorption to complete transparency, divides the area approximately in half; hence, we assume the amount of *S*-radiation that reaches the surface to be equal to one-half of the total S-radiation of a black-body at the temperature of the lowest layer.

In figure 3a, a curve has been drawn that shows the distribution of energy emitted by a black-body at a temperature of 274° A. The amount of radiation that the snow surface receives will be approximately equal to the shaded portion of the area under this curve. Initially, the snow surface, when at a temperature of 273° A., will emit radiation which will be almost equal to the *total* area under this curve; and its temperature will

decrease, since it is losing more radiation than it is receiving, the net loss being nearly equal to the unshaded portion of the area. However, at a certain temperature (in this case, 253° A., as will be shown later) the snow surface will be emitting as much radiation as it is receiving from the atmosphere, the temperature of the latter being assumed unchanged. This equilibrium is shown in figure 3a by the equality of the shaded area under the 274° A. curve and the total area under the 253° A. curve. In this case, the surface temperature will remain constant at 253° A. provided that the temperature of the air remains unchanged.

Application of Weber and Randall's absorption data to an atmosphere containing normal amounts of CO_2.—Water vapor absorption as determined by Weber and Randall is so much less than that found by Hettner in the region 10μ–25μ, that in order to estimate the amount of atmospheric radiation in the manner outlined above, it is necessary to increase the thickness of the layers until each contains 1 millimeter precipitable water and therefore absorbs diffuse radiation as if it contained 2 millimeters. From figures 2a and 2b, we can easily determine the wave-lengths of the radiation which is absorbed by such a layer; radiation having wave-lengths for which $a > 5$ will be almost completely absorbed, while wave-lengths for which $a < 5$ will be only partially absorbed. The inaccuracy involved in regarding these thick layers as elementary layers will not be serious except at low temperatures. The length of a unit column containing 1 millimeter precipitable water is

$$L = 4.62 \frac{T}{e} \text{ meters;}$$

when $T = 273°$, and $e = 6mb.$, then $L = 210$ meters; and when $T = 253°$, and $e = 1\ mb.$, then $L = 1{,}170$ meters.

In figures 2a and 2b, we see from Weber and Randall's absorption curve that a is very small from 10μ to 12μ, increases slightly near 13μ, increases markedly near 17μ, and remains quite large beyond 17μ. For the region 10μ to 13μ, the mean value of a is about 0.21, and the transmission of diffuse radiation in this band through a layer containing 1 millimeter precipitable water vapor is more than 90 percent; for the region 13μ–17μ, the mean value of a is about 0.8, corresponding to about 70 percent transmission, while for wave lengths greater than 17μ, the mean transmission is less than 10 percent.

If, now, assuming Fowle's value of 0.6 gm/m³ as the normal CO_2 content to hold true at all elevations,[3] we also take account of CO_2 absorption in the band 13μ–16μ, then the mean transmission in this band through both the CO_2 and water vapor in a layer 200 millimeters thick is 48 percent; and through a layer 1,000 meters thick, 31 percent. Hence, we shall now define again the W, S, and T bands of radiation to conform with Weber and Randall's absorption data, and Fowle's value of the normal sea-level CO_2 content. The W-radiation will be that contained in the region 5.5—7.0μ, and in the region where wave-lengths are larger than 17μ; the S-radiation in the regions 4.0—5.5μ, 7.0—8.5μ, and 13μ–17μ; and the T radiation in the region 8.5—13μ. At a temperature of 273°, the percentages of radiation from a black body included in these three groups are 46 percent, 27 percent, 27 percent respectively. In this case, as shown in Figure 3b, the atmospheric radiation becomes much less than that shown in figure 3a; and so the surface temperature can fall to a lower value, 240°, as will be seen presently.

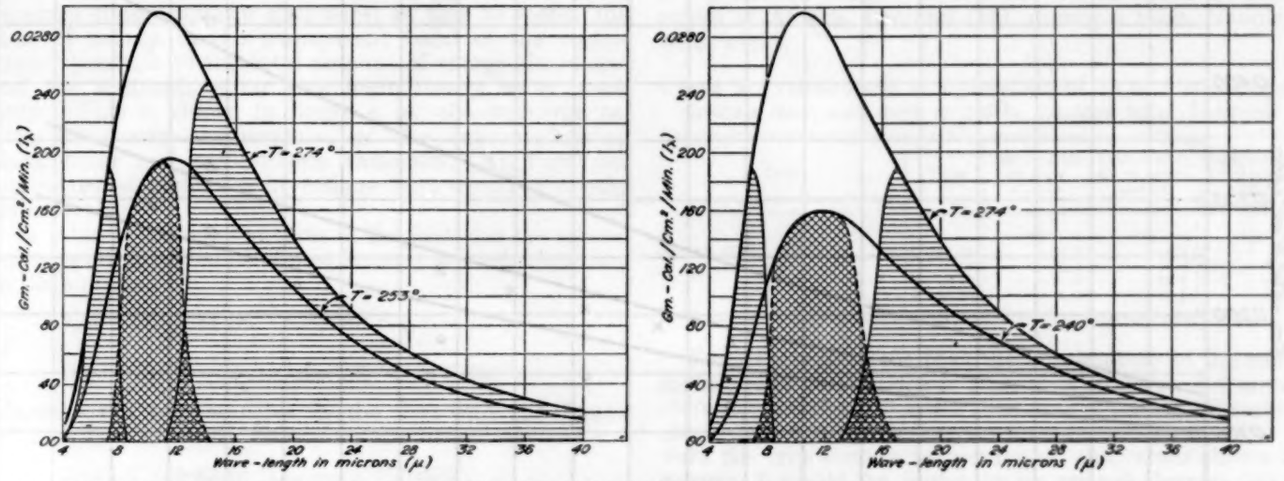

FIGURE 3 (*a* and *b*).—Radiative transfer between a moist atmosphere of surface temperature, 274°, and a snow surface; (*a*) Hettner's water vapor absorption data applied to an atmosphere of abnormal CO_2 content; (*b*) Weber and Randall's water vapor absorption data applied to an atmosphere of normal CO_2 content.

In order to determine, from the two sets of absorption data, the equilibrium surface temperatures for various air temperatures, three curves have been drawn in figure 4, one showing the variation of black-body radiation with temperature, the second showing the variation of atmospheric radiation with temperature, based on Simpson's application of Hettner's data in an atmosphere considerably overcharged with CO_2, and the third showing the same as the second but making use of Weber and Randall's data in an atmosphere containing more nearly a normal amount of CO_2. For comparison, in figure 4, are plotted the mean values of atmospheric radiation against surface temperature as observed on the "Maud" north of the Siberian coast by Sverdrup and discussed by Mosby (11). These are indicated by crosses, and were found by Mosby

[3] This value is probably too large for the free air, and also for surface winter polar conditions where on account of lack of animal and industrial activity the CO_2 content is probably very small.

by subtracting the mean nocturnal radiation from the black body radiation corresponding to the surface temperature. The individual observations, when plotted against surface temperature, exhibit considerable scatter, probably indicating that the radiation was not so much a function of surface temperature as of the air temperature above the inversion; unfortunately, due to lack of sufficient soundings at the time of the radiation measurements, it was not possible to show this. In order to compare the observations with curves (*b*) and (*c*) which represent atmospheric radiation plotted against temperature of the air above the inversion, the crosses must be moved a certain number of degrees to the right, corresponding to the mean value of the surface inversion. If the mean surface inversion were about 10° C. then the points would coincide almost exactly with curve (*c*). Also in figure 4, are plotted values of atmospheric radiation from Ångström's formula, with the constants given by Raman (**12**), $\frac{S}{\sigma T^4}=0.77-0.28\times10^{-0.055e}$, where S=atmospheric radiation, T=temp. of the instrument, σ=Stefan-Boltzmann constant, e=vapor pressure in mb.

From the above formula, the values of atmospheric radiation have been computed *under the assumption that the air is saturated.* At low temperatures, the points fall below the curves (*b*) and (*c*) and also those of the "Maud", but approach them with increasing temperature. The discrepancy at low temperatures should not be taken seriously, since the formula has not yet been verified by observations at those low temperatures. Indeed the "Maud" observations in figure 4, and those taken by Ångström at Abisko (68°21′ N, 18°47′ E.), indicate higher values of atmospheric radiation than found from the formula. This is explained by Mosby as being due to the presence of larger inversions over the polar regions than over the temperate regions.

When curves (*b*) and (*c*) are plotted on logarithmic paper, they are approximately straight lines; and their equations are found to be

(*b*) $R_A=980\times10^{-12}\times T^{3.5}$ gm cal/cm²/min;
(*c*) $R_A=800\times10^{-12}\times T^{3.5}$ gm cal/cm²/min.

The value 3.5 for the exponent was also found by Pekeris (**13**), from the data of Abbot and Fowle (**14**), (**5**). Pekeris plotted logarithm of temperature against logarithm of radiation from layers of air containing normal amounts of CO_2 and the following amounts of precipitable

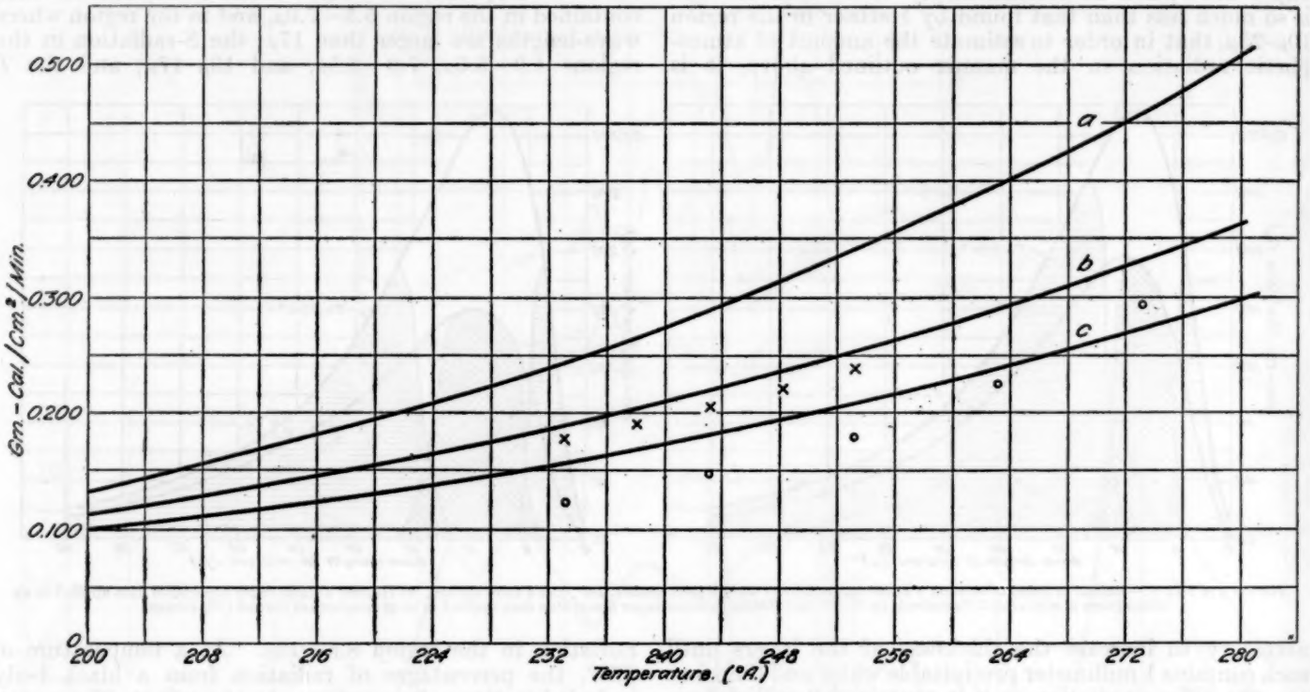

FIGURE 4.—(*a*) Radiation from snow surface; (*b*) radiation from a moist atmosphere of high CO_2 content; (*c*) radiation from a moist atmosphere of normal CO_2 content.

H_2O : 0.0001 gram, 0.003 gram, 0.046 gram, and 0.455 gram. The result was a series of approximately straight and parallel lines, which showed that the radiation could be represented by the equation $I=\text{const.}\times T^n$, where $n=3.5$.

The curves found from equations (*b*) and (*c*) are not shown in figure 4, since they cannot be distinguished from the actual curves.

If now we wish to find the mean temperature of a stratum of air, each of whose unit columns contains 0.15 millimeter precipitable H_2O and 0.03 gram CO_2, that is necessary to maintain a constant surface temperature of 253°, we move the 253° ordinate of curve (*a*) over to curve (*b*); the temperature at which this ordinate fits the latter curve is the desired air temperature. Likewise, the mean temperature of a stratum of air each of whose columns contains 1 millimeter precipitable water and normal CO_2 content, will be found to be 291°. In table 1 are presented air temperatures necessary for the maintenance of various equilibrium surface temperatures.

TABLE 1.—*Mean temperatures of a layer of moist air necessary to maintain given surface temperatures*

	From curve (*b*)		From curve (*c*)	
1	2	3	4	5
$t_{Surf.}$	t_{Air}	t_A-t_S	t_{Air}	t_A-t_S
0° C.	+28°(24)	28	+41°(42)	41
−10	+14 (12)	24	+29 (29)	39
−20	+1 (1)	21	+18 (17)	38
−30	−11 (−11)	19	+4 (4)	34
−40	−23 (−23)	17	−9 (−9)	31
−50	−35 (−35)	15	−21 (−21)	29
−60	−46 (−47)	14	−34 (−34)	26
−70	−59 (−58)	11	−47 (−47)	23

From the table, we see that as the surface temperature decreases, the magnitude of the inversion decreases. This is owing to the well-known shift of maximum intensity of radiation to larger wave-lengths as the temperature of the radiator decreases; as this happens, the ratio of energy in the transparent band of the water-vapor spectrum to the total amount of energy decreases, and the atmosphere radiates more nearly as a black body. This is shown in figure 4 by the convergence, with decreasing temperature, of the curves showing black body and atmospheric radiation. At very low temperatures, instead of inversions there would exist only isothermalcy.

In table 1, the temperatures in the first and the second columns are found to be almost linearly related, according to the equation

$$t_A=1.18t_S+24 \text{ in °C., } -70°\leqq t_S\leqq -20°,$$

or

$$T_A=1.18T_S-25 \text{ in °A., } 203°\leqq T_S\leqq 253°.$$

Likewise the temperatures in the first and the fourth columns conform very closely to the linear relation

$$t_A=1.27t_S+42 \text{ in °C., } -70°\leqq t_S\leqq 0°,$$

or

$$T_A=1.27T_S-32 \text{ in °A., } 203°\leqq T_S\leqq 273°.$$

The air temperatures computed from these formulae are included in table 1, enclosed by parentheses, and it is seen that the agreement with the true values is very close over most of the temperature range considered.

The magnitudes of the inversions shown in table 1 can be checked by comparing them with some large inversions that have been observed. The comparisons are shown in table 2.

TABLE 2.—*Magnitudes of observed inversions compared to those of computed inversions*

1	2	3	4	5	6	7	8
Station	Date and time	Temperature in the surface shelter	Height of top of inversion	Temperature of top of inversion as recorded on meteorograph	Temperature of top of inversion as observed by thermometer	Temperature of inversion top as given in column 2, table 1	Temperature of inversion top as given in column 4, table 1
		°C.	m	°	°	°	°
Fairbanks, Alaska	Dec. 28, 1932: 9.34 h.	−40.5	1,160	−18.5	−17.0	−23.5	−9.0
	20.26 h.	−41.0	840	−16.5	−18.0	24.5	−10.0
	Jan. 25, 1933: 9.48 h.	−37.8	1,830	−19.8	.....	−20.5	−6.0
Fargo, N. Dak.	Jan. 14, 1935: 4.29 h.	−32.0	1,780	−12.7	.....	−13.5	+1.5
Billings, Mont.	Jan. 14, 1935: 3.25 h.	−23.2	800	−2.6	.....	−3.0	+12.5

The temperatures in columns 7 and 8 of table 2 were found from table 1, using the temperatures in column 3 as the argument; and it is seen that the temperatures in column 7 are lower than the observed temperatures in column 5 (and 6), while those in column 8 are higher. In other words, by using Hettner's absorption data, for an atmosphere overcharged with CO_2, smaller inversions result than those found in Nature. On the other hand, using Weber and Randall's data for an atmosphere containing normal amounts of CO_2, the inversions are large enough to account for those observed. The inversions shown in table 2 would have been much larger if temperatures of the snow surface had been observed, since in all cases the surface temperature was observed in a shelter a meter or so above the snow surface, and it is well known that under the conditions here assumed the temperature of the snow is lower than that of the air a short distance above it. To illustrate this, in table 3 are presented some typical observations taken by Ångström at Abisko, Lapland (**14**), during a calm, cloudless polar night.

TABLE 3.—*Temperatures at different heights above a snow surface during a clear, calm night at Abisko, Lapland (after Ångström)*

Date	Time	Temperature at snow surface	Temperature 0.6 m above surface	Temperature 2.0 m above surface
	h.	°C	°C	°C
Jan. 12, 1916	11.00	−12.8	−8.4	−7.6
	12.00	−16.1	−10.6	−9.4
	13.30	−17.0	−12.0	−10.5
	16.00	−18.0	−14.1	−12.5

From table 3 we see that the temperature of the snow surface may be 5° C. lower than that of the air 0.6 meter above it; and 6° or 7° lower than that of the air 2.0 meters above. Hence, if the temperatures in column 3, table 2, were the true surface temperatures, the values shown in column 7 would be found to be several degrees lower and would disagree even more seriously than those in column 5. On the other hand, it is not likely that the temperatures in column 8 would be found to be lower than those observed, even if the true snow surface temperatures were used.

Returning to the question of radiative transfer between the atmosphere and the snow surface, we have seen that the surface temperature will remain unchanged at 253°A. provided that the temperature of the air remains unchanged. However, if we are dealing with the same column of air, it is evident from figures 3a, 3b that its temperature must decrease, since it is emitting more radiation than it receives. As mentioned above, the surface temperature will remain constant at 253° A. because it is receiving radiation from the atmosphere equal to the shaded areas under the 274° A. curve, figure 3a, and emitting an equal amount of energy which is represented by the total area under the 253° A. curve; but the atmosphere does not absorb all this energy that is being emitted by the snow-surface, because the *T*-radiation and about one-half the *S*-radiation escape to space, as indicated by the cross-hatched area under the 253° curve. Hence the mean temperature of any layer that contains 0.15 millimeter precipitable water and larger than normal CO_2 content must fall below 274°. With the initial lapse rate we have assumed, this will apply only to the lowest layers; and the lapse rate in the stratum including these levels will become practically isothermal. Since the temperature of the stratum is then lower than it was originally, it will send less radiation to the snow surface,

and so the surface temperature will decrease. This process will continue to go on, the atmosphere losing energy to space mostly by way of the snow surface; and as the air temperature decreases, the original steep lapse rate will be transformed into approximate isothermalcy up to a certain height. This is illustrated in figure 5, where the original lapse rate is shown by a solid line and the new lapse rates by dashed lines. The lengths of unit columns containing 1 millimeter precipitable water are

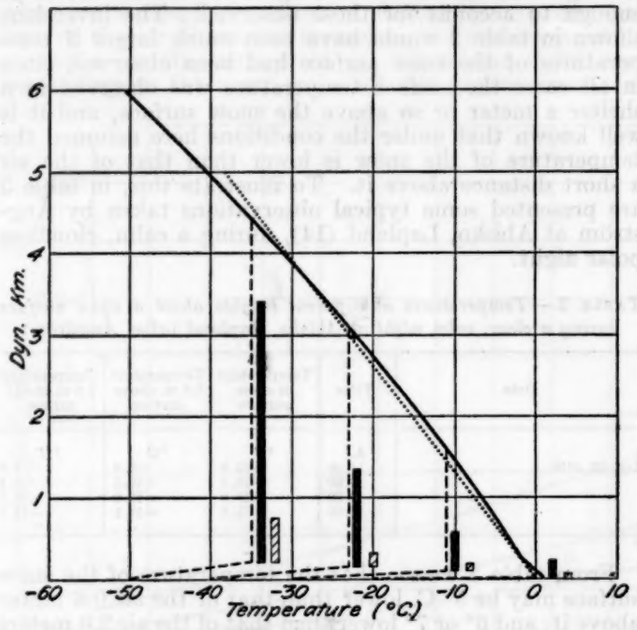

FIGURE 5.—Successive stages in cooling of polar maritime air over a snow surface during a calm, cloudless polar night.

indicated by shaded rectangles, and those containing 0.15 millimeter by cross-hatched rectangles.

A discussion of an example will show why the lapse rates will take on approximately the indicated successive shapes. Let us suppose that the temperature of the surface is −40° C. Then no layer of air, each of whose columns contains 0.15 millimeter precipitable water and 0.03 gram CO_2, can have a mean temperature higher than −23° C.; for if the mean temperature of a certain layer were higher, then the surface and underlying layers would receive more radiation than they would emit and consequently their temperatures would rise. Hence the surface temperature can fall to −40° provided only that the mean temperature of no layer above it is higher than −23°. Similarly it can be shown that by using the data of Weber and Randall, and assuming normal CO_2 content, the mean temperature of no layer of air can be higher than −9°. According to the ideal conditions assumed in this paper the inversion layer will be of infinitesimal thickness. However, in figure 5, for the sake of clarity, the inversions are represented by layers of finite thicknesses.

Looking back now, we see that since only a thin stratum of snow and air will initially be involved, the surface temperature will at first fall very rapidly to a certain value dependent on the maximum mean temperature of a layer of the atmosphere containing in one case 0.15 millimeter precipitable H_2O and 0.03 gram CO_2 and in the second case 1 millimeter precipitable H_2O and a normal amount of CO_2. As the surface temperature falls below this critical value, the temperature of a certain portion of the atmosphere must fall simultaneously; and its rate of fall will become slower as the temperature becomes lower, since for the same drop in temperature the surface must radiate to space a larger amount of energy, as seen from figure 5. Also, the rate of loss of energy to space by the surface becomes smaller with lower temperature; but a fuller account of the rate of decrease of temperature will be given later.

From the above discussion, we see that the top of the isothermal layer marks the height to which cooling from the surface has extended; hence, strictly speaking, this level should be considered to be the top of the polar continental air. The air above, characterized by a steep lapse rate, is, in this case, still polar maritime air. An exception to this general statement will be pointed out later. During January and February 1936, when polar continental outbreaks were very pronounced over the Middle West, the daily cross-sections now prepared at the Central Office of the Weather Bureau were analyzed according to the above principles, with satisfactory results.

From figure 5, it is seen that the lower the surface temperature, the smaller the inversion, and the higher the isothermal layer will extend; the top of the latter marks the height to which the influence of surface cooling has reached. To illustrate the phenomena by observations, in figure 6 are plotted points relating the height of the isothermal layer to its temperature at Fargo, N. Dak. (46°54′ N., 96°48′ W., elevation above m. s. l., 274 meters) during January and February 1936. In many of the soundings, ground inversions also existed, but some of the soundings showed steep lapse rates near the surface because of turbulence within the moving polar mass. Fargo is not situated in a true source region for polar continental air; and when polar air does reach it, the low surface temperatures characteristic of radiative

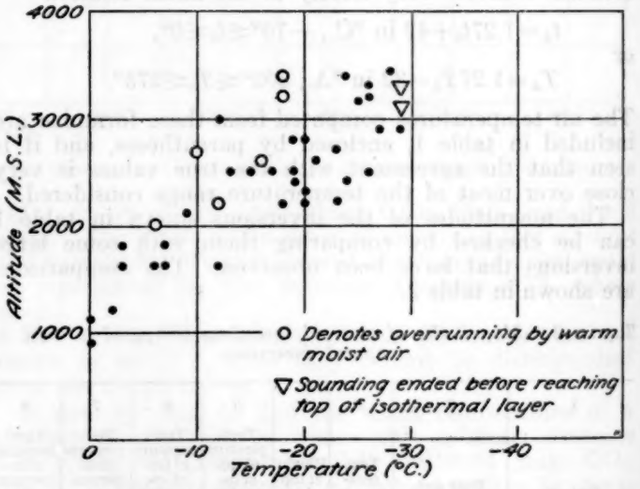

FIGURE 6.—Temperatures and altitudes of isothermal layer above Fargo, N. Dak. (300 m. M. S. L.), January 1–February 19, 1936.

equilibrium are usually lacking because of the wind movement. Therefore no attempt has been made to correlate the magnitude of the ground inversion with the surface temperature.

Although the heights and temperatures of the "isothermal layer" are plotted in figure 6, it must be pointed out that not all of these layers were perfectly isothermal. A strong wind can destroy the lower portion of the isothermal layer, and after the wind dies down the air will cool in

such a way that the lower portion of the isothermal layer becomes an inversion layer of considerable thickness. Also, as will be pointed out later, subsidence of the air mass will tend to transform the upper portion of the isothermal layer into an inversion layer. Hence in plotting figure 6, thick layers, above the surface inversion or adiabatic layer in which the temperature increase or decrease with elevation was less than 0.2°/100 meters, have been considered to have a uniform temperature equal to the mean temperature of the layer.

DIRECT RADIATION LOSS AND THE ROLE OF THE EMISSION LAYER

At this point it is desirable to examine to what extent the atmosphere can lose heat directly to space, and not by way of the surface. In figure 1, by a comparison of soundings (*a*), (*b*), (*c*), we see that because of the convergence of the curves with increasing height the main loss of energy must be by way of the surface, and will be mostly in the form of T-radiation. Nevertheless, an appreciable amount of energy is lost to space from the upper levels of the troposphere, and this loss has an important influence on the lapse rate in upper levels. From figure 1, sounding (*c*), we see that the isothermal layer has a temperature of about −41° C., and extends to 3,300 meters. However, from figure 5 we see that if the cooling is from below only, and the initial lapse rate of the air is that shown by the solid line, then an isothermal layer with temperature −41° C. should extend to about 5,000 meters. Now if in figure 1, sounding (*c*), we extend the isothermal layer to 5,000 meters and then draw an adiabatic lapse rate curve above, this latter curve will intersect the sounding at the next "significant" point. This curve is indicated as a dotted line extending from 3,300 meters to 6,200 meters, and would probably represent the actual lapse rate if cooling had occurred from below only. If this be true, then the area between this curve and the original sounding is nearly proportional to the energy lost to space directly from the atmosphere. That the troposphere at high levels does lose energy directly to space has been shown by Albrecht, (**16**), (**17**), (**18**), according to whom the rapid decrease with height of atmospheric water-vapor content, and consequently of absorbing power, results in a natural upper limit to the region of atmospheric absorption. This critical height, corresponding approximately to the height of the −50° C. isotherm in an atmosphere of normal moisture content, marks the top of the emission layer, about 3 kilometers thick, from which atmospheric radiation is lost to space. In Albrecht's example (**16**), the emission layer, as determined from Peppler's mean summer values of temperature for Germany and Süring's formula for specific humidity, extended from 9 kilometers (−41°) to 12 kilometers (−50°). Applying the analysis described above to sounding (*c*), we find independently that the emission layer in this case extends from 3,300 meters (−41°) to 6,200 meters (−52°), in good agreement with Albrecht's bounding temperatures. It is also interesting to note that in sounding (*c*) the tropopause is found immediately above the emission layer, showing that in this case the emission layer forms the natural limit of the troposphere, which Albrecht pointed out to be true for the temperate and polar regions.

Albrecht found from Hettner's absorption data [(**16**), p. 433, (**17**), p. 65] that the rate of loss of energy to space from the emission layer would be nearly equal to that of the selective radiation from water vapor and carbon dioxide at −50° C., or about 0.170 gram cal/cm²/min. As illustrated in figures 3a, 3b, the loss of energy to space from the surface takes place mostly through the transparent band; and, as can be seen in figure 4 by subtracting from the black body curve either of the two curves of atmospheric radiation, it is much less than that found by Albrecht for the emission layer. Now if Albrecht's value were correct, then it would clearly be impossible for a sunless, cloudless, motionless atmosphere, possessing initially a steep lapse rate, to cool more rapidly in lower than in higher levels. In other words the cooling would proceed in such a manner that a steep lapse rate would always exist. This is contrary to the lapse rates observed in polar continental air masses, which are small, as seen from the examples in figure 1 and from Willett's data for American polar continental air (**19**). Recently, Mügge (**35**) has presented curves showing rates of cooling for a tropical, subtropical, subpolar, and a polar atmosphere. The curves are based on earlier papers by Mügge and Möller (**36**), (**37**), and in each type of atmosphere, he finds ((**35**), p. 169) "* * * that in all latitudes the cooling is greater aloft than below, thereby continually creating atmospheric instability." This conclusion is hardly consistent with the temperature-height curve he presents showing the structure of polar air; according to this curve, the lower portion of the air is very stable, the temperature decrease between the surface and 4 kilometers being about 12° C.

Albrecht's high value of the loss of energy from the emission layer can probably be explained by the fact that he used Hettner's absorption data, which as we have seen seem too high as compared with those of other investigators. In a recent paper, Ramanathan (**20**) applied Hettner's absorption data in a first approximation to the solution of the problem of radiative equilibrium in the upper troposphere; however, instead of assuming a certain amount of absorption in the region 8–13μ, as Hettner observed, Ramanathan assumed complete transparency. Following Simpson's scheme, he assumed an initial lapse rate of 0.6, and used elementary layers of thickness 1 kilometer, each having a mean temperature differing from those of adjacent layers by 6° C. He found that an atmosphere having the assumed lapse rate was not in radiative equilibrium, and that the layers would tend to lose or gain energy at rates shown in table 4.

TABLE 4.—*Net radiation from different layers of the atmosphere*

[Unit=gm. cal/cm²/min.×10⁻² (after Ramanathan)]

Atmospheric layer	Assumed mean temperature of layer	0.0015 cm. ppt. H_2O in stratosphere		0.01 cm. ppt. H_2O in stratosphere		0.03 cm. ppt. H_2O in stratosphere	
		100 per-cent rel. humidity in tropo-sphere	25 per-cent rel. humidity	100 per-cent	25 per-cent	100 per-cent	25 per-cent
−3	205° A	−16	+8	+36	+24	+51	+24
−2	211	−70	−15	31	30	65	44
−1	217	−122	−40	17	18	60	39
1	223	−158	−93	−30	0	17	30
2	229	−158	−155	−77	−34	−39	5
3	235	−112	−197	−76	−78	−57	−39
4	241	−62	−166	−53	−91	−42	−65
5	247	−25	−121	−26	−90	−20	−52
6	253	−9	−84	−9	−61	−9	−51
7	260		−35				−32
Loss from the emission layer		−730	−896	−271	−354	−167	−239

In table 4 it is seen that the maximum loss of energy from the emission layer is about 0.090 gram cal/cm²/min, which is considerably less than that found by Albrecht;

and that the minimum is about 0.017 gram cal/cm²/min. As the moisture in the stratosphere increases, the emission layer becomes lower, and less energy is lost to space. However, an increase in the moisture in the troposphere causes the emission layer to become *higher*, and less energy is then lost to space. It would be valuable to extend Ramanathan's work beyond the first approximation, by the method used by Gowan (**21**), (**22**) to find the temperature distribution satisfying radiative equilibrium in the ozone region.

Now after the cooling process has gone on for some time, and the temperature of the lower atmosphere has become low, then the emission layer, which has been radiating energy to space continuously, can decrease in temperature, since it then receives less intense radiation from below and practically no radiation from above. Of course the very stable stratification below prevents any upward transport of heat by turbulence. As illustrated in sounding (*c*), figure 1, this will result in a certain upper limit to the height to which the isothermal layer can extend (probably about 3,500 meters), and the lapse rate above will be small. In these extreme cases of cooling, it would seem proper to call the whole troposphere polar continental air, since it is only after the lower portion of the atmosphere has cooled considerably by way of the surface that the emission layer can also cool. As the cooling continues, both from the surface and the emission layer, then the latter becomes lower, because its height, as shown by Albrecht, is a function mainly of temperature. Also, because of cooling, the lower atmosphere will contract. To estimate the magnitude of this latter effect, the heights of the 500 mb. surface were compared for soundings of type (*a*) and type (*c*), figure 1. Assuming the surface pressure to be the same, the difference was found to be about 500 meters. In figure 1, we see that the Ellendale sounding meets the tropopause at about 6.2 kilometers, while the As sounding meets it at about 8.1 kilometers; hence contraction of the lower atmosphere by cooling could not account for the difference in height of the tropopause at these two stations. Evidently other factors must enter, and we shall later examine the effects of radiation.

RATE OF DECREASE OF SURFACE AND FREE-AIR TEMPERATURES OVER THE CONTINENT

Let us now examine the rate of decrease of surface and air temperature, assuming that the loss of energy to space takes place from the snow surface. As stated above, the snow temperature will at first fall rapidly, from its initial value of 0° C., to −20° C. (or to −33°), since only a thin stratum of snow and air will cool. Below this temperature, the cooling will become slower and slower, since a larger and larger portion of the air column must be cooled.

Brunt [(**23**), p. 127] gives the following formula for the rate of decrease of surface temperature with time, for a calm, cloudless atmosphere resting above a homogeneous surface, where only conduction of heat from the underlying surface compensates for the loss of heat by nocturnal radiation:

$$\sqrt{t}=\frac{\sqrt{\pi}}{2}\frac{\rho c\sqrt{\kappa}}{E}(T_o-T),$$

where t=time in hours for surface temperature to fall from T_0 to T (from 273° to 253°, or to 240°); ρ=density of the surface=0.5 for old snow and 0.10 for new snow; c=specific heat of the surface=0.5 for snow; κ=conductivity of the surface=0.0011 for old snow and 0.00025 for new snow (**24**), E=effective nocturnal radiation (difference between black-body radiation at temperature T and return atmospheric radiation).

Now in computing the fall of temperature from 0° to −20° C. (or −33°), a mean value of E must be found over the temperature range considered; this can be done from curves (*a*), (*b*), and (*c*) in figure 4. The results are shown in table 5.

TABLE 5.—*Times for cooling of the snow surface from 0° to the critical temperature*

Absorption data	Critical temperature	Mean value of E in gm cal/cm²/min.	Time for cooling	
			Old snow surface	New snow surface
			Hours	*Hours*
Hettner (above normal CO_2 content)	−20° C.	0.11	1.5	0.02
Weber & Randall (normal CO_2 content)	−33°	.14	2.3	.03

In reality, due to the release of latent heat of condensation and the transport of heat downward from the air by mechanical turbulence, the time for cooling is larger than the values in table 5; but these may be regarded as minimum values.

In order for the surface temperature to fall below −20° C. (or −33° C.), the lower portion of the atmosphere must cool; and as shown above, the cooling will transform the original temperature-height curve into those of the forms shown by the dashed lines in figure 5. If the ordinate of this figure were pressure, then the amount of internal and potential energy lost after a certain interval of time would be proportional to the area between the original temperature-height curve and the new curve.

If T_i represents the initial temperature of some point at pressure p, in a unit air column, and T_f represents the final temperature of this point, the difference in energy (internal plus potential) of the air column is given by the following expression [(**25**), p.27]:

$$(1)\qquad U=U_i-U_f=-\frac{c_p.10^3}{g}\int_{p_0}^{p_h}(T_i-T_f)dp \text{ gm. cal.}$$

where p=pressure in mb. p_o, p_h=pressures at bottom and top of the air column, c_p=specific heat of dry air at constant pressure=0.240, g=acceleration due to gravity.

Since T_i represents the known initial temperature distribution and T_f the final distribution, which for the cooled portion of the atmosphere is a function of T_s, the temperature of the snow (as seen from table 1), therefore (1) may be written as a function of T_s:

$$(2)\qquad U=U(T_s).$$

As the saturated air cools, the water vapor will be condensed and the latent heat of condensation released. With an initial lapse rate of the type shown in figure 5, and assuming saturation, the amount of precipitable H_2O is about 1 gm.: and so when the column is cooled sufficiently, a considerable amount of heat may be released. The following equation has been found to represent with sufficient accuracy the latent heat released:

$$(3)\qquad U_w=3440-12.6T_A \text{ gm. cal.}$$

where T_A is the temperature in °A of the isothermal layer, which as we have seen is a linear function of T_s.

Due to the prevalence of subcooled water even at very low temperatures[3], only the latent heat of water has been taken into account, assuming that it equals 600 gm. cal. per gm. of condensed H_2O.

The presence of water droplets (or ice particles) in the atmosphere will have a certain influence on the radiative balance; but this is neglected under the assumption that the foreign particles are small and few in number, and fall rapidly to the surface in the absence of upward currents.

The energy (potential, internal, and latent) of the column will be lost to space principally through the T and S radiations from the snow surface; and the rate of loss will be

$$E=I-R_A=\sigma T_s^4-\kappa T_s^{3.5} \text{ gm. cal/cm}^2\text{/min.}, \tag{4}$$

where σ=Stefan-Boltzmann constant=82.10^{-12}, and κ=980.10^{-12} or 800.10^{-12} according to whether curve (b) or (c) in figure 4 is taken to represent R_A.

Hence, the time required for cooling from −20° C. (or −33° C.) to T_s will be

$$t=\int_{T_c}^{T_s}\frac{d[U(T_s)+U_w(T_s)]}{E(T_s)} \text{ minutes}, \tag{5}$$

where in the one case T_c=253° and in the other, 240°.

In order to evaluate (5), certain approproximations are introduced in order to obtain a simple expression for U: Instead of assuming an initial lapse rate that follows the condensation adiabat above a shallow adiabatic layer (as shown by the solid curve in figure 5), we assume that the initial lapse rate is linear and equal to 0.77 of the dry adiabatic rate (as shown by the dotted line in figure 5). After cooling has occurred the lower levels will become practically isothermal at temperature T_A. This isothermal layer is considered as extending downward to the surface, although actually there is a shallow inversion layer in which the temperature increases from T_s to T_A. The total energy of this layer is so small in comparison with that of the thicker layers considered here that it is regarded as negligible. Hence, in the simplified case, (1) becomes

$$U=U_i-U_f=\frac{-C_p\times 10^3}{g}\int_{p_s}^{p_A}(T_i-T_A)dp; \tag{6}$$

for a linear lapse rate p_0, that is, 0.77 of the dry adiabatic, we have

$$\frac{p}{1000}=\left(\frac{T_i}{273}\right)^{\frac{mg}{R\times 0.77}}=\left(\frac{T_i}{273}\right)^{4.5}, \tag{7}$$

where $\frac{R}{m}$ is the gas constant for dry air, and g is the acceleration due to gravity.

Eliminating p from (6),

$$U=\frac{-4.5\cdot 10^6\cdot C_p}{(273)^{4.5}\cdot g}\int_{273°}^{T_A}(T_i-T_A)T_i^{3.5}dT_i \tag{8}$$

$$=-66{,}860[-0.182(T_A/273)^{5.5}+T_A/273-0.818] \text{ gm. cal.}$$

For T_A=249°, U=1,042 gm. cal. as compared to about 1,092 gm. cal. determined from the original lapse rate of figure 5. Assuming a linear lapse rate of 0.77 the dry adiabatic thus results in an underestimate of U for the temperature range considered here. This difference is in part compensated by assuming that the loss of energy to space is only by way of the snow surface and not also by way of the emission layer; hence, the underestimate of U will be partially corrected by an underestimate in E.

Let us now compute the time required for the cooling of an atmosphere overcharged with CO_2, using Hettner's absorption data, remembering that in this case

$$T_A=1.18T_S-25. \tag{9}$$

Substituting (3), (4), (8) in (5), and eliminating T_A by means of (9), we find

$$t=\int_{253}^{T_s}\frac{\frac{289}{(231)^{4.5}}[T_S-21.2]^{4.5}-304}{\sigma T_S^4-\kappa T_S^{3.5}}dT_S \text{ minutes}, \tag{10}$$

where $\kappa = 980\cdot 10^{-12}$ and $\sigma = 82\cdot 10^{-12}$.

In order to integrate (10) it is necessary to expand $[T_S-21.2]^{4.5}$; since the expansion converges very rapidly, only the first three terms need be retained, and hence (10) may be written as

$$\begin{aligned} t=\frac{289}{(231)^{4.5}}\Bigg\{&\int_{253}^{T_s}\frac{T_S^{4.5}}{\sigma T_S^4-\kappa T_S^{3.5}}dT_S \\ &-95.4\int_{253}^{T_s}\frac{T_S^{3.5}}{\sigma T_S^4-\kappa T_S^{3.5}}dT_S \\ &+3540\int_{253}^{T_s}\frac{T_S^{2.5}}{\sigma T_S^4-\kappa T_S^{3.5}}dT_S\Bigg\} \\ &-304\int_{253}^{T_s}\frac{dT_S}{\sigma T_S^4-\kappa T_S^{3.5}}. \end{aligned} \tag{11}$$

Each of the above integrals can be easily evaluated and the final expression for t becomes

$$\begin{aligned} t=&81.2\{0.667y^3+11.95y^2+94.80y \\ &+2606\cdot\log_{10}(0.0837y-1)\} \\ &-0.6204\cdot 10^4\{0.20x^5+0.021x^4+0.0023x^3 \\ &+0.00029x^2+0.000041x\} \\ &+595\cdot 10^4\cdot\log_{10}(0.0837-x)-1089\cdot 10^4 \text{ minutes}, \end{aligned} \tag{12}$$

where

$$y=T_S^{0.5},\ x=T_S^{-0.5}.$$

Similarly, it is possible to compute the time for the cooling of an atmosphere of normal CO_2 content, using Weber and Randall's absorption data.

In figure 7 are plotted the thermograms for the two cases studied. The inset figure shows the initial rate of cooling. In the first few hours the temperature falls very rapidly from 0° to the critical temperature, −20° (or −33°), while the air temperature remains practically constant. The surface temperature can fall below −20° (or −33°) provided only that the maximum air temperature also falls, so that at t=1.5 hours (or 2.3 hours), the temperature curves show discontinuities in slope; from this point on, the cooling rates become smaller and smaller, so that for the surface temperature to fall to −40° requires about 15 days (or 2 days) of cooling, and to fall to −60° requires about 62 days (or 23 days).

The large difference in the cooling rates for the two cases studied is due to the fact that the return atmospheric radiation is different in the two cases. A larger amount

[3] According to Frost (26) "at Fairbanks dense fog always accompanies temperatures of −45° F. or lower. The records for January 1934, show 348 hours with −45° F. or lower and during this time there were 320 hours of dense fog. On one occasion the fog prevailed for 155 consecutive hours." From 3 polar year airplane soundings taken through low temperature fog at Fairbanks it was found that their heights were 115 m., 200 m., and 75 m.

of return atmospheric radiation allows the surface temperature to fall a lesser number of degrees without a corresponding fall in the temperature of the free air; and because a larger amount of return atmospheric radiation implies a smaller amount of radiation passing to space, it will take more time for the surface temperature to fall to a given value. However, in the cooling of the free air, these two effects tend to compensate each other in the following manner: For the same temperature of the isothermal layer, the loss of radiation to space in one case takes place at a higher surface temperature than in the second case; this tends to equalize the rates of loss of energy, and so the free air thermograms do not diverge as much as the surface thermograms. For the isothermal layer to cool to −10° takes about 3 days as against 2 days; to −20°, 11 days as against 7 days; and to −30°, 25 days as compared to 18 days.

Alaska Section", published by the Weather Bureau, the writer obtained the minimum temperatures that occurred during each of the above months, except the value for January 1934, which was taken from Frost (**26**). The number of clear days also was noted, and to this was added one-half the number of partly cloudy days to find the percentage of clear sky during the month. It was not until the night of October 19–20 that the temperature fell below −20° C., so that this date can be taken as the zero-point on the time scale. In other words, from this date on, the temperature of the free-air began to decrease by surface cooling in the manner described above. From the thermograms in figure 7 were found the number of days necessary for the temperatures to decrease to the observed values. The results, together with the monthly totals of unmelted snow as published in the "Climatological Data", are shown in table 6.

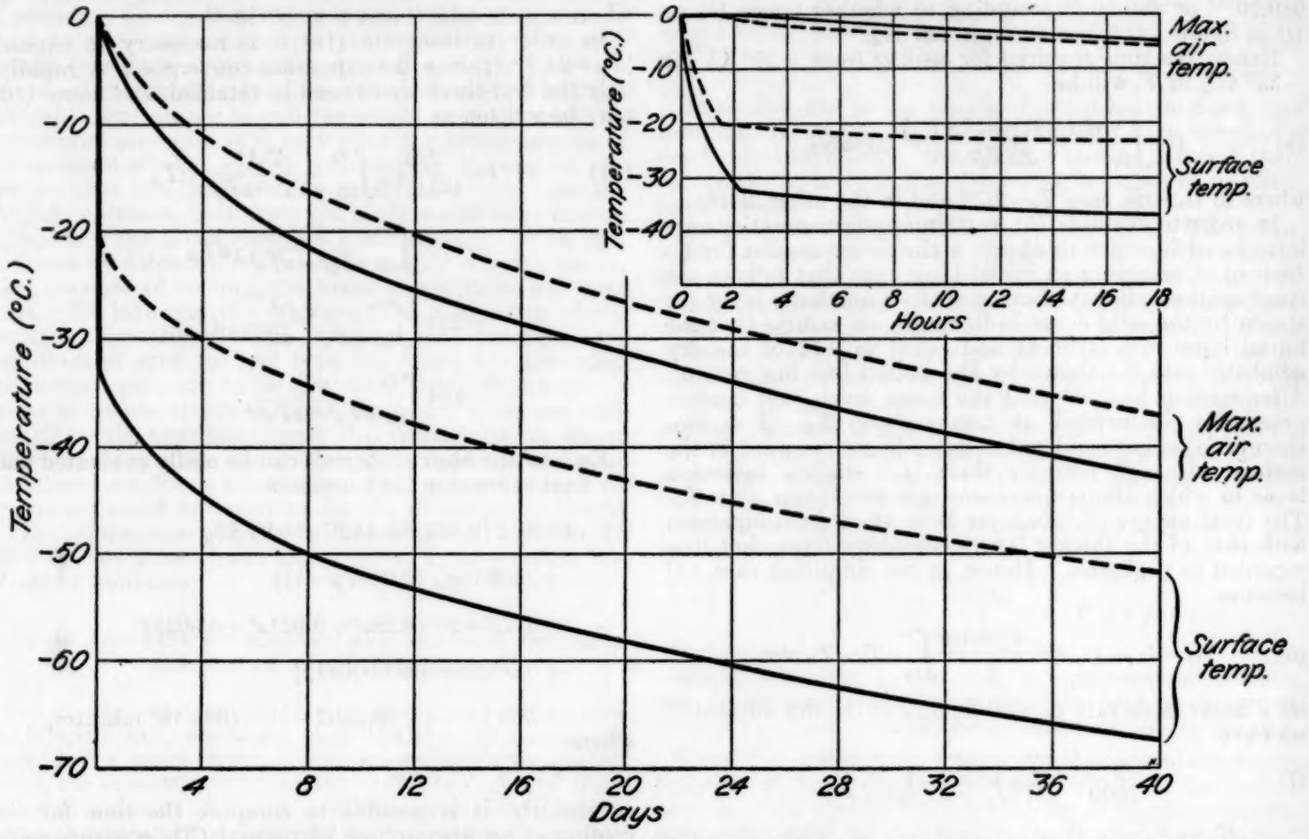

FIGURE 7.—Computed thermograms based on (*a*) Hettner's data in atmosphere of abnormal CO_2 content (shown by broken lines; (*b*) Weber and Randall's data in atmosphere of normal CO_2 content (shown by solid lines).

The rates of cooling presented in figure 7 must be regarded as *maximum rates of cooling*, since *absolutely calm, cloudless conditions have been assumed.* Clouds, or even a small wind movement, would delay the cooling considerably. In order to decide which of the two sets of thermograms is closer to reality, it would be necessary to study the thermogram of a station at a high latitude and situated on a snow-covered continent (or thick ice cover), and to make allowances for cloudiness, wind movement, and advection of colder or warmer air. As this is impossible, we must be satisfied with a less rigorous check. This was done by examining the march of minimum temperature at Fort Yukon, Alaska (66°34′ N, 145°18′ W, 140 meters above mean sea level), from August 1933 to January 1934. From the "Climatological Data for the

TABLE 6.—*March of monthly minimum temperatures at Fort Yukon, Alaska (66°34′ N, 145°18′ W, 139 meters above m. s. l., thermometer shelter 1.3 meters above the ground)*

1 Date	2 Inches of unmelted snow for the month	3 Minimum temperature	4 Number of days from Oct. 20	5 Percent clear sky	6 Number of clear days	7 Number of days—Hettner—high CO_2 content	8 Number of days—Weber & Randall—normal CO_2 content
1933–34		° C.					
Aug. 28	0	0					
Sept. 2	8	−8					
Oct. 20	7	−31	0	42	0	0	0
Nov. 27	13	−42	38	40	16	18	3
Dec. 31	2	−54	72	68	38	43	13
Jan. 14		−61	86	78	49	66	25

In table 6, we see that the number of clear days which elapsed from October 20 to the dates of the various monthly minimum temperatures as given in column 6, is below that of column 7, and above that of column 8, where it must be remembered that the latter values are in terms of "ideal" days—that is, full days during which calm, cloudless, sunless conditions prevailed. Now, the number of days given in column 6, if reduced to "ideal" days, would be much less, because some sunlight, cloudiness, and wind movement undoubtedly occurred during the period. Also it is possible that a temperature 1° higher than the minimum may have occurred at some earlier day in the month, and this too would reduce the number of days in column 6. Even so, the values in column 7 are much higher than those in column 6, showing that the combination of Hettner's absorption data and an abnormal CO_2 content leads to a rate of cooling much slower than that observed in Nature. On the other hand, using the values of Weber and Randall, together with a normal CO_2 content in the atmosphere, a rate of cooling is found which is large enough to account for the march of minimum temperature observed at Fort Yukon.

It may be argued that the low temperatures observed at this station were not created in the vicinity by radiational cooling but rather are due to the importation of colder air from other localities. This may be true, and the fact that −54° was observed at this station on December 31 may mean that it was observed at an earlier date at another, colder locality. This, however, would still mean that the values in column 7 are too high, unless a serious error were made in the selection of October 20 as the zero-point on the time scale. For example, it might have happened that some other colder station reported a temperature below −20° before October 20 and several extra days of cooling occurred before this air moved into Fort Yukon. This would increase the number of days in column 6. To check this possibility, the minimum temperatures for all the weather stations in the Yukon Valley, as published in the October "Climatological Data," have been inspected. On October 17, Eagle (about 200 miles southeast of Fort Yukon) was the first to report a minimum temperature below −20° C. (−21°). On October 19 several more stations reported minimum temperatures below −20°, and finally on October 20 Fort Yukon reported the same. Now if we should start counting the days from October 17, this would increase the number of clear days in column 6 by at most 3. Even if this were done the values in column 7 would still be too large.

Importation of cold air from north of the Yukon Valley is hindered by the Endicott Range; and this air, even if brought down from the north, would usually be warmer than the interior air, since it is well known that air over the frozen ocean is in general warmer than that over a continental snow cover [(27) p. 96 et seq.]. This is illustrated by comparing the mean December temperature for Point Barrow, Alaska (71°23′ N., 156°17′ W., on the Arctic coast) and that for Fort Yukon. The normal temperatures for December are −25.2° C. and −29.6°, respectively; while the mean December 1934 temperatures were −25.8° and −37.3°, respectively.

Another possibility of error lies in the initial lapse-rate assumed. It might be argued that during the summer the air over the Arctic Ocean is much cooler than assumed in figure 5, and that less time would therefore be required to cool the air to the values observed at Fort Yukon. This would then decrease the values in column 7, table 6, and make them agree better with the observed rates of cooling. However, it is a well-known fact that the sea-level temperature over the Arctic during the summer is about 0° C. [(27) p. 89]; and assuming a lapse-rate of the kind shown in figure 5, that is, air in convective equilibrium (above a shallow adiabatic layer) with an ocean surface of temperature 0° C., means that this air would represent the coldest type of air possible over the Arctic during the summer. For this reason, and because of the assumptions of a calm, cloudless, sunless atmosphere, the rates of cooling found above must be regarded as *maximum values*. It must be realized that this is true only for the northern hemisphere, since over the Antarctic the summer temperature is much lower than 0° C.; the mean December ice barrier temperature observed by Simpson was about −6° C. [(28) p. 31, et seq.] and the mean Antarctic Plateau temperature much lower.

HEIGHT AND TEMPERATURE OF TROPOPAUSE OVER POLAR MARITIME AND POLAR CONTINENTAL AIR

In figure 8 we have reproduced the Ås soundings from Palmén's paper [(1) fig. 5]. The time interval between

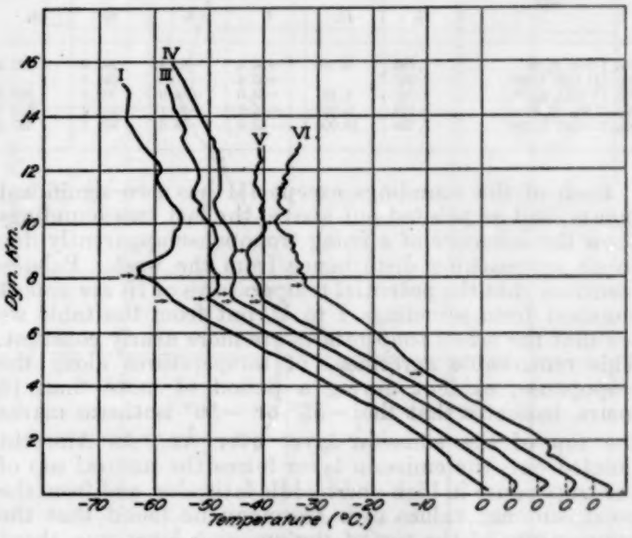

FIGURE 8.—Soundings at Ås. Arrows designate the tropopauses and noteworthy significant points (after Palmén).

soundings I and III is 8 hours; we notice that the tropopause in III is at about 7.3 kilometer, or about 0.8 kilometer lower than in I, and its temperature is −55.4° C. as compared to −62.8° C. in I; but, as Palmén pointed out, in sounding I a discontinuity in lapse rate already appears at 7.2 kilometers at a temperature of −56.6° C. Palmén suggests that this point is at the cold front which had passed Ås during the preceding night; but it appears more reasonable to interpret it as the first sign of a new tropopause, since the tropopauses found in soundings III, IV, V are at approximately the same height and have approximately the same temperature as this discontinuity. (As Palmén points out, the first signs of a second, higher tropopause found in soundings V and VI, apparently are due to an approaching disturbance west of Iceland.) The destruction of the original tropopause in I can be explained by its being bounded above and below by strata of warmer air; the temperature of the top of the tropopause inversion is −54.8°, which is not far different from the temperature of −56.6° found at the discontinuity below the

tropopause, while the temperature at the bottom of the inversion is −62.8°. From considerations of radiative balance, it appears that the temperature of the latter point must rise until it becomes equal to that of the bounding air, provided the inversion is not maintained by convection. An exception would occur in the presence of a discontinuity in moisture, which would allow the sharp inversion to be maintained in the manner of a "dry inversion" (**29**). However, at the low temperatures considered here, the amount of water vapor is so small that differences in it can hardly influence the radiative balance. Hence, provided convection is absent, the original tropopause in sounding I must vanish and the lower discontinuity become the new tropopause. In table 7 (reproduced from Palmén's paper) are presented the heights, temperatures, and potential temperatures at high-level significant points on the Ås soundings:

TABLE 7.—*High-level significant points in the Ås soundings*

[After Palmén]

Soundings 1933	Ht. in dyn. M.		Temperature in °C.		Pot. temperature	
	H_1	H_2	t_1	t_2	θ_1	θ_2
No. I Feb. 2, 15[31]	7,196	8,146	−56.6	−62.8	292.8	297.2
No. III Feb. 2, 23[04]	7,265		−55.4		294.8	
No. IV Feb. 3, 3[00]	7,141	7,401	−55.0	−56.0	293.2	295.6
No. V Feb. 3, 6[35]	7,159	8,912	−55.3	−58.4	292.2	312.7
No. VI Feb. 3, 13[10]	7,758	10,000	−52.6	−58.0	302.4	327.2

Each of the soundings except III has two significant points; and as pointed out above, the last two soundings show the influence of a rising tropopause apparently due to an approaching disturbance from the west. Palmén mentions that the potential temperatures of H_1 are almost constant from soundings I to V, but from the table we see that the *actual temperatures* are more nearly constant. This remarkable agreement of temperatures along the tropopause, evident during a period of more than 16 hours, indicates that the −55° or −56° isotherm marks the top of the emission layer over Ås. As Albrecht pointed out, the emission layer forms the natural top of the tropopause in high and middle latitudes, and from the mean summer values over Germany he found that the temperature of the top of the emission layer was about −50°; in his second paper (**17**), from a theoretical consideration, he found −53°; in the Ellendale sounding (fig. 1), from an independent analysis, the writer computed a temperature of −52°. Although the mean temperature of H_1 from the Ås soundings (−55.6°) is slightly lower than the above values, it appears that this isotherm also marks the top of the emission layer over Ås.

As pointed out by Albrecht and others (**17**, **30**), the tropical tropopause is higher than the emission layer, because of the continuous convection extending to high levels. Radiation currents both from the warmer emission layer and the warmer stratosphere tend to destroy the high cold tropopause, but convection dominates and maintains it. Now, when polar continental air leaves its source region and crosses an open ocean surface, then violent convection ensues; and although it is not yet possible to compute the height of this convection, it is probable that, initially, when the air temperatures are very low it extends to about 8 or 9 kilometers, a few kilometers above the emission layer. However, when the air (now polar maritime) passes over land, the tropopause is no longer maintained at its original height by convection, and its height must now be determined by the emission layer. Radiative balance will wipe out the original tropopause; and a lower, warmer one will form just above the emission layer. As the air moves over a snow surface and cooling of the lower atmosphere occurs, then, as pointed out above, the lower tropopause can contract about 500 meters. This will tend further to lower the tropopause and to raise its temperature. In table 7 we see that the new mean height and mean temperature of the new tropopause (H_1) are about 7.2 kilometers and −56°, respectively. In sounding (*c*), figure 1, the height and the temperature of the tropopause at Ellendale are about 6.2 kilometers and −52°. Hence, we see that after the new tropopause forms above the emission layer, the differences in height and temperature of the tropopause can be very nearly explained by its lowering and adiabatic warming due to the cooling and contraction of the troposphere.

From the arguments presented above we should expect a winter polar continental tropopause to be lower and warmer than a polar maritime tropopause. To verify this by observations, in table 8 is presented a portion of Palmén's table [(**31**), table 1], that gives the mean temperatures of polar (maritime) air over England for the winter half-year (October-March, 1924–29), together with polar continental data for North America. Palmén selected each of the soundings after a careful analysis of the synoptic situation so that they are representative of individual air masses, and grouped them according to high and low surface pressure. Although Palmén calls the air "polar", we assume on account of the maritime exposure of England that it is polar maritime. No other comparable group of observations at high latitudes, giving the mean winter structure of polar continental air to high levels, seems to be available. The observations made at Pawlowsk, Russia (59°41′ N, 30°26′ E), 1902–09, are available only as monthly means, and cannot be used since they probably include many cases of modified polar maritime and tropical air. However, in table 8 are shown means of the sounding balloon observations taken at Ellendale, N. Dak., in the winter half-year of 1932–33, during pronounced polar continental outbreaks. These observations have been discussed by Ballard (**32**); they were taken in two series a month, each series comprising three soundings made within 18 hours, the first at local noon, the second at midnight, and the third at 7 the next morning. Ballard attempted to correct the daytime observations for heating of the bimetal due to insolation and these corrections are included in table 8; for the noon flights they range from −1° C. at the surface to −4° at 10 kilometers, and for the morning flights from 0° at the surface to −1° at 10 kilometers.[4] Since some series did not include all three soundings, means of each series were computed and these were used to find the winter means, equal weight being given to each series. Five series were taken during pronounced cases of polar continental outbreaks in the winter half-year on the following dates: December 14–15, 1932; December 29, 1932; January 11–12, 1933; February 8–9, 1933; March 8–9, 1933. The individual soundings may be seen in Ballard's paper.

[4] These corrections are not included in the soundings reproduced in figures 1 and 9, since they were found from studying the mean differences and should therefore be applied only to mean values.

TABLE 8.—*Thermal Structure of Polar Maritime and Polar Continental Air*

Height in kilometers	England				Ellendale, N. Dak.	
	1022 mb.		996 mb.		1017–1030 mb.	Number of soundings
	Temperature	Number of cases	Temperature	Number of cases	Temperature	
	° C.		° C.		° C.	
Surface	+4.4	31	+6.7	21	−18.1	12
1	−1.1	31	−0.9	21	−20.9	12
2	−5.1	31	−6.7	21	−21.7	12
3	−9.8	31	−13.9	21	−25.0	12
4	−16.1	31	−19.6	21	−30.5	12
5	−22.8	31	−27.1	21	−35.7	12
6	−29.5	31	−34.6	21	−42.1	12
7	−36.6	31	−41.4	21	−46.7	12
8	−43.2	31	−46.2	20	−50.1	12
9	−49.7	31	−48.7	20	−51.5	12
10	−54.3	31	−49.9	20	−51.4	12
11	−57.0	31	−49.7	20	−50.8	12
12	−56.5	31	−49.7	18	−51.6	12
13	−54.4	29	−50.5	17	−51.1	12
14	−55.2	26	−51.4	14	−52.3	11
15	−55.9	21	−52.1	12	−53.7	9
16	−56.1	21	−53.3	12	−52.9	8
TROPOPAUSE						
H km	10.70		8.55		7.4	
T	−58.8		−50.7		−50.3	

In table 8, by comparing polar maritime air in the neighborhoods of low pressure and of high pressure, we see that the former has a colder troposphere (except at the surface layer), a lower, warmer tropopause, and a warmer stratosphere. On the other hand, polar continental air has a much colder, stable troposphere than either of the two types of polar maritime air, and a lower tropopause whose temperature is slightly higher than that of the low-pressure type of maritime air but much higher than that of the high-pressure type; however, the actual stratosphere temperatures for the continental air seem to be between those of the two types of maritime air, although closer to those of the low-pressure type.

An explanation of these differences will not be attempted here, but the following important points should be emphasized. The lowest tropopause of the three types of air is found at Ellendale, a station about 600 kilometers south of the latitude of England, during periods of higher than normal surface pressure (the following are the respective mean sea-level pressures for each series: 1,030 mb., 1,017, 1,021, 1,029, 1,024). The temperature of this tropopause is even slightly higher than that of the warmest type of winter tropopause which occurs in England (in the neighborhood of a deep occluded cyclone).[5] The low, warm tropopause found over Ellendale during polar continental outbreaks probably could be found over all deep polar continental air masses; and its evolution from a higher, colder tropopause over polar maritime air is probably explained by the reasoning above, viz, the cessation of convection as the polar maritime air leaves the open ocean, thus allowing the emission layer to determine the new tropopause, and the contraction of the troposphere due to cooling.

THE EFFECTS OF SUBSIDENCE

As pointed out by Namias (**33**), surfaces of subsidence in American polar continental air extend over large areas and are also surfaces of constant potential temperature. Subsidence inversions will naturally form where some small inversion or weakening of the lapse rate already exists. Formerly it has been thought that radiative transfer across a moisture discontinuity or haze line would cause the initial weakening of the lapse rate, and subsidence would accentuate this into an inversion (**34, 33**); but from the above, it is seen that there also exists another explanation of the initial discontinuity in lapse rate that seems more plausible in the case of subsidence inversions covering large areas. If a homogeneous polar maritime air mass moves over a broad horizontal snow surface, then, after a certain interval of time, the isothermal layer

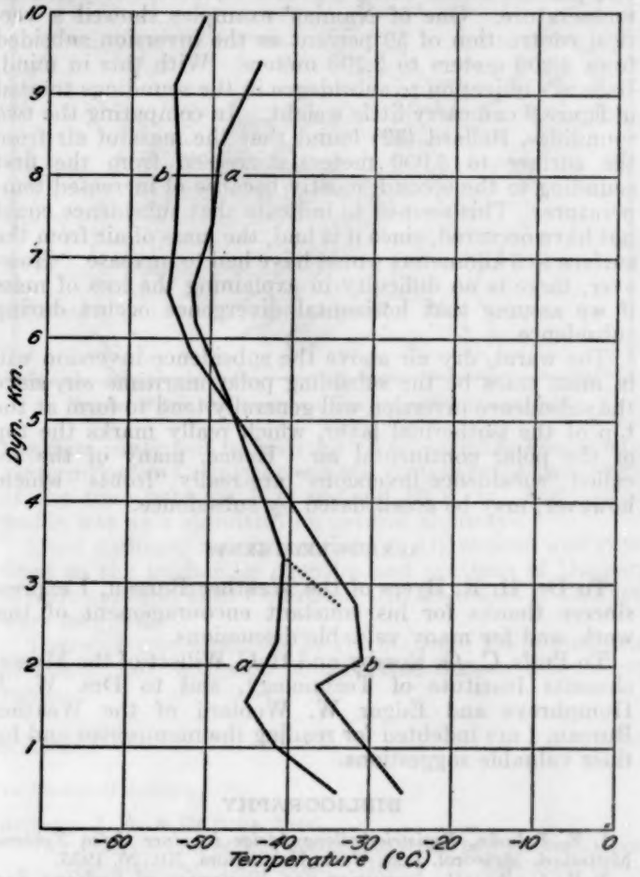

FIGURE 9.—Soundings at Ellendale, N. Dak., (*a*) February 8, 1933, 13.28 h.; (*b*) February 9, 1933, 7.42 h., local time.

will extend up to a certain height which will be nearly the same over the entire area, and so the top of the isothermal layer will have practically the same potential temperature. When the air mass moves southward and subsidence begins, the top of this layer will naturally tend to become the top of the subsidence inversion and will be characterized by almost constant potential temperature over its entire surface. To give an example of this phenomenon, portions of two balloon soundings made at Ellendale, N. Dak., on February 8–9, 1933, have been plotted on figure 9. The first of these soundings [curve (*a*), also plotted in fig. 1] was taken at 13.28 h. on the 8th; the second [curve (*b*)], made 18 hours afterward, shows a higher temperature from the surface to about 5,000 meters, the maximum difference being 12° C. at about 2,000 meters, although the surface temperature increased

[5] The temperature differences may be even larger than those shown in table 8, since it is unlikely that the English daylight soundings were corrected for insolation, as were the Ellendale soundings.

by only 8°. Evidently subsidence occurred above the well-stirred surface layer and this is verified by the close agreement of the potential temperatures at the top of the stable layers, 286° for sounding (*a*) and 288° for sounding (*b*). The decrease in thickness of the stable layer must be compensated by horizontal divergence, as Namias brought out in his example. According to his treatment of three well-defined cases of subsidence, the lapse rate of the air above the inversion decreased as the inversion became lower, but the decrease was much larger than that computed for a layer sinking without any change in its horizontal cross-section. Hence, horizontal divergence was necessary to explain the increased stability, since this process would bring together isotherms of potential temperature. One of Namias' examples showed a vertical contraction of 50 percent as the inversion subsided from 3,200 meters to 2,200 meters. With this in mind, Ballard's objection to subsidence in the soundings treated in figure 9 can carry little weight. In comparing the two soundings, Ballard (**32**) found that the mass of air from the surface to 5,000 meters decreased from the first sounding to the second, mostly because of increased temperature. This seemed to indicate that subsidence could not have occurred, since if it had, the mass of air from the surface to 5 kilometers would have had to increase. However, there is no difficulty in explaining the loss of mass if we assume that horizontal divergence occurs during subsidence.

The warm, dry air above the subsidence inversion will in most cases be the subsiding polar maritime air, since the subsidence inversion will generally tend to form at the top of the isothermal layer, which really marks the top of the polar continental air. Hence, many of the so-called "subsidence inversions" are really "fronts" which, however, may be accentuated by subsidence.

ACKNOWLEDGMENTS

To Dr. H. R. Byers of the Weather Bureau, I express sincere thanks for his constant encouragement of this work, and for many valuable discussions.

To Profs. C.-G. Rossby and H. C. Willett of the Massachusetts Institute of Technology, and to Drs. W. J. Humphreys and Edgar W. Woolard of the Weather Bureau, I am indebted for reading the manuscript and for their valuable suggestions.

BIBLIOGRAPHY

1. E. Palmén, *Registrierballonaufsteige in einer tiefen Zyklone.* Mitteil. d. Meteorol. Inst. Univ. Helsingfors, No. 26, 1935.

2. H. C. Willett, *Discussion and Illustration of Problems Suggested by the Analysis of Atmospheric Cross-sections.* Papers in Phys. Ocean. and Meteor., Mass. Inst. Techn. and Woods Hole Ocean. Inst., IV, 2, 1935.

3. G. Falckenberg, *Absorptionkonstanten einiger meteorologisch wichtiger Körper für infrarote Wellen.* Meteorol. Z., 45, 334, 1928.

4. H. Rubens and E. Aschkinass, *Beobachtungen über Absorption und Emission von Wasserdampf und Kohlensäure im ultrarothen Spectrum.* Ann. d. Phys. u. Chem., 64, 584, 1898.

5. F. E. Fowle, *Water-Vapor Transparency to Low-Temperature Radiation.* Smith. Misc. Coll. Vol. 68, No. 8, 1917.

6. G. Hettner, *Über das ultrarote Absorptionsspektrum des Wasserdampfes.* Ann. d. Phys., 55, 476, 1918.

7. L. R. Weber and H. M. Randall, *Absorption Spectrum of Water Vapor beyond 10μ.* Phys. Rev., 40, 835, 1932.

8. G. C. Simpson, *Further Studies in Terrestrial Radiation.* Mem. Roy. Met. Soc., Vol. III, No. 21, 1928.

9. K. R. Ramanathan and L. A. Ramdas, *Derivation of Ångström's Formula for Atmospheric Radiation, etc.* Proc. Ind. Acad. Sci., 1, 822, 1935.

10. F. E. Fowle, *Smith. Phys. Tables.* 8th Ed., 1933. p. 392.

11. H. Mosby, *Sunshine and Radiation.* Norwegian N. Pole Exp. with the "Maud", 1918–25, Scientific Results, Vol. I, No. 7, 1932.

12. P. K. Raman, *Heat Radiation from the Clear Atmosphere at Night.* Proc. Ind. Acad. Sci. 1, 815, 1935.

13. C. L. Pekeris, *Development and Present Status of the Theory of the Heat Balance in the Atmosphere.* Mass. Inst. Techn., Meteorol. Course, Prof. Notes, No. 5, 1932.

14. C. G. Abbot, *Radiation of the Planet Earth to Space.* Smith. Misc. Coll., Vol. 82, No. 3, 1929.

15. A. Ångström, *Radiation and Temperature of Snow and the Convection of Air at its Surface.* Arkiv f. Mat., Astron., o. Fysik, Bd. 13, No. 21, 1918.

16. F. Albrecht, *Der Wärmeumsatz durch die Wärmestrahlung des Wasserdampfes in der Atmosphäre.* Zeitschr. f. Geophy., 6, 420, 1930.

17. F. Albrecht, *Über die "Glashauswirkung" der Erdatmosphäre und das Zustandekommen der Troposphäre.* Meteorol. Z., 48, 57, 1931.

18. F. Albrecht, *Das Quantentheoretisch gegebene Wasserdampfspektrum über den Wärmeumsatz strahlender Luftschichten.* Meteorol. Z., 48, 476, 1931.

19. H. C. Willett, *American Air Mass Properties.* Papers in Phys. Ocean. and Meteorol., Mass. Inst. Techn. and Woods Hole Ocean. Inst., II, 2, 1933.

20. K. R. Ramanathan, *Effect of Radiation on the Equilibrium of the Higher Layers of the Troposphere, etc.* Beitr. z. Phys. d. fr. Atmos., 18, 196, 1932.

21. E. H. Gowan, *The Effect of Ozone on the Temperature of the Upper Atmosphere.* Proc. Roy. Soc. A, 120, 655, 1928.

22. E. H. Gowan, *The Effect of Ozone on the Temperature of the Upper Atmosphere II.* Proc. Roy. Soc. A, 128, 531, 1930.

23. D. Brunt, *Phys. and Dyn. Meteorology.* Cambridge, 1934, p. 125.

24. M. Jansson, *Über die Wärmeleitungsfahigkeit des Schnees.* Ofversigt af Kongl. Vetenskaps-Akademiens Förhandlingar, Stockholm, 1901, No. 3.

25. C.-G. Rossby, *Thermodynamics Applied to Air Mass Analysis.* Mass. Inst. Techn., Meteorol. Papers, I, 3, 1932.

26. R. L. Frost, *Climatological Review of the Alaska-Yukon Plateau.* Mo. Wea. Rev., 62, 269, 1934.

27. H. U. Sverdrup, *Meteorology, Pt. I, Discussion.* Norwegian N. Polar Exp. with the "Maud", 1918–25, Scient. Res., Vol. II, 1933.

28. G. C. Simpson, *Meteorology, Discussion.* Vol. I. Brit. Antart. Exp., 1910–13, Calcutta, 1919.

29. J. Namias, *The Structure and Maintenance of Dry-Type Moisture Discontinuities not Developed by Subsidence.* To be published shortly.

30. V. and J. Bjerknes, Solberg, Bergeron, *Physikalische Hydrodynamik.* Berlin, 1933, pp. 663–664.

31. E. Palmén, *Aerologische Untersuchungen der Atmosphärischen Storungen, etc.,* Mitteil. d. Meteorol., Inst. Univ. Helsingfors, No. 25, 1933.

32. J. C. Ballard, *Some Results of Sounding-Balloon Observations during the Second International Polar Year.* Mo. Wea. Rev., 62, 45, 1934.

33. J. Namias, *Subsidence within the Atmosphere.* Harvard Meteorol. Studies, No. 2, 1934.

34. S. Mal, S. Basu, and B. N. Desai, *Structure and Development of Temperature Inversions in the Atmosphere.* Beitr. z. Phys. d. fr. Atmos., 20, 56, 1932.

35. R. Mügge, *Energetik des Wetters.* Meteorol. Z., 52, 168, 1935.

36. R. Mügge and F. Möller, *Zur Berechnung von Strahlungsströmen und Temperaturenderungen in Atmosphären von beliebigen Aufbau.* Zeitschr. f. Geophy., 8, 53, 1932.

37. R. Mügge and F. Möller, *Über Abkühlung in der freien Atmosphäre infolge der langwelligen Strahlung des Wasserdampfes.* Meteorol. Z., 49, 95, 1932.

DUSTSTORMS IN THE UNITED STATES, APRIL 1936

By R. J. MARTIN

Dusty conditions which had prevailed during the preceding several months continued into April, but with decreased frequency and mostly with diminished severity. A comparison of the April chart with that for March shows that the center of maximum duststorm frequency migrated slightly to the north, while the greatest number reported diminished from more than 22 in northern Texas in March to 14 in western Oklahoma in April. The extent of the area affected by dense dust is also less; dense dust was reported only occasionally to eastward of the Mississippi River, and no reports of severe duststorms were received from the Lake region, the upper Ohio Valley, or New England.

The shaded area on the April chart delineates those sections in which dense dust was reported, and the lines show the number of occurrences; the larger area, within the dotted line, includes stations reporting only light dust or dusty conditions. Such conditions prevailed on a varying number of days, ranging from only one in portions of Mississippi, Ohio, Tennessee, and southern Texas, to 3 in Illinois, 5 in Montana, 9 in western Nebraska, and 19 in portions of Oklahoma.

A few of the April storms in Colorado were comparable in severity with those of the preceding month in that State. There were complaints of crop damage in several western States; and traffic was hindered, at times for several hours, by decreased visibility. There were several reports of snow tinged with dust; "red snow" fell in Mesa Verde National Park early in the month.

Considerable damage was done to crops in Curry County, N. Mex., by a dust "front" which entered the extreme northeastern corner of the State on the 9th and had moved southward to the extreme southeastern corner on the following day; a severe duststorm on the 23d reduced visibility to one-fourth mile in many sections. The most severe New Mexico storm of the month occurred between the Rio Grande and the eastern State line, on the 25th and 26th; the dust extended upward about 7,000 feet and reduced visibility to approximately one-fourth mile. Dusty conditions were reported at Roswell, N. Mex. on 14 days.

No damage resulted from a duststorm at Pueblo, Colo., on the 15th, where the cloud reached a height of 10,000 feet; but the general storm of the 3d, which enveloped east-central counties from the Kansas border to the one hundred and fourth meridian, reduced visibility to 100 yards in portions of the lower Arkansas Valley, where

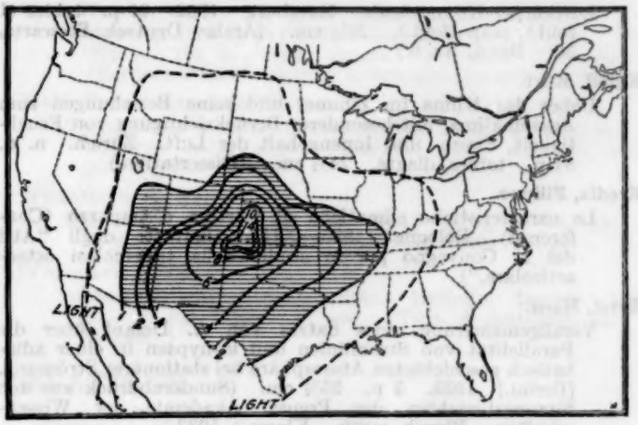

Number of days with duststorms, or dusty conditions, April 1936.

the dust continued to blow for 10 consecutive hours. In eastern Powers County on the 4th visibility was zero much of the time between 5 p. m. and 10 p. m., and motor traffic was at a standstill on several highways.

Dust damage, mostly erosion, in Oklahoma was confined to the panhandle counties and portions of Harper, Woodward, and Ellis Counties. No estimates of damage were received.

There were no reports of loss of life from the duststorms of the month, although considerable human discomfort resulted.

BIBLIOGRAPHY

C. FITZHUGH TALMAN, *in Charge of Library*

RECENT ADDITIONS

The following have been selected from among the titles of books recently received as representing those most likely to be useful to Weather Bureau officials in their meteorological work and studies.

Arctic Institute of the U. S. S. R.

Transactions. v. 1, 18. Leningrad. 1933–35. 25½ cm. v. 1. Scientific results of the Arctic expedition on the "Sedov" in 1930. Hydrology and meteorology. 174 p.—v. 18. Scientific results of the Arctic expedition on the "Lomonosoff" in 1931. Hydrology and Meteorology. 106 p.

Australia. Radio Research Board.

Report No. 5. Atmospherics in Australia. 1. by G. H. Munro and L. G. H. Huxley. Melbourne. 1932. 49 p. tables, diagrs. 24 cm. (Council for scientific and industrial research. Bulletin No. 68.)

——— Report No. 8. 1. Simultaneous observations of atmospherics with cathode ray direction-finders at Toowoomba and Canberra, by G. H. Munroe, H. C. Webster, and A. J. Higgs. 2. Atmospheric interference with reception, by W. J. Wark. Melbourne. 1935. 61 p. tables, diagrs. 24 cm. (Council for scientific and industrial research. Bulletin No. 89.)

Awberry, J. H., & Griffiths, Ezer.

An investigation of the wet-and-dry-bulb hygrometer at low temperatures. Cambridge. [1935.] p. 684–702. tabs., diagrs. 27 cm. (Repr.: Physical socy. of Lond. Proc. v. 47, 1935.)

Beelitz, Paul.

Die Haupttypen des jährlichen Ganges der Niederschläge in Europa. Ohlau i. Schl. 1932. 112 p. tables, diagrs. 24 cm. (Inaug.-Diss.)

Brotzman, W. S.

Observing the weather. Pittsburgh. 1935. p. 138–150. 23 cm. (Railway club of Pittsburgh. Official proceedings. v. 34, no. 6. April 25, 1935.)

Byrd, Richard Evelyn.

Discovery; the story of the second Byrd Antarctic expedition . . . introduction by Claude A. Swanson. New York. 1935. 405 p. front., pls., ports., map. 24 cm. Maps on lining-papers. "First edition."

Canada. Department of Marine.

Meteorological tables, by A. J. Connor. (Reprinted from the Canada year book, 1931.) Ottawa. 1931.

Daniel Guggenheim Airship Institute, Akron, Ohio.

Publication no. 3. Report on airship forum, July 25–26, 1935 . . . edited by Theodor von Karman—Theodor Troller. 1935. 133 p. ill., tables, diagrs. 28 cm.

Deeley, Richard Mountford.

A manual of the principles of meteorology. With frontispiece, 34 other illustrations (including 3 plates) and 27 tables. London. 1935. 285 p. diagrs. 25 cm.

Díaz, Emilio L.

Sobre la circulación atmosférica. n. d. [1935.] p. 215–219. tables. 26½ cm. (De los "Anales de la S. C. Argentina", E. V., T. CXIX.)

Dinies, Erwin.

Luftkörper-Klimatologie. Hamburg. 1932. 21 p. tables (1 fold.), map (fold.). 29½ cm. (Archiv Deutsch. Seewarte, 50. Band, Nr. 6.)

Egloff, Kurt.

Ueber das Klima im Zimmer und seine Beziehungen zum Aussemklima, mit besonderer Berücksichtigung von Feuchtigkeit, Staub- und Ionengehalt der Luft. Zürich. n. d. 84 p. tables, diagrs. 24½ cm. (Dissertation.)

Eredia, Filippo.

Le caratteristiche climatiche di Cortina d'Ampezzo (Conferenza). Bologna. 1935—XIII. (Estratto dagli "Atti del II Convegno per lo studio della tubercolosi osteo-articolare.")

Ertel, Hans.

Verallgemeinerung eines Satzes von A. Defant über die Parallelität von Stromlinien und isohypsen in einer adiabatisch geschichteten Atmosphäre bei stationärer Strömung. [Berlin.] 1933. 3 p. 25½ cm. (Sonderabdruck aus den Sitzungsberichten der Preuss. Akademie der Wissenschaften. Physik.-math. Klasse. 1933.)

Frank, H.

Wetterkunde für den Wassersport. Mit einem Anhang: Windkarten, by Kurt Eichler. Berlin. c1934. 64 p. ill., maps, tabs., diagrs. (all part. fold.) 18½ cm.

Freymann, Rudolf.

Das Klima von Portugal auf Grund der Wetterbeobachtungen 1903–1922. Gieszen. 1935. 126 p. tables, fold. maps. 22 cm. (Dissertation.)

Friedrich, W.

Messungen der Verdunstung vom Erdboden. Breslau. 1935. p. 234–251. tables, diagrs. 24½ cm. (Sonderdruck aus Der Kulturtechniker. Zeitschrift der Deutschen Kulturtechnischen Gesellschaft. 38. Jahrg. Breslau 16. Juli–September 1935. Heft Nr. 3.)

Friez, Julien P., & sons.

Instructions for the installation, operation and care of the Friez wind direction and wind velocity recording and indicating system. Self synchronous motor type. Baltimore. n. d. 9 p. and 3 plates. 27½ cm.

——— Wind news. Baltimore. n. d. 16 p. ill., fold. sheet in back. 28 cm.

Geiger, Rudolf.

Gewitter und Forst. Berlin. 1935. p. 383–385. 25 cm. (Sonderabdruck: Forstwissenschaftliches Centralblatt. 57. Jahrgang, Heft 12. 1935.)

Great Britain. Meteorological office.

Cloud forms. Definitions and photographs. London. 1934. 9 p. 17 pl. 24½ cm.

——— Aviation services division. Aviation meteorological reports. 1–4. n. p. 1934–1935. 4 v. tables, diagrs. 33 cm. 1. Karachi to Singapore. 2. Singapore to Melbourne. 3. Aleppo-Baghdad-Karachi. 4. Cairo to Capetown.

——— Airship meteorology division. Meteorological conditions along airship routes. Upper winds over Italy and neighbouring parts of the Mediterranean. (Tables.) London. 1926. 63 p. 33½ cm. (Mimeographed.)

Gregg, Willis Ray.

Weather. 1933. 9 p. 1 fold. map. 28½ cm. (Paper presented at the Aeronautical session, 22d Annual safety congress, Stevens Hotel, Chicago, Ill., October 5, 1933.)

Guatemala. Observatorio nacional meteorológico de la "Aurora."

Anales. Nos. 1–2. Años 1928–29. Guatemala. n. p. n. d. p. A26–A30. tables. 32 cm.

Hongkong. Observatory.

The upper winds of Hong Kong. From observations made with pilot balloons, 1921–32. By G. S. P. Heywood, under the direction of C. W. Jeffries. Hong Kong. 1933. 13 p. incl. tables. plates. 33 cm. (At head of title: Royal observatory, Hong Kong.)

Hurst, H. E., & Phillips, P.

The Nile basin. v. 3. Supplement. Ten-day means and monthly mean gage readings of the Nile and its tributaries up to 1932. Cairo. 1935. 567 p. tables. 27½ cm. (Physical dept. paper no. 32.)

Jackson, S. P.

Notes on the occurrence of "cold snaps" at Johannesburg. Johannesburg. 1933. p. 27–38. tables, diagrs. 24½ cm. (The South African geogr. jnl. v. 16. Dec. 1933.)

Jeffreys, Harold.

Earthquakes and mountains. London. [1935.] 183 p. front., ill., maps, plates, diagrs. 19 cm.

Jung, Fritz.

Untersuchungen über Regenschwankungen und Häufigkeit unter Berücksichtigung des Anbaus, ausgeführt am Beispiel Südafrikas. Giessen. 1932. 59 p. tables. 20 fold maps and charts 23 cm. (Dissertation.)

Kelliher, S. G. G.

Summary of observations of wind (surface and upper). 1934. Kuala Lumpur. 1935. 53 p. tables. 33½ cm. (Malayan met'l service.)

Kunze, Gerhard.

Beiträge zur Klimatologie des Europäischen Nordmeeres (Skandik). (Dargestellt auf Grund der Beobachtungen der Insel- und Kustenstationen). Schramburg (Württemberg). 1933. 77 p. tabs., fold. map in back. 21½ cm. (Inaug.-Diss.)

Mariolopoulos, E. G., & Livathinos, A. N.

Atlas climatique de la Grèce. Athènes. 1935. 5 p. and 118 plates. 50 x 37½ cm. (Observ. nat. d'Athènes.)

Müller, Karl.

Das Klima Neukastiliens auf Grund der spanischen Wetterbeobachtungen der Jahre 1906 bis 1925. Gieszen. 1933. 145 p. tables. fold. plates in back. 24 cm. (Dissertation.)

Namekawa, Tadao.

A study of the minor fluctuations of the atmospheric pressure. I–III. Kyoto. 1934–1935. p. 405–430; 83–127. Ill., tab., diagr., graphs. 26 cm. (Reprints from Memoirs of the College of science, Kyoto.)

Osorio, Luis H.

Efectos agrícolas de la temperatura y de sus variaciones. p. 157–172. tables. 25 cm. (Excerpt: Boletín agricultura. Bogotá. Números 1 y 2. Febrero 1935.)

Pardé, M.

Le régime de la Garonne. 1935. 160 p. maps (part fold.), tables, diagrs. 25 cm. (Extr.: Revue géogr. des Pyrénées et du Sud-ouest. T. vi, 1935.)

Philip, Charles G.

Stratosphere and rocket flight (astronautics); a popular handbook on space flight of the future, including a section on the problems of interplanetary space navigation . . . London. 1935. 106 p. illus. 19 cm.

Poland. Institut météorologique. Annuaire. 1931.

Supplément A. Résultats des observations météorologiques horaires tirées des enregistrement à Varsovie (Usine des Eaux). Warszawa. 1935. 46 p. tables. Supplément B. Résultats des observations phénologique exécutées en Pologne pendant l'année 1931. Warszawa. 1935. 52 p. diagr., fold. map in back. Supplément C. La grêle en 1931 en Pologne. Warszawa. 1932. 61 p. tables, fold. maps in back. [31 cm. Authors, titles & text in Polish and French.]

[Poland.] **Związku rolniczych zakładow dóswiadczalnych Rzecypospolitej Polskiej. Sekcja fenologiczna.**
Instrukcja do prowadzenia spostrzeżeń fenologiczynch sieci Polskiej . . . Wydano z Zasiłku ministerstwa rolnictwa. Warszawa. 1931. 90 p. 38 col. pls., tabs. 24 cm.

Portugal. Commissão de cartografia das colonias.
Instrucções meteorológicas para uso dos postos das colónias. Coimbra. 1929. 57 p. incl. tables, fold. form. 26 cm.

Poschmann, Albert.
Beiträge zum Studium der nächtlichen Ausstrahlung. Frankfurt. 1932. 21 p. 8 pl. (figs., graphs, etc.), tables, diagrs. 30 cm. (Inaug.-Dissertation.)

Puppo, Agostino.
L'Osservatorio meteorologico di Conegliano e la taratura degli strumenti attinometrici. Pavia. 1935–XIII. 12 p. tables. 23 cm. (Extr.: Boll. del Comitato per la geodesia e la geofisico del Consig. naz. delle ricerche. Serie II, Anno V, N. 3, Luglio 1935–XIII.)

Saedeleer, A. de.
Un nouvel hygromètre de précision. (Communication préliminaire). Brux. p. 872–874. figs. 27 cm. (2me Congrès national des sciences . . . Extrait des "Comptes rendus.")

Stone, Robert G.
Die Entwicklung der amerikanischen Bergobservatorien und das derzeitige Netz von Bergstationen in den Vereiningten Staaten von Amerika. Wien. 1934. p. 11–30. ill. 29 cm. (Repr.: XLIII. Jahresbericht des Sonnblick-Vereines, 1934.)

Tannehill, Ivan Ray.
Preparation and use of weather maps at sea. Wash. 1935. 48 p. illus., maps, charts, diagrs. 23 cm. (U. S. Weather Bureau. Circular R. W. B. 1151.)

Thomas, H.
Das Zustandekommen eines Druckanstieges von 35 mm durch einen stratosphärischen Kaltlufteinbruch ohne Mitwirkung troposphärischer Vorgänge. Berlin. tables, diagrs. 26 cm. (Repr.: Sitzungsber. Preuss. Akad. Wissensch. Phys.-Math. Klasse. 1934. XVII.)

Tsing Hua university meteorological observatory.
Quarterly meteorological bulletin. v. 1–2. 1932–33. Peiping. 1932–33. 34 cm.

U. S. Weather bureau. Aerological division.
Instructions for airway meteorological service. 3d ed. 1935. Wash. 142 p. illus., diagrs. 23½ cm. (Circular N.) (Earlier editions have title: Instructions for airway observers.)

Watt, Robert Alexander Watson.
Through the weather house; or, The wind, the rain, and six hundred miles above. London. 1935. 192 p. front., pls., diagrs. 19 cm.

Weightman, R. Hanson.
Lightning. [Bethesda, Md. 1934.] p. 6, 7, 14, 15. ill. 30 cm. (Extr.: Kenwood magazine. July, 1934.)

[Yugoslavia.] Observatorium Gric.
Meteorologischer Monatsbericht. 1928–31. Zagreb. 1928–31. v. p. tables. 38 cm. (Title & headings also in German.)

SOLAR OBSERVATIONS

SOLAR RADIATION OBSERVATIONS DURING APRIL 1936

By IRVING F. HAND, *Assistant in Solar Radiation Investigations*

For a description of instruments employed and their exposures, the reader is referred to the January 1935, REVIEW, page 24.

Table 1 shows that solar radiation intensities averaged above normal at all three Weather Bureau stations.

Table 2 shows an excess in the amount of total solar and sky radiation at all stations with the exception of Washington, Madison, New York, Blue Hill, and Friday Harbor.

Polarization measurements made at Washington on 3 days give a mean of 61 percent with a maximum of 64 percent on the 16th. At Madison, observations obtained on three days give a mean of 63 percent with a maximum of 71 percent on the 22d. All of these values are slightly above the April normals for the two stations.

TABLE 1.—*Solar radiation intensities during April 1936*

[Gram-calories per minute per square centimeter of normal surface]

WASHINGTON, D. C.

Date	Sun's zenith distance: 8 a.m.	78.7°	75.7°	70.7°	60.0°	0.0°	60.0°	70.7°	75.7°	78.7°	Noon
	75th mer. time	Air mass: A. M.					P. M.				Local mean solar time
	e	5.0	4.0	3.0	2.0	*1.0	2.0	3.0	4.0	5.0	e
	mm.	cal.	cal.	cal.	cal.	cal.	cal.	cal.	cal.	cal.	mm.
Apr. 4	1.96	------	1.04	1.13	1.27	1.45	------	------	------	------	1.60
Apr. 8	1.37	0.93	1.03	1.11	1.32	1.54	------	------	------	------	2.06
Apr. 16	4.37	.70	.81	.91	1.29	1.56	------	------	------	------	3.35
Apr. 20	4.57	------	------	------	------	------	0.99	0.72	------	------	4.75
Apr. 23	3.63	.62	.78	.88	1.08	1.39	1.01	.79	------	------	3.81
Apr. 24	3.81	.42	.53	.63	1.02	1.46	1.10	.94	------	------	2.74
Apr. 25	2.74	------	------	------	------	------	.88	.70	------	------	3.15
Apr. 27	3.63	.71	.84	.96	------	------	------	------	------	------	3.63
Means	------	.68	.84	.94	1.20	1.48	1.00	.79	------	------	------
Departures	------	−.01	+.05	+.05	+.12	+.12	−.09	−.10	------	------	------

TABLE 1.—*Solar radiation intensities during April 1936*—Con.

MADISON, WIS.

Date	Sun's zenith distance: 8 a.m.	78.7°	75.7°	70.7°	60.0°	0.0°	60.0°	70.0°	75.7°	78.7°	Noon
	75th mer. time	Air mass: A. M.					P. M.				Local mean solar time
	e	5.0	4.0	3.0	2.0	*1.0	2.0	3.0	4.0	5.0	e
	mm.	cal.	cal.	cal.	cal.	cal.	cal.	cal.	cal.	cal.	mm.
Apr. 6	1.68	------	1.18	1.28	1.45	1.63	------	------	------	------	1.68
Apr. 11	6.50	------	------	------	------	1.56	------	------	------	------	5.36
Apr. 14	8.18	------	------	------	------	1.54	------	------	------	------	5.79
Apr. 16	3.63	------	------	1.20	------	------	------	------	------	------	3.63
Apr. 17	3.30	------	------	1.14	------	------	------	------	------	------	3.45
Apr. 18	3.00	------	------	------	1.29	------	------	------	------	------	3.15
Apr. 22	2.87	------	------	1.16	1.39	1.56	1.00	------	------	------	2.87
Apr. 23	3.15	------	------	------	1.06	------	------	------	------	------	3.45
Apr. 29	11.38	------	------	------	------	1.47	------	------	------	------	8.48
Means	------	------	(1.18)	1.20	1.30	1.55	(1.00)	------	------	------	------
Departures	------	------	+.27	+.17	+.08	.11	−.19	------	------	------	------

LINCOLN, NEBR.

Apr. 3	1.32	------	1.05	1.24	1.38	1.58	------	------	------	------	1.88
Apr. 6	1.88	------	1.14	1.25	1.43	------	------	------	------	------	1.68
Apr. 7	1.37	------	------	------	------	------	1.29	1.03	0.89	0.78	1.12
Apr. 10	4.95	------	------	.91	1.15	1.54	------	------	------	------	3.99
Apr. 14	5.56	.71	.85	1.00	1.18	1.47	1.14	.93	.77	.67	4.37
Apr. 16	2.74	.87	.99	1.13	1.39	1.60	------	------	------	------	2.16
Apr. 17	2.36	------	.94	1.06	1.27	1.57	1.24	1.00	.87	.74	2.36
Apr. 18	2.26	.84	.94	1.07	1.31	1.57	------	------	------	------	2.62
Apr. 20	6.76	.26	.42	.64	.96	1.20	------	------	------	------	7.04
Means	------	.67	.90	1.04	1.26	1.50	1.22	.97	.84	.73	------
Departures	------	−.04	+.08	+.07	+.07	+.05	+.06	+.01	+.02	+.04	------

BLUE HILL, MASS.

Apr. 1	2.2	------	------	------	------	1.20	1.03	0.94	------	------	2.3
Apr. 4	2.2	------	------	------	1.02	1.18	1.13	1.08	1.03	------	2.2
Apr. 8	2.8	------	------	1.10	1.27	1.40	1.15	.94	------	------	2.9
Apr. 9	3.3	------	------	1.08	1.16	------	------	------	------	------	2.8
Apr. 14	3.6	------	------	------	1.17	1.46	1.26	------	------	------	3.2
Apr. 18	4.0	0.88	0.98	1.11	1.25	1.40	------	------	------	------	4.4
Apr. 19	4.8	.88	.99	1.11	1.27	1.43	------	------	------	------	4.0
Apr. 20	3.8	.82	.91	1.00	1.19	1.29	------	------	------	------	3.0
Apr. 22	2.9	------	------	1.17	1.31	1.51	------	------	------	------	2.4
Apr. 23	2.9	------	1.03	1.14	1.27	1.44	1.49	1.23	1.06	------	2.8
Apr. 24	3.6	------	------	------	1.19	1.47	1.27	1.06	------	------	2.1
Apr. 25	2.6	------	------	------	1.27	------	1.09	------	------	------	2.6
Apr. 27	2.9	------	------	------	1.21	1.32	1.12	.93	------	------	3.8
Apr. 29	9.6	------	------	------	------	1.07	.80	------	------	------	11.1
Means	------	.86	.98	1.10	1.22	1.35	1.15	1.03	.98	------	------

*Extrapolated.

TABLE 2.—*Average daily totals of solar radiation (direct + diffuse) received on a horizontal surface*

Week beginning—	Washington	Madison	Lincoln	Chicago	New York	Fresno	Pittsburgh	Fairbanks	Twin Falls	La Jolla	Miami	New Orleans	Riverside	Blue Hill	Friday Harbor	Ithaca
	Gram-calories per square centimeter															
	cal.	*cal.*	*cal.*	*cal.*	*cal.*	*cal.*	*cal.*	*cal.*	*cal.*	*cal.*	*cal.*	*cal.*	*cal.*	*cal.*	*cal.*	*cal.*
Apr. 1	240	351	394	280	250	483	204	330	480	578	488	353	485	283	407	222
Apr. 8	360	386	527	342	252	628	231	399	605	408	535	507	555	296	299	249
Apr. 15	488	391	564	388	390	558	286	410	522	383	474	546	473	287	483	191
Apr. 22	517	435	313	368	514	652	454	388	534	441	465	428	509	570	478	464
	Departures from weekly normals															
Apr. 1	−131	−21	−19	−18	−79	−28		−4	+46		+17	−5	+10	−94	−3	−43
Apr. 8	−33	−14	+92	+6	−64	+51		+19	+125		−53	+139	+59	−74	−111	−10
Apr. 15	+63	−8	+117	+54	+26	+31		+12	+58		+4	+142	−28	−76	+38	−137
Apr. 22	+67	−4	−137	+11	+103	+79		−4	+23		−13	+48	−5	+134	−6	+91
	Accumulated departures on April 28															
	−2135	+672	−287	+2170	+651	+1764		+252	+1568		−1589	+4347	−826	−917	+805	−476

TABLE 3.—*Total, I_m, and screened, I_y, I_r, solar radiation intensity measurements, obtained during April 1936, and determinations of the atmospheric turbidity factor, β, and water-vapor content, w=depth in millimeters, if precipitated*

AMERICAN UNIVERSITY, WASHINGTON, D. C.

Date and hour angle	Solar altitude	Air mass	I_m	I_y	I_r	$\beta_{I_{m-r}}$	$\beta_{I_{y-r}}$	β_{mean}	$\frac{I_{w-o}}{1.94}$ Percentage of solar constant	$\frac{I_{w-o}-I_m}{1.94}$ Percentage of solar constant	w	Air-mass type
Apr. 8, 1936	° ′	*m*	*gr. cal.*	*gr. cal.*	*gr. cal.*						*mm*	
0:28 p. m.	57 49	1.18	1.430	0.958	0.768	0.052	0.066	0.059	81.2	7.3	3.7	Pc
0:32 p. m.	57 38	1.18	1.322	.960	.768	.052	.066	.059	81.2	7.3	3.7	
Apr. 16, 1936												
1:00 a. m.	58 22	1.18	1.494	1.016	.802	.036	.032	.034	84.8	7.3	3.7	P_p
0:56 a. m.	58 51	1.17	1.494	1.016	.802	.036	.032	.034	84.8	7.3	3.7	
Apr. 25, 1936												
3:52 p. m.	33 04	1.83	.953	.701	.590	.170	.170	.170	57.1	6.1	2.2	N_p
3:56 p. m.	32 17	1.87	.948	.700	.586	.164	.168	.166	57.3	6.6	2.3	

Meteorological conditions during turbidity measurements

Apr. 8. Temperature 5° C; wind, S. 12; visibility, 30 miles; polarization, 61.4 percent; blueness of sky, 5.
Apr. 16. Temperature 10° C; wind, NW. 20; visibility, 50 miles; polarization, 63.6 percent; blueness of sky, 6.
Apr. 25. Temperature 8° C; wind, S. 12; visibility, 20 miles; polarization, 57.8 percent; blueness of sky, 5.

BLUE HILL METEOROLOGICAL OBSERVATORY OF HARVARD UNIVERSITY

Apr. 1, 1936												
2:35 p. m.	34 30	1.76	1.058	0.712	0.584	0.098	0.098	0.098	67.9	13.4	7.8	Pc
4:56 p. m.	14 47	3.86	.708	.529	.455	.100	.122	.111	47.8	1.4	.7	
Apr. 4, 1936												
3:06 a. m.	35 01	1.74	1.111	.804	.670	.143	.146	.144	66.5	9.0	8.1	Pc
1:12 a. m.	50 00	1.30	1.367	.927	.766	.084	.129	.106	73.6	3.1	2.8	
9:10 p. m.	52 16	1.26	1.360	.919	.751	.081	.105	.093	75.0	4.4	3.0	
2:54 p. m.	36 51	1.67	1.341	.915	.705	.021	.005	.013	85.5	16.3	11.3	
Apr. 8, 1936												
4:07 a. m.	23 15	2.53	1.167	.832	.708	.092	.112	.102	67.6	7.3	4.7	Pc: N_{PP} aloft
Apr. 9, 1936												
4:19 a. m.	23 36	2.49	1.131	.782	.663	.122	.117	.120	73.0	14.6	9.2	N_{PC}
Apr. 14, 1936												
3:46 a. m.	30 45	1.95	1.186	.825	.692	.075	.103	.089	66.0	4.5	3.2	N_{PP}
1:10 a. m.	53 38	1.24	1.424	.934	.768	.100	.118	.109	75.2	1.8	1.6	
1:38 p. m.	50 28	1.29	1.400	.949	.760	.061	.062	.062	79.5	6.9	6.1	
Apr. 18, 1936												
4:40 a. m.	21 55	2.66	1.155	.815	.663	.033	.029	.031	73.3	13.2	7.8	P_P+P_A
Apr. 19, 1936												
3:11 a. m.	38 07	1.62	1.330	.891	.710	.037	.061	.049	78.0	8.8	6.9	P_P+P_A
Apr. 22, 1936												
4:51 a. m.	20 49	2.80	1.200	.847	.701	.039	.061	.050	67.0	4.5	2.9	Pc: P_P aloft
1:58 a. m.	50 26	1.29	1.414	.959	.737							
Apr. 23, 1936												
4:02 a. m.	30 02	2.00	1.267	.851	.703							
2:49 a. m.	51 56	1.27	1.371	.901	.741	.066	.126	.096	75.0	3.5	2.8	P_C+P_A
12:28 p. m.	59 39	1.16	1.416	.946	.755	.063	.073	.068	80.0	6.1	5.4	
1:51 p. m.	51 40	1.27	1.424	.948	.749	.034	.038	.036	79.9	5.6	4.7	
4:24 p. m.	25 16	2.33	1.153	.801	.615	.029	.014	.022	77.7	17.5	10.3	
Apr. 24, 1936												
1:38 a. m.	59 24	1.16	1.403	.948	.756	.058	.056	.057	80.0	6.8	6.1	N_{PC}
1:53 p. m.	59 40	1.16	1.442	.952	.776	.051	.096	.074	79.0	3.8	3.3	
3:53 p. m.	32 45	1.88	1.300	.890	.731	.047	.078	.062	72.3	4.5	2.9	
Apr. 25, 1936												
3:26 a. m.	36 57	1.66	1.322	.900	.726	.041	.049	.045	79.6	10.6	7.2	N_P
4:12 p. m.	28 39	2.08	1.080	.755	.620	.074	.100	.087	63.6	7.5	5.0	
Apr. 27, 1936												
4:04 a. m.	30 21	1.96	1.218	.793	.682	.055	.166	.110	65.0	1.3	1.0	N_{PC}
0:16 a. m.	61 18	1.14	1.308	.859	.686	.139	.110	.124	74.3	5.9	5.3	
2:31 p. m.	46 45	1.37	1.277	.863	.686	.059	.073	.066	78.6	11.9	9.9	
5:03 p. m.	19 40	2.95	.946	.678	.550	.062	.071	.066	62.2	12.8	7.4	
Apr. 29, 1936												
0:20 a. m.	61 47	1.13	1.030	.701	.566	.145	.044	.094	75.6	21.7	20.2	Tc

Atmospheric conditions during solar radiation measurements. Blue Hill Observatory of Harvard University, April 1936

Date and time from apparent noon	Air temperature	Wind, Beaufort scale	Visibility (scale 0–10)	Sky blueness	Cloudiness and remarks
	°C.				
4; 0.15 a. m.	+2.4	WNW 5	9	8	1 Frcu, wind gusty.
22; 2.13 a. m.	+4.6	W 5	9	8	2 Ci, few Cu.
23; 3.03 a. m.	+5.7	NW 4	8	8	5 Ci, light haze.
23; 1.34 p. m.	+12.6	W 3	9	7	1 Ci, few Cu; light haze.
24; 3.38 p. m.	+6.7	NW 5	10	8	Few Cu, light haze N.
25; 3.13 a. m.	+3.5	NW 2	9	8	Few Ci, mod. haze NE.
27; 3.56 a. m.	+4.3	NW 4	9	8	Zero clouds, light haze.
27; 0.08 a. m.	+8.7	NW 3	9	8	Zero clouds, light haze.

POSITIONS AND AREAS OF SUN SPOTS

[Communicated by Capt. J. F. Hellweg, U. S. Navy (Ret.), Superintendent U. S. Naval Observatory. Data furnished by the U. S. Naval Observatory in cooperation with Harvard and Mount Wilson Observatories. The difference in longitude is measured from the central meridian, positive west. The north latitude is positive. Areas are corrected for foreshortening and are expressed in millionths of the sun's visible hemisphere. The total area for each day includes spots and groups]

MEAN DAILY AREA FOR 30 DAYS, 944

Date	Eastern standard time	Heliographic			Area		Total area for each day	Observatory
		Diff. in longitude	Longitude	Latitude	Spot	Group		
1936	h m	°	°	°				
Mar. 1	13 5	−30.0	273.0	+24.0		187		Harvard.
		−21.0	282.0	−15.5		143		
		+16.0	319.0	+11.5	158			
		+79.5	22.5	−35.0	119		607	
Mar. 2	12 45	−55.0	234.9	+17.0		85		Mt. Wilson.
		−21.0	268.9	+21.0		109		
		−10.0	279.9	−18.0		122		
		+26.0	315.9	+12.0	97			
		+27.0	316.9	+18.0	52		465	
Mar. 3	13 3	−39.5	237.1	+19.5		123		U. S. Naval.
		−8.0	268.6	+21.0		123		
		+3.0	279.6	−18.0		108		
		+39.5	316.1	+11.5	123			
		+41.0	317.6	+16.5	31		508	
Mar. 4	11 8	−27.0	237.5	+19.5		123		Do.
		+4.5	269.0	+21.5		123		
		+14.5	279.0	−18.0		123		
		+40.0	304.5	+24.0		31		
		+51.5	316.0	+12.0	123			
		+55.0	319.5	+16.5	15		538	
Mar. 5	11 30	−87.0	164.1	−24.0	53			Mt. Wilson.
		−15.0	236.1	+18.0		90		
		−8.0	243.1	+32.0		95		
		+9.0	260.1	+17.0		12		
		+14.0	265.1	+21.0		65		
		+27.0	278.1	−18.0		121		
		+64.0	315.1	+11.5	69		515	
		+68.0	319.1	+17.5	10			
Mar. 6	11 2	−74.0	164.2	−22.0	77			U. S. Naval.
		+1.0	239.2	+18.0	31			
		+8.0	246.2	+33.0		432		
		+29.0	267.2	+21.0	31			
		+29.5	267.7	+18.5		46		
		+40.5	278.7	−18.0		62		
		+79.0	317.2	+11.0	46		725	
Mar. 7	11 30	−60.0	164.7	−22.0	123			Do.
		+15.0	239.7	+17.5	31			
		+22.0	246.7	+32.5		494		
		+27.0	251.7	−21.5		154		
		+31.5	256.2	+18.0	15			
		+42.0	266.7	+21.0	31			
		+42.5	267.2	+18.5		154		
		+50.5	275.2	−19.5	31			
		+58.0	282.7	−17.0	15		1,048	
Mar. 8	12 50	−79.0	131.9	−22.0	15			Mt. Wilson.
		−60.0	150.9	−25.0		15		
		−47.0	163.9	−23.0	119			
		+30.0	240.9	+18.0	21			
		+32.0	242.9	+32.0		614		
		+40.0	250.9	−22.0		466		
		+57.0	267.9	+18.0		393		
		+59.0	269.9	+21.0	22			
		+64.0	274.9	−19.0	14		1,679	
Mar. 9	11 10	−68.0	130.6	−21.0	31			U. S. Naval.
		−35.0	163.6	−22.5	123			
		−18.5	180.1	+20.0		46		
		+41.0	239.6	+18.0	15			
		+47.0	245.6	+32.5		556		
		+53.0	251.6	−21.0		494		
		+67.0	265.6	+18.0		154	1,419	
Mar. 10	11 1	−79.0	106.5	−30.5		123		Do.
		−75.0	110.5	−21.0	31			
		−55.0	130.5	−21.0	15			
		−21.0	164.5	−23.0	108			
		−3.0	182.5	+20.0		108		
		+59.0	244.5	+32.5		494		
		+66.0	251.5	−22.0		617	1,496	
Mar. 11	11 40	−65.0	106.9	−33.0		168		Mt. Wilson.
		−64.0	107.9	−22.0		25		
		−61.0	110.9	−30.0		88		
		−37.0	134.9	−23.0		18		
		−9.0	162.9	−24.0	157			
		−2.0	169.9	+24.0		24		
		+12.0	183.9	+20.0		145		
		+13.0	184.9	−16.0		5		
		+68.0	239.9	+32.0		433		
		+76.0	247.9	−22.0		733	1,796	

POSITIONS AND AREAS OF SUN SPOTS—Continued

MEAN DAILY AREA FOR 30 DAYS, 944—Continued

Date	Eastern standard time	Heliographic			Area		Total area for each day	Observatory
		Diff. in longitude	Longitude	Latitude	Spot	Group		
1936	h m	°	°	°				
Mar. 12	11 40	−54.0	104.7	−32.0		253		Mt. Wilson.
		−49.0	109.7	−29.0		359		
		−47.0	111.7	−21.0		36		
		+4.0	162.7	−24.0		171		
		+15.0	173.7	+24.0		4		
		+24.0	182.7	−16.0	12			
		+26.0	184.7	+20.0	69			
		+85.0	243.7	−23.0	293			
		+89.0	247.7	+32.0	111		1,308	
Mar. 13	11 15	−39.5	106.3	−31.5		432		U. S. Naval.
		−36.0	109.8	−20.5		93		
		+18.0	163.8	−23.0	123			
		+39.0	184.8	+21.0	39		687	
Mar. 14	11 50	−43.0	89.3	+16.5		93		Do.
		−25.0	107.3	−31.0		370		
		−20.0	112.3	−21.0		46		
		+30.0	162.3	−22.5	123			
		+51.0	183.3	+21.0	31		663	
Mar. 15	12 30	−54.0	64.8	+18.0		15		Mt. Wilson.
		−30.0	88.8	+16.0		134		
		−18.0	100.8	−32.0	137			
		−10.0	108.8	−29.0		230		
		−7.0	111.8	−21.0		24		
		+42.0	160.8	−24.0	191			
		+68.0	186.8	−16.0	8		739	
Mar. 16	11 40	−16.0	90.0	+16.0		154		U. S. Naval.
		−0.5	105.5	−31.0		309		
		+7.0	113.0	−20.0	23			
		+36.0	162.0	−22.5		123	609	
Mar. 17	12 8	+11.0	103.5	−29.0		421		Harvard.
		+70.0	162.5	−23.0	241		662	
Mar. 18	12 50	−27.0	52.1	−7.0		23		Mt. Wilson.
		+5.0	84.1	−25.0		9		
		+20.0	99.1	−32.0		111		
		+23.0	102.1	−16.0		192		
		+30.0	109.1	−29.0		234		
		+78.0	157.1	−19.0	15			
		+80.0	159.1	−24.0	55		639	
Mar. 19	15 18	−10.5	54.0	−7.5		230		Harvard.
		+18.5	83.0	−26.5		117		
		+39.5	104.0	−16.0		368		
		+42.0	106.5	−29.5		387	1,102	
Mar. 20	13 28	−71.0	341.3	−18.0		247		U. S. Naval.
		+1.0	53.3	−9.0	23			
		+28.0	80.3	−29.0		340		
		+40.0	92.3	+13.5		77		
		+50.0	102.3	−18.0		216		
		+52.5	104.8	−30.5		216	1,119	
Mar. 22	11 18	−44.0	343.1	−18.0		247		Do.
		+24.0	51.1	−8.5		154		
		+53.0	80.1	−29.0		309		
		+66.0	93.1	+15.0		123		
		+75.0	102.1	−29.5		154		
		+80.0	107.1	−16.0	62		1,051	
Mar. 23	14 51	−29.0	343.0	−17.0		247		Do.
		−40.0	332.0	−8.5		93		
		+68.0	80.0	−29.0		370		
		+86.0	98.0	−30.5	23		733	
Mar. 24	10 34	−13.5	348.0	−17.0	240			Harvard.
		−11.5	350.0	−12.5	39			
		+70.5	72.0	+19.0	38			
		+71.5	73.0	+12.5	43			
		+83.5	85.0	−30.0	856		1,216	
Mar. 25	11 45	−58.0	289.3	−24.0	7			Mt. Wilson.
		−31.0	316.3	−29.0		22		
		−11.0	336.3	−16.0		29		
		−3.0	344.3	−19.0		272		
		−1.0	346.3	−15.0		35		
		+2.0	349.3	−11.0		5		
		+80.0	67.3	−23.0		33	403	
Mar. 26	15 35	−76.5	255.5	−19.0	209			Harvard.
		−67.0	265.0	−12.0		104		
		−44.0	288.0	−22.0		341		
		−1.0	331.0	−12.5		26		
		+7.5	339.5	−13.5		19		
		+14.0	346.0	−17.0	240			
		+17.0	349.0	−14.0	26		965	
Mar. 27	12 50	−74.0	246.4	−23.0		505		Mt. Wilson.
		−56.0	264.4	−18.0		147		
		−35.0	285.4	−25.0		361		
		+7.0	327.4	−14.0		23		
		+18.0	338.4	−15.0	7			
		+25.0	345.4	−18.0		214		
		+27.0	347.4	−15.0	8		1,265	
Mar. 28	10 57	−70.0	238.2	−24.5	154			U. S. Naval.
		−58.0	250.2	−21.0		108		
		−45.0	263.2	−15.0		154		
		−22.0	286.2	−25.0		309		
		+21.0	329.2	−14.5		123		
		+36.0	344.2	−17.5		247	1,095	
Mar. 29	12 6	−58.0	236.4	−24.0	185			Do.
		−46.0	248.4	−21.0		93		
		−32.0	262.4	−15.0		154		
		−8.5	285.9	−25.0		309		
		+36.0	330.4	−14.5		123		
		+50.0	344.4	−17.5		185	1,049	

POSITIONS AND AREAS OF SUN SPOTS—Continued

MEAN DAILY AREA FOR 30 DAYS, 944—Continued

Date	Eastern standard time	Heliographic: Diff. in longitude	Heliographic: Longitude	Heliographic: Latitude	Area: Spot	Area: Group	Total area for each day	Observatory
1936	h m	°	°	°				
Mar. 30	11 3	−43.0	238.8	−23.0		216		U. S. Naval.
		−30.0	251.8	−21.0		62		
		−25.0	256.8	+20.0		46		
		−17.0	264.8	−15.0		216		
		−2.0	279.8	−27.0		185		
		+11.0	292.8	−22.0		123		
		+48.5	330.3	−14.0		123		
		+63.0	344.8	−17.5		123	1,094	
Mar. 31	11 19	−30.0	238.4	−23.0		309		Do.
		−17.0	251.4	−20.5		31		
		−10.5	257.9	+20.0		123		
		−9.0	259.4	−13.0	15			
		−2.0	266.4	−15.0		185		
		+9.5	277.9	−26.0		123		
		+23.0	291.4	−22.0		185		
		+63.0	331.4	−15.0		93		
		+77.0	345.4	−19.5		62	1,126	

MEAN DAILY AREA FOR 30 DAYS, 812

Date	Eastern standard time	Heliographic: Diff. in longitude	Heliographic: Longitude	Heliographic: Latitude	Area: Spot	Area: Group	Total area for each day	Observatory
Apr. 1	15 27	−64.0	189.1	−13.5		29		Harvard.
		−13.0	240.1	−22.5	335			
		−8.0	245.1	−20.5	27			
		0.0	253.1	−18.0		13		
		+1.0	254.1	−20.0	8			
		+7.5	260.6	+19.5		198		
		+18.0	271.1	−15.5		176		
		+25.5	278.6	−27.0		78		
		+40.5	293.6	−21.0		52		
		+41.5	294.6	−24.5	130			
		+59.5	312.6	+35.0	47		1,093	
Apr. 2	13 20	−60.0	181.0	+19.0		72		Mt. Wilson.
		−53.0	188.0	+29.0	8			
		−52.0	189.0	−15.0		9		
		−4.0	237.0	−22.0		324		
		+16.0	257.0	+20.0		270		
		+28.0	269.0	−15.0		170		
		+49.0	290.0	−23.0		91		
		+65.0	306.0	+36.0		15	959	
Apr. 3	11 20	−75.0	153.8	−24.0	62			U. S. Naval.
		−53.0	175.8	+19.5		93		
		+10.0	238.8	−22.5		278		
		+28.0	256.8	+20.5		216		
		+40.5	269.3	−16.0		108		
		+63.0	291.8	−23.0	62		819	
Apr. 4	11 6	−61.0	154.8	−24.0	77			Do.
		−42.0	173.8	+20.5		154		
		−34.0	181.8	+18.0		93		
		+20.0	235.8	−23.0		247		
		+40.0	255.8	+20.5		154		
		+53.0	268.8	−16.5		123		
		+77.0	292.8	−24.0	62		910	
Apr. 5	11 30	−48.0	154.3	−24.0	66			Mt. Wilson.
		−25.0	177.3	+22.0		326		
		+32.0	234.3	−22.0		68		
		+54.0	256.3	+21.0		24		
		+66.0	268.3	−14.0		40	524	
Apr. 6	14 48	−80.0	107.3	−30.0	62			U. S. Naval.
		−70.0	117.3	+13.5		154		
		−35.0	152.3	−24.0	31			
		−14.5	172.8	+21.0		494		
		−5.5	181.8	+18.5		93		
		+48.0	235.3	−23.0		216	1,050	
Apr. 7	14 46	−70.0	104.2	+17.5	31			Do.
		−66.0	108.2	−30.0	123			
		−57.0	117.2	+13.0		247		
		−21.0	153.2	−25.0	23			
		−2.0	172.2	+21.5		617		
		+8.0	182.2	+19.0	31			
		+61.0	235.2	−22.5		154	1,226	
Apr. 8	11 28	−60.0	102.8	+17.5	31			Do.
		−55.0	107.8	−30.0	123			
		−45.0	117.8	+12.5		216		
		+9.0	171.8	+21.0		679		
		+19.5	182.3	+20.0	15			
		+70.0	232.8	−22.0	93		1,157	
Apr. 9	9 50	−80.0	70.4	+21.0	9			Mt. Wilson.
		−75.0	75.4	−28.0	235			
		−67.0	83.4	−33.0	5			
		−50.0	100.4	+18.0		36		
		−43.0	107.4	−31.0		146		
		−32.0	118.4	+13.0		218		
		+22.0	172.4	+21.0		520		
		+65.0	215.4	+16.0		23		
		+80.0	230.4	−22.0	164		1,356	
Apr. 10	9 50	−78.0	59.2	−18.0		15		Do.
		−70.0	67.2	+17.0		24		
		−63.0	74.2	+21.0		5		
		−61.0	76.2	−28.0	194			
		−35.0	102.2	+18.0		14		
		−29.0	108.2	−31.0	148			
		−19.0	118.2	+13.0		208		
		+34.0	171.2	+21.0		691		
		+61.0	198.2	−19.5		19		
		+78.0	215.2	+16.0	5		1,323	

POSITIONS AND AREAS OF SUN SPOTS—Continued

MEAN DAILY AREA FOR 30 DAYS, 812—Continued

Date	Eastern standard time	Heliographic: Diff. in longitude	Heliographic: Longitude	Heliographic: Latitude	Area: Spot	Area: Group	Total area for each day	Observatory
1936	h m	°	°	°				
Apr. 11	11 22	−71.0	52.2	+10.0		31		U. S. Naval.
		−68.0	55.2	−19.0		62		
		−59.0	64.2	+16.5		77		
		−49.0	74.2	−29.0	154			
		−9.5	122.7	+11.5		154		
		+46.0	169.2	+21.0		556	1,034	
Apr. 12	13 0	−55.0	54.1	+12.0		64		Mt. Wilson.
		−49.0	60.1	−19.0	34			
		−42.0	67.1	+18.0		100		
		−33.0	76.1	−29.0		205		
		−9.0	100.1	+18.0		35		
		−2.0	107.1	−31.0	119			
		+15.0	124.1	+12.0		205		
		+60.0	169.1	+21.0		358	1,120	
Apr. 13	11 4	−44.0	53.0	+11.5		247		U. S. Naval.
		−33.0	64.0	+16.0		93		
		−22.5	74.5	−29.0	154			
		+9.0	106.0	−31.5	93			
		+26.0	123.0	+12.0		123		
		+72.0	169.0	+22.0		154	864	
Apr. 14	11 0	−31.0	52.8	+11.0		247		Do.
		−28.0	55.8	−19.0		46		
		−18.0	65.8	+16.5	31			
		−10.0	73.8	−29.0	123			
		+21.0	104.8	−31.0	93			
		+39.0	122.8	+12.0		154	694	
Apr. 15	10 58	−82.0	348.6	−19.0	93			Do.
		−23.0	47.6	+11.0	15			
		−14.0	56.6	−19.5		46		
		−12.0	58.6	+11.0		185		
		−5.0	65.6	+16.5	31			
		+2.5	73.1	−29.5	123			
		+34.0	104.6	−31.0	93			
		+52.0	122.6	+12.0		77	663	
Apr. 16	11 7	−79.0	338.3	−11.5		123		Do.
		−70.0	347.3	−19.5		309		
		−1.0	56.3	−19.5		46		
		+1.0	58.3	+12.0		123		
		+9.0	66.3	+19.0	31			
		+16.0	73.3	−29.0	123			
		+45.5	102.8	−30.0	93			
		+65.0	122.3	+12.0		62	910	
Apr. 17	11 15	−65.0	339.1	−11.5		216		Do.
		−55.0	349.1	−19.5		370		
		+12.0	56.1	−18.0	15			
		+16.5	60.6	+12.0	46			
		+20.0	64.1	−19.0		46		
		+29.0	73.1	−28.5	123			
		+59.0	103.1	−30.0	62			
		+85.0	129.1	+12.0	46		924	
Apr. 18	11 4	−53.0	338.0	−12.0		216		Do.
		−42.0	349.0	−19.5		340		
		+30.0	61.0	+11.0	23			
		+33.0	64.0	−19.0		62		
		+35.0	66.0	+19.5	15			
		+40.0	71.0	−28.0	93			
		+66.0	97.0	−26.0		93		
		+70.0	101.0	−29.5	77		919	
Apr. 19	12 30	−38.0	339.0	−12.0		474		Mt. Wilson.
		−36.0	341.0	−14.0	57			
		−24.0	353.0	−19.0		302		
		+46.0	63.0	+10.0	20			
		+47.0	64.0	−27.0		27		
		+50.0	67.0	−21.0	17			
		+54.0	71.0	−29.0	138			
		+77.0	94.0	−28.0		16	1,060	
		+80.0	97.0	−32.0	9			
Apr. 20	11 51	−25.5	338.6	−12.0		370		U. S. Naval.
		−21.0	343.1	−20.0	31			
		−10.0	354.1	−19.5	216			
		+60.0	64.1	−25.0	15			
		+66.0	70.1	−27.0	62		694	
Apr. 21	11 0	−23.0	328.4	−18.0		62		Do.
		−14.0	337.4	−12.0		401		
		−8.0	343.4	−20.0	15			
		+2.0	353.4	−19.0		278		
		+80.0	71.4	−27.0	46		802	
Apr. 22	13 45	−72.0	264.7	+37.0	5			Mt. Wilson.
		−6.0	330.7	+10.0		7		
		+4.0	340.7	−15.0	61			
		+6.0	342.7	−11.0		304		
		+8.0	344.7	−9.0		68		
		+16.0	352.7	−18.0		253		
		+56.0	32.7	+18.0		7		
		+79.0	55.7	−22.0	5			
		+88.0	64.7	−25.0		18	728	
Apr. 23	11 6	+16.0	340.9	−12.0		401		U. S. Naval.
		+28.0	352.9	−19.0	247		648	
Apr. 24	11 48	−51.0	260.3	+36.5	77			Do.
		−22.0	289.3	+37.0		93		
		+28.0	339.3	−11.5		370		
		+40.0	351.3	−19.0	216		756	
Apr. 25	12 16	−39.0	258.8	+37.0	46			Do.
		−8.0	289.8	+37.0		77		
		+37.0	334.8	−27.0		62		
		+45.0	342.8	−11.0		309		
		+53.0	350.8	−19.5	185		679	

POSITIONS AND AREAS OF SUN SPOTS—Continued

MEAN DAILY AREA FOR 30 DAYS, 812—Continued

Date	Eastern standard time	Heliographic			Area		Total area for each day	Observatory
		Diff. in longitude	Longitude	Latitude	Spot	Group		
1936	h m	°	°	°				
Apr. 26	14 40	−26.0	257.3	+37.0	-------	12	-------	Mt. Wilson.
		+5.0	288.3	+36.0	-------	14	-------	
		+5.0	288.3	+12.0	-------	19	-------	
		+23.0	306.3	−16.0	-------	15	-------	
		+51.0	334.3	−26.0	-------	197	-------	
		+57.5	340.8	−13.0	17	-------	-------	
		+58.0	341.3	−12.0	-------	125	-------	
		+68.0	351.3	−18.0	185	-------	584	
Apr. 27	13 50	−16.0	254.6	+36.0	-------	16	-------	Do.
		+19.0	289.6	+13.0	-------	35	-------	
		+35.0	305.6	−16.0	-------	9	-------	
		+64.0	334.6	−26.0	-------	226	-------	
		+68.0	338.6	−13.0	23	-------	-------	
		+68.0	338.6	−10.0	25	-------	-------	
		+79.0	349.6	−18.0	227	-------	561	
Apr. 28	11 44	+33.0	291.5	+12.0	-------	46	-------	U. S. Naval.
		+74.0	332.5	−26.0	46	-------	-------	
		+87.0	345.5	−27.0	62	-------	154	
Apr. 29	11 6	−68.0	177.6	−18.0	-------	77	-------	Do.
		+50.0	295.6	+12.0	15	-------	92	
Apr. 30	11 13	−54.0	178.3	−18.0	-------	46	46	Do.

PROVISIONAL SUN-SPOT RELATIVE NUMBERS, APRIL 1936

[Dependent alone on observations at Zurich and its station at Arosa]

[Data furnished through the courtesy of Prof. W. Brunner, Eidgen. Sternwarte, Zurich, Switzerland]

April 1936	Relative numbers	April 1936	Relative numbers	April 1936	Relative numbers
1	*Wac*93	11	*a*91	21	*a*67
2	100	12	*Ec*92	22	*a*49
3	*a*91	13	*a*83	23	56
4	*Ec*74	14	86	24	*Ec*53
5	85	15	*a*73	25	*Wc*72
6	*d*91	16	*ad*88	26	77
7	*b*—	17	—	27	56?
8	*b*76	18	73	28	—
9	*d*89	19	83	29	32
10	99	20	75	30	—

Mean, 26 days = 77.1.

a=Passage of an average-sized group through the central meridian.
b=Passage of a large group or spot through the central meridian.
c=New formation of a center of activity: *E*, on the eastern part of the sun's disk; *W*, on the western part; *M*, in the central circle.
d=Entrance of a large or average-sized center of activity on the east limb.

AEROLOGICAL OBSERVATIONS

[Aerological Division, D. M. LITTLE in charge]

By L. T. SAMUELS

At those stations with a sufficient period of record for the determination of approximate normals, upper-air temperatures during April averaged below normal except over San Diego where the departures were positive. (See table 1.) In practically all cases the departures were of moderate to small magnitude.

Upper-air relative humidity departures were mostly of opposite sign to those for temperature, and of small to moderate magnitude. The comparatively pronounced increase in the mean relative humidity with elevation found at El Paso is characteristic of the approach of the warm season.

The directions of the upper-air wind resultants were close to normal at the 3-kilometer level. (See table 2.) Resultant velocities at that level exceeded the normals over the northern half and southeastern section of the country, and were below normal elsewhere. Departures were of small to moderate magnitude.

TABLE 1.—*Mean free-air temperatures and relative humidities obtained by airplanes during April 1936*

TEMPERATURE (° C.)

Stations	Altitude (meters) m. s. l.																Number of observations
	Surface		500		1,000		1,500		2,000		2,500		3,000		4,000		5,000		
	Mean	Departure from normal	Mean	Departure from normal	Mean	Departure from normal	Mean	Departure from normal	Mean	Departure from normal	Mean	Departure from normal	Mean	Departure from normal	Mean	Departure from normal	Mean	Departure from normal	
Barksdale Field (Shreveport), La.[1] (52 m)	13.4	-------	15.1	-------	13.2	-------	11.0	-------	8.9	-------	6.4	-------	3.5	-------	−2.7	-------	−9.9	-------	30
Billings, Mont.[2] (1,088 m)	2.9	-------	3.1	-------	1.1	-------	4.2	-------	1.8	-------	−1.2	-------	−4.5	-------	−11.1	-------	−17.7	-------	30
Boston, Mass.[1] (5 m)	4.2	−2.4	3.1	−1.1	1.1	−1.2	−1.2	−1.8	−3.6	−2.0	−5.6	−1.8	−7.8	−1.7	−12.2	−1.3	−18.3	−1.2	13
Cheyenne, Wyo.[2] (1,873 m)	1.6	-------	-------	-------	-------	-------	-------	-------	2.4	-------	.4	-------	−2.7	-------	−9.7	-------	−17.6	-------	30
El Paso, Tex.[2] (1,194 m)	14.0	-------	-------	-------	-------	-------	15.9	-------	13.1	-------	9.4	-------	5.4	-------	−2.5	-------	−10.1	-------	30
Fargo, N. Dak.[2] (274 m)	−1.9	-------	−.8	-------	−2.6	-------	−4.0	-------	−5.8	-------	−8.2	-------	−10.6	-------	−16.0	-------	−21.8	-------	30
Kelly Field (San Antonio), Tex.[1] (206 m)	14.3	-------	15.2	-------	14.4	-------	13.1	-------	11.5	-------	9.1	-------	5.9	-------	−.8	-------	−7.4	-------	30
Lakehurst, N. J.[2] (39 m)	5.8	-------	4.7	-------	2.5	-------	.7	-------	−1.0	-------	−3.1	-------	−5.4	-------	−10.8	-------	-------	-------	25
Maxwell Field (Montgomery), Ala.[1] (52 m)	15.0	-------	15.6	-------	13.2	-------	10.7	-------	8.1	-------	5.8	-------	2.7	-------	−2.8	-------	−8.7	-------	22
Mitchel Field (Hempstead, Long Island), N. Y.[1] (29 m)	5.3	-------	5.2	-------	3.2	-------	.7	-------	−1.2	-------	−3.6	-------	−6.0	-------	−10.3	-------	−16.7	-------	22
Murfreesboro, Tenn.[2] (174 m)	8.9	-------	10.7	-------	8.9	-------	7.3	-------	5.1	-------	2.9	-------	.6	-------	−4.8	-------	−11.0	-------	30
Norfolk, Va.[2] (10 m)	9.5	−2.0	9.6	−1.6	7.0	−2.1	4.9	−1.9	2.7	−1.7	.4	−1.5	−2.6	−1.8	−8.3	−2.1	−13.7	−2.0	20
Oklahoma City, Okla.[2] (391 m)	12.1	-------	13.9	-------	13.1	-------	11.2	-------	9.1	-------	5.9	-------	2.4	-------	−4.8	-------	-------	-------	30
Omaha, Nebr.[2] (300 m)	5.6	−1.0	6.0	−1.3	5.2	−1.7	3.1	−2.0	1.2	−1.7	−1.1	−1.5	−3.8	−1.4	−10.1	−1.4	−16.9	−1.1	30
Pearl Harbor, Territory of Hawaii[3] (6 m)	20.3	−2.3	18.4	−1.3	15.0	−1.1	12.6	−.8	11.5	+.1	10.0	−.1	7.4	−.9	1.5	−2.6	-------	-------	30
Pensacola, Fla.[3] (2 m)	17.2	−.6	16.4	−.1	14.6	0	12.5	0	9.9	−.4	7.1	−.5	4.1	−.7	−1.5	−.1	−7.9	0	27
San Diego, Calif.[1] (10 m)	13.0	−2.5	12.2	−1.0	13.6	+.9	13.2	+2.0	11.2	+1.9	8.4	+1.8	5.6	+1.6	−.1	+1.4	−6.5	+1.8	29
Scott Field (Belleville), Ill.[1] (135 m)	5.6	-------	9.2	-------	8.0	-------	5.4	-------	2.8	-------	.1	-------	−2.1	-------	−7.5	-------	−13.6	-------	24
Seattle, Wash.[2] (10 m)	10.5	+.7	6.6	−1.2	4.8	−.6	2.2	−.4	−.2	0	−3.0	−.1	−5.8	−.3	−12.6	−1.3	−20.2	−2.0	15
Spokane, Wash.[2] (596 m)	5.9	-------	-------	-------	8.8	-------	8.2	-------	5.3	-------	1.8	-------	−1.4	-------	−7.9	-------	−15.3	-------	30
Washington, D. C.[2] (13 m)	7.1	−3.2	7.1	−1.5	4.5	−1.8	2.4	−2.2	.5	−2.4	−1.9	−3.2	−4.2	−3.9	−8.7	−3.6	−13.4	−3.0	26
Wright Field (Dayton), Ohio[1] (244 m)	5.3	-------	6.5	-------	4.6	-------	2.7	-------	.8	-------	−1.5	-------	−3.9	-------	−9.1	-------	−14.9	-------	26

RELATIVE HUMIDITY (PERCENT)

Barksdale Field (Shreveport), La.	71	-------	58	-------	54	-------	51	-------	40	-------	37	-------	34	-------	33	-------	31	-------	-------
Billings, Mont.	67	-------	-------	-------	-------	-------	60	-------	60	-------	63	-------	66	-------	68	-------	64	-------	-------
Boston, Mass.	73	+3	65	−1	64	+1	64	+3	63	+1	63	+1	64	+4	60	+6	55	+4	-------
Cheyenne, Wyo.	69	-------	-------	-------	-------	-------	-------	-------	64	-------	59	-------	59	-------	59	-------	61	-------	-------
El Paso, Tex.	31	-------	-------	-------	-------	-------	33	-------	33	-------	35	-------	38	-------	43	-------	47	-------	-------
Fargo, N. Dak.	82	-------	65	-------	60	-------	57	-------	56	-------	53	-------	53	-------	55	-------	55	-------	-------
Kelly Field (San Antonio), Tex.	79	-------	75	-------	63	-------	55	-------	43	-------	39	-------	37	-------	35	-------	33	-------	-------
Lakehurst, N. J.	71	-------	65	-------	59	-------	59	-------	62	-------	58	-------	53	-------	42	-------	-------	-------	-------
Maxwell Field (Montgomery), Ala.	72	-------	58	-------	53	-------	51	-------	53	-------	53	-------	46	-------	36	-------	34	-------	-------
Mitchel Field (Hempstead, Long Island), N. Y.	77	-------	67	-------	62	-------	62	-------	65	-------	62	-------	59	-------	57	-------	54	-------	-------
Murfreesboro, Tenn.	79	-------	69	-------	69	-------	66	-------	66	-------	59	-------	55	-------	47	-------	45	-------	-------
Norfolk, Va.	76	+7	62	+3	60	+4	60	+5	58	+5	53	+2	54	+5	51	+9	48	+11	-------
Oklahoma City, Okla.	54	-------	56	-------	54	-------	49	-------	46	-------	45	-------	46	-------	49	-------	-------	-------	-------
Omaha, Nebr.	62	−8	61	−6	56	−5	54	−3	52	−2	51	−2	51	−1	57	+5	57	+6	-------
Pearl Harbor, Territory of Hawaii.	83	+13	82	+8	85	+7	81	+6	67	−1	52	−2	46	+3	39	+10	-------	-------	-------
Pensacola, Fla.	78	−1	65	−5	62	−1	56	−1	56	+5	53	+5	51	+7	38	+2	28	−3	-------
San Diego, Calif.	87	+13	81	+5	58	−5	38	−11	29	−10	24	−10	21	−8	18	−5	18	−4	-------
Scott Field (Belleville), Ill.	76	-------	55	-------	49	-------	51	-------	54	-------	57	-------	58	-------	53	-------	51	-------	-------
Seattle, Wash.	74	+2	77	+7	74	+7	73	+9	69	+9	65	+8	60	+6	50	+3	46	+1	-------
Spokane, Wash.	74	-------	-------	-------	61	-------	57	-------	59	-------	61	-------	61	-------	60	-------	60	-------	-------
Washington, D. C.	71	+6	56	−3	55	−2	54	−3	55	−1	56	+3	50	+1	45	0	48	+3	-------
Wright Field (Dayton), Ohio	77	-------	71	-------	69	-------	67	-------	65	-------	66	-------	67	-------	68	-------	62	-------	-------

[1] Army. [2] Weather Bureau. [3] Navy.

Observations taken about 4 a. m., 75th meridian time, except along the Pacific coast and Hawaii where they are taken at dawn.

NOTE.—The departures are based on "normals" covering the following total number of observations made during the same month in previous years, including the current month: Boston, 84; Norfolk, 141; Omaha, 149; Pearl Harbor, 112; Pensacola, 190; San Diego, 175; Seattle, 84; Washington, 226.

TABLE 2.—*Free-air resultant winds (meters per second) based on pilot-balloon observations made near 5 a. m. (E. S. T.) during April 1936*

[Wind from N=360°, E=90°, etc.]

Altitude (m) m. s. l.	Albuquerque, N. Mex. (1,554 m)		Atlanta, Ga. (309 m)		Billings, Mont. (1,088 m)		Boston, Mass. (15 m)		Cheyenne, Wyo. (1,873 m)		Chicago, Ill. (192 m)		Cincinnati, Ohio (153 m)		Detroit, Mich. (204 m)		Fargo, N. Dak. (274 m)		Houston, Tex. (21 m)		Key West, Fla. (11 m)		Medford, Oreg. (410 m)		Murfreesboro, Tenn. (180 m)	
	Direction	Velocity	Direction	Velocity	Direction	Velocity	Direction	Velocity	Direction	Velocity	Direction	Velocity	Direction	Velocity	Direction	Velocity	Direction	Velocity	Direction	Velocity	Direction	Velocity	Direction	Velocity	Direction	Velocity
	°		°		°		°		°		°		°		°		°		°		°		°		°	
Surface	335	0.9	290	0.9	299	1.4	266	1.9	284	3.4	294	0.3	259	0.6	269	1.4	329	1.0	15	1.7	74	2.2	108	0.2	202	0.9
500	-----	-----	263	2.0	-----	-----	286	8.9	-----	-----	259	3.6	255	2.7	284	3.1	343	2.8	122	2.0	95	3.6	308	.4	217	2.9
1,000	-----	-----	283	4.1	-----	-----	294	9.8	-----	-----	289	5.2	281	6.4	292	6.1	323	4.4	125	2.2	130	2.6	303	.9	250	5.1
1,500	-----	-----	273	5.9	284	4.7	288	10.8	-----	-----	300	6.5	281	8.6	274	7.8	305	5.7	204	1.2	180	1.4	180	.5	280	6.0
2,000	279	3.3	288	8.2	289	5.2	290	11.0	277	5.9	303	8.7	296	10.5	288	10.7	307	8.4	234	2.2	219	1.9	196	2.4	298	7.3
2,500	271	5.8	282	9.2	284	7.4	283	10.7	287	8.8	298	10.4	298	9.8	289	11.3	304	8.8	261	2.7	232	2.5	225	2.7	287	7.8
3,000	284	6.8	285	8.8	291	8.2	280	12.7	298	9.4	301	13.3	301	11.0	276	11.9	307	8.5	275	3.0	255	3.3	225	5.5	264	5.9
4,000	291	5.4	-----	-----	304	7.8	-----	-----	297	7.4	307	15.9	-----	-----	-----	-----	-----	-----	295	7.1	271	4.3	230	8.4	-----	-----
5,000	302	5.1	-----	-----	313	7.6	-----	-----	284	6.2	-----	-----	-----	-----	-----	-----	-----	-----	-----	-----	-----	-----	230	8.9	-----	-----

Altitude (m) m. s. l.	Newark, N. J. (14 m)		Oakland, Calif. (8 m)		Oklahoma City, Okla. (402 m)		Omaha, Nebr. (306 m)		Pearl Harbor, Territory of Hawaii [1] (68 m)		Pensacola, Fla.[1] (24 m)		St. Louis, Mo. (170 m)		Salt Lake City, Utah (1,294 m)		San Diego, Calif. (15 m)		Sault Ste. Marie, Mich. (198 m)		Seattle, Wash. (14 m)		Spokane, Wash. (603 m)		Washington, D. C. (10 m)	
	Direction	Velocity	Direction	Velocity	Direction	Velocity	Direction	Velocity	Direction	Velocity	Direction	Velocity	Direction	Velocity	Direction	Velocity	Direction	Velocity	Direction	Velocity	Direction	Velocity	Direction	Velocity	Direction	Velocity
	°		°		°		°		°		°		°		°		°		°		°		°		°	
Surface	265	2.1	199	0.7	182	1.9	36	0.7	-----	-----	70	1.5	253	0.9	138	2.2	360	0.1	331	1.8	180	1.5	139	0.9	291	1.8
500	277	6.9	288	2.5	177	5.2	110	0.8	-----	-----	189	1.2	241	3.8	-----	-----	333	1.9	342	3.8	201	2.6	-----	-----	278	4.8
1,000	279	9.0	315	4.4	211	8.6	234	3.6	-----	-----	240	4.4	282	5.2	-----	-----	346	2.8	340	4.6	193	2.4	223	2.5	276	6.7
1,500	276	9.1	321	3.0	245	6.6	269	6.3	-----	-----	263	5.1	293	7.9	148	2.6	294	3.7	322	5.2	210	2.7	242	3.6	289	9.7
2,000	284	10.1	315	3.0	259	4.8	304	9.9	-----	-----	278	7.3	290	9.0	210	1.2	320	3.0	255	3.4	223	4.2	250	4.7	286	10.4
2,500	287	12.9	321	3.8	278	4.5	310	11.0	-----	-----	287	7.5	296	9.4	262	2.3	297	4.8	-----	-----	224	6.3	258	5.5	271	9.9
3,000	287	12.4	284	4.2	301	5.7	310	12.4	-----	-----	269	6.6	300	9.4	276	3.6	328	4.8	-----	-----	221	5.7	257	5.9	270	10.4
4,000	-----	-----	-----	-----	299	5.8	312	12.0	-----	-----	-----	-----	-----	-----	283	6.5	338	8.3	-----	-----	233	7.0	266	8.2	-----	-----
5,000	-----	-----	-----	-----	-----	-----	-----	-----	-----	-----	-----	-----	-----	-----	295	7.5	-----	-----	-----	-----	-----	-----	250	10.8	-----	-----

[1] Navy stations.

RIVERS AND FLOODS

[River and Flood Division, MONTROSE W. HAYES in charge]

By W. J. MOXOM

The winter of 1935–36 was unusually cold over the region east of the Rocky Mountains, and the snowfall was the heaviest in many years in the country north of the Potomac, Ohio, and Missouri Rivers. These conditions usually bring about floods when there is a sudden melting of snow and breaking up of ice by rain and warm weather; and in March floods occurred in Iowa, Minnesota, and in all the States east of the Mississippi River, except Michigan. They were light to moderate, except along the Atlantic seaboard from Virginia northward and in the upper Ohio Valley, where they were extremely high and exceeded all previous records.

Late in February and early in March, mild, rainy weather caused rises and ice gorges in the rivers of Virginia and Maryland, and some damage resulted from ice movement, but the combined run-off from the rain and melted snow was insufficient to give injurious floods. New England, New York, and Pennsylvania were not so fortunate, and there was considerable damage from both the crushing effects of ice and from floodwaters.

By March 16 the streams in Virginia and Maryland had fallen considerably and a fall had begun north of Maryland. Conditions were approaching normal, but on March 17 a storm that originated on March 15 in Texas had moved to south-central North Carolina and was causing general rains over the Middle Atlantic seaboard and the upper Ohio Basin. These rains were phenomenally heavy in the country to the west of the Coastal Plains and along the divide between the eastern rivers and the upper Ohio Basin. Amounts of nearly 5 inches occurred in 12 hours or less over a large area in the mountainous regions of Virginia, Maryland, and western Pennsylvania, and more than 6 inches fell at some stations in a period of 48 hours or less. The storm moved slowly in a northeasterly direction and the rains were heavy over all of the North Atlantic seaboard. To the northeastward the amounts were not so heavy, but from a flood-producing viewpoint the results were about the same, because the rivers in the southern part of the area under consideration were much lower at the beginning of the rain than they were in Pennsylvania, New York, and New England.

The rains fell on well-saturated and semifrozen soil, and the percentage of run-off was unusually high. This, coupled with the fact that the northern rivers were at or above flood stage, and those in Maryland and Virginia, while not in flood were higher than normal, gave the most disastrous floods of record in the James, Potomac, Susquehanna, Connecticut, and Merrimack Rivers, in some of the tributaries of the Ohio River in Pennsylvania and in the Ohio River from Pittsburgh, Pa., to below Wheeling, W. Va.

The Ohio River flood, which gave a record crest stage of 46.0 feet at Pittsburgh, Pa., on March 18, crested at Evansville, Ind., on March 31. The rise in the Ohio below Evansville was prolonged, due to early April floods in the Cumberland and Tennessee Rivers, and a crest stage of 52.8 feet occurred at Cairo, Ill., on April 16.

In the lower Mississippi River, flood stages were exceeded at all points between Cairo, Ill., and Helena, Ark. At Helena the crest was 50.6 feet on April 22–24. Flood stage was not reached below the mouth of the Arkansas River; and the crest of the rise reached New Orleans, La., on May 3, 1936, giving a stage of 14.4 feet which was 2.6 feet below flood stage at that place.

In April, river stages in the Carolinas were the highest since 1929, and the highest since 1916 at a few points in the Saluda Basin in South Carolina. Moderately high floods prevailed in Georgia and Alabama; they were light to moderate elsewhere. All of the rivers in North Carolina have been in flood one or more times during each month from January to April, inclusive, with high water prevailing in the lower portions for prolonged periods.

Flood losses in the Northeastern States in March were undoubtedly the greatest of record, but it is not practicable at this time to give the estimated money value. Several hundred thousand people were made homeless by the floodwaters and many homes were completely destroyed. The actual number of drownings may never be known, but unofficial figures place it at more than 170. Business was partially or completely paralyzed in many of the large industrial sections, and losses to wage earners and retailers amounted to large sums. In April rather large losses occurred in Alabama, Georgia and the Carolinas, but elsewhere they were light.

A full report of these floods will be made in a later number, or perhaps a supplement, of the MONTHLY WEATHER REVIEW, when all data are available.

The following table shows for a few stations the gage heights of the March 1936 flood, compared with the previous highest records:

Station	River	1936 stage	Previous record	
			Stage	Year
Columbia, Va.	James	35.9	35.4	1635
Richmond, Va.	do	28.5	23.6	1935
Hancock, Md.	Potomac	47.6	39.7	1889
Washington, D. C.	do	19.8	19.5	1889
Sunbury, Pa.	Susquehanna	26.8	21.0	1889
Harrisburg, Pa.	do	30.3	26.1	1889
Holyoke, Mass.	Connecticut	16.8	14.8	1927
Springfield, Mass.	do	28.6	22.4	1927
Hartford, Conn.	do	37.3	29.8	1854
Saltsburg, Pa.	Kiskiminitas	33.1	22.1	1859
McKeesport, Pa.	Monongahela	28.8	25.8	1907
Pittsburgh, Pa.	Ohio	46.0	41.1	1763
Old Dam No. 2, Coraopolis, Pa.	do	43.6	36.5	1907
Dam No. 6, Beaver, Pa.	do	54.8	46.6	1907
Dam No. 13, Wheeling, W. Va.	do	57.8	53.4	1884
Parkersburg, W. Va.	do	48.0	58.9	1913

Table of flood stages in March and April 1936

River and station	Flood stage	Above flood stages—dates		Crest	
		From—	To—	Stage	Date
ST. LAWRENCE DRAINAGE					
Lake Erie	*Feet*			*Feet*	
Sandusky: Upper Sandusky, Ohio	13	Mar. 25	Mar. 25	13.7	Mar. 25.
ATLANTIC SLOPE DRAINAGE					
Connecticut:					
White River Junction, Vt.	18	Mar. 12	Mar. 14	19.8	Mar. 12.
		Mar. 17	Mar. 26	33.4	Mar. 19.
Bellows Falls, Vt.	16	Mar. 19	Mar. 22	24.6	Do.
Holyoke, Mass.	9	Mar. 14	Mar. 16	9.9	Mar. 15.
		Mar. 19	Mar. 25	16.8	Mar. 20.
Springfield, Mass.	20	do	Mar. 24	38.6	Do.
Hartford, Conn.	16	Mar. 13	Apr. 1	37.3	Mar. 21.
		Apr. 7	Apr. 11	18.5	Apr. 8.
Mohawk: Tribes Hill, N. Y.	23	Mar. 18	Mar. 19	25.4	Mar. 18.
Hudson: Albany, N. Y.	12	Mar. 13	Mar. 13	15.1	Mar. 13.
		Mar. 18	Mar. 20	18.7	Mar. 19.
Lackawaxen: Hawley, Pa.	9	Mar. 12	Mar. 12	13.4	Mar. 12.
		Mar. 17	Mar. 19	15.2	Mar. 18.

Table of flood stages in March and April 1936—Continued

River and station	Flood stage	Above flood stages—dates		Crest	
		From—	To—	Stage	Date
ATLANTIC SLOPE DRAINAGE—con.					
	Feet			*Feet*	
Lehigh: Lehighton, Pa.	9	Mar. 9	Mar. 12	11.3	Mar. 11.
		Mar. 18	Mar. 19	13.1	Mar. 18.
Schuylkill: Reading, Pa.	10	Mar. 12	Mar. 13	15.5	Mar. 12.
		Mar. 18	Mar. 19	12.4	Mar. 18.
		Apr. 6	Apr. 6	10.2	Apr. 6.
Delaware:					
Port Jervis, N. Y.	18	Mar. 18	Mar. 18	18.6	Mar. 18.
Phillipsburg, N. J.	22	Mar. 12	Mar. 13	27.6	Mar. 12.
		Mar. 18	Mar. 20	30.7	Mar. 19.
Trenton, N. J.	12	Mar. 12	Mar. 13	15.5	Mar. 12.
		Mar. 18	Mar. 20	16.6	Mar. 19.
Chenango:					
Sherburne, N. Y.	8	Mar. 12	Mar. 13	9.6	Mar. 12.
		Mar. 16	Mar. 22	10.6	Mar. 18.
Binghamton, N. Y.	16	Mar. 11	Mar. 14	22.0	Mar. 13.
		Mar. 16	Mar. 22	27.0	Mar. 18.
Chemung: Corning, N. Y.	16	Mar. 12	Mar. 12	19.3	Mar. 12.
		Mar. 18	Mar. 18	17.8	Mar. 18.
West Branch—Susquehanna:					
Clearfield, Pa.	10	do	Mar. 19	[1] 17.8	Do.
Renovo, Pa.	16	Mar. 17	do	29.3	Do.
Williamsport, Pa.	20	Mar. 12	Mar. 13	23.7	Mar. 12.
		Mar. 17	Mar. 20	[1] 33.7	Mar. 19.
Frankstown Branch: Huntingdon, Pa.	12	do	do	[1] 22.0	Mar. 18.
Juniata: Newport, Pa.	26	Mar. 18	Mar. 19	34.2	Mar. 19.
Susquehanna:					
Oneonta, N. Y.	12	Mar. 11	Mar. 25	19.5	Mar. 18.
Bainbridge, N. Y.	12	do	Mar. 14	18.0	Mar. 13.
		Mar. 16	Mar. 22	21.5	Mar. 18.
Binghamton, N. Y.	14	Mar. 12	Mar. 14	18.0	Mar. 13.
		Mar. 17	Mar. 21	22.8	Mar. 18.
Towanda, Pa.	16	Mar. 12	Mar. 14	22.3	Mar. 13.
		Mar. 17	Mar. 21	25.0	Mar. 19.
Wilkes-Barre, Pa.	22	Mar. 12	Mar. 14	28.9	Mar. 13.
		Mar. 17	Mar. 22	33.1	Mar. 20.
Sunbury, Pa.	20	Mar. 18	Mar. 20	26.8	Mar. 19.
Harrisburg, Pa.	18	Mar. 12	Mar. 14	21.8	Mar. 13.
		Mar. 18	Mar. 22	30.3	Mar. 19.
North Branch—Potomac: Cumberland, Md.	17	Mar. 17	Mar. 19	29.1	Mar. 18.
Shenandoah: Riverton, Va.	22	do	do	37.5	Do.
Potomac:					
Hancock, Md.	32	do	do	47.6	Do.
Harpers Ferry, W. Va.	18	Mar. 18	Mar. 20	36.5	Mar. 19.
Sycamore Island, Md.	11	do	Mar. 21	28.5	Do.
Washington, D. C.	8	do	do	19.8	Do.
James:					
Buchanan, Va.	17	Mar. 17	Mar. 19	28.0	Mar. 18.
Lynchburg, Va.	18	Mar. 18	do	24.7	Do.
Columbia, Va.	10	Mar. 1	Mar. 1	10.2	Mar. 1.
		Mar. 13	Mar. 13	10.2	Mar. 13.
		Mar. 17	Mar. 31	35.8	Mar. 19.
		Apr. 3	Apr. 4	10.5	Apr. 4.
		Apr. 6	Apr. 15	17.1	Apr. 8.
Richmond, Va.	8	Mar. 18	Mar. 23	26.5	Mar. 20.
Dan:					
Danville, Va.	11	do	Mar. 18	12.7	Mar. 18.
Clarksville, Va.	13	do	Mar. 20	16.3	Mar. 20.
Roanoke:					
Randolph, Va.	18	do	Mar. 21	20.1	Mar. 19.
		Apr. 7	Apr. 8	19.5	Apr. 8.
Weldon, N. C.	31	Mar. 18	Mar. 24	44.8	Mar. 21.
		Apr. 7	Apr. 13	38.1	Apr. 8, 9.
Williamston, N. C.	10	Mar. 1	Mar. 3	10.5	Mar. 1.
		Mar. 17	Apr. 24	14.0	Mar. 25.
Fishing Creek: Enfield, N. C.	14	Apr. 8	Apr. 10	14.9	Apr. 9, 10.
Tar:					
Rocky Mount, N. C.	8	Mar. 18	Mar. 22	9.4	Mar. 22.
		Apr. 5	Apr. 12	11.1	Apr. 11.
Tarboro, N. C.	18	Mar. 22	Mar. 24	18.5	Mar. 23.
		Apr. 7	Apr. 15	24.3	Apr. 12, 13.
Greenville, N. C.	13	Mar. 21	Mar. 26	14.5	Mar. 24, 25.
		Apr. 8	Apr. 18	18.2	Apr. 14.
		Mar. 18	Mar. 23	18.1	Mar. 20.
Neuse, N. C.	14	Mar. 29	Mar. 30	16.9	Mar. 29.
		Apr. 4	Apr. 13	19.6	Apr. 9.
		Mar. 18	Mar. 24	17.5	Mar. 23.
Smithfield, N. C.	13	Mar. 31	Mar. 31	13.4	Mar. 31.
		Apr. 3	Apr. 15	20.7	Apr. 9.
		Mar. 18	Mar. 19	25.8	Mar. 18.
Haw: Moncure, N. C.	20	Apr. 3	Apr. 3	21.2	Apr. 3.
		Apr. 7	Apr. 10	29.0	Apr. 7.
Cape Fear:					
Fayetteville N. C.	35	Mar. 18	Mar. 21	43.2	Mar. 19.
		Apr. 4	Apr. 4	37.1	Apr. 4.
		Apr. 7	Apr. 12	54.9	Apr. 8.
Lock No. 2 Elizabethtown N. C.	20	Mar. 18	Mar. 24	30.8	Mar. 20.
		Mar. 29	Apr. 2	26.4	Mar. 30.
		Apr. 4	Apr. 16	31.8	Apr. 10.
Lynches: Effingham S. C.	14	Apr. 8	Apr. 17	18.6	Apr. 12
Waccamaw: Conway S. C.	7	Apr. 14	Apr. 25	9.3	Apr. 18, 19.
Peedee:					
Cheraw S. C.	30	Mar. 18	Mar. 20	36.2	Mar. 18.
		Mar. 29	Mar. 30	34.9	Mar. 29.
		Apr. 3	Apr. 5	37.2	Apr. 3.
		Apr. 7	Apr. 12	42.8	Apr. 8.
Mars Bluff Bridge S. C.	17	Mar. 15	Mar. 16	17.3	Mar. 15.
		Mar. 20	Apr. 21	27.1	Apr. 11.
Poston S. C.	18	Mar. 24	Apr. 23	27.8	Apr. 13.

[1] Subject to correction when high water marks are tied in by leveling.

Table of flood stages in March and April 1936—Continued

River and station	Flood stage	Above flood stages—dates		Crest	
		From—	To—	Stage	Date
ATLANTIC SLOPE DRAINAGE—con.					
	Feet			*Feet*	
Black: Kingstree S. C.	12	Apr. 4	Apr. 17	13.1	Do.
Saluda:					
Pelzer S. C.	6	Mar. 28	Mar. 30	7.0	Mar. 28.
		Apr. 2	Apr. 13	15.0	Apr. 7.
Chappells S. C.	13	Mar. 26	Mar. 30	19.0	Mar. 26.
		Apr. 2	Apr. 13	28.6	Apr. 8.
Columbia S. C.	8	...do...	...do...	13.9	Do.
Broad: Blairs S. C.	14	Mar. 27	Mar. 30	18.4	Mar. 29.
		Apr. 2	Apr. 11	33.8	Apr. 8.
Congaree: Columbia S. C.	19	...do...	Apr. 12	33.3	Do.
Catawba:					
Catawba N. C.	10	Apr. 2	Apr. 3	13.0	Apr. 2.
		Apr. 6	Apr. 6	17.7	Apr. 6.
Catawba S. C.	11	Mar. 28	Mar. 28	12.1	Mar. 28.
		Apr. 2	Apr. 3	16.0	Apr. 3.
		Apr. 7	Apr. 10	25.0	Apr. 7.
Wateree: Camden S. C.	23	Mar. 29	Mar. 29	25.0	Mar. 29.
		Apr. 2	Apr. 12	36.6	Apr. 7.
Santee:					
Rimini, S. C.	12	Feb. 5	Mar. 1	17.1	Feb. 10.
		Mar. 6	Mar. 7	12.1	Mar. 6, 7.
		Mar. 12	Mar. 15	13.0	Mar. 14
		Mar. 18	May 4	33.0	Apr. 10.
Ferguson, S. C.	12	Jan. 6	Mar. 9	14.8	Jan. 26.
		Mar. 13	May 6	20.4	Apr. 12.
Broad: Carlton, Ga.	15	Apr. 2	Apr. 3	22.0	Apr. 2.
		Apr. 6	Apr. 8	[1] 28.0	Apr. 7.
Savannah:					
Calhoun Falls, S. C.	8	...do...	...do...	11.5	Do.
Augusta, Ga.	32	Apr. 2	Apr. 4	34.7	Apr. 3.
		Apr. 6	Apr. 11	41.2	Apr. 8.
Ellenton, S. C.	14	Mar. 19	Mar. 22	16.0	Mar. 21.
		Mar. 24	Apr. 28	36.9	Apr. 9.
Clyo, Ga.	13	Mar. 31	...do...	26.0	Apr. 13.
Ogeechee:					
Midville, Ga.	6	Apr. 6	Apr. 16	9.1	Apr. 11.
Dover, Ga.	7	Apr. 3	Apr. 23	12.8	Apr. 14.
Ocmulgee:					
Macon, Ga.	15	Apr. 2	Apr. 11	25.1	Apr. 9.
Hawkinsville, Ga.	25	Apr. 6	Apr. 15	33.0	Apr. 12.
Abbeville, Ga.	11	Apr. 3	Apr. 21	19.7	Apr. 13.
Lumber City, Ga.	15	Apr. 7	Apr. 22	22.7	Apr. 16.
Oconee:					
Milledgeville, Ga.	22	Apr. 2	Apr. 12	36.8	Apr. 10.
Dublin, Ga.	22	Apr. 6	Apr. 17	33.4	Apr. 12.
Altamaha:					
Charlotte, Ga.	12	Mar. 1	Mar. 2	12.9	Mar. 1.
		Apr. 1	Apr. 27	27.9	Apr. 16.
Doctortown, Ga.	10	Apr. 13	Apr. 23	12.0	Apr. 18.
EAST GULF OF MEXICO DRAINAGE					
Chattahoochee:					
West Point, Ga.	19	Apr. 7	Apr. 11	22.4	Apr. 8.
Eufaula, Ala.	40	Apr. 9	Apr. 13	50.4	Apr. 11.
Columbia, Ala.	42	Apr. 10	Apr. 14	46.7	Apr. 12.
Alaga, Ala.	32	Apr. 8	Apr. 15	40.5	Do.
Flint:					
Montezuma, Ga.	20	Apr. 5	Apr. 5	20.4	Apr. 5.
		Apr. 11	Apr. 13	22.8	Apr. 12.
Albany, Ga.	20	Apr. 7	Apr. 18	29.4	Apr. 15.
Bainbridge, Ga.	25	Apr. 11	Apr. 20	31.0	Apr. 17.
Apalachicola:					
River Junction, Fla.	20	Apr. 9	Apr. 18	23.8	Apr. 15.
Blountstown, Fla.	15	Mar. 1	Mar. 9	17.6	Mar. 1, 2.
		Mar. 27	Apr. 30	23.6	Apr. 15.
Choctawhatchee: Caryville, Fla.	12	Apr. 13	Apr. 13	12.2	Apr. 13.
Oostanaula:					
Resaca, Ga.	22	Apr. 2	Apr. 11	30.9	Apr. 3.
Rome, Ga.	25	...do...	Apr. 12	33.7	Apr. 8.
Etowah: Canton, Ga.	17	Apr. 2	Apr. 3	23.0	Apr. 2.
		Apr. 6	Apr. 7	22.3	Apr. 7.
Coosa:					
Mayos Bar Lock, Ga.	28	Apr. 2	Apr. 13	36.9	Apr. 8.
Gadsden, Ala.	20	Mar. 28	Apr. 18	31.5	Apr. 11, 12.
Lock No. 4, Lincoln, Ala.	17	Apr. 3	Apr. 17	23.5	Apr. 10.
Wetumpka, Ala.	45	Apr. 7	Apr. 14	50.6	Apr. 9.
Tallapoosa: Milstead, Ala.	40	...do...	Apr. 10	42.2	Apr. 10.
Cahaba: Centerville, Ala.	23	Apr. 7	Apr. 7	25.0	Apr. 7.
		Apr. 9	Apr. 9	25.5	Apr. 9.
Alabama:					
Montgomery, Ala.	35	Apr. 7	Apr. 18	51.5	Apr. 11.
Selma, Ala.	45	Apr. 9	Apr. 19	52.2	Apr. 14.
Millers Ferry, Ala.	40	Apr. 7	Apr. 23	52.0	Apr. 16.
Black Warrior: Lock No. 10, Tuscaloosa, Ala.	46	Apr. 3	Apr. 5	51.3	Apr. 4.
		Apr. 10	Apr. 11	49.5	Apr. 10.
Tombigbee:					
Aberdeen, Miss.	34	...do...	Apr. 12	36.3	Apr. 11.
Lock No. 4, Demopolis, Ala.	39	Apr. 1	Apr. 20	51.6	Apr. 12.
Lock No. 3, Ala.	33	Mar. 30	Apr. 22	53.1	Apr. 11.
Lock No. 2, Ala.	46	Apr. 4	Apr. 21	54.5	Apr. 11, 12.
Lock No. 1, Ala.	31	Apr. 3	Apr. 24	37.1	Apr. 13–18.
Pearl: Pearl River, La.	12	Mar. 1	Mar. 3	13.6	Mar. 1.
		Apr. 13	Apr. 16	12.1	Apr. 14.

Table of flood stages in March and April 1936—Continued

River and station	Flood stage	Above flood stages—dates		Crest	
		From—	To—	Stage	Date
MISSISSIPPI SYSTEM					
Upper Mississippi Basin					
	Feet			*Feet*	
Minnesota: Mankato, Minn.	19	Mar. 22	Mar. 24	20.2	Mar. 23.
Chippewa: Durand, Wis.	11	Mar. 25	Mar. 26	11.5	Mar. 26.
		Apr. 14	Apr. 18	12.1	Apr. 14.
Wisconsin:					
Knowlton, Wis.	12	Mar. 24	Mar. 26	17.2	Mar. 24.
Portage, Wis.	17	Mar. 29	Mar. 30	17.6	Mar. 29.
Iowa: Wapello, Iowa.	10	Mar. 15	Mar. 20	11.6	Mar. 17, 18.
Raccoon: Van Meter, Iowa.	13	Mar. 5	Mar. 6	14.0	Mar. 5.
Des Moines:					
Tracy, Iowa.	14	Mar. 4	Mar. 5	14.3	Do.
		Mar. 12	Mar. 12	14.0	Mar. 12.
Ottumwa, Iowa.	9	Mar. 4	Mar. 6	9.5	Mar. 6.
Illinois:					
Morris, Ill.	13	Feb. 25	Mar. 1	14.5	Feb. 27.
Peru, Ill.	17	Feb. 26	Mar. 8	21.7	Feb. 28.
Peoria, Ill.	18	Mar. 1	Mar. 12	19.8	Mar. 4, 5.
Havana, Ill.	14	Feb. 27	Mar. 22	18.0	Mar. 3, 4.
Beardstown, Ill.	14	Feb. 28	Mar. 24	19.8	Mar. 4, 5.
Mississippi:					
St. Paul, Minn.	8	Mar. 24	Apr. 5	10.9	Mar. 30.
La Crosse, Wis.	12	.....	.....	11.9	Apr. 20.
Keokuk, Iowa.	12	Apr. 9	Apr. 12	12.3	Apr. 9.
Hannibal, Mo.	13	Mar. 17	Mar. 20	13.3	Mar. 18.
		Apr. 6	Apr. 15	13.9	Apr. 10–12.
Missouri Basin					
Big Sioux: Akron, Iowa.	12	Mar. 5	Mar. 16	18.7	Mar. 12.
Floyd: Merrill, Iowa.	13	Mar. 6	Mar. 11	14.5	Mar. 10.
Platte: Ashland, Nebr.	7	Mar. 5	Mar. 5	7.4	Mar. 5.
Missouri: Nebraska City, Nebr.	15	Mar. 6	Mar. 7	15.2	Mar. 6.
Ohio Basin					
Stony Creek: Johnstown, Pa.	15	Mar. 17	Mar. 18	30.2	Mar. 17.
Kiskiminetas: Saltsburg, Pa.	8	...do...	...do...	33.1	Mar. 18.
Allegheny:					
Olean, N. Y.	12	Mar. 19	Mar. 20	12.8	Mar. 19.
		Mar. 28	Mar. 28	12.8	Mar. 28.
Warren, Pa.	12	Mar. 27	Mar. 29	13.9	Do.
Franklin, Pa.	17	...do...	Mar. 28	18.9	Do.
Lock No. 8, Mosgrove, Pa.	24	Mar. 12	Mar. 13	28.7	Mar. 12.
		Mar. 17	Mar. 19	37.6	Mar. 18.
		Mar. 25	Mar. 30	27.7	Mar. 28.
Lock No. 5, Schenley, Pa.	24	Mar. 12	Mar. 14	28.5	Mar. 12.
		Mar. 17	Mar. 20	45.7	Mar. 18.
		Mar. 26	Mar. 29	27.2	Mar. 28.
Lock No. 4, Natrona, Pa.	24	Mar. 12	Mar. 14	26.8	Mar. 12.
		Mar. 17	Mar. 20	43.6	Mar. 18.
		Mar. 26	Mar. 29	26.3	Mar. 28.
Lock No. 3, Acmetonia, Pa.	25	Mar. 12	Mar. 13	26.7	Mar. 13.
		Mar. 17	Mar. 20	45.2	Mar. 18.
		Mar. 28	Mar. 29	26.3	Mar. 28.
Tygart:					
Elkins, W. Va.	14	Mar. 17	Mar. 18	15.8	Mar. 18.
		Mar. 25	Mar. 25	15.8	Mar. 25.
Philippi, W. Va.	20	.....	.....	19.1	Mar. 18.
		Mar. 24	Mar. 25	24.0	Mar. 24, 25
Youghiogheny:					
Connellsville, Pa.	13	Mar. 17	Mar. 18	20.3	Mar. 18.
West Newton, Pa.	20	...do...	...do...	26.0	Do.
Monongahela:					
Lock No. 15, Hoult, W. Va.	22	...do...	...do...	25.8	Mar. 17, 18
Lock No. 10, Morgantown, W. Va.	25	Mar. 24	Mar. 25	27.2	Mar. 25.
		Mar. 18	Mar. 18	25.3	Mar. 18.
		Mar. 25	Mar. 25	27.2	Mar. 25.
Lock No. 7, Greensboro, Pa.	30	Mar. 17	Mar. 19	40.4	Mar. 18.
		Mar. 24	Mar. 26	39.3	Mar. 25.
		Apr. 7	Apr. 7	31.0	Apr. 7.
Lock No. 4, Charleroi, Pa.	30	Mar. 17	Mar. 19	40.1	Mar. 18.
		Mar. 25	Mar. 26	36.0	Mar. 25
McKeesport, Pa.	20	Mar. 17	Mar. 19	28.8	Mar. 18.
Walhonding: Walhonding, Ohio.	8	Mar. 24	Mar. 25	10.3	Mar. 24.
Tuscarawas: Coshocton, Ohio.	11	Mar. 1	Mar. 1	12.6	Mar. 1.
		Mar. 24	Mar. 28	13.8	Mar. 26.
Muskingum:					
Lock No. 7, McConnelsville, Ohio.	22	Mar. 1	Mar. 1	22.1	Mar. 1.
Lock No. 3, Lowell, Ohio.	25	Mar. 20	Mar. 22	28.2	Mar. 21.
Lock No. 1, Marietta, Ohio.	35	Mar. 18	Mar. 24	48.1	Mar. 20.
		Mar. 25	Mar. 30	40.4	Mar. 28.
Little Kanawha:					
Glenville, W. Va.	23	Mar. 17	Mar. 18	24.7	Mar. 17.
		Mar. 24	Mar. 25	24.8	Mar. 25.
		Apr. 6	Apr. 6	23.5	Apr. 6.
Creston, W. Va.	20	Mar. 17	Mar. 18	21.4	Mar. 18.
		Mar. 25	Mar. 25	20.3	Mar. 25.
		Apr. 6	Apr. 7	21.9	Apr. 6.
Hocking: Athens, Ohio.	17	...do...	...do...	17.9	Apr. 7.
Gauley: Summersville, W. Va.	10	Mar. 17	Mar. 18	15.5	Mar. 18.
		Mar. 24	Mar. 28	14.7	Mar. 24.
Elk: Clay, W. Va.	18	Mar. 18	Mar. 18	18.8	Mar. 18.
		Mar. 25	Mar. 25	23.1	Mar. 25.

[1] Estimated.

Table of flood stages in March and April 1936—Continued

River and station	Flood stage	Above flood stages—dates		Crest	
		From—	To—	Stage	Date
MISSISSIPPI SYSTEM—continued					
Ohio Basin—Continued					
Scioto:	*Feet*			*Feet*	
LaRue, Ohio	11	Mar. 25	Mar. 25	11.8	Mar. 25
Prospect, Ohio	10	Mar. 26	Mar. 26	10.0	Mar. 26.
Circleville, Ohio	14	Mar. 25	...do...	15.5	Do.
Barren: Bowling Green, Ky	20	Mar. 27	Mar. 29	21.5	Mar. 28.
		Apr. 11	Apr. 12	21.0	Apr. 11.
Green:					
Lock No. 6, Brownsville, Ky	28	Mar. 27	Mar. 30	29.4	Mar. 29.
		Apr. 8	Apr. 13	29.5	Apr. 11.
Lock No. 4, Woodbury, Ky	33	Mar. 27	Mar. 31	39.2	Mar. 29.
		Apr. 7	Apr. 15	39.8	Apr. 12.
Lock No. 2, Rumsey, Ky	34	Mar. 26	Apr. 21	40.8	Apr. 15, 16.
West Fork—White River:					
Anderson, Ind	8	Mar. 25	Mar. 29	9.4	Mar. 28.
		Apr. 7	Apr. 9	9.1	Apr. 7.
Elliston, Ind	18	...do...	Apr. 7	18.0	Do.
Edwardsport, Ind	12	Mar. 23	Apr. 1	14.2	Mar. 30.
		Apr. 7	Apr. 11	15.9	Apr. 9.
White:					
Petersburg, Ind	16	Mar. 28	Apr. 1	17.0	Mar. 30, 31.
		Apr. 10	Apr. 12	16.7	Apr. 11.
Hazleton, Ind	16	Mar. 28	Apr. 2	17.7	Mar. 31.
		Apr. 10	Apr. 14	17.2	Apr. 11.
Wabash: Lafayette, Ind	11	Mar. 26	Mar. 26	12.6	Mar. 26.
New: New River, Tenn	18	Mar. 25	Mar. 25	19.2	Mar. 25.
Cumberland:					
Williamsburg, Ky	19	...do...	Mar. 27	20.6	Mar. 25.
Celina, Tenn	28	Mar. 19	Mar. 20	29.5	Mar. 19.
		Mar. 26	Mar. 31	40.9	Mar. 28.
		Apr. 6	Apr. 12	42.3	Apr. 10.
Carthage, Tenn	40	Mar. 28	Mar. 30	44.2	Mar. 29.
		Apr. 8	Apr. 11	40.5	Apr. 8.
Nashville, Tenn	40	Mar. 28	Apr. 3	43.6	Mar. 31.
		Apr. 9	Apr. 14	43.4	Apr. 11.
Clarksville, Tenn	46	Mar. 28	Apr. 4	48.2	Apr. 2.
		Apr. 10	Apr. 16	49.2	Apr. 13.
Lock F, Eddyville, Ky	50	Mar. 28	Apr. 20	60.0	Apr. 16.
North Fork-Holston: Mendota, Va	8	Apr. 6	Apr. 7	9.7	Apr. 6.
Holston: Rogersville, Tenn	13	Apr. 7	...do...	13.5	Apr. 7.
Pigeon: Newport, Tenn	6	Mar. 27	Mar. 28	12.6	Mar. 28.
		Apr. 2	Apr. 2	10.8	Apr. 2.
		Apr. 6	Apr. 7	13.7	Apr. 6.
French Broad:					
Rosman, N. C	8	...do...	Apr. 6	8.8	Do.
Asheville, N. C	6	Mar. 26	Mar. 28	6.7	Mar. 26.
		Apr. 2	Apr. 3	[1] 7.2	Apr. 2.
		Apr. 6	Apr. 10	8.0	Apr. 6.
Marshall, N. C	10	...do...	Apr. 6	10.6	Do.
Hot Springs, N. C	14	...do...	...do...	14.2	Do.
Oldtown (near Newport), Tenn	6	Apr. 2	Apr. 4	10.8	Apr. 2.
		Apr. 6	Apr. 10	12.3	Apr. 6.
Dandridge, Tenn	12	Mar. 25	Mar. 28	15.1	Mar. 28.
		Apr. 2	Apr. 3	13.3	Apr. 2.
		Apr. 6	Apr. 7	16.4	Apr. 6.
Little Tennessee: McGhee, Tenn	18	Mar. 28	Mar. 28	20.8	Mar. 28.
		Apr. 3	Apr. 3	18.2	Apr. 3.
		Apr. 7	Apr. 7	24.0	Apr. 7.
Hiwassee: Charleston, Tenn	22	Apr. 3	Apr. 3	25.3	Apr. 3.
		Apr. 7	Apr. 8	26.0	Apr. 7.
Tennessee:					
Knoxville, Tenn	20	Mar. 26	Mar. 29	23.8	Mar. 28.
		Apr. 7	Apr. 8	21.7	Apr. 7.
Loudon, Tenn	22	Mar. 27	Mar. 29	25.8	Mar. 28.
		Apr. 7	Apr. 8	23.5	Apr. 7.
Chattanooga, Tenn	30	Mar. 27	Mar. 31	37.1	Mar. 29.
		Apr. 4	Apr. 5	30.4	Apr. 4.
		Apr. 8	Apr. 11	35.4	Apr. 9.
Hales Bar Lock, Tenn.:					
Upper gage	50	Mar. 29	Mar. 30	50.6	Mar. 30.
		Apr. 9	Apr. 9	50.2	Apr. 9.
Lower gage	30	Mar. 29	Mar. 31	31.9	Mar. 30.
		Apr. 9	Apr. 10	30.3	Apr. 9.
Bridgeport, Ala	18	Mar. 27	Apr. 12	25.8	Mar. 30.
Widows Bar Lock, Ala.:					
Upper Gage	17	Mar. 26	Apr. 13	26.9	Mar. 30.
Lower Gage	26	do	do	34.9	Do.
Guntersville, Ala	25	Mar. 27	Apr. 14	35.5	Apr. 2.
Decatur, Ala	20	Mar. 31	Apr. 13	22.5	Apr. 3.
Florence, Ala	18	Mar. 30	Apr. 15	24.4	Apr. 6.
Riverton Lock, Ala	33	Mar. 28	Apr. 18	47.7	Apr. 7.
Savannah, Tenn	39	Apr. 2	do	47.4	Apr. 10.
Johnsonville, Tenn	31	Apr. 4	Apr. 20	39.6	Apr. 12.
Ohio:					
Pittsburgh, Pa	25	Mar. 12	Mar. 13	25.8	Mar. 13.
		Mar. 17	Mar. 21	46.0	Mar. 18.
		Mar. 25	Mar. 29	30.6	Mar. 26.
		Apr. 7	Apr. 7	25.5	Apr. 7.
Dam No. 2, Coraopolis, Pa	26	Mar. 17	Mar. 20	43.8	Mar. 18.
				25.9	Mar. 26.

[1] Estimated.

Table of flood stages in March and April 1936—Continued

River and station	Flood stage	Above flood stages—dates		Crest	
		From—	To—	Stage	Date
MISSISSIPPI SYSTEM—continued					
Ohio Basin—continued					
Ohio—Continued.	*Feet*			*Feet*	
Dam No. 6, Beaver, Pa	30	Mar. 17	Mar. 20	54.8	Mar. 19.
		Mar. 24	Mar. 29	37.7	Mar. 26.
Dam No. 12, near Wheeling, W. Va	36	Mar. 18	Mar. 21	55.5	Mar. 19.
		Mar. 26	Mar. 28	39.6	Mar. 26.
Dam No. 13, near Wheeling, W. Va	45	Mar. 18	Mar. 21	57.8	Mar. 19.
				42.9	Mar. 26.
Parkersburg, W. Va	36	Mar. 18	Mar. 24	48.0	Mar. 20.
		Mar. 26	Mar. 30	40.3	Mar. 28.
Dam No. 19, Little Hocking, Ohio	40	Mar. 19	Mar. 24	50.5	Mar. 21.
		Mar. 26	Mar. 29	43.1	Mar. 28.
Dam No. 20, near Belleville, W. Va	45	Mar. 19	Mar. 23	50.6	Mar. 21.
				43.2	Mar. 28, 29.
Dam No. 22, Ravenswood, W. Va	44	Mar. 19	Mar. 24	52.1	Mar. 21.
		Mar. 28	Mar. 29	44.9	Mar. 28.
Dam No. 25, near Addison, Ohio	43	Mar. 18	Apr. 1	57.9	Mar. 22.
		Apr. 7	Apr. 9	44.9	Apr. 8.
Point Pleasant, W. Va	40	Mar. 18	Apr. 1	54.4	Mar. 22.
		Apr. 7	Apr. 9	42.2	Apr. 8.
Dam No. 26, Chambersburg, Ohio	50	Mar. 19	Mar. 31	61.2	Mar. 23.
Dam No. 28, Huntington, W. Va	50	Mar. 20	...do...	58.6	Do.
Dam No. 29, Ashland, Ky	51	...do...	Apr. 1	62.7	Do.
		Apr. 7	Apr. 10	53.6	Apr. 8.
Dam No. 30, Greenup, Ky	52	Mar. 20	Apr. 1	62.0	Mar. 23.
		Apr. 8	Apr. 10	53.6	Apr. 8.
Portsmouth, Ohio	50	Mar. 20	Apr. 1	59.2	Mar. 23, 24.
		Apr. 8	Apr. 10	51.5	Apr. 9.
Dam No. 32, near Vanceburg, Ky	53	Mar. 21	Apr. 1	59.4	Mar. 24.
Dam No. 33, Maysville, Ky	50	Mar. 20	Apr. 2	59.1	Mar. 27.
		Apr. 8	Apr. 11	52.3	Apr. 9.
Dam No. 35, New Richmond, Ohio	48	Mar. 21	Apr. 2	56.5	Mar. 27, 28.
		Apr. 9	Apr. 12	49.9	Apr. 10.
Dam No. 36, Brent, Ky	52	Mar. 21	Apr. 2	60.4	Mar. 28.
		Apr. 9	Apr. 11	53.6	Apr. 10.
Cincinnati, Ohio	52	Mar. 21	Apr. 3	60.6	Mar. 28.
		Apr. 9	Apr. 12	54.0	Apr. 10.
Dam No. 37, Fernbank, Ohio	50	Mar. 21	Apr. 3	59.6	Mar. 28.
		Apr. 8	Apr. 12	53.2	Apr. 10.
Dam No. 38, Grant, Ky	51	Mar. 22	Apr. 3	59.1	Mar. 28.
		Apr. 9	Apr. 12	52.7	Apr. 11.
Dam No. 39, Markland, Ind	48	Mar. 23	Apr. 2	53.5	Mar. 28, 29.
		Apr. 10	Apr. 12	48.6	Apr. 11.
Dam No. 41, Louisville, Ky.:					
Upper Gage	28	Mar. 23	Apr. 4	36.6	Mar. 29, 30.
		Apr. 9	Apr. 14	31.6	Apr. 12.
Low-water Gage	51	Mar. 23	Apr. 4	59.6	Mar. 29, 30.
		Apr. 9	Apr. 14	54.7	Apr. 12.
Dam No. 43, Evans Landing, Ind	57	Mar. 24	Apr. 4	64.3	Mar. 30.
		Apr. 10	Apr. 14	59.5	Apr. 12.
Dam No. 44, Leavenworth, Ind	53	Mar. 22	Apr. 15	63.6	Mar. 29, 30.
Dam No. 45, Addison, Ky	47	Mar. 23	Apr. 16	54.9	Mar. 30.
Dam No. 46, Owensboro, Ky	41	Mar. 25	...do...	45.1	Mar. 31.
Dam No. 47, Newburgh, Ind	38	Mar. 22	Apr. 19	46.7	Do.
Evansville, Ind	35	...do...	Apr. 20	44.4	Do.
Dam No. 48, Henderson, Ky	38	Mar. 23	...do...	46.7	Apr. 1.
Dam No. 49, Uniontown, Ky	37	Mar. 25	Apr. 22	46.4	Apr. 4.
Dam No. 50, Fords Ferry, Ky	34	Mar. 5	Mar. 11	36.2	Mar. 8.
		Mar. 22	Apr. 23	50.1	Apr. 5, 6.
Dam No. 51, Golconda, Ill	40	Mar. 28	Apr. 22	47.8	Apr. 6.
Paducah, Ky	39	Mar. 27	Apr. 23	49.1	Apr. 16.
Dam No. 52, Brookport, Ill	37	Mar. 26	Apr. 24	50.9	Apr. 15, 16.
Dam No. 53, Mound City, Ill	42	Mar. 25	Apr. 25	55.3	Do.
Cairo, Ill	40	...do...	...do...	52.8	Apr. 16.
White Basin					
Black: Black Rock, Ark	14	Apr. 6	Apr. 7	16.4	Apr. 6.
Lower Mississippi Basin					
Big Lake Outlet: Manila, Ark	10	Apr. 11	Apr. 18	10.8	Apr. 14, 15.
Tallahatchie: Swan Lake, Miss	26	Apr. 6	Apr. 21	27.6	Apr. 13.
Mississippi:					
New Madrid, Mo	34	Mar. 28	Apr. 25	41.4	Apr. 13–18.
Memphis, Tenn	34	Apr. 5	Apr. 28	39.3	Apr. 22.
Helena, Ark	44	Apr. 7	Apr. 30	50.6	Apr. 22–24.
Arkansas City, Ark	42	----------	----------	41.4	Apr. 27, 28.
GULF OF CALIFORNIA DRAINAGE					
Colorado Basin					
Gunnison: Delta, Colo	9	Apr. 22	Apr. 24	9.3	Apr. 23.
		Apr. 27	Apr. 27	9.0	Apr. 27.
PACIFIC SLOPE DRAINAGE					
Columbia Basin					
Clearwater: Kamiah, Idaho	12	Apr. 17	Apr. 26	13.6	Apr. 24.

WEATHER ON THE ATLANTIC AND PACIFIC OCEANS

[The Marine Division, I. R. TANNEHILL in charge]

NORTH ATLANTIC OCEAN, APRIL 1936

By H. C. HUNTER

Atmospheric pressure.—There were marked fluctuations of pressure over most parts of the North Atlantic during April. On the average, pressure considerably exceeded normal over the northeastern portion, and it slightly exceeded normal in most waters near the American coast and eastward to well beyond Newfoundland and Bermuda, the excess here being of greater amount around latitudes 30° to 35° than either to northward or to southward. Near the Azores and to eastward and southeastward, pressure averaged a trifle less than normal.

The extremes of pressure so far reported are 30.74 and 28.87 inches. The higher was noted on two liners, the British *Empress of Australia* and the German *Hamburg*, at about latitude 45° N., longitude 48° W., during the forenoon of the 29th. The lower was recorded at a late hour of the 8th on the U. S. cutter *Champlain*, on ice patrol duty, near 49° N., 52° W.

TABLE 1.—*Averages, departures, and extremes of atmospheric pressure (sea level) at selected stations for the North Atlantic Ocean and its shores, April 1936*

Station	Average pressure	Departure	Highest	Date	Lowest	Date
	Inches	*Inch*	*Inches*		*Inches*	
Julianehaab, Greenland	29.75		30.39	15	29.02	9
Reykjavik, Iceland	29.94	+0.14	30.52	13	29.16	25
Lerwick, Shetland Islands	29.93	+.13	30.29	5	29.45	25
Valencia, Ireland	30.01	+.12	30.51	29	29.30	21
Lisbon, Portugal	29.96	−.03	30.32	21	29.38	14
Madeira	30.01	.00	30.34	21	29.57	6
Horta, Azores	30.13	−.02	30.53	29	29.51	2
Belle Isle, Newfoundland	29.86	+.03	30.52	6	29.18	1
Halifax, Nova Scotia	29.95	+.02	30.48	28	29.32	8
Nantucket	30.00	+.03	30.53	9	29.32	2
Hatteras	30.08	+.07	30.52	9	29.49	2
Bermuda	30.14	+.05	30.40	9	29.88	13, 19
Turks Island	30.03	+.01	30.17	9	29.94	17, 18
Key West	30.04	+.02	30.24	4	29.84	2
New Orleans	30.06	+.06	30.41	3	29.63	1

NOTE.—All data based on a. m. observations only, with departures compiled from best available normals related to time of observation, except Hatteras, Key West, Nantucket, and New Orleans which are 24-hour corrected means.

Cyclones and gales.—Cyclonic activity was considerable in many parts of the North Atlantic area at scattered times, the periods from 6th to 10th and from 20th to 27th being the more noteworthy, while the last 3 days were particularly quiet. No instance of force-12 wind has been reported.

On the morning of the 6th a low-pressure system extended from western Greenland across the lower Lake region to the west Gulf of Mexico, and in the last named area some sharp shifts of wind were experienced. This system moved eastward, and the situations on the 8th and 9th are indicated on charts IX and X. A well-marked cyclone was near Newfoundland on these days, and two vessels noted storm winds (force 11).

To westward and southwestward of the Iberian peninsula there was a notable LOW on the 14th and 15th, causing winds of greater force than are often met in those waters. This LOW, however, soon passed northeastward over Spain and France.

From the 21st to 27th there was considerable storminess along parts of the chief steamship route to northern Europe, and at times strong to whole gales were met not only along the routes but also to southward of them west of the 50th meridian, even to near the latitude of Bermuda. Two well-marked cyclones were associated with most of the gales, the preceding cyclone moving northeastward past Iceland on the 25th, about the time the following cyclone was close to eastern Newfoundland. Once on the 23d, and once on the 26th, force 11 was noted near the eastern edge of the Grand Banks.

Fog.—Over waters to westward of the 45th meridian, fog during April was as frequent as usual, for the most part, or somewhat more frequent. There was a little fog noted over the northern Gulf of Mexico at times, chiefly during the first few days of the month. Near the middle Atlantic coast there was more fog than normal for April, most of it occurring before the middle of the month; the fog here was especially dense and widespread about the 10th, when the fishing schooner *Thelma* was sunk by collision with the Danish steamship *Elfi*, off the New Jersey coast, fortunately without loss of life. There was less fog than April usually brings over waters to the eastward of New England, about as far as meridian 60°; but from 60° to 45° there was an unusually large amount of fog, the 5°-square 45° to 50° N., 45° to 50° W. reporting fog on 14 days, the greatest amount indicated for any Atlantic area during the month. From the 13th to 25th scarcely any day was without fog.

About 300 miles to east-southeastward of Bermuda, where fog is decidedly uncommon, two vessels noted it on the 3d.

Between the 45th meridian and the coasts of the European continent and the British Isles fog was decidedly infrequent, most of the few reports received relating to the first 3 days of April.

OCEAN GALES AND STORMS, APRIL 1936

Vessel	Voyage		Position at time of lowest barometer		Gale began April	Time of lowest barometer April	Gale ended April	Lowest barometer	Direction of wind when gale began	Direction and force of wind at time of lowest barometer	Direction of wind when gale ended	Direction and highest force of wind	Shifts of wind near time of lowest barometer
	From—	To—	Latitude	Longitude									
NORTH ATLANTIC OCEAN			° ′	° ′				*Inches*					
Topa Topa, Am. S. S.	Mobile	Liverpool	45 30 N.	41 30 W.	[1] 29	4a, 1	1	29.23	WNW	NW, 8	NNW	NNW, 10	None.
Burgerdijk, Du. S. S.	New Orleans	Habana	26 24 N.	85 54 W.	1	4a, 2	2	29.69	SSE	S, 7	S	SSE, 8	SSE-SSW.
Yankee Arrow, Am. S. S.	Boston	Beaumont	32 50 N.	73 54 W.	2	Noon, 2	2	29.77	SW	SW, 7	W	W, 8	SW-W.
Eastern Sun, Am. M. S.	Marcus Hook	Port Arthur	34 06 N.	75 28 W.	2	do	3	29.66	SW	SW, 6	NW	SW, 9	SW-NW.
Gulfwing, Am. S. S.	Philadelphia	Las Piedras	35 30 N.	73 40 W.	2	2p, 2	4	29.64	SW	SW, 8	NW	WNW, 8	SW-NW.
Lekhaven, Du. S. S.	Antwerp	Wilmington, N. C.	[2] 43 41 N.	20 16 W.	4	4p, 2	6	[3] 29.39	NNW	WNW, 3	NNE	NNW, 10	N-W.
West Irmo, Am. S. S.	St. Vincent	New York	36 54 N.	67 30 W.	3	3p, 3	4	29.48	SSW	SSW, 8	WNW	SW, 9	SSW-NW.
Ary Lensen, Br. M. S.	Cristobal	do	10 53 N.	79 05 W.	6	4a, 6	10	30.02	NNE	NNE, 6	ENE	ENE, 9	NNE-ENE.
Imlay, Am. S. S.	Philadelphia	Tampico	[2] 22 48 N.	95 37 W.	6	do	7	29.58	WNW	S, 4	N	NNE, 7	S-WNW.
Paris, Fr. S. S.	Havre	New York	40 50 N.	68 10 W.	7	8p, 7	8	29.57	SE	SSW, 7	WNW	SW, 8	{ESE-SSW-WSW.
Beemsterdijk, Du. S. S.	Rotterdam	do	41 45 N.	63 40 W.	8	1a, 8	8	29.45	WSW	SW, 7	WNW	W, 9	{SSE-SW-WNW.
Amapala, Hond. S. S.	New York	Santiago, Cuba	[2] 20 00 N.	74 15 W.	7	4a, 8	8	30.03	E	E, 7	E	E, 7	None.
Tennessee, Dan. S. S.	Drammen	Portland, Maine	43 40 N.	57 36 W.	8	8a, 8	9	29.52	WSW	WSW, 9	NW	WSW, 10	
Mahsud, Br. S. S.	Cardiff	Philadelphia	38 47 N.	55 20 W.	8	4p, 8	8	29.86	SW	SW, 9	NW	SW, 9	SW-NW.
Virginia, Am. S. S.	Port Arthur	Portland, Maine	28 30 N.	91 15 W.	8	do	8	29.98	NE	NE, 8	SW	NE, 8	NE-SW.
Champlain, U. S. C.	On ice patrol out	from St. Johns	49 03 N.	52 07 W.	8	9p, 8	9	28.87	NW	NW, 7	W	NW, 11	SSW-NW.
Braheholm, Swed. S. S.	Newcastle	Portland, Maine	47 49 N.	49 48 W.	8	Mdt., 8	9	29.17	SW	WSW, —	NW	NW, 11	WSW-NW.
American Trader, Am. S. S.	London	Boston	45 30 N.	42 00 W.	8	4a, 9	9	29.52	SSW	W, 7	NNW	WNW, 9	SSW-W.
Ariadne, Du. S. S.	Amsterdam	Santo Domingo	39 02 N.	39 10 W.	9	4p, 10	10	30.06	SW	NNW, 8	N	NNW, 9	SW-N.
Exporter, Am. S. S.	Gibraltar	New York	35 48 N.	25 58 W.	10	Mdt., 10	13	29.74	NW	W, 7	WNW	WNW, 8	Steady.
Prusa, Am. S. S.	Seville	Wilmington, N. C.	35 29 N.	10 46 W.	14	7a, 14	15	29.50	S	W, 10	WNW	W, 11	S-W.
Athelsultan, Br. M. S.	Gibraltar	Antwerp	38 06 N.	9 12 W.	14	11a, 15	14	29.60	SSW	WSW, 6	SW	SSW, 8	
Wellfield, Br. M. S.	Horta	New York	38 50 N.	47 22 W.	15	Mdt., 15	17	29.76	W	W, 8	SSW	W, 8	None.
Fernlane, Nor. M. S.	Rotterdam	do	38 25 N.	47 30 W.	15	4p, 17	17	29.78	WSW	WSW, 8	WSW	WSW, 9	Steady.
Exporter, Am. S. S.	Gibraltar	do	36 10 N.	59 04 W.	20	8a, 19	20	29.85	N	SSW, 5	NNW	N, 10	
Kinai Maru, Jap. M. S.	Cristobal	do	15 47 N.	76 05 W.	20	7a, 21	22	29.98	NE	NE, 8	NE	NE, 8	None.
Teteia, Br. S. S.	Swansea	Jamaica	49 00 N.	10 05 W.	21	8p, 21	22	29.36	S	WNW, 8	N	W, 9	W-NW.
Exporter, Am. S. S.	Gibraltar	New York	38 10 N.	69 17 W.	21	2a, 22	22	29.86	SW	W, 9	N	SW, 9	SW-NNW.
Fernlane, Nor. M. S.	Rotterdam	do	38 30 N.	65 14 W.	21	8a, 22	22	29.92	WSW	WSW, 9	NW	WSW, 10	WSW-NW.
Chesapeake, Br. M. S.	Aruba	Bowling	54 00 N.	13 45 W.	22	4a, 23	23	29.45	SSE	SSW, —	SSW	SSE, 8	SSE-SSW.
Scanmail, Am. S. S.	Copenhagen	New York	48 54 N.	42 48 W.	23	9p, 23	24	29.32	WSW	WSW, 11	W	WSW, 11	SW-NW.
Chinese Prince, Br. M. S.	Dakar	Halifax	39 18 N.	50 23 W.	25	2p, 25	25	29.60	SSW	SW, 10	NW	SW, 10	SW-WNW.
Samala, Br. S. S.	Pto. Cortez	Rotterdam	42 18 N.	17 55 W.	25	2a, 26	27	29.72	S	WSW, —	NW	S, 8	S-NW.
Pontchartrain, U. S. C.	On ice patrol out	from Halifax	48 20 N.	48 22 W.	25	do	26	29.00	ENE	NE, 9	WNW	NW, 11	NE-NNE.
Breedijk, Du. S. S.	Rotterdam	New York	44 14 N.	37 00 W.	26	8a, 26	27	29.69	SSE	S, 8	WNW	WSW, 10	SSE-W.
Sarcoxie, Am. S. S.	Havre	do	47 30 N.	28 30 W.	26	10p, 26	27	30.01	SW	SSW, 9	NW	SSW, 9	SSW-WSW.
Satartia, Am. S. S.	Ceara, Brazil	Boston	38 16 N.	66 52 W.	26	2a, 27	27	30.11	WSW	N, 8	NNE	WSW, 9	WSW-NNE.
Washington, Am. S. S.	Cobh	New York	48 48 N.	28 35 W.	26	4a, 27	27	29.94	S	WSW, 9	W	W, 10	SW-W.
NORTH PACIFIC OCEAN													
Athelchief, Br. M. S.	Yokohama	San Francisco	43 15 N.	162 47 E.	[1] 31	6a, 1	3	28.78	WSW	WSW, 11	NNW	SSW, 12	SSW-WNW.
Aden Maru, Jap. S. S.	Manila	Los Angeles	38 17 N.	136 00 W.	[1] 29	3p, 2	5	29.40	SE	WNW, 8	NNW	WNW, 8	WSW-WNW.
Nichiyo Maru, Jap. M. S.	Los Angeles	Yokohama	34 34 N.	171 00 E.	1	4p, 1	2	29.85	W	W, 7	WNW	W, 9	
Tricolor, Nor. M. S.	Yokohama	San Francisco	41 36 N.	156 36 E.	2	10p, 2	3	29.77	WNW	WNW, 9	W	WNW, 10	None.
Makua, Am. S. S.	Ahukini, T. H.	do	36 01 N.	129 21 W.	3	3a, 3	4	29.60	NW	SW, 6	NW	NW, 9	
Birchbank, Br. M. S.	Dairen	Los Angeles	33 51 N.	125 13 E.	3	4p, 3	4	29.76	WNW	WNW, 8	NW	WNW, 9	Steady.
Nichiyo Maru, Jap. M. S.	Los Angeles	Yokohama	33 30 N.	157 20 E.	4	Mdt., 4	4	29.51	S	SW, 7	S	S, 9	S-SW.
Rakuyo Maru, Jap. S. S.	do	do	36 32 N.	168 57 W.	4	4a, 4	5	29.36	WNW	W, 5	WSW	WNW, 8	Steady.
Pres. Grant, Am. S. S.	Victoria, B. C.	do	48 00 N.	165 00 E.	5	6p, 5	5	29.01	SE	S, 5	SE	ESE, 9	ESE-SW.
Pres. Jackson, Am. S. S.	Yokohama	Victoria, B. C.	[3] 39 28 N.	148 18 E.	6	4a, 6	6	29.47	WNW	WNW, 8	NNW	WNW, 9	
Empress of Canada, Br. S. S.	do	Honolulu	34 47 N.	141 12 E.	10	Noon, 10	10	29.88	NE	NE, 7	N	N, 8	NE-N.
Toorak, Br. S. S.	Tanjong Oeban	Yokohama	35 12 N.	139 46 E.	12	Noon, 13	13	29.60	SE	NE, 4	NE	ESE, 9	ENE-NE.
Niagara, Br. S. S.	Honolulu	Vancouver	32 22 N.	147 20 W.	13	4p, 13	13	29.93	NNW	NNW, 9	NNE	NNW, 9	None.
Rakuyo Maru, Jap. S. S.	Los Angeles	Yokohama	35 45 N.	146 11 E.	14	6a, 14	14	29.00	SSW	SW, 6	NNW	NW, 8	S-NW.
Peter Maersk, Dan. M. S.	Yokohama	Los Angeles	45 42 N.	178 50 W.	15	4a, 15	15	29.55	SSE	S, 8	SSW	S, 8	S-SSW.
Maliko, Am. S. S.	Seattle	Honolulu	39 40 N.	139 30 W.	15	5p, 15	16	29.50	WNW	WNW, 8	NW	WNW, 9	SE-WNW.
Siantar, Du. M. S.	Manila	Los Angeles	45 10 N.	164 30 W.	15	10p, 15	16	30.03	S	S, 8	SSW	S, 8	None.
Sangstad, Nor. M. S.	Calatagan, P. I.	do	38 10 N.	165 50 E.	15	8p, 15	16	[2] 29.68	SW	SW, 9	WNW	W, 11	SW-WSW.
Tacoma, Am. S. S.	Legaspi, P. I.	do	39 20 N.	138 36 W.	15	8a, 16	16	[3] 29.26	NNW	W, 8	NW	WNW, 8	W-NW.
General Sherman, Am. S. S.	Yokohama	San Francisco	38 30 N.	149 30 E.	17	10a, 17	18	29.49	W	W, 9	NW	W, 9	WSW-NW.
Saparoea, Du. M. S.	Singapore	do	38 42 N.	151 12 E.	25	10a, 26	26	29.51	S	S, 8	W	S, 10	S-W.
Empress of Asia, Br. S. S.	Vancouver, B. C.	Yokohama	48 23 N.	152 24 E.	26	11p, 26	27	29.21	SSE	S, 8	W	S, 8	S-SW.
Saparoea, Du. M. S.	Singapore	San Francisco	45 42 N.	173 19 E.	29	11p, 29	30	28.68	S	SW, 12	W	W, 12	S-W.
Michigan, Am. S. S.	Otaru	do	49 15 N.	178 50 E.	29	6a, 30	30	28.48	SSE	SSE, 9	W	SW, 10	SE-SW.

[1] March.
[2] Position approximate.
[3] Barometer uncorrected.

NORTH PACIFIC OCEAN, APRIL 1936

By WILLIS E. HURD

Atmospheric pressure.—The general pressure situation over the North Pacific Ocean and adjoining coasts during April 1936 exhibited few departures of moment from normal. The Aleutian LOW was developed as usual except in the vicinity of Kodiak, where the average pressure for the month, 29.89, was 0.14 inch above the normal. Off the Washington coast, pressures were also appreciably above normal, as they were at Midway Island. Anticyclonic conditions were somewhat better developed than normal in middle latitudes.

TABLE 1.—*Averages, departures, and extremes of atmospheric pressure at sea level, North Pacific Ocean, April 1936, at selected stations*

Stations	Average pressure	Departure from normal	Highest	Date	Lowest	Date
	Inches	*Inch*	*Inches*		*Inches*	
Point Barrow	30.08	−0.01	30.76	4, 5	29.56	8
Dutch Harbor	29.79	+.01	30.26	20,21, 25	29.20	12
St. Paul	29.77	−.02	30.26	26	28.62	12
Kodiak	29.89	+.14	30.36	2	29.08	6
Juneau	29.95	−.01	30.36	1	29.33	8
Tatoosh Island	30.10	+.10	30.62	5	29.70	3
San Francisco	30.06	+.01	30.40	5	29.60	3
Mazatlan	29.90	+.01	29.98	4, 8	29.84	2, 17, 18, 23
Honolulu	30.04	−.02	30.13	17	29.91	28
Midway Island	30.19	+.07	30.36	19	29.94	27
Guam	29.88	−.01	29.94	20	29.80	3
Manila	29.83	+.01	29.92	14	29.76	21
Hong Kong	29.85	------	30.05	15	29.72	24, 25
Naha	29.93	+.01	30.14	13	29.70	24
Chichishima	30.00	+.03	30.26	17	29.60	3
Nemuro [1]	------	------	30.20	17	29.62	22

[1] For 14 days.

NOTE.—Data based on 1 daily observation only, except those for Juneau, Tatoosh Island, San Francisco, and Honolulu, which are based on two observations. Departures are computed from best available normals related to time of observation.

Cyclones and gales.—The month was only moderately stormy as a whole, despite the fact that hurricane velocities occurred locally on 3 days, and winds of force 11 on 2 days. These high winds were experienced by ships within the region 38°–46° N., 160°–175° E. Scattered gales of force 9–10 were encountered on a few other days, but the majority of the Pacific gales in April did not exceed force 8.

The deepest April cyclones occurred on the first and last days of the month. The earlier lay to the eastward of the Kuril Islands and affected the western part of the northern sailing routes until about the 5th, during a slow northward passage into the Bering Sea. It was on the 1st, however, that it acquired greatest intensity, the British motorship *Athelchief* on that day reporting a south-southwest wind of hurricane force, lowest barometer 28.78, near 43° N., 163° E.

In the final cyclone of the month, which lay south of the western Aleutians on the 29th and 30th, pressure fell to unusually low values for the type, locality, and season of the storm. On the 29th, with a southwest hurricane accompanied by snow, the Dutch motorship *Saparoea* reported a barometer reading of 28.68 inches, near 46° N., 173° E. On the 30th the American steamer *Michigan*, with strong to whole accompanying gales, observed a corrected pressure of 28.48 inches, near 49° N., 179° E. This is the lowest reported reading of the month.

Storminess was most widespread on the 15th and 16th. On these dates gales were experienced in middle latitudes between 150° and 175° E.; over a considerable region south of the Aleutians and the peninsula of Alaska; and in middle latitudes some 10° to 15° off the California coast. The heaviest winds of this midmonth period were of force 11, experienced by the Norwegian motorship *Sangstad*, near 38° N., 166° E.

Cyclones covered the northwestern part of the ocean during the greater part of the month. Some were progressive storms from Japanese waters, while others were more fluctuating and less progressive disturbances of the nature of the Aleutian LOW. Gales resulting from this continuous unsettled condition were for the most part of a minor nature, except during the periods previously mentioned.

East of 160° west longitude no gales were reported except those due to disturbances originating generally to the northeastward of the Hawaiian Islands. These LOWS were of brief duration except that which formed during the 13th near 30° N., 145° W. and, moving north-northeastward, entered British Columbia on the 18th. Local accompanying gales, force 8 to 9, occurred on the 13th, 15th, and 16th. Within the region 35°–40° N., 128°–150° W., local gales arising from earlier disturbed conditions occurred on the 2d, 4th, and 6th.

Tehuantepecers.—Moderate gales (force 7) of the norther type occurred in the Gulf of Tehuantepec on the 13th and 18th. No other winds of equal force were reported as occurring this month to the southward of the thirtieth parallel.

Fog.—Along the northern and middle routes, fogs were reported on several days, but were widely scattered as to location and occurred on not more than 1 or 2 days in any locality, except in far eastern waters, where they were observed on 6 days, and along the American coast. There were two days with fog reported near Vancouver Island; 8 days with fog off California; and 7 with fog off Lower California. Off the latter two coasts, the 10th to 12th were the most extensively foggy. Two small vessels were damaged during this period as a result of the thick weather.

CLIMATOLOGICAL TABLES

CONDENSED CLIMATOLOGICAL SUMMARY

In the following table are given for the various sections of the climatological service of the Weather Bureau the monthly average temperature and total rainfall; the stations reporting the highest and lowest temperatures, with dates of occurrence; the stations reporting the greatest and least total precipitation; and other data as indicated by the several headings.

The mean temperature for each section, the highest and lowest temperatures, the average precipitation, and the greatest and least monthly amounts are found by using all trustworthy records available.

The mean departures from normal temperatures and precipitation are based only on records from stations that have 10 or more years of observations. Of course, the number of such records is smaller than the total number of stations.

Condensed climatological summary of temperature and precipitation by sections, April 1936

[For description of tables and charts, see REVIEW, January, p. 29]

Section	Temperature								Precipitation					
	Section average	Departure from the normal	Monthly extremes						Section average	Departure from the normal	Greatest monthly		Least monthly	
			Station	Highest	Date	Station	Lowest	Date			Station	Amount	Station	Amount
	°F.	°F.		°F.			°F.		In.	In.		In.		In.
Alabama	62.5	−1.1	Greensboro	93	[1] 13	3 stations	28	3	6.80	+2.26	Goodwater	12.96	Elba	1.66
Arizona	62.6	+2.5	Quartzite	111	18	Snowflake	8	5	.14	−.45	Pinedale	.75	41 stations	.00
Arkansas	59.7	−1.8	2 stations	96	[1] 13	2 stations	17	3	2.64	−2.20	Mammoth Spring	6.17	Magnolia	.60
California	56.7	+.5	do	107	17	Twin Lakes	−9	1	1.59	−.65	Kennett	7.37	9 stations	.00
Colorado	45.5	+1.9	Las Animas	95	29	Pearl	−20	6	.80	−.97	Willow Creek	3.10	3 stations	.00
Florida	70.0	+.1	Avon Park	99	3	2 stations	35	[1] 19	2.20	−.68	Garniers	9.28	Cedar Key	.00
Georgia	62.1	−1.3	Fort Gaines	94	15	Blairsville	21	4	7.92	+4.20	Washington	15.21	Brunswick	1.33
Idaho	46.8	+1.7	2 stations	96	17	Alpha	−21	1	1.00	−.40	Lake	2.24	Rupert	.16
Illinois	49.0	−3.1	Havana	91	20	Freeport	9	4	2.44	−.93	Casey	5.45	Havana	.97
Indiana	47.8	−4.0	Shoals	91	28	Wheatfield	15	8	3.17	−.32	Leavenworth	4.73	Columbia City	1.28
Iowa	45.9	−2.8	Corydon (near)	92	20	Sibley	0	3	1.10	−1.61	Keosauqua	2.28	Omaha, Nebr.	.23
Kansas	54.5	−.2	3 stations	98	14	2 stations	−2	2	1.17	−1.39	Centralia	3.83	Elkhart	.08
Kentucky	53.1	−3.0	2 stations	90	15	Anchorage	19	8	4.79	+.82	Mount Sterling	7.58	Oneonta	3.25
Louisiana	65.2	−1.9	Dodson	96	14	2 stations	26	3	4.32	−.32	Bogalusa	10.00	Minden	.70
Maryland-Delaware	49.8	−2.3	Takoma, Md	90	15	Friendsville, Md	11	4	2.86	−.59	Grantsville, Md	4.58	Great Falls, Md	1.09
Michigan	38.3	−4.4	St. Joseph	80	30	Vanderbilt	−7	4	2.04	−.42	Eloise	3.73	Houghton	.49
Minnesota	36.4	−6.6	Redwood Falls	86	19	Warroad	−18	[1] 1	1.30	−.74	Willmar	4.16	Crookston	.28
Mississippi	62.4	−2.2	Booneville	94	15	5 stations	28	3	4.78	−.07	Shubuta	9.16	Holly Springs	1.63
Missouri	53.0	−2.2	Lamar	95	14	2 stations	9	3	2.45	−1.46	Parma	5.45	Booneville	.61
Montana	41.8	−1.1	Ballantine	94	19	Chessman Reservoir	−28	1	.82	−.32	Hebgen Dam	2.49	Mildred	.02
Nebraska	47.0	−2.2	Newport	97	13	2 stations	−15	[1] 2	1.59	−.82	Madrid	4.36	Omaha	.23
Nevada	52.8	+4.9	Logandale	102	15	San Jacinto	−3	2	.29	−.48	Lamoille	2.37	3 stations	.00
New England	41.9	−1.8	Waterbury, Conn.	85	30	First Conn. Lake, N. H.	10	5	3.97	+.64	Pinkham Notch, N. H.	6.90	Nantucket, Mass.	2.2
New Jersey	48.0	−1.7	Burlington	90	30	2 stations	19	25	3.23	−.38	Little Falls	4.55	Indian Mills	2.05
New Mexico	52.0	+.4	San Marcial	100	12	Lake Alice (near)	−7	[1] 2	.31	−.57	Tierra Amarilla	2.65	17 stations	.00
New York	42.1	−2.1	Port Jarvis	87	30	Andover	10	10	3.45	+.47	Stillwater Reservoir	5.75	Brockport	1.55
North Carolina	56.4	−1.4	2 stations	92	15	Mt. Mitchell	3	4	5.59	+2.03	Highlands	11.06	Hatteras	.97
North Dakota	35.6	−6.0	do	87	19	2 stations	−15	[1] 5	.39	−.87	Wahpeton	1.52	Langdon	.00
Ohio	46.2	−3.5	4 stations	85	[1] 15	Mt. Vernon (near)	14	4	2.92	−.19	Ironton	5.89	Catawba Island	1.52
Oklahoma	61.0	+.7	2 stations	100	[1] 14	Boise City	6	2	.99	−2.36	Wyandotte	3.82	Norman	.00
Oregon	49.9	+2.7	Prairie City	91	16	Mescham	−23	1	1.52	−.45	Brookings	4.63	Big Eddy	.26
Pennsylvania	46.1	−2.5	York	90	30	Brookville	14	4	3.01	−.38	Corry	5.49	Center Hall	1.09
South Carolina	59.9	−2.4	Garnett	94	15	Caesars Head	18	4	8.27	+5.10	Caesars Head	12.56	Georgetown	1.96
South Dakota	41.6	−4.3	4 stations	90	[1] 13	Vale	−13	3	1.[illegible]	−.78	2 stations	3.07	Pollock	.54
Tennessee	56.1	−2.6	2 stations	94	[1] 15	Rugby	15	4	4.[illegible]	−.11	Copperhill	9.63	Memphis	1.21
Texas	65.0	−1.1	do	109	5	Romero	5	[1] 2	1.69	−1.34	Falfurrias	6.35	2 stations	.00
Utah	49.8	+2.8	St. George	96	[1] 15	Woodruff	−10	2	.65	−.53	Silver Lake	2.81	Escalante	.00
Virginia	52.2	−2.2	Pennington Gap	93	30	Big Meadows	15	[1] 4	3.43	+.13	Wallaceton	6.24	Sexton Shelter	1.39
Washington	50.9	+2.7	2 stations	93	[1] 16	Lake Keechelus	−7	1	1.11	−1.20	Wishkah Headworks	4.83	White Swan	.03
West Virginia	49.3	−2.4	Hastings	90	30	2 stations	12	[1] 4	3.66	+.15	Davis	6.28	Wardenville	2.03
Wisconsin	38.1	−5.5	Lancaster	77	9	Mellen	−5	6	1.28	−1.23	Blair	3.27	Prairie du Sac	.41
Wyoming	39.9	−.2	Colony	88	20	3 stations	−28	[1] 2	1.13	−.45	Bechler River	3.81	Dubois	T
Alaska (March)	13.0	−2.0	Dutch Harbor	69	25	Allakaket	−44	20	1.84	+.10	View Cove	14.84	3 stations	T
Hawaii	70.3	+.1	Waimanalo	90	[1] 3	Kanalohuluhulu	39	20	8.95	+.70	Korean Camp	46.46	Ka Lae	.03
Puerto Rico	75.8	+1.1	Mayaguez No. 2	95	24	Guineo Reservoir	43	5	2.10	−2.59	Lares	7.19	Potala	.00

[1] Other dates also.

TABLE 1.—*Climatological data for Weather Bureau stations, April 1936*

[Compiled by Annie E. Small, by official authority, U. S. Weather Bureau]

District and station	Elevation of instruments: Barometer above sea level	Elevation of instruments: Thermometer above ground	Elevation of instruments: Anemometer above ground	Pressure: Station, reduced to mean of 24 hours	Pressure: Sea level, reduced to mean of 24 hours	Pressure: Departure from normal	Temperature of the air: Mean max. + mean min. ÷ 2	Temperature of the air: Departure from normal	Temperature of the air: Maximum	Temperature of the air: Date	Temperature of the air: Mean maximum	Temperature of the air: Minimum	Temperature of the air: Date	Temperature of the air: Mean minimum	Temperature of the air: Greatest daily range	Mean wet thermometer	Mean temperature of the dew-point	Mean relative humidity	Precipitation: Total	Precipitation: Departure from normal	Precipitation: Days with 0.01 inch or more	Wind: Total movement	Wind: Prevailing direction	Wind: Maximum velocity: Miles per hour	Wind: Maximum velocity: Direction	Wind: Maximum velocity: Date	Clear days	Partly cloudy days	Cloudy days	Average cloudiness, tenths	Total snowfall	Snow, sleet, and ice on ground at end of month
	Ft.	Ft.	Ft.	In.	In.	In.	°F.	°F.	°F.		°F.	°F.		°F.	°F.	°F.	°F.	%	In.	In.		Miles								0–10	In.	In.
New England							43.1	−0.8										72	3.34	+0.3										6.8		
Eastport	76	67	85	29.86	29.94	+0.01	38.6	−0.4	52	19	44	27	25	33	20	36	32	81	2.64	−0.2	16	8,649	sw.	37	sw.	6	5	4	21	7.6	1.0	0.0
Greenville, Maine	1,070	6	40	.....	.....	.....	.....	.....	.....	.....	.....	.....	.....	.....	.....	.....	.....	.....	.....	.....	.....	.....	.....	.....	.....	.....	.....	.....	.....	.....	.....	.....
Portland, Maine	103	82	117	29.85	29.97	+.01	42.4	−.6	74	30	49	28	4	36	21	37	31	67	4.54	+1.2	14	7,509	nw.	43	s.	6	9	9	12	5.9	3.4	.0
Concord	289	60	.....	.....	.....	.....	.....	.....	.....	.....	.....	.....	.....	.....	.....	.....	.....	.....	.....	.....	.....	.....	.....	.....	.....	.....	.....	.....	.....	.....	.....	.....
Burlington	403	11	48	29.50	29.95	−.04	41.2	−2.1	73	30	48	24	25	34	29	37	30	71	3.48	+1.3	16	7,705	s.	38	s.	26	5	6	19	7.7	7.1	.0
Northfield	876	12	60	29.00	29.97	−.02	39.2	−1.1	74	29	47	20	25	31	31	35	31	69	3.97	+1.7	19	6,094	s.	30	s.	6	3	5	22	8.1	8.9	.0
Boston[1]	29	31	50	29.95	29.98	+.01	45.2	−1.2	80	30	53	29	4	38	27	39	33	66	3.54	+.2	14	8,832	w.	36	s.	6	5	11	14	6.7	T	.0
Nantucket	12	14	90	29.98	30.00	+.03	44.6	+1.2	64	30	50	32	4	39	20	40	36	74	2.21	−.8	12	11,772	sw.	43	s.	6	9	10	11	5.5	.0	.0
Block Island	26	11	46	29.98	30.01	+.03	43.1	−.9	61	30	48	31	4	38	16	40	37	82	2.53	−1.0	13	11,662	w.	39	w.	8	6	11	13	6.3	.0	.0
Providence	160	215	251	29.83	30.01	+.03	45.4	−1.2	80	30	54	29	4	37	30	39	32	65	3.79	+.6	13	9,172	nw.	44	nw.	8	8	9	13	6.3	T	.0
Hartford	159	70	104	29.82	30.00	+.01	45.8	−.9	78	30	54	30	4	38	35	.....	.....	.....	3.21	−.2	16	6,944	s.	30	s.	6	6	7	17	6.9	T	.0
New Haven	106	74	153	29.91	30.03	+.04	45.9	−1.3	78	21	53	30	4	39	35	41	35	69	3.46	−.1	16	7,256	s.	33	s.	6	6	10	14	6.7	T	.0
Middle Atlantic States							49.9	−1.7										65	3.04	0.0									6.5		
Albany	97	97	112	29.90	30.01	+0.01	45.0	−1.8	78	29	53	28	4	37	27	40	35	72	3.12	+.7	17	6,042	s.	31	s.	6	5	5	20	7.5	T	.0
Binghamton	871	57	79	29.06	30.00	−.02	44.1	−1.3	82	29	53	24	25	35	36	.....	.....	.....	2.65	+.2	18	5,599	nw.	27	nw.	16	4	4	22	8.4	.4	.0
New York	314	415	454	29.68	30.03	+.03	47.2	−2.2	78	21	55	30	8	40	37	41	34	64	3.13	−.1	13	12,057	nw.	56	nw.	8	6	11	13	6.6	.0	.0
Harrisburg	374	94	104	29.62	30.03	+.01	48.6	−2.3	84	30	58	29	4	39	39	42	35	63	3.61	+.9	16	6,379	w.	28	w.	16	5	11	14	6.7	T	.0
Philadelphia	114	174	367	29.92	30.05	+.04	50.2	−1.9	83	30	59	31	8	41	38	43	36	62	2.25	−.8	13	10,007	s.	46	s.	6	6	11	13	6.4	T	.0
Reading	323	283	306	29.68	30.04	.....	48.9	−1.4	85	30	58	28	8	40	35	42	34	60	2.41	−.9	17	9,754	nw.	49	sw.	6	5	15	10	6.6	T	.0
Scranton	805	72	104	29.14	30.02	+.01	45.9	−2.2	82	29	55	25	8	37	35	39	32	64	2.85	+.1	14	5,434	nw.	25	nw.	21	4	13	13	6.8	T	.0
Atlantic City	52	37	172	29.99	30.05	+.05	47.6	−.2	70	15	54	31	8	41	24	43	38	71	3.32	+.3	15	11,890	w.	57	s.	6	5	11	14	6.8	T	.0
Sandy Hook	22	10	57	30.00	30.02	.....	47.2	.....	77	21	54	32	8	41	33	42	37	73	2.25	−1.4	14	11,01	5w.	55	s.	6	8	10	12	6.1	T	.0
Trenton	190	88	106	29.83	30.04	.....	48.6	−1.2	84	30	58	30	8	39	39	42	36	65	2.11	−.8	14	8,265	s.	38	s.	6	7	9	14	6.3	.0	.0
Baltimore	123	100	215	29.92	30.05	+.04	51.8	−1.8	86	21	61	32	8	43	41	44	37	61	2.56	−.8	14	8,794	sw.	40	nw.	21	6	9	15	6.5	T	.0
Washington	112	62	85	29.93	30.05	+.03	52.2	−1.1	86	21	62	30	4	43	43	44	34	55	1.98	−1.3	11	6,333	nw.	31	nw.	21	7	10	13	6.3	T	.0
Cape Henry	18	8	54	30.05	30.07	.....	54.6	.0	88	15	63	37	4	46	34	49	44	72	4.50	+1.2	10	8,376	se.	39	n.	15	12	10	8	5.3	.0	.0
Lynchburg	686	5	.....	29.32	30.08	+.06	54.0	−3.3	89	15	67	28	4	41	45	.....	.....	.....	4.54	+1.6	13	.....	nw.	.....	.....	.....	3	24	3	.....	T	.0
Norfolk	91	80	125	29.99	30.09	+.08	55.9	−.9	86	15	65	34	4	47	34	48	43	68	4.71	+1.5	11	7,315	s.	29	n.	15	8	10	12	6.1	.0	.0
Richmond	144	11	52	29.92	30.08	+.06	54.0	−2.6	87	15	64	30	4	43	37	46	40	64	2.68	−.8	10	6,582	sw.	31	sw.	21	9	10	11	5.7	T	.0
Wytheville	2,304	49	55	.....	30.04	+.01	49.1	−2.9	78	15	59	21	4	39	38	.....	.....	63	3.03	.0	10	5,896	w.	29	w.	21	6	13	11	.....	.....	.....
South Atlantic States							60.6	−1.2										68	4.90	+1.9									5.1		
Asheville	2,253	89	104	27.72	30.08	+.05	53.3	−.6	83	15	65	22	4	42	45	45	37	61	4.38	+1.4	10	7,722	nw.	32	nw.	7	6	14	10	5.9	.2	.0
Charlotte	779	63	86	29.24	30.09	+.06	57.3	−2.5	89	15	68	29	4	47	33	49	42	63	9.01	+5.7	10	5,847	ne.	26	sw.	2	8	11	11	5.7	T	.0
Greensboro	886	6	56	29.12	30.08	.....	53.4	.....	87	15	65	26	4	42	40	47	41	67	6.19	.....	.....	6,788	sw.	29	nw.	2	8	12	10	5.9	T	.0
Hatteras	11	5	50	.....	30.08	+.07	58.2	−1.6	73	29	64	38	4	52	23	.....	.....	81	.97	−2.6	8	10,122	ne.	34	nw.	3	15	7	8	.....	.0	.0
Raleigh	376	103	146	29.66	30.07	+.04	57.2	−2.2	89	15	68	30	4	47	34	50	45	69	5.21	+1.7	11	7,055	sw.	28	nw.	3	12	11	7	4.8	.0	.0
Wilmington	72	73	107	30.02	30.09	+.06	60.8	−1.2	87	16	70	34	4	52	27	54	49	70	1.56	−1.1	7	7,713	sw.	35	sw.	6	15	6	9	4.7	.0	.0
Charleston	48	11	92	30.04	30.09	+.06	64.5	.0	91	16	72	39	4	47	24	57	52	72	2.20	−.3	7	8,404	sw.	28	e.	25	13	7	10	4.7	.0	.0
Columbia, S. C	347	67	73	29.70	30.09	+.06	60.6	−2.7	89	15	71	32	4	50	34	52	45	61	10.76	+7.9	8	5,282	se.	21	sw.	16	13	8	9	5.0	.0	.0
Greenville, S. C	1,039	139	.....	.....	.....	.....	57.3	−1.3	87	16	68	29	4	47	40	.....	.....	.....	8.40	+4.7	10	.....	ne.	.....	.....	.....	10	8	12	.....	.0	.0
Augusta	182	62	77	29.87	30.06	+.03	62.2	−2.0	90	15	73	34	4	52	35	54	47	65	7.99	+4.8	10	4,984	sw.	24	w.	16	11	7	12	5.5	.0	.0
Savannah	65	73	152	30.01	30.08	+.05	66.2	+.2	92	15	75	38	4	57	35	58	54	72	1.67	−.9	6	8,650	nw.	37	nw.	2	13	6	11	4.7	.0	.0
Jacksonville	43	86	110	30.04	30.09	+.05	68.9	+.2	89	15	78	40	4	59	27	60	55	69	1.77	−.6	5	6,573	ne.	28	w.	2	18	4	8	3.7	.0	.0
Florida Peninsula							74.4	+1.3										72	1.37	−0.8									3.7		
Key West	22	10	64	30.02	30.04	+.02	76.7	+1.0	87	2	82	66	14	71	16	69	66	73	1.02	−.3	3	7,517	e.	22	n.	12	19	6	5	3.6	.0	.0
Miami	25	124	168	30.05	30.08	+.05	74.5	+1.7	85	26	80	57	4	69	21	67	63	71	2.15	−.9	7	7,607	se.	25	s.	2	15	11	4	4.2	.0	.0
Tampa	35	88	197	30.04	30.08	+.02	72.0	+1.1	87	15	81	47	4	63	28	64	60	73	.93	−1.1	2	8,339	e.	31	w.	2	18	8	4	3.4	.0	.0
Titusville	43	5	36	30.03	30.08	.....	70.4	.....	90	7	82	44	4	59	32	.....	.....	.....	.57	.....	5	.....	se.	.....	.....	.....	17	8	5	.....	.0	.0
East Gulf States							63.4	−1.3										70	6.18	+2.0									5.1		
Atlanta[1]	976	5	53	29.04	30.06	+.03	58.8	−2.2	87	15	70	30	4	48	44	51	45	67	9.86	+6.2	12	7,200	nw.	30	nw.	7	9	9	12	5.6	.0	.0
Macon	370	79	87	29.68	30.06	+.05	62.6	−1.3	91	15	73	34	4	52	40	54	46	62	7.20	+4.0	9	5,693	nw.	25	sw.	6	13	7	10	4.8	.0	.0
Thomasville	273	49	58	29.80	30.09	+.06	66.1	−.6	88	15	77	35	4	55	39	59	56	76	4.99	+1.6	6	.....	e.	.....	.....	.....	11	8	11	.....	.0	.0
Apalachicola	35	11	.....	30.04	30.08	.....	67.0	.....	83	15	74	45	4	60	24	61	.....	.....	.89	−1.9	5	.....	s.	.....	.....	.....	11	11	8	.....	.0	.0
Pensacola	56	149	185	30.02	30.08	+.06	65.4	−1.3	79	12	72	42	3	59	25	61	58	81	6.03	+2.0	11	9,204	se.	40	s.	9	15	7	8	4.3	.0	.0
Anniston	741	9	.....	.....	.....	.....	60.8	+.4	89	15	72	30	3	50	43	.....	.....	.....	6.99	+2.6	10	.....	nw.	.....	.....	.....	11	8	11	.....	T	.0
Birmingham	700	11	48	29.30	30.07	+.05	60.9	−2.4	88	15	71	31	3	50	37	52	46	65	5.20	+.4	11	5,823	nw.	32	s.	5	10	7	13	5.6	.0	.0
Mobile	57	86	105	30.01	30.07	+.05	65.6	−.7	86	13	74	39	3	57	26	59	55	76	5.94	+1.3	11	6,345	s.	26	s.	1	11	9	10	4.8	.0	.0
Montgomery	218	92	105	29.83	30.08	+.05	64.2	−1.1	89	15	74	36	3	54	33	56	50	67	6.16	+1.9	11	5,568	n.	20	sw.	1	12	2	16	5.4	.0	.0
Meridian	378	67	92	29.67	30.06	+.04	62.1	−1.9	90	14	74	33	3	51	36	54	48	68	6.71	+1.9	9	4,944	sw.	22	s.	5	11	7	12	5.1	.0	.0
Vicksburg	247	65	73	29.80	30.07	+.07	63.7	−1.9	89	13	74	38	3	53	32	54	47	64	7.58	+2.4	6	6,047	s	26	nw.	1	13	5	12	5.2	.0	.0
New Orleans	53	76	84	30.01	30.06	+.06	67.8	−1.0	88	13	77	46	3	59	29	60	55	70	6.55	+1.3	9	5,513	se.	21	se.	8	13	6	11	4.7	.0	.0
West Gulf States							64.8	−1.6										64	1.84	−.8									4.4		
Shreveport	249	92	227	29.79	30.06	+.09	64.8	−1.0	92	13	76	35	3	54	34	54	46	58	2.18	−2.4	5	8,916	s.	35	sw.	5	13	7	10	4.9	.0	.0
Bentonville	1,303	12	38	28.67	30.04	+.08	56.6	−.3	88	14	69	20	3	44	40	.....	.....	.....	1.45	−3.4	8	5,786	s.	22	sw.	4	11	9	10	.....	.3	.0
Fort Smith	457	79	94	29.54	30.02	+.06	60.8	−1.0	90	13	73	26	2	48	42	49	39	51	.73	−3.2	6	6,642	e.	28	sw.	20	15	9	6	4.1	.0	.0
Little Rock	357	94	102	29.67	30.05	+.07	59.8	−2.3	87	14	71	30	3	49	40	50	40	55	3.10	−2.1	7	6,580	s.	30	nw.	1	11	8	11	5.3	.0	.0
Austin	605	136	148	29.39	30.02	.....	66.6	−1.2	94	5	79	38	3	54	43	56	47	58	.66	−3.7	6	7,430	se.	35	sw.	28	14	7	9	4.3	.0	.0
Brownsville	57	88	96	29.92	29.98	.....	70.8	−2.9	92	1	79	48	9	63	29	64	61	80	2.02	+.6	6	8,792	se.	35	nw.	12	13	10	7	4.9	.0	.0
Corpus Christi	20	11	78	29.99	30.01	+.06	68.6	−2.2	95	5	75	48	9	62	27	62	59	78	1.92	+.1	7	9,152	se.	31	n.	2	11	13	6	4.4	.0	.0
Dallas	512	220	227	29.46	30.00	.....	64.2	.....	93	13	76	31	2	52	43	53	42	51	.59	−3.7	3	10,079	se.	40	sw.	5	17	5	8	3.6	.0	.0
Fort Worth	679	92	110	29.32	30.03	+.09	64.8	−.2	94	12	78	32	2	52	44	.....	.....	.....	.99	−3.0	2	8,666	s.	35	n.	5	21	5	4	2.7	.0	.0
Galveston	54	106	114	29.99	30.05	+.08	66.3	−2.4	80	28	72	46	3	60	21	61	58	82	1.93	−1.1	7	8,311	s.	39	w.	28	12	13	5	4.	.0	.0
Houston	138	292	314	29.91	30.06	.....	67.0	−2.3	89	1	77	39	3	57	31	.....	.....	.....	2.03	−1.6	5	9,212	s.	34	sw.	28	12	11	7	4.7	.0	.0
Palestine	510	64	72	29.52	30.05	+.09	63.7	−2.3	92	13	75	33	3	52	37	54	46	61	2.88	−1.5	5	6,213	s.	23	s.	4	16	5	9	4.2	.0	.0
Port Arthur	34	58	66	30.02	30.07	.....	66.4	.....	86	12	75	38	3	58	27	.....	.....	.....	2.45	−.5	8	6,562	s.	26	nw.	2	13	12	5	4.5	.0	.0
San Antonio	693	242	301	29.28	30.00	+.07	68.0	−1.1	93	5	80	38	3	56	39	57	49	61	2.77	−.4	7	7,572	s.	43	e.	16	10	11	9	.51	.0	.0

[1] Observations taken at airport.

TABLE 1.—*Climatological data for Weather Bureau stations, April 1936*—Continued

District and station	Elevation of instruments: Barometer above sea level	Elevation of instruments: Thermometer above ground	Elevation of instruments: Anemometer above ground	Pressure: Station, reduced to mean of 24 hours	Pressure: Sea level, reduced to mean of 24 hours	Pressure: Departure from normal	Temperature of the air: Mean max. + mean min. ÷ 2	Temperature of the air: Departure from normal	Temperature of the air: Maximum	Temperature of the air: Date	Temperature of the air: Mean maximum	Temperature of the air: Minimum	Temperature of the air: Date	Temperature of the air: Mean minimum	Temperature of the air: Greatest daily range	Mean wet thermometer	Mean temperature of the dew-point	Mean relative humidity	Precipitation: Total	Precipitation: Departure from normal	Precipitation: Days with 0.01 inch or more	Wind: Total movement	Wind: Prevailing direction	Wind: Maximum velocity: Miles per hour	Wind: Maximum velocity: Direction	Wind: Maximum velocity: Date	Clear days	Partly cloudy days	Cloudy days	Average cloudiness, tenths	Total snowfall	Snow, sleet, and ice on ground at end of month
Ohio Valley and Tennessee	Ft.	Ft.	Ft.	In.	In.	In.	°F.	°F.	°F.		°F.	°F.		°F.	°F.	°F.	°F.	%	In.	In.		Miles								0–10	In.	In.
							51.3	−3.5										63	3.77	+0.1										6.4		
Chattanooga	762	71	214	29.26	30.07	+0.04	59.0	−1.3	87	15	69	31	3	48	41	49	40	56	6.40	+1.6	8	6,761	w.	38	sw.	6	11	10	9	5.3	T	0.0
Knoxville	995	66	84	29.01	30.07	+.04	57.2	−.8	87	15	68	28	3	46	36	48	41	61	4.76	+.6	10	5,088	w.	25	w.	2	10	11	9	5.1	T	.0
Memphis	399	78	86	29.63	30.06	+.06	58.6	−3.2	85	14	68	30	3	50	33	50	42	61	1.21	−3.6	9	6,670	sw.	24	sw.	5	12	8	10	5.0	.0	.0
Nashville	546	168	191	29.50	30.09	+.08	56.2	−2.8	87	15	67	27	3	46	41	47	40	62	3.70	−.4	11	8,150	nw.	44	nw.	5	9	8	13	5.9	.1	.0
Lexington	989	6	----	----	----	----	50.2	−4.1	83	15	62	21	8	39	39	----	----	----	5.76	+2.3	14	----	sw.	----	----	----	14	3	13	----	.5	.0
Louisville	525	188	234	29.48	30.08	+.07	52.0	−4.4	84	15	62	24	3	42	35	45	38	64	4.10	+.2	10	8,668	sw.	35	nw.	16	10	7	13	6.0	.1	.0
Evansville	431	76	116	29.59	30.06	+.06	52.4	−4.3	80	27	61	25	3	44	31	45	38	62	3.00	−.9	9	7,357	s.	40	s.	5	8	11	11	5.9	T	.0
Indianapolis	822	194	230	29.16	30.06	+.06	47.7	−4.4	78	20	57	23	3	39	39	41	33	62	3.89	+.3	16	8,487	w.	37	w.	7	7	10	13	6.4	.6	.0
Terre Haute	575	96	129	29.41	30.04	----	50.2	----	82	20	60	24	3	40	39	42	35	63	3.86	+.2	11	7,675	se.	31	nw.	7	10	7	13	5.8	1.0	.0
Cincinnati	627	11	51	29.37	30.06	+.05	49.2	−3.2	79	15	58	23	8	40	37	43	37	67	3.11	.0	11	6,493	w.	30	w.	7	6	6	18	6.9	.4	.0
Columbus	822	90	210	29.17	30.05	+.03	47.2	−4.0	80	30	56	24	8	38	35	42	35	67	3.17	+.3	13	7,435	s.	38	sw.	28	3	12	15	7.2	.2	.0
Dayton	900	58	153	29.08	30.05	----	47.7	−3.9	79	28	57	24	4	38	35	----	----	----	3.81	+.6	14	6,732	sw.	36	w.	7	5	8	17	7.1	.8	.0
Elkins	1,947	59	78	27.99	30.07	+.04	46.1	−2.7	79	28	58	20	8	35	42	40	34	68	4.07	+.4	15	5,913	w.	30	nw.	7	2	9	19	7.6	3.0	.0
Parkersburg	637	77	84	29.42	30.08	+.05	49.4	−4.0	85	30	60	25	8	39	42	43	36	63	3.54	+.4	12	5,402	sw.	34	nw.	15	3	10	17	7.4	1.3	.0
Pittsburgh[1]	842	164	410	28.65	30.02	.00	45.4	−5.8	78	29	55	21	4	36	38	39	33	66	2.11	−.8	15	8,685	nw.	49	nw.	15	3	6	21	7.8	1.6	.0
Lower Lake Region							42.6	−2.8										74	2.55	0.0									7.8		
Buffalo	768	243	280	29.15	30.00	−.01	39.2	−3.6	70	27	46	22	4	32	36	36	32	80	1.78	−.8	18	10,836	sw.	57	w.	7	2	6	22	8.1	2.3	0
Canton	448	10	61	29.46	29.94	----	40.3	−2.2	70	29	48	21	1	33	36	38	34	79	3.50	+1.3	21	7,272	w.	30	sw.	3	3	7	20	7.9	2.8	.0
Ithaca	836	77	100	29.09	30.01	----	42.7	−2.3	81	29	52	23	4	34	36	38	33	72	2.74	+.2	18	7,499	nw.	31	se.	2	2	6	22	8.1	T	.0
Oswego	335	71	85	29.62	29.99	−.02	41.0	−2.6	75	29	48	26	3	34	29	37	32	74	2.81	+.5	20	8,054	w.	28	w.	3	3	5	22	7.9	4.3	.0
Rochester	523	86	102	29.43	30.01	.00	41.9	−3.0	77	29	49	23	8	35	35	38	34	76	1.83	−.5	20	6,939	w.	35	w.	7	3	6	21	8.2	2.3	.0
Syracuse	596	65	79	29.34	30.00	−.01	43.5	−.9	82	29	51	24	4	36	34	----	----	----	2.85	+.4	22	6,064	w.	25	sw.	16	1	5	24	8.5	3.5	.0
Erie	714	130	166	29.24	30.02	.00	42.4	−2.7	74	29	50	23	8	35	30	37	34	78	2.97	+.2	16	9,001	w.	38	s.	5	5	3	22	8.0	9.0	.0
Cleveland	762	267	318	29.19	30.03	+.01	44.3	−1.9	78	29	52	23	8	36	31	39	34	71	2.18	−.3	17	10,765	nw.	54	w.	7	4	4	22	7.8	3.6	.0
Sandusky	629	5	67	29.36	30.05	+.03	44.6	−2.6	76	20	53	22	4	37	33	----	----	----	2.08	−.5	18	7,244	w.	31	w.	7	3	8	19	7.5	.7	.0
Toledo	628	79	87	29.35	30.04	+.03	43.9	−3.7	76	20	52	23	4	36	31	39	33	70	1.75	−.9	15	7,393	w.	33	nw.	15	5	9	16	6.9	2.1	.0
Fort Wayne	857	69	84	29.10	30.04	----	44.9	−4.4	78	20	53	21	8	37	33	39	34	70	2.47	−.6	15	7,366	nw.	34	nw.	15	2	13	15	7.4	2.0	.0
Detroit	626	5	78	29.33	30.03	+.01	42.3	−3.9	74	20	50	21	3	35	34	37	32	73	3.61	+1.2	18	7,645	nw.	34	w.	7	3	8	19	7.3	1.2	.0
Upper Lake Region							37.7	−3.9										73	2.02	−0.4									7.2		
Alpena	609	13	89	29.34	30.03	+.01	35.8	−2.8	75	29	43	10	4	28	41	32	28	77	1.91	−.3	15	8,676	nw.	31	se.	14	5	10	15	6.7	13.0	.0
Escanaba	612	54	60	29.37	30.06	+.04	34.0	−3.9	60	29	41	13	8	27	24	30	26	75	.96	−1.3	12	7,379	s.	27	n.	17	3	9	18	7.4	2.4	.0
Grand Rapids	707	70	244	29.26	30.04	+.02	42.2	−4.8	74	29	50	22	3	34	30	36	31	70	2.27	−.5	16	8,283	n.	44	sw.	14	3	9	18	7.6	10.1	.0
Lansing	878	5	90	29.06	30.03	----	41.1	−4.5	74	14	50	16	4	33	35	37	32	74	3.37	+.8	16	7,217	nw.	28	nw.	7	3	8	19	7.8	7.8	.0
Ludington	637	5	54	29.32	30.04	----	38.2	−3.7	67	30	44	22	7	32	29	34	----	----	1.99	−.6	13	----	n.	----	----	----	5	11	14	----	5.4	.0
Marquette	734	77	111	29.22	30.04	+.02	34.0	−3.8	58	27	40	17	7	28	24	31	27	77	1.02	−1.4	8	6,822	nw.	31	s.	14	2	10	18	7.3	3.8	.0
Sault Sainte Marie	614	11	52	29.32	30.04	+.01	32.7	−4.7	63	28	39	12	1	27	29	30	27	82	1.95	−.2	13	6,965	nw.	30	nw.	16	5	3	22	7.4	5.5	.0
Chicago	673	7	131	29.32	30.06	+.06	43.6	−3.3	82	20	51	22	7	36	47	38	32	68	2.54	−.2	13	7,739	ne.	35	nw.	15	5	12	13	6.7	4.8	.0
Green Bay	617	109	141	29.36	30.03	+.02	38.8	−4.4	70	28	47	16	7	31	34	34	28	68	1.26	−1.4	11	8,430	n.	31	ne.	20	2	7	21	8.0	2.1	.0
Milwaukee	681	97	221	29.29	30.05	+.04	40.8	−3.0	74	29	48	18	7	34	37	38	30	69	2.30	−.4	13	9,120	n.	41	n.	15	3	10	17	7.3	13.0	.0
Duluth	1,133	5	47	28.79	30.04	+.03	33.4	−3.6	62	19	42	2	7	25	30	29	23	71	2.65	+.6	8	9,295	nw.	38	nw.	7	8	8	14	5.9	3.4	.0
North Dakota							36.2	−4.6										68	0.42	−1.2									5.3		
Moorhead, Minn	940	50	58	29.05	30.09	+.10	35.9	−4.7	72	13	46	2	7	26	36	31	26	71	.74	−1.4	5	6,748	n.	24	nw.	15	7	14	9	5.8	1.1	.0
Bismarck	1,674	8	57	28.27	30.09	+.12	38.1	−4.0	81	19	50	3	7	27	45	32	25	64	.37	−1.2	5	7,069	nw.	31	nw.	13	11	9	10	5.3	.1	.0
Devils Lake	1,478	11	44	29.48	30.11	+.12	33.8	−5.0	73	13	45	−1	7	23	36	29	24	72	.44	−1.1	6	7,596	nw.	32	nw.	13	10	10	10	5.6	.3	.0
Grand Forks	833	12	67	----	----	----	33.8	----	70	13	44	−5	7	23	37	30	----	----	.40	----	6	----	nw.	38	s.	13	6	20	4	----	1.7	.0
Williston	1,878	42	50	28.06	30.09	+.13	37.2	−4.8	82	19	49	−2	5	26	46	31	24	63	.12	−1.1	2	6,021	se.	30	nw.	13	12	12	6	4.5	.4	.0
Upper Mississippi Valley							46.9	−3.4										63	1.94	−1.0									5.7		
Minneapolis	919	105	208	29.05	30.05	----	39.8	−6.6	73	28	48	6	7	32	29	35	27	63	1.48	−.8	11	8,585	nw.	36	nw.	15	4	13	13	6.6	2.6	.0
La Crosse	714	11	48	29.26	30.04	+.06	42.7	−4.5	75	19	52	13	7	34	39	37	30	66	2.55	+.1	11	5,031	nw.	24	nw.	15	7	7	16	6.6	5.5	.0
Madison	974	70	78	28.97	30.04	+.05	41.4	−4.0	70	19	50	16	7	33	37	36	31	70	.95	−1.8	9	7,218	nw.	32	nw.	15	5	12	13	6.8	7.3	.0
Charles City	1,015	10	51	28.96	30.06	+.08	42.7	−3.7	78	30	53	12	7	32	45	37	30	65	2.34	−.2	7	6,177	n.	24	sw.	30	12	6	12	5.2	5.0	.0
Davenport	606	66	161	29.38	30.05	+.07	47.4	−2.5	84	30	57	18	3	38	42	40	33	61	1.80	−.9	11	8,112	nw.	37	nw.	15	7	12	11	5.8	5.3	.0
Des Moines	861	5	99	29.13	30.05	+.08	47.8	−2.3	87	30	59	12	3	37	43	40	31	59	1.33	−1.6	9	8,109	n.	34	nw.	15	13	4	13	5.4	4.7	.0
Dubuque	700	60	79	29.28	30.04	+.06	45.2	−3.4	79	30	54	16	7	36	42	38	31	61	.84	−2.0	9	5,545	nw.	27	nw.	15	9	6	15	6.0	5.7	.0
Keokuk	614	64	78	29.39	30.06	+.08	49.6	−2.7	87	20	60	15	3	40	39	41	32	56	1.57	−1.4	12	6,271	nw.	27	nw.	20	12	8	10	5.2	2.9	.0
Cairo	358	87	93	29.67	30.05	+.06	55.0	−3.1	84	15	64	26	3	46	32	48	43	69	3.79	+.1	10	7,437	s.	30	n.	21	10	6	14	5.7	T	.0
Peoria	609	11	45	29.40	30.07	+.08	48.2	−2.7	87	20	59	18	3	38	44	41	34	64	1.64	−1.7	12	6,023	nw.	26	nw.	11	15	6	9	4.8	3.0	.0
Springfield, Ill	636	5	191	29.36	30.05	+.07	50.4	−2.3	89	20	61	20	3	40	41	42	35	64	2.20	−1.3	10	8,903	e.	35	nw.	15	12	7	11	5.4	.3	.0
St. Louis	568	179	303	29.43	30.05	+.07	52.4	−3.4	89	20	62	20	3	42	38	44	37	61	2.80	−1.0	11	9,017	nw.	43	sw.	27	12	9	9	4.6	T	.0
Missouri Valley							50.3	−1.5										57	1.59	−1.3									4.7		
Columbia, Mo	784	6	84	29.20	30.04	+.06	53.0	−1.9	90	30	64	18	3	42	37	----	----	----	.63	−3.1	10	6,949	s.	26	sw.	20	16	6	8	4.3	0.2	.0
Kansas City[1]	750	32	45	29.22	30.03	+.07	54.3	−.5	91	30	66	16	3	42	43	44	34	53	1.89	−1.2	12	8,256	n.	34	sw.	20	13	7	8	4.6	1.1	.0
St. Joseph	967	11	49	29.00	30.04	----	52.7	----	90	30	65	13	3	41	40	42	31	51	2.91	−.1	8	7,374	n.	32	nw.	15	18	5	7	3.6	2.2	.0
Springfield, Mo	1,324	98	104	28.63	30.04	+.07	54.6	−1.4	88	14	65	17	3	44	37	45	37	58	2.37	−1.5	9	7,978	se.	32	s.	4	19	4	7	3.7	.3	.0
Iola	984	11	50	28.97	30.02	+.07	57.6	+1.4	96	14	72	16	3	43	44	----	----	----	.29	−3.2	5	----	sw.	----	----	----	11	14	5	----	1.0	.0
Topeka	987	65	87	----	----	----	54.4	−.3	91	13	68	16	3	41	43	----	----	----	3.02	+.2	8	7,639	n.	29	sw.	20	17	8	5	3.8	1.5	.0
Lincoln	1,189	11	81	28.76	30.04	+.10	49.6	−1.9	89	13	62	9	3	37	45	40	29	54	2.29	−.2	6	8,329	n.	37	n.	20	9	13	8	5.2	2.2	.0
Omaha	1,105	170	200	28.98	30.05	+.10	49.1	−2.1	88	13	61	10	3	37	46	40	30	55	23	−2.3	6	9,513	nw.	39	n.	15	10	9	11	5.2	1.6	.0
Valentine	2,598	47	54	27.33	30.09	+.15	42.3	−3.4	83	13	54	−8	3	30	43	36	28	64	1.63	−.2	11	6,824	n.	26	n.	20	8	14	8	5.6	3.6	.0
Sioux City	1,138	64	106	28.82	30.05	+.10	46.1	−1.7	84	13	58	8	3	34	42	38	29	59	.62	−2.1	5	7,939	n.	38	w.	30	14	7	9	4.7	1.8	.0
Huron	1,307	59	74	28.66	30.09	+.13	41.8	−3.3	85	13	54	7	3	30	49	35	28	65	1.62	−.6	8	7,396	nw.	33	nw.	15	13	10	7	4.7	1.8	.0
Northern Slope							43.0	−0.1										62	1.04	−0.5									6.0		
Havre	2,505	11	67	27.38	30.06	+.13	40.9	−2.8	86	18	54	−8	2	28	47	33	26	64	.44	−.6	7	6,989	e.	32	sw.	11	10	8	12	5.7	1.8	.0
Helena	4,124	85	111	25.82	30.05	+.08	43.8	+.3	80	18	55	−10	1	33	36	36	27	57	.99	−.1	7	5,952	sw.	31	w.	5	4	10	16	6.8	3.8	.0
Missoula	3,263	80	91	----	----	----	48.6	----	88	18	61	2	1	37	43	----	----	----	.51	−.5	9	5,739	nw.	37	w.	13	7	7	16	6.5	1.1	.0
Kalispell	2,973	48	56	----	30.02	+.06	44.7	+1.1	85	18	57	−8	1	32	45	----	----	----	1.33	+.5	9	4,903	w.	22	sw.	12	9	9	12	----	.0	.0
Miles City	2,371	48	55	27.51	30.10	+.14	43.7	−1.0	85	19	56	0	5	31	40	36	29	62	.23	−.9	6	5,124	nw.	31	n.	13	6	13	11	6.3	1.4	.0
Rapid City	3,259	50	58	26.64	30.12	+.17	41.1	−3.2	85	19	52	−8	2	30	41	35	28	65	1.21	−.8	11	5,923	n.	31	nw.	20	8	10	12	5.7	4.0	.0
Cheyenne	6,094	50	71	23.94	29.99	+.08	43.0	+2.1	74	23	57	−6	2	29	40	34	27	61	1.26	−.7	10	9,556	nw.	37	nw.	10	7	10	13	5.9	5.0	.0
Lander	5,372	60	68	24.64	30.02	+.08	44.5	+2.1	77	18	58	−11	2	31	43	35	26	57	1.39	−.7	8	4,327	sw.	32	sw.	23	5	20	5	5.5	3.3	.0
Sheridan	3,790	10	47	26.11	30.05	----	42.2	----	81	19	57	−10	2	28	45	35	27	63	.88	−1.0	11	4,283	nw.	22	nw.	10	6	14	10	5.8	.9	.0
Yellowstone Park	6,241	12	46	23.87	30.09	+.13	38.5	+1.5	71	18	50	−8	1	27	40	32	25	65	1.64	+.2	14	5,719	sw.	26	sw.	22	5	6	19	7.1	9.7	.0
North Platte	2,821	11	51	27.08	30.04	+.12	47.2	−1.4	85	23	60	−3	2	34	43	38	30	60	1.59	−.5	6	6,370	n.	27	w.	29	9	12	9	5.2	2.4	.0

[1] Observations taken at airport.

TABLE 1.—*Climatological data for Weather Bureau stations, April 1936*—Continued

District and station	Elevation of instruments: Barometer above sea level	Elevation of instruments: Thermometer above ground	Elevation of instruments: Anemometer above ground	Pressure: Station, reduced to mean of 24 hours	Pressure: Sea level, reduced to mean of 24 hours	Pressure: Departure from normal	Temperature of the air: Mean max. + mean min. ÷ 2	Temperature of the air: Departure from normal	Temperature of the air: Maximum	Temperature of the air: Date	Temperature of the air: Mean maximum	Temperature of the air: Minimum	Temperature of the air: Date	Temperature of the air: Mean minimum	Temperature of the air: Greatest daily range	Mean wet thermometer	Mean temperature of the dew-point	Mean relative humidity	Precipitation: Total	Precipitation: Departure from normal	Precipitation: Days with 0.01 inch or more	Wind: Total movement	Wind: Prevailing direction	Wind: Maximum velocity: Miles per hour	Wind: Maximum velocity: Direction	Wind: Maximum velocity: Date	Clear days	Partly cloudy days	Cloudy days	Average cloudiness, tenths	Total snowfall	Snow, sleet, and ice on ground at end of month
	Ft.	*Ft.*	*Ft.*	*In.*	*In.*	*In.*	°*F.*	°*F.*	°*F.*		°*F.*	°*F.*		°*F.*	°*F.*	°*F.*	°*F.*	%	*In.*	*In.*		*Miles*								*0–10*	*In.*	*In.*
Middle Slope							**54.6**	**+1.2**										**46**	**0.71**	**−1.6**										**4.4**		
Denver	5,292	106	113	24.71	29.97	+0.07	50.5	+3.4	77	19	63	11	1	38	33	39	27	48	.72	−1.3	8	6,178	s.	32	n.	5	7	15	8	5.7	2.7	0.0
Pueblo	4,685	80	86	25.27	29.96	+.08	52.4	+2.3	81	29	67	8	2	37	38	38	23	42	.29	−1.0	5	5,678	e.	30	w.	23	11	12	7	4.7	.3	.0
Concordia	1,392	50	58	28.57	30.06	+.13	52.1	−1.4	89	13	65	14	3	40	42	42	31	52	2.06	−.3	7	7,389	ne.	27	ne.	15	16	7	7	4.6	2.5	.0
Dodge City	2,509	10	86	27.41	30.02	+.12	54.2	+.6	89	13	69	9	2	39	43	41	29	47	.56	−1.4	6	9,918	s.	36	n.	5	19	6	5	3.0	1.2	.0
Wichita	1,358	85	93	28.56	30.00	+.07	56.5	+.1	93	14	69	15	3	44	38	45	32	45	.58	−2.3	5	9,254	sw.	37	sw.	20	15	8	7	4.1	T	.0
Oklahoma City	1,214	10	47	28.72	30.00	+.08	61.7	+1.9	94	13	75	20	2	48	40	48	35	44	.03	−3.3	2	8,426	s.	30	nw.	5	13	9	8	4.6	T	.0
Southern Slope							**62.8**	**0.0**										**42**	**1.42**	**−0.4**										**3.7**		
Abilene	1,738	10	52	28.19	29.99	+.09	64.0	−.4	95	29	78	28	7	50	42	50	37	45	4.09	+1.4	6	8,633	s.	35	s.	4	20	3	7	3.3	.0	.0
Amarillo	3,676	10	49	26.27	29.98	+.11	58.0	+2.2	91	14	73	14	2	43	38	43	28	40	.25	−1.6	1	7,901	s.	31	w.	4	15	9	6	4.0	T	.0
Del Rio	960	63	71	28.97	29.95	+.06	69.0	−1.6	92	12	82	40	6	56	43	57	47	54	1.30	−.5	4	7,955	se.	32	n.	26	13	12	5	4.0	.0	.0
Roswell	3,566	75	85	26.35	29.93	+.08	60.4	−.2	90	14	76	26	7	44	43	44	25	31	.04	−.8	2	6,593	s.	35	w.	4	15	12	3	3.4	.0	.0
Southern Plateau							**61.4**	**+4.1**										**35**	**0.15**	**−0.3**										**3.1**		
El Paso	3,778	152	175	26.16	29.90	+.07	65.8	+2.4	91	15	79	34	6	53	39	46	25	26	.11	−.2	2	7,349	e.	43	w.	4	21	7	2	2.2	.0	.0
Albuquerque	4,972	5	39	25.03	29.89	------	55.4	------	85	15	72	18	2	38	47	40	24	38	.09	−.5	3	7,330	w.	41	nw.	8	11	12	7	4.4	.7	.0
Santa Fe	7,013	38	53	23.25	29.92	+.08	49.2	+2.5	73	12	62	17	6	37	34	37	24	43	.20	−.8	3	4,878	e.	25	w.	4	11	14	5	4.8	.1	.0
Flagstaff	6,907	10	59	23.39	29.89	+.05	46.6	+4.4	76	15	63	16	2	30	44	35	----	50	.10	------	1	6,840	sw.	30	sw.	3	8	11	11	----	T	.0
Phoenix	1,108	10	107	28.73	29.87	.00	73.1	+6.1	100	17	89	42	2	58	40	51	28	23	.14	−.3	3	4,649	e.	24	w.	3	19	9	2	2.6	.0	.0
Yuma	141	9	54	29.74	29.88	−.01	73.8	+4.3	103	17	91	45	2	57	45	55	36	32	.00	−.1	0	4,598	w.	32	nw.	4	23	7	0	1.7	.0	.0
Independence	3,957	5	26	25.95	29.96	+.06	59.8	+4.7	87	16	76	28	1	43	41	43	----	----	.38	+.3	1	------	nw.	----	------	----	22	5	3	----	.0	.0
Middle Plateau							**52.5**	**+4.1**										**45**	**0.41**	**−0.6**										**4.5**		
Reno	4,527	61	76	25.49	30.00	+.03	52.6	+5.3	83	15	67	23	1	38	41	41	29	48	.04	−.4	1	5,574	w.	27	w.	21	16	10	4	3.4	T	.0
Tonopah	6,090	12	20	------	------	------	52.4	------	78	16	64	18	1	40	45	39	23	37	.13	------	2	------	nw.	----	------	----	----	----	----	----	----	----
Winnemucca	4,344	18	56	25.63	30.01	+.05	51.3	+4.6	86	17	68	17	2	35	49	40	29	52	.61	−.2	5	5,451	sw.	34	nw.	27	11	14	5	4.5	.2	.0
Modena	5,473	10	46	24.59	29.91	+.03	50.0	+4.0	82	15	67	18	1	32	47	37	21	41	.08	−.8	2	7,405	w.	38	s.	3	14	8	8	4.6	.2	.0
Salt Lake City	4,357	86	210	25.72	29.96	+.04	53.2	+3.6	84	16	66	14	2	40	39	42	32	52	.85	−1.2	7	6,226	se.	40	nw.	19	9	12	9	5.2	.2	.0
Grand Junction	4,602	60	68	25.35	29.92	+.04	55.2	+2.8	81	15	68	20	2	42	35	41	26	39	.45	−.4	4	5,228	se.	28	nw.	8	13	10	7	4.7	T	.0
Northern Plateau							**53.2**	**+3.9**										**52**	**0.67**	**−0.5**										**5.7**		
Baker	3,471	48	53	26.48	30.07	+.07	49.1	+3.9	83	17	62	7	1	37	40	41	33	60	1.15	+.1	10	4,423	se.	26	n.	4	5	14	11	6.2	1.4	.0
Boise	2,739	79	87	27.18	30.04	+.06	54.1	+3.7	88	17	66	11	1	42	38	44	34	53	.70	−.5	6	4,516	se.	26	nw.	4	9	12	9	5.4	T	.0
Pocatello	4,477	60	68	25.46	29.98	+.04	49.9	+3.9	80	17	61	12	5	38	35	40	30	52	.97	−.5	10	6,524	se.	30	sw.	8	9	13	8	4.9	4.0	.0
Spokane	1,929	101	110	27.97	30.02	+.03	52.2	+3.8	86	17	63	14	1	41	34	42	32	53	.18	−1.0	3	5,210	s.	22	sw.	7	9	10	11	5.6	.0	.0
Walla Walla	991	57	65	28.96	30.03	+.02	57.8	+4.7	89	17	68	19	1	48	37	47	37	50	.74	−.8	5	4,491	s.	22	sw.	7	8	13	9	5.8	.8	.0
Yakima	1,076	58	67	28.88	30.03	------	56.0	+3.5	88	17	68	21	1	44	40	45	33	46	.27	−.2	4	4,916	nw.	34	w.	7	4	16	10	6.5	T	.0
North Pacific Coast Region							**52.8**	**+3.6**										**74**	**1.69**	**−1.4**										**7.0**		
North Head	211	11	56	29.90	30.13	+.08	49.8	+2.3	68	16	54	33	1	46	21	47	45	87	.85	−3.3	14	8,591	nw.	33	se.	18	2	6	22	8.0	.7	.0
Seattle	125	90	321	29.95	30.08	+.05	53.8	+4.4	74	16	62	31	1	46	28	48	42	69	.72	−1.7	7	6,285	se.	28	sw.	11	4	10	16	6.6	.9	.0
Tatoosh Island	86	10	54	30.00	30.10	+.10	48.4	+2.3	61	15	52	34	1	45	16	45	43	84	3.98	−1.6	15	8,197	s.	40	e.	15	3	6	21	8.0	T	.0
Medford	1,329	29	58	28.64	30.06	------	55.4	------	87	15	69	21	1	41	43	48	41	68	1.52	+.3	7	------	nw.	----	------	----	11	6	13	5.7	T	.0
Portland, Oreg	153	68	106	29.93	30.09	+.03	55.6	+3.8	85	15	64	31	1	47	37	49	43	69	.80	−2.1	9	4,038	nw.	21	w.	17	1	9	20	7.6	5.2	.0
Roseburg	510	45	76	29.52	30.08	+.01	56.4	+5.4	84	12	69	25	1	44	39	49	43	70	2.25	.0	10	3,012	n.	17	w.	1	6	10	14	6.4	T	.0
Middle Pacific Coast Region							**56.7**	**+2.4**										**70**	**2.42**	**+0.2**										**5.4**		
Eureka	62	73	89	30.05	30.12	+.01	51.0	+1.1	75	16	56	34	1	46	25	48	47	88	2.13	−1.2	10	5,540	n.	30	n.	4	3	9	18	7.2	.0	.0
Redding	722	20	34	------	------	------	61.5	------	86	12	72	30	1	51	33	51	42	56	4.76	+2.1	9	5,455	nw.	26	se.	3	8	8	14	6.0	.0	.0
Sacramento	69	92	115	29.96	30.04	+.03	60.2	+2.1	85	11	72	36	1	49	31	52	46	64	1.69	+.2	4	5,225	sw.	24	se.	3	14	14	2	3.2	.0	.0
San Francisco	155	208	243	29.89	30.06	+.01	58.9	+3.9	83	11	66	43	1	51	31	52	46	70	1.09	−.5	6	5,302	w.	28	nw.	4	11	8	11	5.1	.0	.0
South Pacific Coast Region							**60.8**	**+1.4**										**71**	**0.66**	**−0.3**										**4.6**		
Fresno	327	97	105	29.68	30.04	+.05	63.6	+3.4	91	12	76	38	1	51	33	54	46	60	.54	−.4	2	4,889	nw.	24	nw.	4	14	10	6	3.8	.0	.0
Los Angeles	338	159	191	29.66	30.03	+.04	60.6	+1.2	90	11	69	46	1	52	38	53	48	73	.95	−.1	3	4,229	se.	19	sw.	4	9	16	5	4.7	.0	.0
San Diego	87	62	70	29.93	30.03	+.04	58.2	−.3	77	7	64	45	6	53	27	53	50	79	.48	−.3	5	5,170	nw.	28	w.	4	11	8	11	5.4	.0	.0
West Indies																																
San Juan, P. R.	82	9	54	29.93	30.02	------	77.2	+.6	89	19	82	70	1	73	15	----	----	----	2.38	−2.0	15	9,804	e.	35	e.	9	4	23	3	5.3	.0	.0
Panama Canal																																
Balboa Heights	118	6	92	------	[1]29.83	.00	82.4	+.8	94	15	91	70	30	74	23	----	----	[2]74	1.64	−1.3	5	6,459	nw.	25	n.	11	2	23	5	5.8	.0	.0
Cristobal	36	6	97	------	[1]29.86	.00	82.2	+.4	88	23	86	76	13	79	11	76	74	[2]78	3.29	−.9	16	9,646	n.	28	nw.	12	3	17	10	6.5	.0	.0
Alaska																																
Fairbanks	454	11	87	[1]29.47	[1]30.00	------	27.6	------	63	23	40	−13	11	15	45	24	15	57	T.	------	0	4,642	n.	32	n.	4	17	9	4	3.4	T.	.0
Juneau	80	96	116	[1]29.86	[1]29.95	------	42.0	------	62	24	49	24	2	35	27	38	31	68	7.18	------	14	4,922	w.	24	se.	8	8	3	19	6.7	4.8	.0
Hawaiian Islands																																
Honolulu	38	86	100	[1]30.00	[1]30.04	------	72.6	−.4	82	10	77	63	23	68	13	66	62	72	1.40	−.7	13	7,429	ne.	27	ne.	7	9	11	10	5.7	.0	.0

[1] Observations taken hourly.
[2] Pressure not reduced to mean of 24 hours.

TABLE 2.—*Data furnished by the Canadian Meteorological Service, April 1936*

Station	Altitude above mean sea level, Jan. 1, 1919	Pressure			Temperature of the air						Precipitation		
		Station reduced to mean of 24 hours	Sea level reduced to mean of 24 hours	Departure from normal	Mean Max. + mean min. ÷2	Departure from normal	Mean maximum	Mean minimum	Highest	Lowest	Total	Departure from normal	Total snowfall
	Ft.	*In.*	*In.*	*In.*	*° F.*	*° F.*	*° F.*	*° F.*	*° F.*	*° F.*	*In.*	*In.*	*In.*
Cape Race, Newfoundland	99												
Sydney, Cape Breton Island	48	29.83	29.88	−0.01	39.9	+4.9	48.5	31.3	65	22	6.19	+2.34	5.8
Halifax, Nova Scotia	88	29.66	29.77	−.19	39.8	+2.0	46.0	33.5	59	26	4.79	+.61	1.5
Yarmouth, Nova Scotia	65	29.84	29.91	−.05	40.0	+1.1	44.9	35.2	52	29	3.51	−.31	4.3
Charlottetown, Prince Edward Island	38	29.81	29.85	−.05	38.2	+3.0	44.9	31.5	63	20	3.07	+.42	19.5
Chatham, New Brunswick	28	29.78	29.81	−.09	38.0	+2.5	45.9	30.2	74	22	2.18	−.45	15.2
Father Point, Quebec	20	29.84	29.86	−.07	35.5	+2.3	40.8	30.3	61	21	2.44	+.86	9.8
Quebec, Quebec	296	29.57	29.90	−.09	37.7	+2.6	43.8	31.7	70	22	5.30	+3.21	24.3
Doucet, Quebec	1,236				25.9		37.6	14.2	55	−20	3.57		24.8
Montreal, Quebec	187												
Ottawa, Ontario	236	29.68	29.95	−.07	38.8	−1.2	46.1	31.6	64	17	4.06	+2.56	4.5
Kingston, Ontario	285	29.64	29.96	−.06	39.4	−.6	45.9	32.9	61	20	3.17	+1.38	1.6
Toronto, Ontario	379	29.58	30.00	−.02	39.6	−1.2	45.8	33.4	64	24	3.00	+.63	1.8
Cochrane, Ontario	930				27.7		36.2	19.3	55	2	1.60		10.4
White River, Ontario	1,244	28.65	30.00	−.04	26.0	−7.0	38.1	13.8	58	−17	1.95	+.70	9.9
London, Ontario	808				38.0		45.5	30.6	65	17	3.26		6.8
Southampton, Ontario	656	29.27	30.00	−.03	34.8	−3.9	41.4	28.2	66	14	3.26	+1.46	9.0
Parry Sound, Ontario	688	29.26	29.96	−.06	35.2	−2.4	40.5	27.9	60	6	1.85	−.06	8.2
Port Arthur, Ontario	644	29.38	30.12	+.09	29.1	−4.4	39.5	18.7	54	−10	1.95	+.23	.9
Winnipeg, Manitoba	760	29.24	30.11	+.09	29.8	−6.1	40.1	19.6	65	−16	.44	−.61	3.5
Minnedosa, Manitoba	1,690	28.23	30.10	+.09	29.4	−6.6	40.7	18.2	69	−15	.47	−.59	3.1
Le Pas, Manitoba	860				26.6		39.4	13.8	64	−21	1.23		9.4
Qu'Appelle, Saskatchewan	2,115	27.74	30.04	+.05	30.6	−6.8	41.8	19.4	72	−13	.50	−.55	4.8
Moose Jaw, Saskatchewan	1,759				35.2		46.4	23.9	76	−9	.48		3.2
Swift Current, Saskatchewan	2,392	27.45	30.02	+.06	37.6	−3.7	49.1	26.2	82	26	.50	−.43	4.0
Medicine Hat, Alberta	2,365	27.51	30.02	+.10	40.4	−4.1	51.2	29.6	86	0	.67	−.07	3.9
Calgary, Alberta	3,540	26.32	30.05	+.15	36.9	−2.7	48.2	25.7	81	−4	.64	.00	6.4
Banff, Alberta	4,521												
Prince Albert, Saskatchewan	1,450	28.47	30.09	+.11	32.2	−3.9	43.0	21.4	66	−12	.62	−.21	1.6
Battleford, Saskatchewan	1,592	28.30	30.08	+.11	33.6	−3.6	45.5	21.6	74	−13	.23	−.24	1.1
Edmonton, Alberta	2,150	27.70	30.02	+.13	35.4	−4.5	46.4	24.4	76	−13	.97	+.09	8.2
Kamloops, British Columbia	1,262	28.70	30.00	+.07	52.0	+3.1	65.4	38.7	86	15	.66	+.27	.0
Victoria, British Columbia	230	29.83	30.09	+.08	49.9	+3.1	56.3	43.6	67	32	.90	−1.47	.2
Barkerville, British Columbia	4,180												
Estevan Point, British Columbia	20				46.6		51.8	41.3	58	26	8.92		.0
Prince Rupert, British Columbia	170				42.0		49.1	35.0	68	22	6.23		.0
Hamilton, Bermuda	151												
LATE REPORTS FOR MARCH 1936													
Port Arthur, Ontario	644	29.14	29.87	−0.18	21.0	+4.2	29.9	12.0	45	−12	0.55	−0.42	5.3

SEVERE LOCAL STORMS, APRIL 1936

[Compiled by Mary O. Souder from reports submitted by Weather Bureau officials]

[The table herewith contains such data as have been received concerning severe local storms that occured during the month. A revised list of tornadoes will appear in the Annual Report of the Chief of Bureau]

Place	Date	Time	Width of path, yards	Loss of life	Value of property destroyed	Character of storm	Remarks
Tignall, near, Georgia	1	8:30 p. m.		3		Tornado	5 persons injured; 11 houses, 5 barns, and a store demolished; numerous animals killed.
Lincolnton, Ga., and vicinity	1	9 p. m.		0		do	2 persons injured; 50 houses wrecked; the courthouse, church, and a hotel damaged.
Gordo, Ala., vicinity of	1	11 p. m.	300	1		Tornadic winds	5 persons injured; several buildings destroyed; path 1 mile long.
Wills Valley, Ala	1	p. m.				Heavy rain and hail.	Wills Creek overflowed its banks, some flooding resulting; 200 feet of road washed out.
Hopkins County, Ky	1				$15,000	Wind and hail	Barns and small buildings unroofed or blown down; hail at Madisonville damaged windows and greenhouses.
Concord, N. C	2	5:57 a. m.	[1] 2		15,000	Wind	2 persons injured; storm moved from northwest to southeast causing scattered damage; noise like a nearby passing freight train; trees fell toward southeast; path 5 miles long.
Sasser, Ga	2	6 a. m.	200–500	1	3,000	Tornado	Several persons injured; number of buildings wrecked.
Leesburg, Ga	2	7 a. m.		1	4,300	do	8 persons injured; property damaged.
Greensboro, N. C	2	7:12–7:20 p. m.	13–267	14	2,000,000	do	144 persons injured, 88 seriously; 56 buildings totally wrecked and 233 damaged; path 7 miles long.
Cordele, Ga	2	7:30 a. m.		23	3,000,000	do	500 persons injured; 287 buildings demolished, 165 damaged. This may be same tornado that previously passed through Sasser and Leesburg, Ga.
Lodge, near S. C	2	8:30 a. m.	80	1	1,000	do	Farmer killed by a falling tree in his yard; path 1 mile long.
Mebane to Arcola, N. C., vicinity of.	2	8–9:15 p. m.		1	10,000	do	Continuation of the Greensboro tornado; appears to have passed ½ mile north of Mebane at 8 p. m., and was traced in an easterly direction for 6 miles; 4 persons injured; slight damage 3 miles north of Hillsboro; heavy cloud with a loud roar passed north of Arcola, a point 40 miles from Greensboro, at 9:15 p. m.
Cherry Lake, Fla	2				5,000	Thundersquall	Trees and chicken houses blown down; houses unroofed; some chickens killed by lightning.
Aiken, S. C., and vicinity	2				2,000	Wind	Property damaged.
Hampton, Colleton, Barnwell, and Allendale Counties, S. C.	2				5,000	do	Trees blown down; houses unroofed

[1] Miles instead of yards.

SEVERE LOCAL STORMS, APRIL 1936—Continued

Place	Date	Time	Width of path, yards	Loss of life	Value of property destroyed	Character of storm	Remarks
Valentine, Nebr.	3-4	p. m.				Dust	A heavy deposit of yellow dust settled over the entire landscape turning the snow to mud color and approaching 1/16 inch in depth on sidewalks.
Izard County, Ark.	5	2 p. m.	400	1	40,000	Tornado	4 persons injured and property damaged; path narrow and 440 yards long from southwest to northeast.
Nashville, Tenn.	5	7:30-9:30 p. m.			1,000	Thundersquall	Storm started with severe thunder at 7:30 p. m.; lightning interrupted power and light service; wind of 44 miles from the northwest; period of damaging winds less than 10 minutes.
Booneville, Miss.	5	8:05 p. m.	400-500	4	20,000	Tornado	12 persons injured; property loss; path 25 miles long, not continuous.
Coffeeville-Tupelo, Miss., Red Bay, Ala.	5	8:10 p. m.	440	4	10,000	do	At Coffeeville, 7 persons injured; property damaged; path 18 to 20 miles long.
Tupelo, Miss.	5	8:55 p. m.	400	216	3,000,000-4,000,000	do	700 persons injured; much property damaged; storm southwest to northeast; path 50 miles long.
Red Bay to Elkwood, Ala.	5			6		do	In Elkwood 6 persons killed and 15 injured; storm traveled 110 miles in a general northeasterly direction; amount of damage not estimated.
Henderson and Jefferson Counties, Ky.	5				25,000	Hail, heavy rain, and wind.	Fruit crop and tobacco-plant beds, windows, and automobile tops damaged; buildings unroofed and trees blown down; $25,000 loss estimated from hail alone.
Gainesville and New Holland, Ga.	6	8:27-8:37 a. m.		203	13,000,000	Tornadoes	934 persons injured, not including over 700 who required first-aid treatment; 750 houses demolished and 254 badly damaged; 1,662 families registered for Red Cross aid. The first tornado struck on the campus of Brenau College at 8:27 a. m.; only minor damage occurred to the college buildings, but the trees on the campus were torn to pieces and the trunks thrown down in all directions; the course of destruction was narrow and extended nearly eastward through New Holland, then northeastward into the country. The other tornadoes came along 10 minutes later, 2 distinct funnel clouds appearing at once. These destroyed all but a few buildings in the business section. One course of destruction led into the city from the southwest, just to the west of the Atlanta highway; the other came in from nearly west along the Dawsonville highway. These 2 paths came together west of Grove Street, and an area 4 blocks in width was laid waste across the entire city beyond which separate courses of destruction again appeared. Where the tornadoes finally disappeared is uncertain, but Lavonia, Ga., nearly 40 miles from Gainesville, experienced a tornado about an hour later, and Anderson, S. C., had one the same day. The wreckage was astounding. In many places the debris was piled up 8 or 10 feet deep in the streets. 3-story buildings were flattened into 1.
Acworth, near, Ga.	6	8:30 a. m.		0		do	2 persons injured; 4 houses and a mill demolished; other buildings damaged.
Anderson, S. C., and vicinity.	6	10:05 a. m.	400-500	1	250,000	do	Man killed in his home by falling bricks; 30 persons injured, some seriously; more than 50 homes wrecked; trees uprooted; power and communication lines disrupted.
Atlantic City, Absecon, and Corbin City, N. J.	6	10:20-10:25 a. m.				Wind	In Atlantic City extreme wind velocity of 65 miles per hour was registered; a 2,000-pound brick-tile wall collapsed under pressure of high wind, injuring a man and damaging an automobile; in Absecon a 2-story barn blown down; at Corbin City windows were broken in 2 houses.
Hardin, Wayne, Lewis, and Maury Counties, Tenn.	6	7:45 p. m.	100-1,320	10	202,000	Tornado	55 persons injured; more than 30 houses demolished and many damaged leaving 250 persons homeless.
McNairy County, Tenn.	6	8:30 p. m.			2,500	Thunderstorm	Property damaged.
Lawrence, Giles, Marshall, Lincoln, and Franklin Counties, Tenn.	6	9:15-11:30 p. m.		1	24,000	Electrical and wind.	4 persons injured; 2 families marooned; property damaged.
Warren County, Tenn.	6	11 p. m.	200		20,000	Wind	3 persons injured and 15 made homeless; property damaged.
Blackville, S. C., and vicinity.	6				2,000	Severe winds	Trees uprooted and roofs damaged.
Pennington, N. Mex.	9					Wind	Many fences destroyed due to Russian thistle and other debris being blown against them.
Hardin County, Iowa.	13				2,500	do	Property damaged.
Orange and Marshalltown, near, Iowa.	13				2,000	do	Do.
Lincoln, Nebr.	13					do	Small building overturned; plate glass windows and globes on street lights broken.
Ada, Minn., and vicinity.	13-16					Flood	High temperatures melted accumulated snows causing several rivers and creeks to overflow their banks in northern Minnesota; greatest damage at Ada where a hospital, 40 residences, and 6 buildings were flooded; dam east of Ada washed out; many acres of farm lands and several highways inundated; 2 bridges and part of railroad siding washed out.
Bedford County, Va.	15	4-5 p. m.			1,000	Thunderstorm	Damage to orchards and small buildings over a path several miles long.
Midland, Tex.	15	7:30 p. m.	1,320		25,000	Tornado	Property damaged.
Norfolk, Va.	15	9:25-10 p. m.			1,200	Thunderstorm	Damage by lightning to soft drink plant.
Tuscola, Tex.	15	10:30 p. m.	[1] 4	0	800	Tornado	Property damaged.
Abilene, Tex., and vicinity.	15	p. m.			1,175	Wind	Do.
Fond du Lac and Milwaukee Counties, Wis.	15				18,000	Wind and hail	Squalls most severe in northeastern Dodge County and in the vicinity of Milwaukee and Waukesha. In Dodge and Fond du Lac Counties a number of small buildings were demolished; considerable damage to telephone lines; in Waukesha an ice house was unroofed and a large barn demolished; in Milwaukee windows were broken and a shelter shed of a school collapsed; 5 second-grade pupils were caught under the shed, their injuries necessitating hospital treatment; woman injured when blown against a pole, another slightly injured by flying glass from a broken window; small damage from hail.
Glendale, Kans., and vicinity.	20	6 p. m.			500	Wind and dust	Storm had tornadic characteristics; dust entirely obscured the sky; garage demolished; outbuildings blown down.
Caldwell, Idaho.	23	4-5 p. m.	880			Hail	Windows broken; roofs damaged; chickens killed; some loss to apricots crop; path 3 miles long.
Miami and Opa Locka, Fla.	26	5 p. m.	1,320		50,000	Thunderstorm and hail.	Light to heavy hail over a small area northwest of the city in the vicinity of the municipal airport and Opa Locka; over a small area, 1,320 yards wide and 2½ miles in length, the fall was exceptionally heavy and unprecedented in this section; depth of fall in the open 4 or 5 inches and 2 feet deep when banked against the Goodyear airship hangar, remaining on the ground 3 days; property damaged including at least 41 residences in Opa Locka; many windows broken including 1,000 in the southwest side of the airship hangar; many automobiles and an airplane at the Naval Reserve base damaged.
Tracy, Tex.	27	2 a. m.		2		Tornado	11 persons injured; property damaged.
Holyoke, Colo.	27	6:30 p. m.	[1] 10		1,500	Heavy hail	Considerable damage to vegetable gardens.
Bush, La.	27	p. m.	[1] 6			Wind and hail	Heavy hailstones caused much damage to growing crops and fruit trees; several houses unroofed; amount of damage not estimated.
Haxtun, Colo.	27					Heavy hail	Loss to small grain.

[1] Miles instead of yards.

SEVERE LOCAL STORMS, APRIL 1936—Continued

Place	Date	Time	Width of path, yards	Loss of life	Value of property destroyed	Character of storm	Remarks
Montgomery, Ill.	27				8,750	Wind	4 persons slightly injured; property damaged.
Cuero, Tex.	28	2 a. m.	[1] 3			do	3 persons injured.
Fort Bend County, Tex.	28	do			5,000	do	5 persons injured.
Wharton County, Tex.	28	3 a. m.		2	2,000	do	7 persons injured; storm had tornadic characteristics.
Winnie to Orangefield, Tex.	28	4:30–6 a. m.				do	2 persons injured.
Webster and Nuckolls Counties, Nebr., southern portions.	28	5–8 a. m.			15,000	Hail	Damage to greenhouses, roofs, and windows.
York and Butler Counties, Nebr.	28	Noon	[1] 10		1,000	do	Property damaged.
Edgerly, Hathaway, Jennings, Plaucheville, and Bayou Jacque, La.	28	a. m.			1,000	Squalls	Do.
Galveston, Tex.	28	do			15,000	Thundersquall	In the school park a wood and steel grandstand, 240 feet in length, was blown to the ground and the steel supports badly bent; 6 small residences, supported on piling, were toppled over toward the north; a board fence 10 feet high surrounding the athletic field undamaged; large oak tree uprooted fell toward the north.
Lincoln, Nebr.	28	2–2:30 p. m.	333		5,000	Hail	Damage to windows and roofs.
Fort Wayne, Ind.	28					Heavy hail	Damage to greenhouses; automobile tops punctured; some loss in trucking.
Riverton, near, and Manson, Iowa.	28					Thundersquall and hail.	Gardens and trees damaged by hail in Riverton; in Manson an empty circus tent blown over.
Braddyville, Iowa.	29					Hail and wind	Garage wrecked; windows broken; telephone lines down.
Rock and Nobles Counties, Minn.	29–30	Midnight			10,000	Thunderstorm	Number of barns unroofed; small buildings and silos wrecked; some livestock and much poultry perished; some damage by lightning.
Lyons and Richland, Iowa.	30	3:15 a. m.				Wind and hail	Sheds and several windmills blown down; several sheep killed; considerable damage reported.
Rice, Dakota, Ramsey, and Washington Counties, Minn.	30	7:30–9 a. m.				Thundersquall	Number of buildings moved from their foundations; roofs lifted; windows blown in; poles and wires down; boathouses wrecked; tree uprooted. Greatest damage in St. Paul and vicinity.
Columbia, Ind.	30	3–4 p. m.		0		Tornado	Property damaged; path short.
Clay, Dickinson, and Emmet Counties, Iowa.	30	3–5:30 p. m.	880–1,760	2	565,000	do	More than 36 persons seriously injured; 62 farm and city homes totally destroyed and 79 badly damaged. Storm started as a windstorm in Sheldon, O'Brien County, at 2 p. m. At 3 p. m. the tornado made its first appearance in the extreme northwest portion of Waterford, Clay County, where 1 person was killed, 8 houses destroyed and a number of others badly damaged. Near Milford 2 funnel clouds were observed and a waterspout over west Lake Okobji also reported. Just after this the storm lifted, although heavy hail fell along the path to the northeast, with some stones measuring 8 inches in circumference. The next destruction occurred in Estherville, Emmet County, at 4:17 p. m. Because of the short lapse of time, it is believed that this was a new storm developing in advance of the original tornado, which followed along a short time later. The first storm passed over the northern part of the city, wrecked or badly damaged 12 homes, blew down power and telephone lines, and uprooted trees. The hospital was damaged, making care of the injured difficult. After this storm had struck Estherville a second one appeared and passed along the southern edge of the city, destroying hundreds of trees and tearing out 800 feet of railroad track. It is believed the second storm was the redevelopment of the Clay-Dickinson County tornado. After passing Estherville the paths of the 2 storms followed somewhat erratic but generally parallel courses across Center Township, joined for a short distance, then separated again to pass on opposite sides of Dolliver. The paths once more united and the storms passed into Minnesota, east of Tuttle Lake, about 5:30 p. m.; path of storm 60 miles long.
Martin, Faribault, and Blue Earth Counties, Minn.	30	5:30–6 p. m.	[1] 1–2	3	850,000	do	Tornado originated near Sheldon, in northwestern Iowa, entered Minnesota in the vicinity Tenhassen, south-central Martin County. Storm moved northeastward into Faribault County and was last reported near Pleasant Prairie shortly after 6 p. m. Greatest destruction in Blue Earth, Faribault County; about 300 buildings demolished or badly damaged; silos and windmills wrecked; trees uprooted; poles and wires down; farm machinery damaged; 20 persons injured; much livestock and poultry perished; path of storm 25 miles long; damage in Martin County $500,000, in Faribault and Blue Earth Counties $350,000.
Union, Iowa.	30	6 p. m.		0		Tornado and hail	Barn, a number of small buildings, and trees destroyed; path 1 mile long.
Preston, Minn., and vicinity.	30	8 p. m.	110	0	25,000	Tornado	Number of outbuildings wrecked; many trees uprooted; path 880 yards long.
Frankville, Iowa.	30	9 p. m.			1,000	Wind and hail	Damage to buildings.
Spring Valley and Perry, Iowa.	30	do	33–333	0	3,000	Tornado and hail	Trees broken; damage to electric and telephone wires; path 10 miles long.
Winona, Fillmore, and Houston Counties, Iowa.	30	p. m.			566,000	Rain and flood	Long stretches of railroad track, bridges, culverts, and dams washed out; highways damaged; creosote block pavements buckled; basements flooded; much cordwood washed away; some livestock and much poultry drowned; considerable damage to prospective crops; rockslides blocked highway traffic.
Varina, Iowa.	30				18,000	Electrical	Grain elevator destroyed by fire after being struck by lightning.
Morrison County, Minn.	30				10,000	Rain and flood	Bridge washed away, 2 others damaged; highways inundated.
Hanson, Lincoln, Minor, and McCook Counties, S. Dak.	30					Wind	Communication and power lines damaged and poles down; 2 farm buildings in Canton moved from their founuations.

[1] Miles instead of yards.

U. S. GOVERNMENT PRINTING OFFICE: 1936

Chart I. Departure (°F.) of the Mean Temperature from the Normal, April 1936

Chart I. Departure (°F.) of the Mean Temperature from the Normal, April 1936

Chart II. Tracks of Centers of Anticyclones, April 1936. (Inset) **Departure of Monthly Mean Pressure from Normal**

(Plotted by W. P. Day)

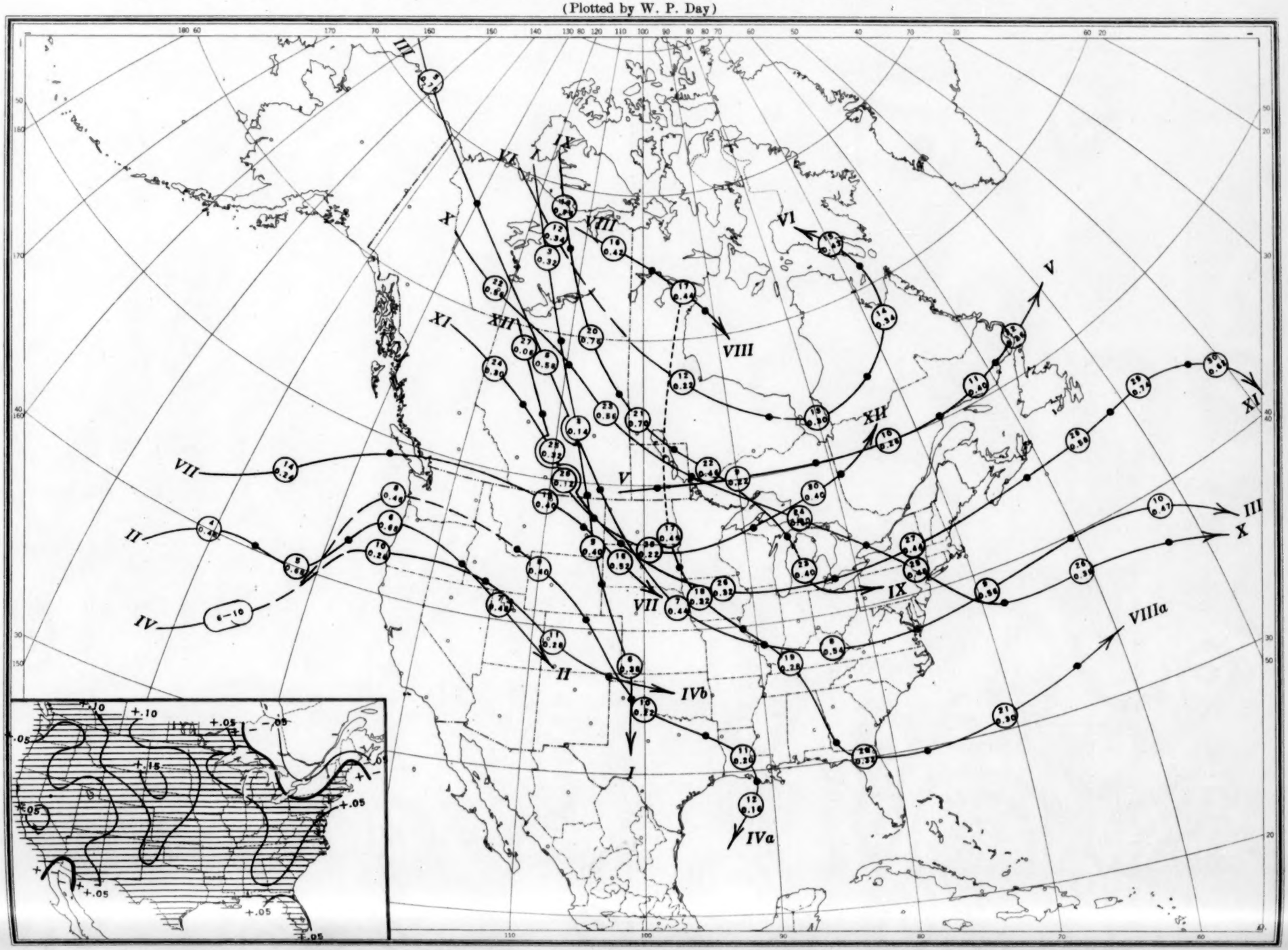

Circle indicates position of anticyclone at 8 a. m. (75th meridian time), with barometric reading. Dot indicates position of anticyclone at 8 p. m. (75th meridian time).

Chart III. Tracks of Centers of Cyclones, April 1936. (Inset) **Change in Mean Pressure from Preceding Month**

(Plotted by W. P. Day)

Circle indicates position of anticyclone at 8 a. m. (75th meridian time), with barometric reading. Dot indicates position of anticyclone at 8 p. m. (75th meridian time).

Chart III. Tracks of Centers of Cyclones, April 1936. (Inset) **Change in Mean Pressure from Preceding Month**

(Plotted by W. P. Day)

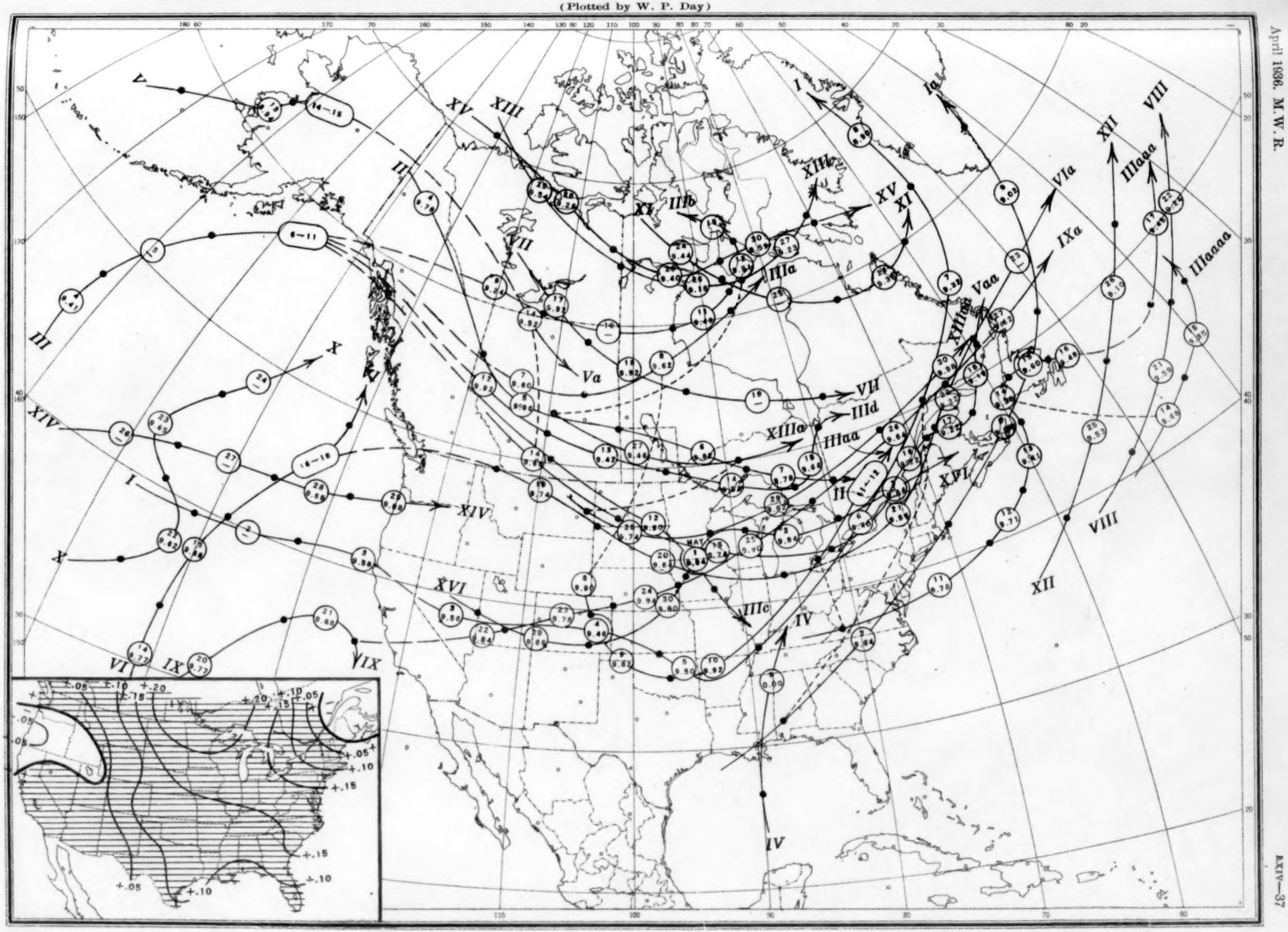
I
Ia
II
III
IIIa
IIIb
IIIc
IIIaa
IIIaaa
IIIaaaa
IIIaaaaa
IIIaaaaaa
IIIaaaaaaa
IIIaaaaaaaa
IIIaaaaaaaaa
IIIaaaaaaaaaa
IIIaaaaaaaaaaa
IIIaaaaaaaaaaaa
IIIaaaaaaaaaaaaa
IIIaaaaaaaaaaaaaa
IIIaaaaaaaaaaaaaaa
IIIaaaaaaaaaaaaaaaa
IIIaaaaaaaaaaaaaaaaa
IIIaaaaaaaaaaaaaaaaaa
IIIaaaaaaaaaaaaaaaaaaa
IIIaaaaaaaaaaaaaaaaaaaa
IIIaaaaaaaaaaaaaaaaaaaaa
IIIaaaaaaaaaaaaaaaaaaaaaa
IIIaaaaaaaaaaaaaaaaaaaaaaa
IIIaaaaaaaaaaaaaaaaaaaaaaaa
IIIaaaaaaaaaaaaaaaaaaaaaaaaa
IIIaaaaaaaaaaaaaaaaaaaaaaaaaa
IIIaaaaaaaaaaaaaaaaaaaaaaaaaaa
IIIaaaaaaaaaaaaaaaaaaaaaaaaaaaa
IIIaaaaaaaaaaaaaaaaaaaaaaaaaaaaa
IIIaaaaaaaaaaaaaaaaaaaaaaaaaaaaaa
IIIaaaaaaaaaaaaaaaaaaaaaaaaaaaaaaa
IIIaaaaaaaaaaaaaaaaaaaaaaaaaaaaaaaa
IIIaaaaaaaaaaaaaaaaaaaaaaaaaaaaaaaaa
IIIaaaaaaaaaaaaaaaaaaaaaaaaaaaaaaaaaa
IIIaaaaaaaaaaaaaaaaaaaaaaaaaaaaaaaaaaa
IIIaaaaaaaaaaaaaaaaaaaaaaaaaaaaaaaaaaaa
IIIaaaaaaaaaaaaaaaaaaaaaaaaaaaaaaaaaaaaa
IIIaaaaaaaaaaaaaaaaaaaaaaaaaaaaaaaaaaaaaa
IIIaaaaaaaaaaaaaaaaaaaaaaaaaaaaaaaaaaaaaaa
IIIaaaaaaaaaaaaaaaaaaaaaaaaaaaaaaaaaaaaaaaa
IIIaaaaaaaaaaaaaaaaaaaaaaaaaaaaaaaaaaaaaaaaa
IIIaaaaaaaaaaaaaaaaaaaaaaaaaaaaaaaaaaaaaaaaaa
IIIaaaaaaaaaaaaaaaaaaaaaaaaaaaaaaaaaaaaaaaaaaa
IIIaaaaaaaaaaaaaaaaaaaaaaaaaaaaaaaaaaaaaaaaaaaa
IIIaaaaaaaaaaaaaaaaaaaaaaaaaaaaaaaaaaaaaaaaaaaaa
IIIaaaaaaaaaaaaaaaaaaaaaaaaaaaaaaaaaaaaaaaaaaaaaa
IIIaaaaaaaaaaaaaaaaaaaaaaaaaaaaaaaaaaaaaaaaaaaaaaa
IIIaaaaaaaaaaaaaaaaaaaaaaaaaaaaaaaaaaaaaaaaaaaaaaaa
IIIaaaaaaaaaaaaaaaaaaaaaaaaaaaaaaaaaaaaaaaaaaaaaaaaa
IIIaaaaaaaaaaaaaaaaaaaaaaaaaaaaaaaaaaaaaaaaaaaaaaaaaa
IIIaaaaaaaaaaaaaaaaaaaaaaaaaaaaaaaaaaaaaaaaaaaaaaaaaaa
IIIaaaaaaaaaaaaaaaaaaaaaaaaaaaaaaaaaaaaaaaaaaaaaaaaaaaa
IIIaaaaaaaaaaaaaaaaaaaaaaaaaaaaaaaaaaaaaaaaaaaaaaaaaaaaa
IIIaaaaaaaaaaaaaaaaaaaaaaaaaaaaaaaaaaaaaaaaaaaaaaaaaaaaaa
IIIaaaaaaaaaaaaaaaaaaaaaaaaaaaaaaaaaaaaaaaaaaaaaaaaaaaaaaa
IIIaaaaaaaaaaaaaaaaaaaaaaaaaaaaaaaaaaaaaaaaaaaaaaaaaaaaaaaa
IIIaaaaaaaaaaaaaaaaaaaaaaaaaaaaaaaaaaaaaaaaaaaaaaaaaaaaaaaaa
IIIaaaaaaaaaaaaaaaaaaaaaaaaaaaaaaaaaaaaaaaaaaaaaaaaaaaaaaaaaa
IIIaaaaaaaaaaaaaaaaaaaaaaaaaaaaaaaaaaaaaaaaaaaaaaaaaaaaaaaaaaa
IIIaaaaaaaaaaaaaaaaaaaaaaaaaaaaaaaaaaaaaaaaaaaaaaaaaaaaaaaaaaaa
IIIaaaaaaaaaaaaaaaaaaaaaaaaaaaaaaaaaaaaaaaaaaaaaaaaaaaaaaaaaaaaa
IIIaaaaaaaaaaaaaaaaaaaaaaaaaaaaaaaaaaaaaaaaaaaaaaaaaaaaaaaaaaaaaa
IIIaaaaaaaaaaaaaaaaaaaaaaaaaaaaaaaaaaaaaaaaaaaaaaaaaaaaaaaaaaaaaaa
IIIaaaaaaaaaaaaaaaaaaaaaaaaaaaaaaaaaaaaaaaaaaaaaaaaaaaaaaaaaaaaaaaa
IIIaaaaaaaaaaaaaaaaaaaaaaaaaaaaaaaaaaaaaaaaaaaaaaaaaaaaaaaaaaaaaaaaa
IIIaaaaaaaaaaaaaaaaaaaaaaaaaaaaaaaaaaaaaaaaaaaaaaaaaaaaaaaaaaaaaaaaaa
IIIaaaaaaaaaaaaaaaaaaaaaaaaaaaaaaaaaaaaaaaaaaaaaaaaaaaaaaaaaaaaaaaaaaa
IIIaaaaaaaaaaaaaaaaaaaaaaaaaaaaaaaaaaaaaaaaaaaaaaaaaaaaaaaaaaaaaaaaaaaa
IIIaaaaaaaaaaaaaaaaaaaaaaaaaaaaaaaaaaaaaaaaaaaaaaaaaaaaaaaaaaaaaaaaaaaaa
IIIaaaaaaaaaaaaaaaaaaaaaaaaaaaaaaaaaaaaaaaaaaaaaaaaaaaaaaaaaaaaaaaaaaaaaa
IIIaaaaaaaaaaaaaaaaaaaaaaaaaaaaaaaaaaaaaaaaaaaaaaaaaaaaaaaaaaaaaaaaaaaaaaa
IIIaaaaaaaaaaaaaaaaaaaaaaaaaaaaaaaaaaaaaaaaaaaaaaaaaaaaaaaaaaaaaaaaaaaaaaaa
IIIaaaaaaaaaaaaaaaaaaaaaaaaaaaaaaaaaaaaaaaaaaaaaaaaaaaaaaaaaaaaaaaaaaaaaaaaa
IIIaaaaaaaaaaaaaaaaaaaaaaaaaaaaaaaaaaaaaaaaaaaaaaaaaaaaaaaaaaaaaaaaaaaaaaaaaa
IIIaaaaaaaaaaaaaaaaaaaaaaaaaaaaaaaaaaaaaaaaaaaaaaaaaaaaaaaaaaaaaaaaaaaaaaaaaaa
IIIaaaaaaaaaaaaaaaaaaaaaaaaaaaaaaaaaaaaaaaaaaaaaaaaaaaaaaaaaaaaaaaaaaaaaaaaaaaa
IIIaaaaaaaaaaaaaaaaaaaaaaaaaaaaaaaaaaaaaaaaaaaaaaaaaaaaaaaaaaaaaaaaaaaaaaaaaaaaa
IIIaaaaaaaaaaaaaaaaaaaaaaaaaaaaaaaaaaaaaaaaaaaaaaaaaaaaaaaaaaaaaaaaaaaaaaaaaaaaaa
IIIaaaaaaaaaaaaaaaaaaaaaaaaaaaaaaaaaaaaaaaaaaaaaaaaaaaaaaaaaaaaaaaaaaaaaaaaaaaaaaa
IIIaaaaaaaaaaaaaaaaaaaaaaaaaaaaaaaaaaaaaaaaaaaaaaaaaaaaaaaaaaaaaaaaaaaaaaaaaaaaaaaa
IIIaaaaaaaaaaaaaaaaaaaaaaaaaaaaaaaaaaaaaaaaaaaaaaaaaaaaaaaaaaaaaaaaaaaaaaaaaaaaaaaaa
IIIaaaaaaaaaaaaaaaaaaaaaaaaaaaaaaaaaaaaaaaaaaaaaaaaaaaaaaaaaaaaaaaaaaaaaaaaaaaaaaaaaa
IIIaaaaaaaaaaaaaaaaaaaaaaaaaaaaaaaaaaaaaaaaaaaaaaaaaaaaaaaaaaaaaaaaaaaaaaaaaaaaaaaaaaa
IIIaaaaaaaaaaaaaaaaaaaaaaaaaaaaaaaaaaaaaaaaaaaaaaaaaaaaaaaaaaaaaaaaaaaaaaaaaaaaaaaaaaaa
IIIaaaaaaaaaaaaaaaaaaaaaaaaaaaaaaaaaaaaaaaaaaaaaaaaaaaaaaaaaaaaaaaaaaaaaaaaaaaaaaaaaaaaa
IIIaaaaaaaaaaaaaaaaaaaaaaaaaaaaaaaaaaaaaaaaaaaaaaaaaaaaaaaaaaaaaaaaaaaaaaaaaaaaaaaaaaaaaa
IIIaaaaaaaaaaaaaaaaaaaaaaaaaaaaaaaaaaaaaaaaaaaaaaaaaaaaaaaaaaaaaaaaaaaaaaaaaaaaaaaaaaaaaaa
IIIaaaaaaaaaaaaaaaaaaaaaaaaaaaaaaaaaaaaaaaaaaaaaaaaaaaaaaaaaaaaaaaaaaaaaaaaaaaaaaaaaaaaaaaa
IIIaaaaaaaaaaaaaaaaaaaaaaaaaaaaaaaaaaaaaaaaaaaaaaaaaaaaaaaaaaaaaaaaaaaaaaaaaaaaaaaaaaaaaaaaa
IIIaaaaaaaaaaaaaaaaaaaaaaaaaaaaaaaaaaaaaaaaaaaaaaaaaaaaaaaaaaaaaaaaaaaaaaaaaaaaaaaaaaaaaaaaaa
IIIaaaaaaaaaaaaaaaaaaaaaaaaaaaaaaaaaaaaaaaaaaaaaaaaaaaaaaaaaaaaaaaaaaaaaaaaaaaaaaaaaaaaaaaaaaa
IIIaaaaaaaaaaaaaaaaaaaaaaaaaaaaaaaaaaaaaaaaaaaaaaaaaaaaaaaaaaaaaaaaaaaaaaaaaaaaaaaaaaaaaaaaaaaa
IIIaaaaaaaaaaaaaaaaaaaaaaaaaaaaaaaaaaaaaaaaaaaaaaaaaaaaaaaaaaaaaaaaaaaaaaaaaaaaaaaaaaaaaaaaaaaaa
IIIaaaaaaaaaaaaaaaaaaaaaaaaaaaaaaaaaaaaaaaaaaaaaaaaaaaaaaaaaaaaaaaaaaaaaaaaaaaaaaaaaaaaaaaaaaaaaa
IIIaaaaaaaaaaaaaaaaaaaaaaaaaaaaaaaaaaaaaaaaaaaaaaaaaaaaaaaaaaaaaaaaaaaaaaaaaaaaaaaaaaaaaaaaaaaaaaa
IIIaaaaaaaaaaaaaaaaaaaaaaaaaaaaaaaaaaaaaaaaaaaaaaaaaaaaaaaaaaaaaaaaaaaaaaaaaaaaaaaaaaaaaaaaaaaaaaaa
IIIaaaaaaaaaaaaaaaaaaaaaaaaaaaaaaaaaaaaaaaaaaaaaaaaaaaaaaaaaaaaaaaaaaaaaaaaaaaaaaaaaaaaaaaaaaaaaaaaa
IIIaaaaaaaaaaaaaaaaaaaaaaaaaaaaaaaaaaaaaaaaaaaaaaaaaaaaaaaaaaaaaaaaaaaaaaaaaaaaaaaaaaaaaaaaaaaaaaaaaa
IIIaaaaaaaaaaaaaaaaaaaaaaaaaaaaaaaaaaaaaaaaaaaaaaaaaaaaaaaaaaaaaaaaaaaaaaaaaaaaaaaaaaaaaaaaaaaaaaaaaaa
IIIaaaaaaaaaaaaaaaaaaaaaaaaaaaaaaaaaaaaaaaaaaaaaaaaaaaaaaaaaaaaaaaaaaaaaaaaaaaaaaaaaaaaaaaaaaaaaaaaaaaa
IIIaaaaaaaaaaaaaaaaaaaaaaaaaaaaaaaaaaaaaaaaaaaaaaaaaaaaaaaaaaaaaaaaaaaaaaaaaaaaaaaaaaaaaaaaaaaaaaaaaaaaa
IIIaaaaaaaaaaaaaaaaaaaaaaaaaaaaaaaaaaaaaaaaaaaaaaaaaaaaaaaaaaaaaaaaaaaaaaaaaaaaaaaaaaaaaaaaaaaaaaaaaaaaaa
IIIa

Chart IV. Percentage of Clear Sky Between Sunrise and Sunset, April 1936

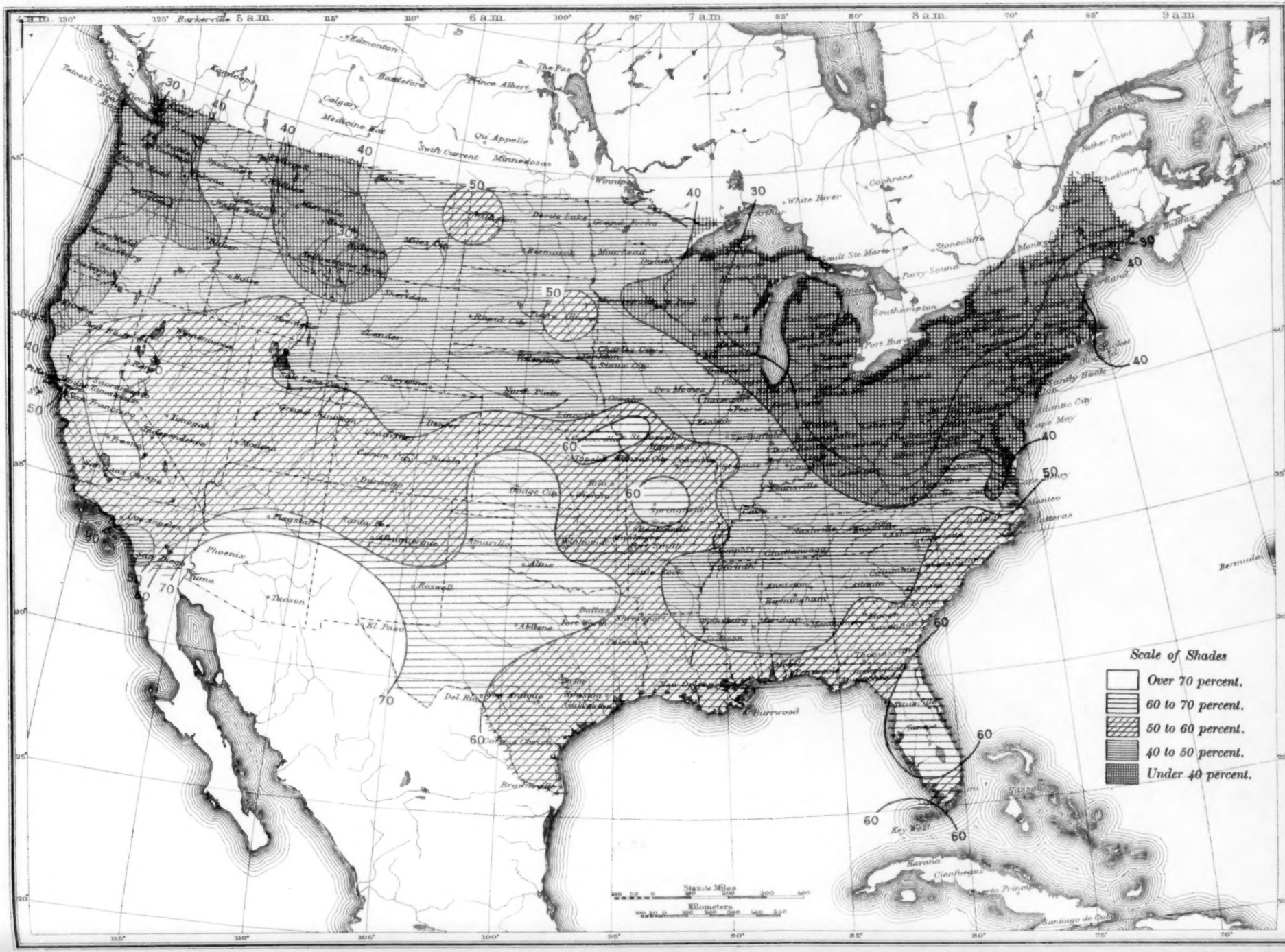

Chart V. Total Precipitation, Inches, April 1936. (Inset) Departure of Precipitation from Normal

Chart V. Total Precipitation, Inches, April 1936. (Inset) Departure of Precipitation from Normal

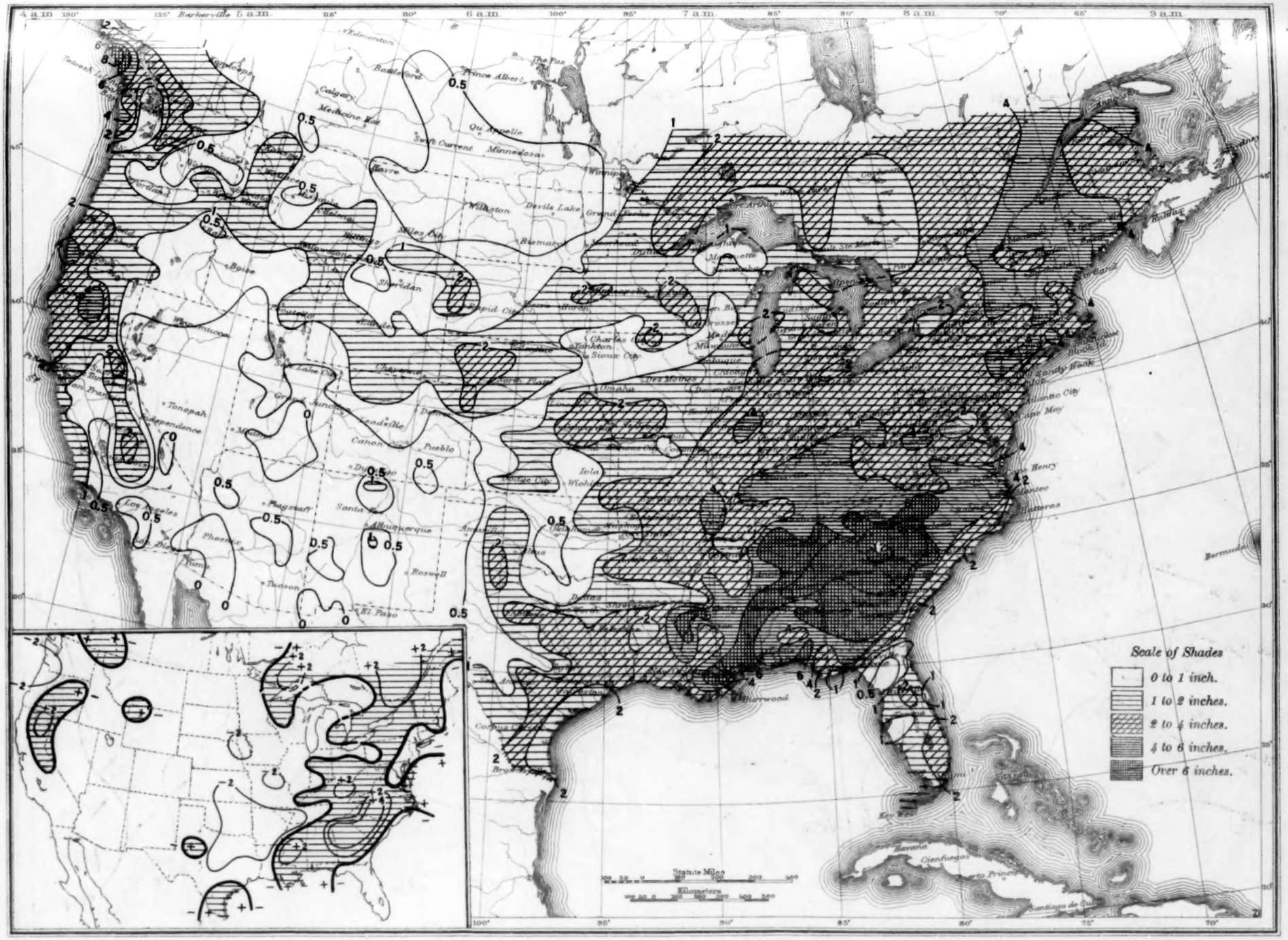

Chart VI. Isobars at Sea Level and Isotherms at Surface; Prevailing Winds, April 1936

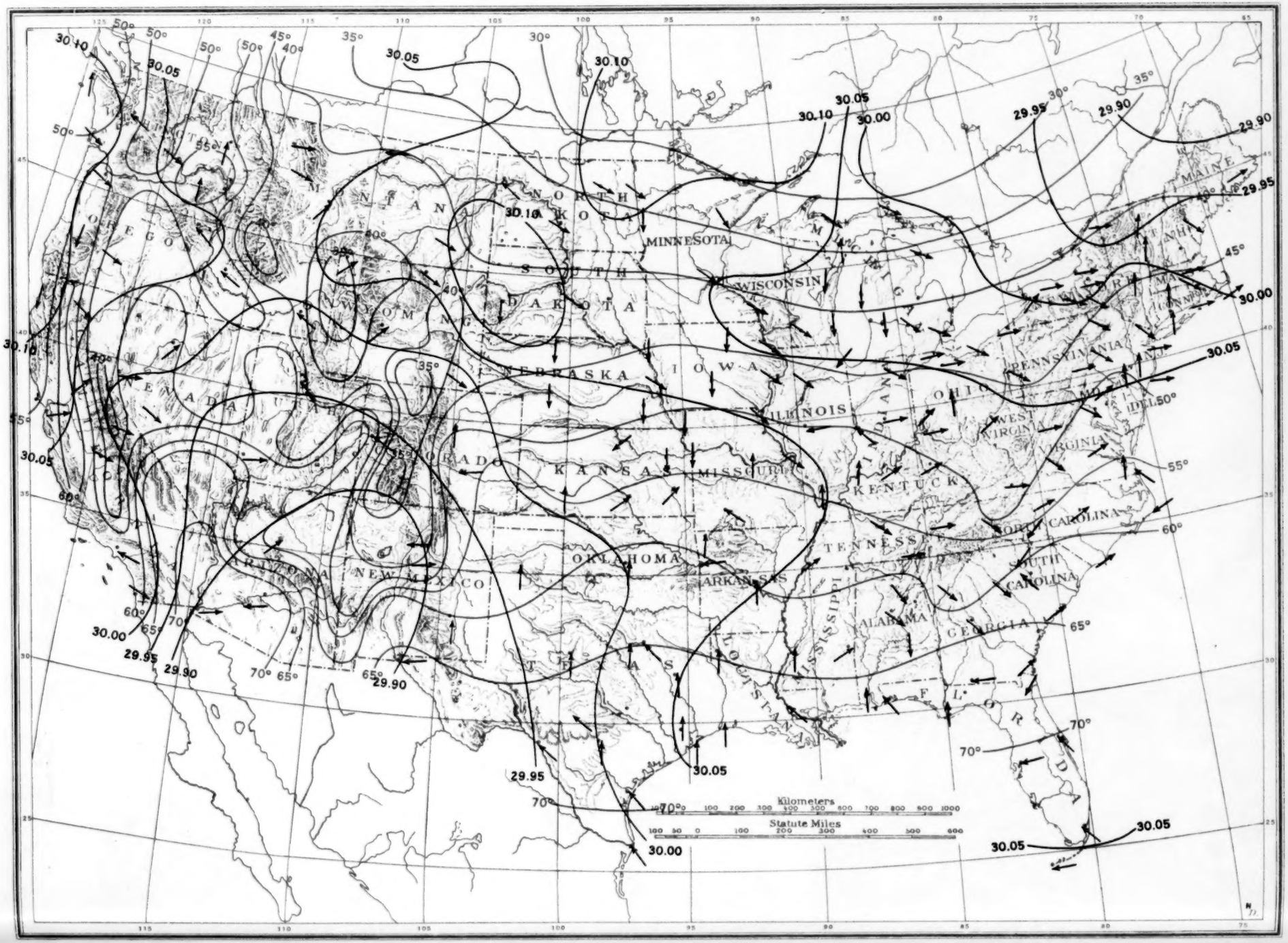

Chart VII. Wind Roses for Selected Stations, April 1936

(Plotted by W. W. Reed)

Chart VII. Wind Roses for Selected Stations, April 1936

(Plotted by W. W. Reed)

Chart VIII. Total Snowfall, Inches, April 1936

Chart IX. Weather Map of North Atlantic Ocean, April 8, 1936

(Plotted from the Weather Bureau Northern Hemisphere Chart)

Chart IX. Weather Map of North Atlantic Ocean, April 8, 1936

(Plotted from the Weather Bureau Northern Hemisphere Chart)

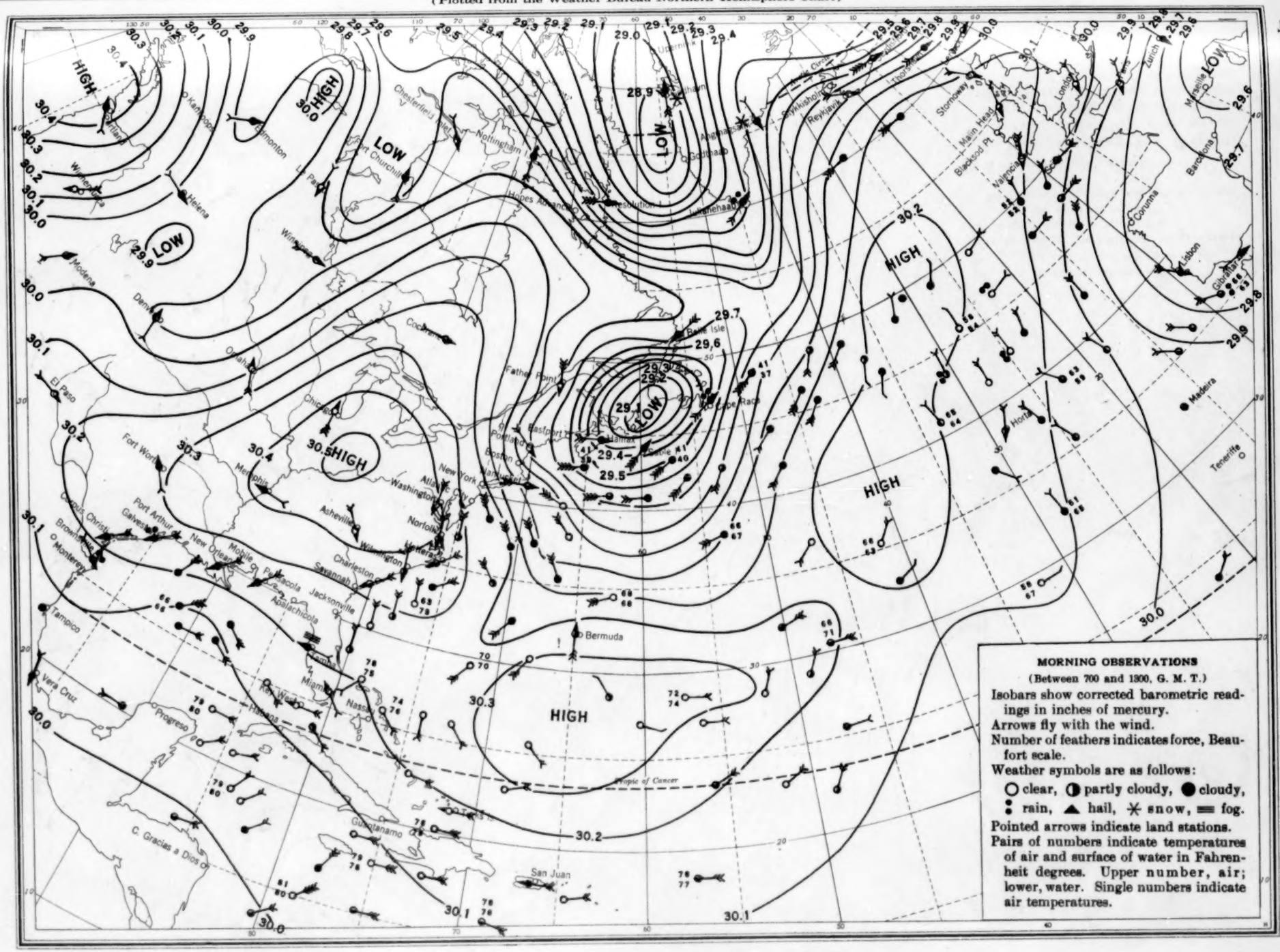
HIGH
LOW
30.5HIGH
Bermuda
Tropic of Cancer
MORNING OBSERVATIONS
(Between 700 and 1300, G. M. T.)
Isobars show corrected barometric readings in inches of mercury.
Arrows fly with the wind.
Number of feathers indicates force, Beaufort scale.
Weather symbols are as follows:
clear, partly cloudy, cloudy,
rain, hail, snow, fog.
Pointed arrows indicate land stations.
Pairs of numbers indicate temperatures of air and surface of water in Fahrenheit degrees. Upper number, air; lower, water. Single numbers indicate air temperatures.

Chart X. Weather Map of North Atlantic Ocean, April 9, 1936

(Plotted from the Weather Bureau Northern Hemisphere Chart)

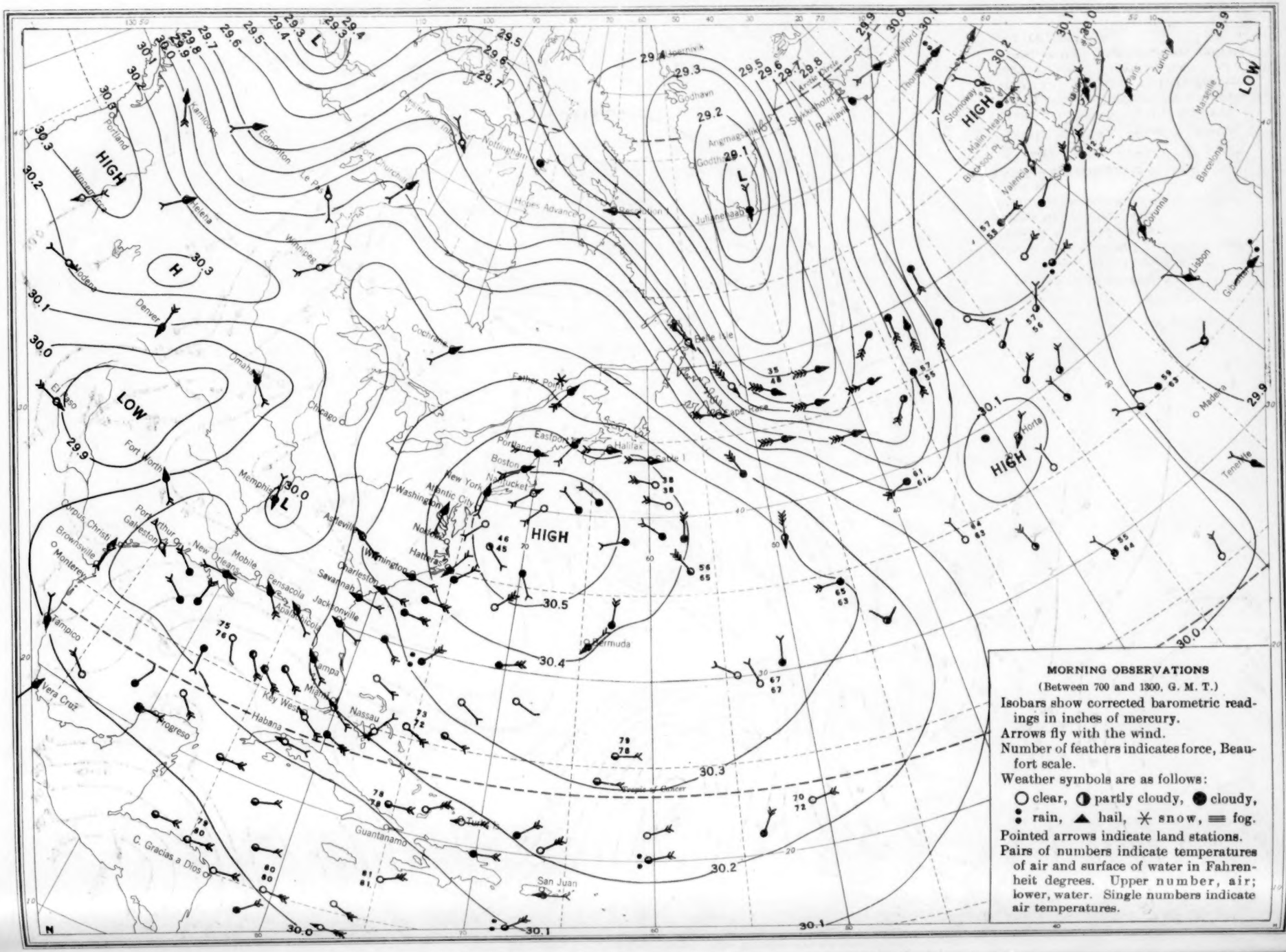

MORNING OBSERVATIONS

(Between 700 and 1300, G. M. T.)

Isobars show corrected barometric readings in inches of mercury.

Arrows fly with the wind.

Number of feathers indicates force, Beaufort scale.

Weather symbols are as follows:

○ clear, ◑ partly cloudy, ● cloudy, : rain, ▲ hail, ✳ snow, ≡ fog.

Pointed arrows indicate land stations.

Pairs of numbers indicate temperatures of air and surface of water in Fahrenheit degrees. Upper number, air; lower, water. Single numbers indicate air temperatures.